

ORNL  
MASTER COPY

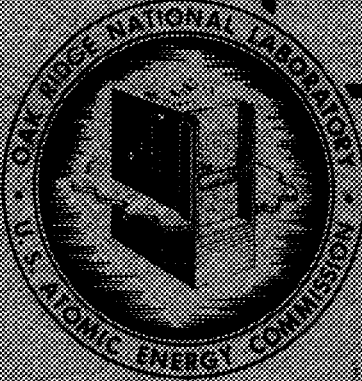
THIS DOCUMENT HAS BEEN REPRODUCED  
EXACTLY AS RECEIVED FROM THE  
PERSON OR ORGANIZATION ORIGINATING  
THE SAME. POINTS OF VIEW OR  
OPINIONS STATED HEREIN DO NOT  
NECESSARILY REPRESENT THE  
OFFICIALS OF THE U.S. GOVERNMENT

P. S. RILEY, ORNL/AD *J.F. 12/18/60*  
INITIALS DATE

*CONFIDENTIAL*

HOMOGENEOUS REACTOR PROJECT  
QUARTERLY PROGRESS REPORT  
FOR PERIOD ENDING AUGUST 15, 1951

*J.V.*  
*62*



DECLASSIFIED

By Authority Of:  
*E.J. Murphy 3-28-62*  
*W. H. ...*

For: J. I. ...  
Laboratory Science Dept.

OAK RIDGE NATIONAL LABORATORY

OPERATED BY

CARBIDE AND CARBON CHEMICALS COMPANY

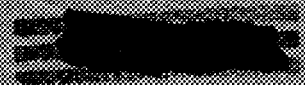
A DIVISION OF UNION CARBIDE AND CARBON CORPORATION

CLASSIFICATION *CONFIDENTIAL*  
DATE *JUL 6 1970*  
*Doc Review*  
*Order*

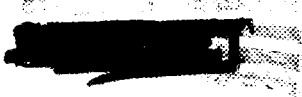
*[Signature]*

REPRODUCTION PERMITTED  
BY THE U.S. GOVERNMENT  
AUTHORITY DERIVED FROM E.O. 12958

POST OFFICE BOX P  
OAK RIDGE, TENNESSEE





## DISTRIBUTION LIST

ORNL 1121  
Progress Report

### INTERNAL

1	G. T. Felbeck (C&CCC)	38	A. S. Householder
2-3	Chemistry Library	39	C. S. Harrill
4	Physics Library	40	D. W. Cardwell
5	Biology Library	41	K. Z. Morgan
6	Health Physics Library	42	E. M. King
7	Metallurgy Library	43	C. E. Winters
8-9	Training School Library	44	C. H. Secoy
10-19	Central Files	45	J. A. Lane
20	C. E. Center	46	C. G. Graham
21	C. E. Larson	47	J. L. English
22	W. B. Humes (K-25)	48	W. R. Gall
23	W. D. Lavers (Y-12)	49	L. R. Quarles
24	A. M. Weinberg	50	E. P. Blizzard
25	E. H. Taylor	51	W. H. Davenport
26	E. J. Murphy	52	R. N. Lyon
27	E. D. Shipley	53	C. P. Keim
28	J. A. Swartout	54	C. D. Susano
29	F. C. VonderLage	55	R. S. Livingston
30	R. C. Briant	56	S. E. Beall
31	S. C. Lind	57	J. P. Gill
32	F. O. Steahly	58	G. E. Boyd
33	A. H. Snell	59	E. G. Bohlmann
34	A. Hollaender	60	J. H. Buck
35	M. T. Kelley	61	D. D. Cowen
36	G. H. Clewett	62	P. M. Reyling
37	J. S. Felton	63-66	Central Files (OP)

### RESTRICTED DATA

This document contains restricted data as defined in the Atomic Energy Act of 1946.

### CAUTION

This document contains information affecting the National Defense of the United States. Its transmission or the disclosure of its contents in any manner to any unauthorized person is prohibited and may result in severe criminal penalties under applicable Federal laws.

EXTERNAL

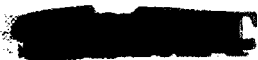
67-69	Aircraft Nuclear Propulsion Project
70-79	Argonne National Laboratory
80	Armed Forces Special Weapons Project (Sandia)
81-88	Atomic Energy Commission, Washington
89	Battelle Memorial Institute
90-92	Brookhaven National Laboratory
93	Bureau of Ships
94-99	Carbide and Carbon Chemicals Company (Y-12 Area)
100	Chicago Patent Group
101	Chief of Naval Research
102-106	du Pont Company
107	H. K. Ferguson Company
108-111	General Electric Company, Richland
112	Hanford Operations Office
113-116	Idaho Operations Office
117	Iowa State College
118-121	Knolls Atomic Power Laboratory
122-124	Los Alamos
125	Massachusetts Institute of Technology (Kaufmann)
126-127	Mound Laboratory
128	National Advisory Committee for Aeronautics
129-130	New York Operations Office
131-132	North American Aviation, Inc.
133	Patent Branch, Washington
134	Savannah River Operations Office
135-136	University of California Radiation Laboratory
137-140	Westinghouse Electric Corporation
141-143	Wright-Air Development Center
144-158	Technical Information Service, Oak Ridge

RESTRICTED DATA

This document contains restricted data as defined in the Atomic Energy Act of 1946.

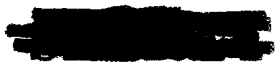
CAUTION

This document contains information affecting the National Defense of the United States. Its transmission or the disclosure of its contents in any manner to any unauthorized person is prohibited and may result in severe criminal penalties under applicable Federal laws.



Reports previously issued in this series are as follows:

ORNL-527	Date Issued December 28, 1949
ORNL-630	Period Ending February 28, 1950
ORNL-730	Feasibility Report - Date Issued, July 6, 1950
ORNL-826	Period Ending August 31, 1950
ORNL-925	Period Ending November 30, 1950
ORNL-990	Period Ending February 28, 1951
ORNL-1057	Period Ending May 15, 1951



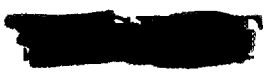
[REDACTED]

## TABLE OF CONTENTS

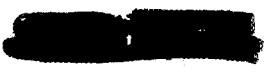
	PAGE NO.
SUMMARY	1
Part I. HOMOGENEOUS REACTOR EXPERIMENT	
1. CONSTRUCTION OF HRE	9
D <sub>2</sub> O system	9
Fuel system	9
Steam system	9
Shield	9
Instrumentation and control	9
Welding and Inspection of Welds in the Fuel System	13
2. DESIGN PROGRESS	15
Flow diagram	15
Sampler	15
Insulation	17
Pressure drop in soup circulating system	17
Removal of heat from core after shutdown	18
Pressure drop in D <sub>2</sub> O circulating system	18
Stress analysis of core tank	18
Low-pressure D <sub>2</sub> O catalytic recombiner	18
3. CORROSION	20
Scouting Studies	20
Anodic and cathodic treatment of type 347 stainless steel during passivation with nitric or chromic acid solutions	20
Electrochemical corrosion studies	22
Static Tests	25
Pretreatment films	26
Uranyl sulfate corrosion studies	28
Corrosion of reflector materials	37
Dynamic Corrosion Studies	42
Loop A, runs A-7 and A-8	43
Loop B	44
Thermal loops	46
Results and discussion	46
Future work	49
4. RADIATION STABILITY	51
Radiation experiments in the graphite pile	51

	PAGE NO.
Out-of-pile bomb experiments	51
Experiments at higher fluxes	53
Radiation effects on the HRE reflector system	54
Plans for next quarter	55
 5. ENGINEERING COMPONENT STUDIES	 56
Mechanical Aspects of Soup Recirculating Test Loops	56
Examination of loop after operation	57
Pretreatment of the loops	57
Westinghouse pump, model 100A	58
Bearings	59
Double-discharge pump	60
Pulsafeeder pumps	60
Operation of the HRE Mock-up	60
Letdown system	61
Apparatus	61
Performance of the letdown system	63
Development of Pulsafeeder pump	63
40- and 10-kw boilers	64
Soup pressurizer	64
Recombiner system	64
Mixing in the HRE Core	65
 6. RECOMBINATION OF HYDROGEN AND OXYGEN	 68
Laboratory Scale Studies	68
100% conversion	68
Conversion inside tubes	69
Catalysts other than platinum	70
Pressurizer tests	70
High-pressure recombination-reflector system	71
Removal of iodine from the gas stream	71
Pilot Plant Tests	72
Pilot plant runs with low gas flow rates	72
Pilot plant runs with high gas flow rates	74
 7. CHEMICAL CONTROL	 75
Electromagnetic Densitometer	75
Princo Densitrol	77
Pyrex	79
Stainless steel	79
Titanium	79
Q Measurement	80
Radiation Resistant Glasses	81

	PAGE NO.
8. PHYSICS	84
Criticality Calculations	84
Constants	84
Light-water reflector	85
Operation with low-enrichment fuel	87
Kinetics of the HRE	87
Linearized treatment of HRE with pressurizer	88
Nonlinear mechanics of HRE with pressurizer	93
Effect of pressurizer on limiting power surges	96
Damping produced by delayed neutrons	99
Numerical calculation of a power surge	102
Possibility of slow, undamped power excursions	104
A method for treating certain second-order nonlinear differential equations	105
Fluid Friction Coefficients in the Pressurizer Tube and Their Effects on the Reactivity of the Core Materials	107
Heat Transfer Coefficients for the Steam Generator	108
Safety Calculations for the HRE	110
9. CONTROLS	113
Part II. ALTERNATE SYSTEMS	
10. SOLUTION CHEMISTRY	119
The Uranium Trioxide-Phosphoric Acid-Water System	119
Experimental	119
Conclusions	120
The Effect of Carbon Dioxide on the Sodium Uranyl Carbonate- Water System	120
Vapor Pressures of Uranyl Salt Solutions	122
Studies of Electrical Conductivities of Aqueous Uranyl Sulfate Solutions	122
Preparation of Pure Uranyl Sulfate for Experimental Purposes	124
Uranyl Sulfate Production — Acidities, Refractive Indices, and Densities of Uranyl Sulfate Solutions	124
Experimental	124
11. CORROSION	129
Corrosion of Titanium	129
Corrosion of Rem-Cru Titanium sheet and plate	129
Corrosion of welded titanium tubing	129
Corrosion of welded titanium	130
Corrosion of titanium coupled to type 347 stainless steel	131
Corrosion of sintered titanium	132



	PAGE NO.
Corrosion of Zirconium	132
Corrosion of Bureau of Mines resistance-melted zirconium-tin alloys	133
Corrosion of Bureau of Mines induction-melted zirconium-tin alloys	133
Corrosion of arc-melted crystal bar zirconium containing 5% tin	134
Corrosion of Bureau of Mines zirconium tubing containing 5% tin	135
Corrosion of crystal bar zirconium	135
Uranyl Fluoride Stability and Corrosion Studies	136
Solution stability of uranyl fluoride contained in untreated type 347 stainless steel bombs	136
Effect of pretreatment films on solution stability	138
12. RADIATION DAMAGE	143
Specific and net gas production in homogeneous reactor systems	143
Survey of the stability of HRP systems	144
Hydrolysis of iron, chromium, and nickel salts in uranyl sulfate solutions	146
Hydrogenation of uranyl sulfate solutions	146
Recombination of hydrogen and oxygen at high pressures	148
Hydrogen embrittlement	149
Out-of-pile bomb studies	149
Plans for next quarter	150
13. SLURRY FUEL STUDIES	151
Uranium Trioxide Studies	151
Uranium Dioxide Studies	153
Magnesium Uranate and Magnesium Diuranate Studies	153
Slurry Circulators and Boilers	153
14. SLURRY PUMPING STUDIES	155
Heat transfer and apparent viscosity of $UO_3$ slurries	155
$UO_3$ abrasion tests	156
Particle-size reduction of circulated slurry	159
Particle-size change in a circulated slurry	159
Temperature cycle loop	160
Part III. LONG RANGE STUDIES	
15. PLUTONIUM CHEMISTRY AND FISSION PRODUCT SOLUBILITIES	165
Plutonium Chemistry in Aqueous Uranyl Sulfate at 100 to 250°C	165
Measurement of the Solubility of Yttrium Sulfate in Aqueous Uranyl Sulfate Solutions from 200 to 300°C	165
Solubility of Fission Product Sulfates	166





	PAGE NO.
16. CHEMICAL PROCESSING	171
Frequency of chemical processing for an aqueous homogeneous plutonium producer	171
Heavy-water recovery	173
Extraction of plutonium and nitric acid from solutions con- taining uranyl sulfate	173
Plutonium chemistry in uranyl sulfate solutions	178
Fission product calculations	180
Alternate processing schemes	182
APPENDIX	
NATURE OF LIQUID FLOW WITHIN A SPHERICAL CONTAINER	187
Introduction	187
Experimental program and facilities	187
Pressure-drop measurement in glass spheres	188
Literature survey and theoretical considerations	190
Program for September 1 to December 1, 1951	191



[REDACTED]

## LIST OF TABLES

TABLE NO.	TITLE	PAGE NO.
3.1	Analyses of $UO_2SO_4$ Solutions Heated in Type 347 Passivated Steel Bomb at 250°C	24
3.2	Analyses of $UO_2SO_4$ Solutions Containing KCl Heated in a Type 347 Passivated Steel Bomb at 250°C	24
3.3	Analyses of a $UO_2SO_4$ Solution Containing KCl Heated 16 hr in a Type 347 Passivated Steel Bomb at 250°C in the Absence of Oxygen	25
3.4	Chemical Analyses of Uranyl Sulfate Solutions	29
3.5	Corrosion Rates of Nitric Acid --- Pretreated Type 347 Stainless Steel	29
3.6	Chemical Analyses of Nitric Acid --- Pretreatment Solution After Use at 250°C	30
3.7	Chemical Analyses of Nitric Acid --- Pretreatment Solution After Use at 250°C	31
3.8	Chemical Analyses of Uranyl Sulfate Solutions in Run S197	32
3.9	Chemical Analyses of Uranyl Sulfate Solutions in Run S198	34
3.10	Chemical Analyses of Uranyl Sulfate Solutions from Run S203	36
3.11	Corrosion of SAE 1030 Carbon Steel Uncoupled and Coupled with Type 347 Stainless Steel in 0.005 M Hydrogen Peroxide at 200°C	38
3.12	Effect of Trisodium Phosphate Concentration on Corrosion Behavior of Uncoupled SAE 1030 Carbon Steel in 0.005 M Hydrogen Peroxide at 200°C	40
3.13	Effect of Trisodium Phosphate on the Corrosion Behavior of SAE 1030 Carbon Steel Coupled to Type 347 Stainless Steel in 0.005 M Hydrogen Peroxide at 200°C	41
4.1	In-Pile Radiation Experiments with HRE Constituents	52
4.2	Effect of Oxygen on Stability of HRE System	53
4.3	G Values for HRE Reflector Solutions	54
6.1	Two-Stage Catalytic Recombination 0.3% Pt on $Al_2O_3$	68
6.2	Conversion of Undiluted Electrolytic Gas in Copper Tube	69
6.3	Summary of Pressurizer Test Data	70

TABLE NO.	TITLE	PAGE NO.
6.4	Effect of Variables on Recombination in the Burner Chamber and Follow-up Recombiner at Low Gas Flow Rates	73
6.5	Summary of Results of Pilot Plant Runs with Gas Flow Rates of 16, 19, and 28 cfm	74
7.1	Composition of Glass Samples	81
8.1	Values of Macroscopic Two-Group Constants	85
8.2	Microscopic Capture Cross-Sections	86
8.3	Concentrations Required for Criticality Under Various Conditions	86
8.4	Calculated Values of Velocity and Time of Passage Through Steam Generator Tubes	111
8.5	Rate of Diluent Addition to Keep $2H_2 + O_2$ Above Reflector at Nonexplosive Concentration (15%) for a Reflector Pressure of 1000 psi and Reactor Power of 1000 kw	112
10.1	Solubility of Uranium Trioxide in Orthophosphoric Acid Solutions at $250^\circ C$	120
10.2	Refractive Indices and Densities of Aqueous Uranyl Sulfate at $25.0 \pm 0.2^\circ C$	124
11.1	Corrosion of Rem-Cru Titanium in $0.17 M UO_2SO_4$ at $250^\circ C$	129
11.2	Corrosion of Welded Titanium Tubing in $0.17 M UO_2SO_4$ at $250^\circ C$	130
11.3	Corrosion of Welded Titanium Sheet in $0.17 M UO_2SO_4$ at $250^\circ C$	131
11.4	Corrosion of Annealed Titanium — Type 347 Stainless Steel Couples in $0.17 M UO_2SO_4$ at $100^\circ C$	131
11.5	Corrosion of Sintered Titanium in $0.17 M UO_2SO_4$ at $250^\circ C$	132
11.6	Corrosion of BuMines Resistance-Melted Zirconium-Tin Alloys in $0.17 M UO_2SO_4$ at $250^\circ C$	133
11.7	Corrosion of Induction-Melted Zirconium Containing 5% Tin in $0.17 M$ Uranyl Sulfate Solution at $250^\circ C$	134
11.8	Corrosion of Arc-Melted Crystal Bar Zirconium Containing 5% Tin in $0.17 M UO_2SO_4$ at $250^\circ C$	135
11.9	Corrosion of Extruded Zirconium Tubing Containing 5% Tin in $0.17 M$ Uranyl Sulfate at $250^\circ C$	135
11.10	Solution Stability Data for $0.13 M UO_2F_2$ Exposed at $150^\circ C$ in Untreated Type 347 Stainless Steel Bombs	136

TABLE NO.	TITLE	PAGE NO.
11.11	Solution Stability Data for 0.13 M $\text{UO}_2\text{F}_2$ Exposed in Untreated Type 347 Stainless Steel Bombs	137
11.12	Solution Stability Data for 1.26 M $\text{UO}_2\text{F}_2$ Exposed at 150°C in $\text{HNO}_3$ -Pretreated Type 347 Stainless Steel Bombs	139
11.13	Solution Stability Data for 1.26 M $\text{UO}_2\text{F}_2$ Exposed at 150°C in $\text{CrO}_3$ -Pretreated Type 347 Stainless Steel Bombs	140
11.14	Solution Stability Data for 1.26 M $\text{UO}_2\text{F}_2$ Exposed at 250°C in $\text{HNO}_3$ -Pretreated Type 347 Stainless Steel Bombs	140
11.15	Solution Stability Data for 1.26 M $\text{UO}_2\text{F}_2$ Exposed at 250°C in $\text{CrO}_3$ -Pretreated Type 347 Stainless Steel Bombs	141
11.16	Corrosion Data for $\text{CrO}_3$ -Pretreated Type 347 Stainless Steels Exposed to 1.26 M Uranyl Fluoride at 250°C	142
12.1	Possible HRP Fuel Solutions	144
12.2	Survey of the Stability of HRP Fuel-Metal Combinations	145
12.3	Hydrolysis of Iron, Chromium, and Nickel Salts in Uranyl Sulfate Solution	147
12.4	Results of Hydrogen Embrittlement Tests	149
12.5	Out-of-Pile Bomb Experiments with High Concentrations of Uranyl Sulfate	150
15.1	Solubility of $\text{Ce}_2(\text{SO}_4)_3$ in Water	167
15.2	Solubility of $\text{Ce}_2(\text{SO}_4)_3$ in $\text{UO}_2\text{SO}_4$ Solution	168
15.3	Solubility of $\text{La}_2(\text{SO}_4)_3$ in Water	169
15.4	Solubility of $\text{BaSO}_4$ in $\text{UO}_2\text{SO}_4$ Solution	170
16.1	Effect of $\text{HNO}_3$ Concentration on Extraction of Pu(IV) and $\text{HNO}_3$ by 30% TBP	174
16.2	Effect of $\text{HNO}_3$ Concentration on Extraction of Pu(IV) and $\text{HNO}_3$ by 30% TBP from 0.5 N $\text{H}_2\text{SO}_4$	174
16.3	Effect of $\text{HNO}_3$ Concentration on Extraction of Pu(IV) and $\text{HNO}_3$ by 30% TBP	175
16.4	Effect of TBP Concentration on Extraction of Pu(IV) and $\text{HNO}_3$ from $\text{HNO}_3$ Solutions	175
16.5	Effect of TBP Concentration on Extraction of Pu(IV) and $\text{HNO}_3$ from $\text{HNO}_3$ Solutions	175

TABLE NO.	TITLE	PAGE NO.
16.6	Effect of Sodium Nitrate Concentration on Extraction of Pu(IV) and HNO <sub>3</sub> by 30% TBP from HNO <sub>3</sub> Solutions	175
16.7	Effect of TBP Concentration on Extraction of Pu(IV) and HNO <sub>3</sub> from 2 M NaNO <sub>3</sub> Solutions of HNO <sub>3</sub>	176
16.8	Comparison of Observed and Calculated Pu(IV) Distribution Coefficient	176
16.9	Effect of HNO <sub>3</sub> Concentration on Extraction of Pu(IV) and HNO <sub>3</sub> by 30% TBP at Constant Ionic Strength *	177
16.10	Values of the Thermodynamic Equilibrium Constant at 25°C for the Reaction $\text{H}^+ + \text{NO}_3^- + \text{TBP} \rightleftharpoons \text{TBP} \cdot \text{HNO}_3$	177
16.11	Plutonium Solubility vs. Uranium Concentration at 250°C	178
16.12	Plutonium Solubility vs. H <sub>2</sub> SO <sub>4</sub> Concentration at 250°C	179
16.13	Plutonium Solubility vs. H <sub>2</sub> SO <sub>4</sub> Concentration at 150°C	179
16.14	Total Radiation Intensities Under Varying Operating Conditions	180
16.15	Radiation Intensities from Nongaseous Fission Products	180
16.16	Radiation Intensities of Neptunium Under Varying Conditions	181
16.17	Radiation Intensities of Uranium Under Varying Conditions	181
16.18	Decontamination Factors Required to Reduce Beta Activity of Uranium to 150 disintegrations/min/mg U Under Conditions Given in Table 16.17	182
16.19	Fission Product Build-up	182
APPENDIX		
1	Dimensions of Glass Spheres Used in Pressure-Drop Experiments	188

**LIST OF FIGURES**

FIGURE NO.	TITLE	PAGE NO.
1.1	D <sub>2</sub> O Cell Installations.	10
1.2	Reflector Pressure Vessel.	11
1.3	Shield and Components.	12
1.4	Control Room.	13
2.1	HRE Simplified Flow Diagram at 1000-kw Operation.	16
2.2	Sampling Equipment Arrangement.	17
3.1	Effect of Anodic Treatment of Type 347 Stainless Steel at Various Current Densities During Passivation in 1% HNO <sub>3</sub> .	21
3.2	Effect of Anodic Treatment of Type 347 Stainless Steel at Various Current Densities During Passivation in 2% CrO <sub>3</sub> Solution.	22
5.1	Flow Diagram of the HRE Mock-up.	62
5.2	Liquid Flow Rate vs. Temperature Entering Letdown Heat Exchanger.	63
6.1	Recombination of Undiluted Electrolytic Gas in Metal Tubes.	69
7.1	Pipeline Model Densitrol Assembly with Modified 600-lb Ring Joint Flanges.	78
7.2	Irradiated Glass Sample No. 1-M.	82
7.3	Irradiated Glass Sample No. 2-M	82
7.4	Irradiated Glass Sample No. 3-M.	83
7.5	Irradiated Glass Sample No. 4-M.	83
8.1	Effective Multiplication Constant of HRE with Light-Water Reflector, 93.4% Enriched Uranium	86
8.2	Power as a Function of Time Following a Step in <i>k</i> .	103
8.3	Temperature as a Function of Time Following a Step in <i>k</i> .	103
8.4	Number of Delayed Neutron Emitters Present as a Function of Time Following a Step in <i>k</i> .	103
8.5	Paths in a Phase Plane Given by	

$$\frac{dn}{dz} = \frac{u(z - u)}{z^2 - uz - \alpha z^3 + \alpha z^2}, \quad \alpha = 5. \quad 106$$



FIGURE NO.	TITLE	PAGE NO.
8.6	Fractional Energy Loss Per Cycle of Pressurizer Oscillation as a Function of Amplitude.	108
8.7	Heat Transfer Coefficients for the HRE Boiler.	110
8.8	Heat Required to Change the Steam Temperature in the Boiler by Unit Amount with No Efflux of Steam.	110
9.1	Flow Sheet for Pressurizer Control.	113
9.2	Pressurizer Liquid-Level Float.	114
10.1	The Solubility of Uranium Trioxide in Phosphoric Acid at 250°C.	121
10.2	pH of Uranyl Sulfate Solutions as a Function of Temperature and Concentration.	125
10.3	Density of UO <sub>2</sub> SO <sub>4</sub> Solutions at 25°C.	126
10.4	Refractive Index of SO <sub>4</sub> Solutions at 25°C.	127
14.1	Abrasion Testing Apparatus.	157
14.2	Abrasion of Stainless Steel Surfaces.	158
14.3	UO <sub>3</sub> Particle Breakdown.	160
14.4	Particle Distribution in Sphere.	160
14.5	Slurry Thermal Loop.	161
15.1	Solubility of Ce <sub>2</sub> (SO <sub>4</sub> ) <sub>3</sub> in H <sub>2</sub> O from 100 to 350°C.	167
15.2	Solubility of Ce <sub>2</sub> (SO <sub>4</sub> ) <sub>3</sub> in 0.126 M UO <sub>2</sub> SO <sub>4</sub> Solution from 150 to 340°C.	168
15.3	Solubility of La <sub>2</sub> (SO <sub>4</sub> ) <sub>3</sub> in H <sub>2</sub> O from 100 to 350°C.	169
15.4	Solubility of BaSO <sub>4</sub> in 0.126 M UO <sub>2</sub> SO <sub>4</sub> Solution.	170
16.1	Chemical Processing by Purex for Batch Operation of Reactor.	172
16.2	Chemical Processing Period for a Homogeneous Plutonium Producer as a Function of Flux To Give 2% Pu <sup>240</sup>	173
16.3	Solubility of Plutonium Sulfate in H <sub>2</sub> SO <sub>4</sub> — 1 M UO <sub>2</sub> SO <sub>4</sub> .	179
16.4	Dowex-50 Cation and Dowex-A-1 Anion Resin Capacity Loss from Irradiation.	183

APPENDIX

1	Experimental Equipment for Pressure Loss Studies.	189
2	Pressure Losses in Spherical Containers.	190



1998

1998



## SUMMARY

### Part I

#### HOMOGENEOUS REACTOR EXPERIMENT

The over-all construction for the HRE is approximately 60% complete as of August 15, 1951. The final revisions of HRE designs are nearing completion, and significant research and development progress has been made as summarized below.

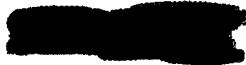
**Corrosion. Scouting Studies.** Anodic and cathodic treatments of type 347 stainless steel during nitric and chromic acid "passivation" have been investigated in an effort to improve the corrosion resistance of the film produced. The results were negative in that the films produced without anodic or cathodic treatment were better than those produced with the treatment. The criterion used was the time required for film breakdown when exposed to a 100°C solution containing 30 g of uranium per liter which was 0.2 M in KCl. An interesting observation made in the course of these studies was that film resistance was improved by a 48-hr exposure under these conditions.

An investigation of the relation between oxygen concentration and solution stability and corrosion in the uranyl sulfate solution-type 347 stainless steel system has been begun. Sufficient data for valid evaluation have not been obtained thus far, primarily because of questions introduced by impurities in the uranyl sulfate used.

**Static Tests.** Some studies of the structure of the pretreatment film

obtained on type 347 stainless steel and factors affecting it were begun. When a specimen is given the nitric acid pretreatment in a newly machined bomb, at the end of a 24-hr exposure it is covered with a lustrous film about 1  $\mu$  thick. In the case of pretreatment in an old, chemically cleaned bomb which had previously been exposed to a number of pretreatments and also to  $\text{UO}_2\text{SO}_4$  solution, the resultant film is dull gray in color and about 3  $\mu$  in thickness. Microscopic examination of the films indicates that  $\alpha\text{-Fe}_2\text{O}_3$  is the basic constituent with a possibility of  $\text{Cr}_2\text{O}_3$  also being present. A two-layer effect was also observed, the substrate layer appearing almost structureless while the outer layer contained fairly large and uniform crystallites. This outer layer had sloughed off in numerous areas, suggesting that the protection is actually related to the substrate layer. Other investigations into the effects of etching specimens before pretreatment indicated that samples which had been etched tended to pit during pretreatment and that the film did not cover these pits. The films on the etched samples also seemed to be slightly more ferromagnetic than those from the unetched specimens.

The corrosion resistance of 1% nitric acid-pretreated type 347 stainless steel appears to be a straight line function of uranyl sulfate concentration in the range 0.17 to 0.86 M. Indicated corrosion rates for these respective concentrations were 0.01 and 0.06 mpy, based on 11-week exposures.



## HRP QUARTERLY PROGRESS REPORT

It appears that the minimum trisodium phosphate concentration necessary to reduce corrosion attack (to less than 1 mpy) by water on SAE 1030 carbon steel, coupled and uncoupled with type 347 stainless steel, is in the range 300 to 400 ppm.

*Dynamic Tests.* The necessity of the presence of dissolved oxygen in the uranyl sulfate solution to assure solution stability in a type 347 stainless steel system at 250°C appears quite well established. Preliminary indications are that the nitric acid pretreatment has no effect on corrosion rate, as estimated from nickel concentration build-up in the solution during operation, provided oxygen is present. It appears, however, that an oxygen pretreatment, in effect, is required since it has been observed that higher oxygen concentrations are required to stabilize the solution in a system which has had no previous exposure than in a system which has been previously exposed to oxygenated uranyl sulfate for some period of time. The function of the oxygen in limiting corrosion has not yet been determined; one possible mechanism might involve the prevention of the existence of iron(II) in the solution.

Substantially accelerated corrosion has been observed in high flow areas. Whether this is caused by film failure or inability of the film to form under high flow conditions is not clearly established.

*Radiation Stability.* Five bombs irradiated for 95 days in the ORNL graphite reactor disclosed no deleterious effects in comparison with shorter term irradiations. The solution appears stable, and the corrosion rate appears no greater than in

the case of either short irradiation experiments or out-of-pile corrosion tests. The percent of uranium recovered as soluble uranium was not as great (average of five, 78%) in the 95-day exposures as in the 5-day exposures (average of three, 90%).

A series of out-of-pile tests gave no evidence that oxygen pretreatment added significantly to the protection afforded by the use of oxygen during the test run. This observation is not in conflict with the statement appearing elsewhere in this report (see section on corrosion) that oxygen pretreatment reduces the required oxygen partial pressure to maintain stability. In each test of this series the oxygen partial pressure was greater than the minimum requirement for stability.

A second experiment was conducted in the LITR at power levels up to 1 mw. Mechanical difficulties terminated the experiment and dictated the necessity of redesigning the apparatus.

The gas yield for the reflector has been measured using light water containing small amounts of corrosion inhibitors. At the full flux of hole 12 in the ORNL graphite reactor solutions of 250 to 500 ppm of trisodium phosphate gave  $0.75 \pm .05$  hydrogen molecules per 100 ev with steady-state pressures of less than 100 psi at 100 to 140°C.

*Engineering Component Studies. Mechanical Aspects of Soup Test Loops and Pumps.* The Model 100A Westinghouse pump modified with Stellite 98M2 journals, improved thrust pads, and tantalum seal rings are expected to give a minimum of 3000 to 4000 hr of trouble-free operation, providing

[REDACTED]

FOR PERIOD ENDING AUGUST 15, 1951

the seal rings continue to operate satisfactorily. The metal bearings appear to be just as satisfactory, but less operating experience has been accumulated.

A double-discharge pump showed a radial load  $1/2$  to  $1/3$  that of a single-discharge pump. The double discharge induced undesirable vibrations in the pump.

Soup recirculating test loops have shown that:

1. By using a bypass of 0.5 gph from the top of the pressurizer to the rear of the pump rotor cavity, solution stability can be maintained with 50 psi (measured cold) of oxygen pressure in the pressurizer.
2. Without this bypass, 300 to 500 psi oxygen pressure is required in the pressurizer.
3. An oxygen concentration as low as 20 ppm has maintained solution stability.
4. Acid etching and passivation is not required; however, loops must be clean and free of grease.

*Operation of the HRE Mock-Up.* The system for removing gas from the HRE core operates satisfactorily with the following limitations:

1. The liquid flow from the Pulsafeeder pump must be kept greater than 0.8 gpm. Since the normal output is 1.5 to 1.6 gpm, the condition is met except in the case of gas binding, which is still under investigation.

2. The level control system must be maintained in proper adjustment.

The performance of the soup pressurizer is rather sluggish, as the response to system pressure changes is slow.

The HRE soup off-gas recombiner system operates satisfactorily at steady flows between 1 and 15 scfm. However, when the flow rate is rapidly reduced to 1 scfm, the gas flow to the burner is stopped long enough to cause a flashback from the burner to the condenser, where the flashback is extinguished.

*Mixing in the HRE Core.* Mixing characteristics of the HRE core have been studied. Should stagnant regions limit operating power and temperature, core baffles can distribute the flow properly. The arrangement and construction of optimum baffles are specified.

**Recombination of Hydrogen and Oxygen.** Pilot plant testing of the HRE recombiner system has been continued with a series of runs designed to determine the efficiency of recombination and the temperature distribution over the catalyst bed with and without steam in the inlet stream. Conclusions were that the full flow of cooling water to the burner chamber shell should be maintained at all gas flow rates and that about 0.5 cfm of steam should be added on the inlet side of the catalytic recombiner.

Three pilot plant tests at high flow rates (16, 19, and 28 cfm, respectively) gave satisfactory performance although the vapor temperature in the off-gas line was 774°C at 28 cfm.

## HRP QUARTERLY PROGRESS REPORT

An experimental two-stage catalytic recombiner has been operated giving better than 99.99% over-all conversion.

A study of the efficiency of metal tubes indicates that large-scale catalytic recombination on copper may be feasible. Approximately 15 sq ft of copper surface is capable of converting 1 cfm of electrolytic gas at an operating temperature of 440°C. A  $V_2O_5$ - $Al_2O_3$  catalyst gave poor results.

The violence of implemented explosions in a typical loop test pressurizer unit emphasize the hazard involved in high-pressure loop tests employing hydrogen-oxygen mixtures.

Two experiments with the high-pressure catalytic recombiner for the reflector system indicated satisfactory performance.

The efficiency of a trap packed with stainless steel turnings for the removal of iodine from the gas stream has been demonstrated.

**Chemical Control.** The determination of density using the electromagnetic densitometer appears to be feasible on the basis of laboratory testing. The first of three Princo Densitrol Instruments has been received and most of the effort is now being directed towards the completion of the testing of this unit.

Development work on Q-coil ceramics, glazes, and gasketing is continuing.

Optical spectra of slow-neutron absorbing optical glasses have been measured before and after exposures in the ORNL graphite pile.

**Physics.** Some further criticality calculations have been performed, mainly aimed at determining the feasibility of a light-water reflector. Light water is less favorable on several points than heavy water, but there are no insurmountable difficulties.

A stability analysis (linearized) has been made for the current design (8/15/51). An unexpected instability of the pressurizer system appeared, whereby the presence of delayed neutrons induce oscillations of the liquid level in the pressurizer. Steps are being taken to correct this difficulty.

Some general work has been done on the mechanism of damping of power surges by the delayed neutrons and the calculations of power surges induced by reactivity changes. An attempt has been made on this point to include the effect of the inertia of the fluid in the pressurizer pipe. No additional effects (except the previously noted instability) of practical importance are found, and, aside from some easily met requirements on the pressurizer design, previous impressions of stability against large changes in reactivity are confirmed.

**Controls.** Minor changes have been made in the control scheme, and progress is being made in the development of monitoring devices.

### Part II

#### ALTERNATE SYSTEMS

**Solution Chemistry.** The solubility of  $UO_3$  in orthophosphoric acid solutions at 250°C has been measured as

[REDACTED]

FOR PERIOD ENDING AUGUST 15, 1951

a function of phosphoric acid concentration. From the solubility data and capture cross-sections it appears that such solutions would be feasible for an enriched reactor but marginal for a natural uranium machine.

A survey of the uranyl carbonate-carbon dioxide-water system indicates insufficient solubility for use at 250°C.

Development and construction of apparatus for the study of vapor pressures over a wide temperature range has been completed, and the measurements at high temperatures on uranyl sulfate solutions are under way.

Work is also under way on the electrical conductivity of solutions over a wide temperature range.

**Corrosion.** Static tests on titanium (not pretreated) in 0.17 M  $\text{UO}_2\text{SO}_4$  at 250°C contained in 1%  $\text{HNO}_3$ -pretreated type 347 stainless steel bombs continue to give uniformly good results.

Static tests on zirconium (with 5% tin addition) continue to show improved corrosion resistance over regular Bureau of Mines zirconium on exposure to 0.17 M  $\text{UO}_2\text{SO}_4$  solution in 1%  $\text{HNO}_3$ -pretreated type 347 stainless steel bombs.

Static tests with  $\text{UO}_2\text{F}_2$  solutions in stainless steel bombs still give erratic results with no particular pattern discernible thus far. A number of successful tests have been run, but a high percentage of failures does not allow any conclusions to be drawn.

**Radiation Damage.** Studies of the gas production from uranyl sulfate, uranyl nitrate, and uranyl fluoride solutions are under way. An acid gas formed in the irradiation of uranyl sulfate solutions has been shown to be  $\text{CO}_2$  arising from an impurity in the salt. Irradiations with cobalt gamma source failed to yield any measurable  $\text{SO}_2$  from 0.4 M  $\text{H}_2\text{SO}_4$  or 1.24 M  $\text{UO}_2\text{SO}_4$ .

The nitrate ion in uranyl nitrate solutions appears to decompose yielding nitrogen gas.

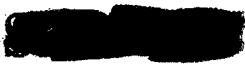
A survey of the corrosion of titanium and zirconium in solutions of uranyl nitrate, uranyl sulfate, and uranyl fluoride indicated excellent behavior of the titanium toward the sulfate. In each of the other combinations some deleterious effects were noted.

The kinetics of the noncatalytic reduction of uranyl ion by hydrogen gas and of the oxidation of  $\text{UO}_2$  in dilute acid solutions by oxygen gas are under study. Such knowledge may be of use in understanding and explaining the recombination reaction encountered in radiation tests.

Type 347 stainless steel tubes which had been used in irradiation experiments show no evidence of hydrogen embrittlement.

**Slurry Fuel Studies.** Considerable effort has been devoted to the preliminary steps of setting up an expanded program on slurry preparation and study.

A slurry of  $\text{UO}_3$  containing 300 g of uranium per liter stabilized with



bentonite was found unstable, settling very rapidly, after being heated for 24 hr at 250°C. A uranium dioxide slurry, upon being boiled under an atmosphere of oxygen, gave indications that the uranium is oxidized. Magnesium uranate and magnesium diuranate slurries were prepared, but both were found unstable on being heated at 250°C.

A slurry circulating loop is under construction in which the effect of pumping on particle size will be studied and observations will be made on erosion, power requirements, and heat transfer.

### Part III

#### LONG RANGE STUDIES

**Fission Product Solubilities.** The solubilities of yttrium sulfate,

barium sulfate, and cerous sulfate, respectively, in uranyl sulfate solutions have been measured over the temperature range of approximately 100 to 350°C. The solubilities of cerous sulfate and lanthanum sulfate in water over the same temperature range have also been determined.

**Chemical Processing.** A chemical processing scheme for a uranyl sulfate-D<sub>2</sub>O homogeneous reactor is proposed, and a discussion of the factors involved is given. The scheme is designed to limit the Pu<sup>240</sup> content of 2% of the total plutonium in a reactor operating at 250°C and producing 2000 g of plutonium per day.

The solubility of plutonium in uranyl sulfate solutions has been measured and found to be very low. The implications of these results with reference to chemical processing are discussed.



**Part I**

**HOMOGENEOUS REACTOR EXPERIMENT**



100

100



## 1. CONSTRUCTION OF HRE

S. E. Beall, Leader  
D. T. Jones      J. W. Hill  
J. J. Hairston

Construction work on the Homogeneous Reactor Experiment is approximately 60% complete as of August 15, 1951. The status of various phases of the reactor is given below.

**D<sub>2</sub>O System.** The D<sub>2</sub>O system is complete except for the installation of three equipment items: (1) the high-pressure gas recombiner, (2) the low-pressure gas recombiner, and (3) the Pulsafeeder pumps. Fabrication of the recombiners should be accomplished by September 15, and delivery of the Pulsafeeder pumps is expected during September. The low-pressure piping has been pressure tested at 500 psi; the high-pressure system will be tested at 2000 psi before September 1.

A Triplex piston pump is being installed temporarily in lieu of Pulsafeeder pumps so that the entire system can be operated for component testing. This testing involves measurements of pressure drops, capacities, and flow rates in various equipment pieces and calibration of instruments. Such experimental work in the heavy-water system is expected to continue through September.

Figures 1.1 and 1.2 show the D<sub>2</sub>O cell and the reflector pressure vessel.

**Fuel System.** Effort on the soup system has been devoted entirely to fabrication of components. Compo-

nents completed include condensate weight tanks, inner dump tanks, outer dump tanks, soup condensers, and cold traps. Remaining to be fabricated are the letdown heat exchanger, flame and catalytic recombiners, charcoal adsorbers, soup pressurizer, and reactor sphere. Although the erection of piping in the soup system has just begun, completion is expected before November 1.

**Steam System.** The steam system has not been started because delivery of the turbine generator is not expected until November. However, the construction schedule calls for completion of piping fabrication by that time, and start-up of the reactor should not be delayed if the November delivery date is met.

**Shield.** One wall of the shield structure has been completed and another has been begun. Construction of the shield necessarily follows the installation of cell equipment and therefore will probably not be completed before December 1. Figure 1.3 shows the shielding status as of August 1.

**Instrumentation and Control.** This phase of the job is 60 to 75% complete. Wiring of the console and control relays has been finished, as has that portion of the instrumentation associated with the D<sub>2</sub>O system. Figure 1.4 is a recent photograph of the control room.

[REDACTED]

HRP QUARTERLY PROGRESS REPORT

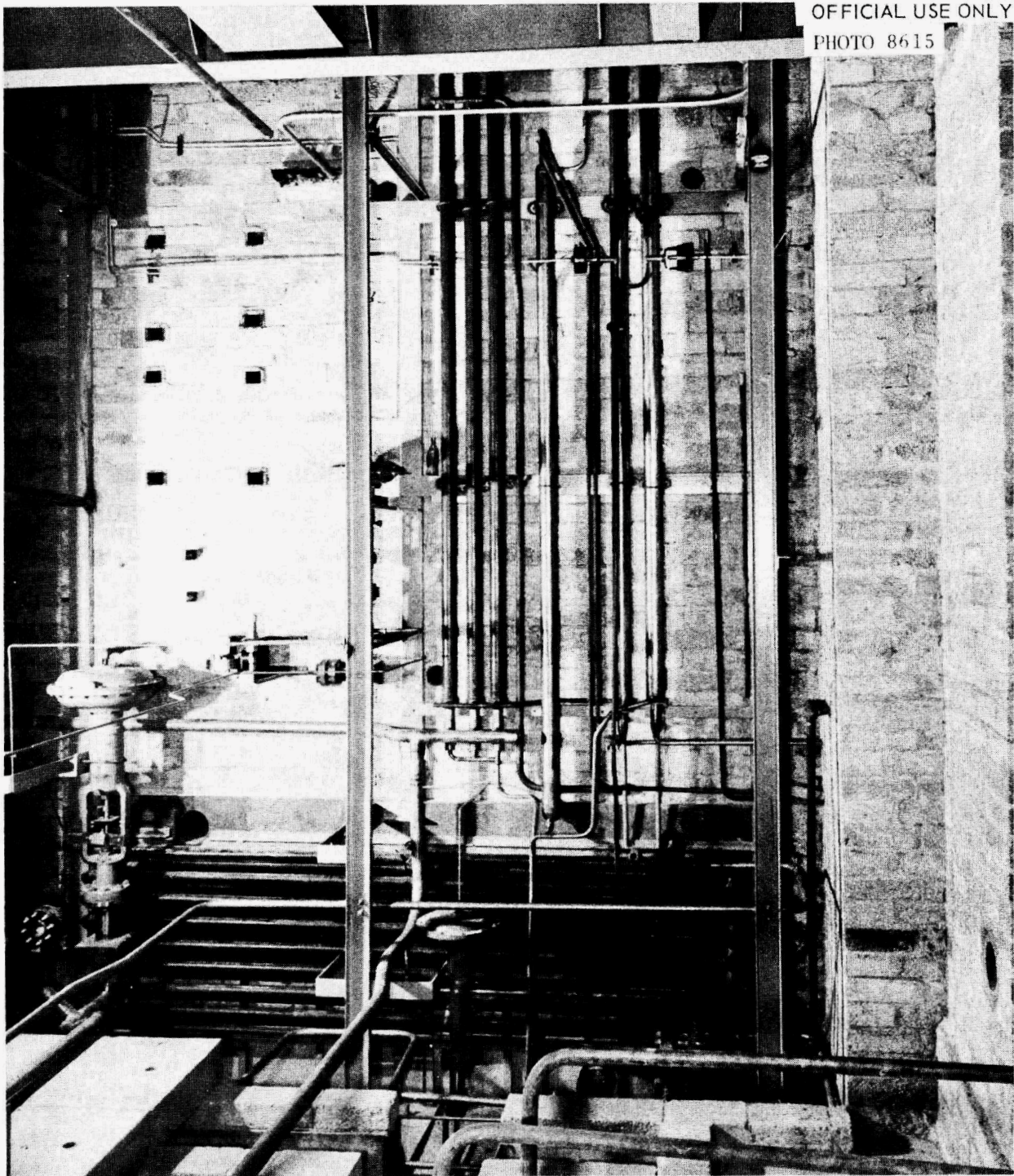


Fig. 1.1 - D<sub>2</sub>O Cell Installations.

[REDACTED]

FOR PERIOD ENDING AUGUST 15, 1951

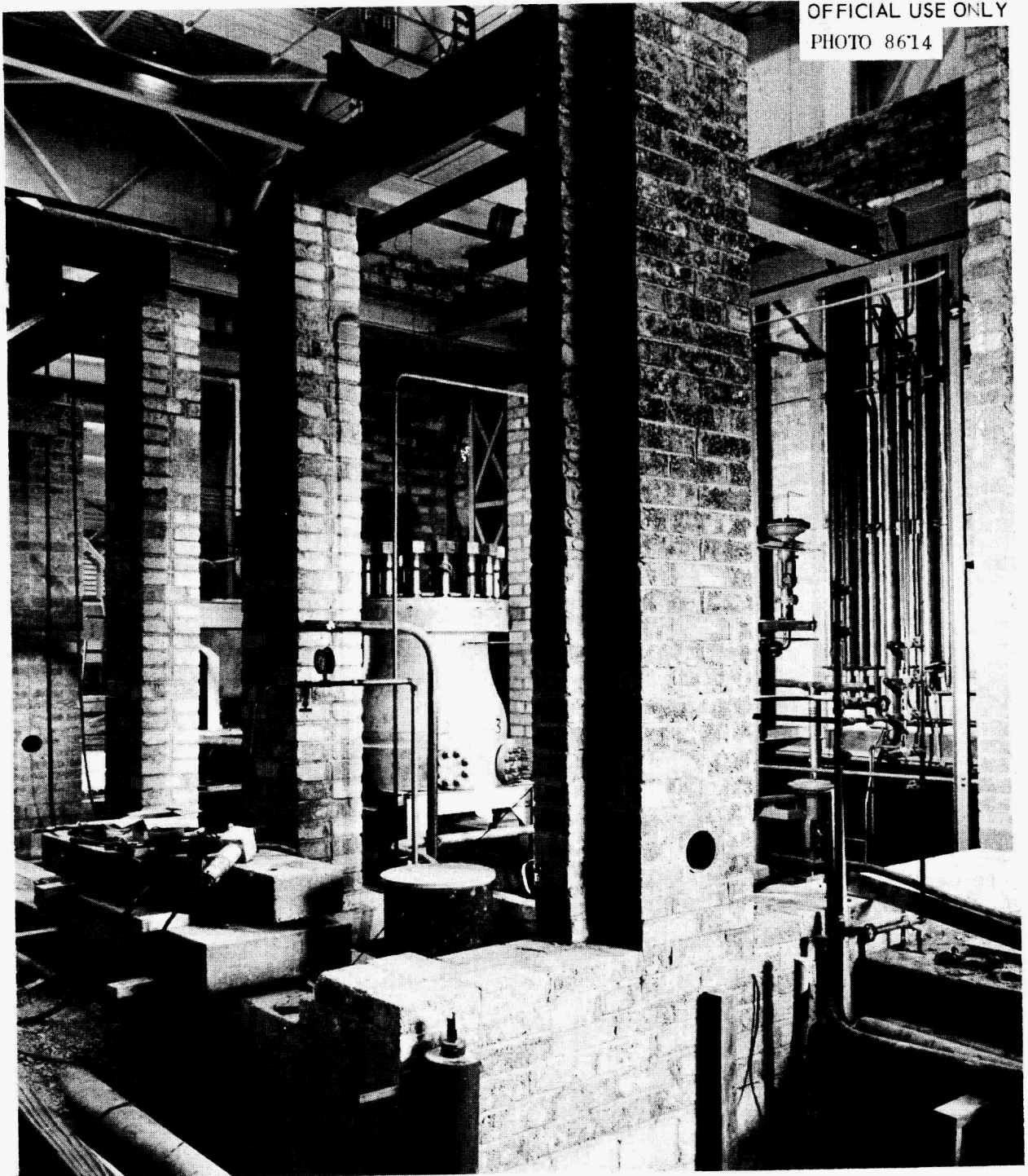
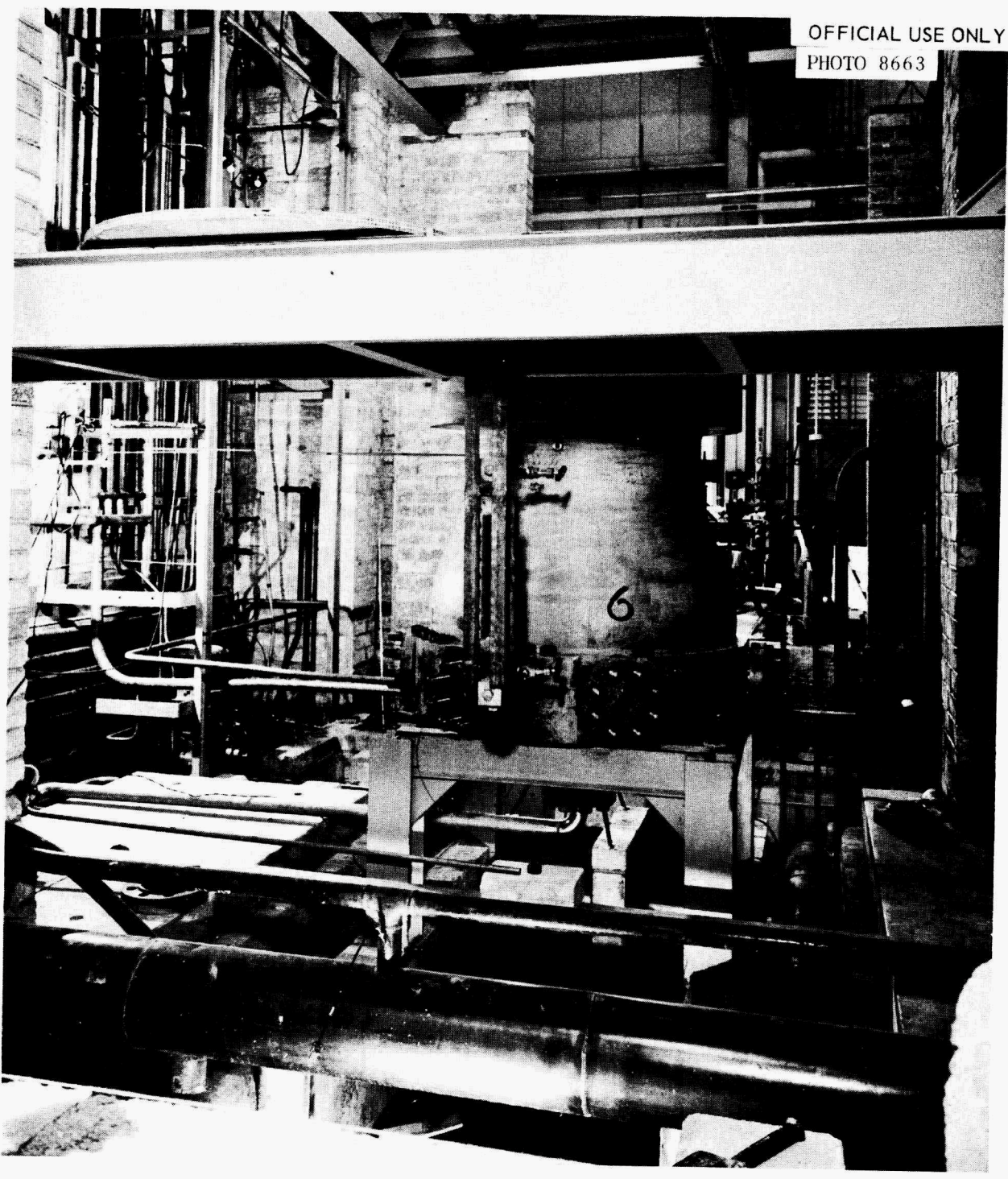


Fig. 1.2 - Reflector Pressure Vessel.

**HRP QUARTERLY PROGRESS REPORT**

[REDACTED]



**Fig. 1.3 - Shield and Components.**

[REDACTED]

FOR PERIOD ENDING AUGUST 15, 1951



Fig. 1.4 - Control Room.

#### WELDING AND INSPECTION OF WELDS IN THE FUEL SYSTEM

The necessity of high-quality welding in the fuel system, a portion of which operates at 1000 psig and 250°C, has led to extraordinary welding and inspection practices. All joints are made by the Heliarc method to rigid specifications which allow no defects such as incomplete or over

penetration, gas pockets, cracks, or oxidation of the metal. Special procedures have been set up to insure the proper qualification of the welding operators, and a full-time welding inspector is employed to see that the procedures are followed. In spite of the fact that the welders are highly skilled, roughly 50% of the joints must be repaired before the acceptance tests are passed. The

[REDACTED]

## HRP QUARTERLY PROGRESS REPORT

program of inspection is outlined below:

- I. Analysis of Welding Rod, Pipe, and Fittings
  - A. Welding rod - each package sampled for wet chemical analysis.
  - B. Pipe - each length sampled for spectrographic analysis.
  - C. Fittings - samples of each size fitting received in one shipment from a particular vendor submitted for spectrographic analysis.
- II. Inspection of Welding Process
  - A. Certified welding inspector observes preparation and welding of each joint.
- III. Nondestructive Testing of Finished Welds
  - A. Visual examination - boroscope and magnifying glass.
  - B. For minute surface imperfections - Dyckek penetrant applied; no cracks or pinholes allowed.
  - C. X-ray or  $\gamma$ -ray examination - welds may be rejected because of incomplete penetration, over penetration, cracks, pinholes, slag, or gas pockets; for the high-pressure fuel system any defect is cause for rejection.
- D. Hydraulic testing - system filled with water and pressure raised to double the normal operating pressure.
- E. Helium leak testing - system evacuated and probed for leaks with Westinghouse helium leak detector.
- IV. Quality Control Samples
  - A. Source of samples -
    1. Each welder to prepare quality sample after making each ten process welds.
    2. One joint per welder per week to be cut out of process line.
  - B. Destructive tests required -
    1. Tensile - strength not less than 95% of base metal.
    2. Free and root bends - no visible defects after bending through 180°.
    3. Metallographic examination - no cracks permissible; ferrite not to exceed 10%.
    4. Corrosion testing - boiling nitric acid according to A.S.T.M. specification; uranyl sulfate at 250°C.

A detailed description of the welding, inspecting, and testing procedures is given in an undocumented paper entitled *Welding and Inspection Techniques in the Fabrication of HRE Fuel System*. Copies are available for distribution to AEC installations upon request.

## 2. DESIGN PROGRESS

W. R. Gall, Leader

F. C. Zapp	R. L. Cauble
C. W. Day	A. F. Strauchman
C. L. Segaser	R. W. French
W. Terry	J. D. Maloney
R. B. Chapman	L. Cooper

T. H. Thomas

Design progress during this quarter includes completion of fuel cell and steam generation cell piping drawings and details of fuel dump tanks, evaporator, condensate tanks, low-pressure cooler, and Pulsafeeder pump installation drawings. Final designs of catalytic recombiners for the reflector and fuel systems are now complete.

**Flow Diagram.** Figure 2.1 shows a simplified flow diagram of the process for the HRE. The only changes of importance in the diagram during this quarter are the following:

1. A high-pressure catalytic recombiner has been added to the reflector gas system. A liquid jet in the circulating reflector stream will be used to aspirate approximately 0.3 cfm of gas from the reflector vessel through a chamber containing approximately 2 lb of platinized alumina. The gas will return to the vessel mixed with the liquid stream as shown.
2. Provision has been made to admit oxygen to the fuel system in accordance with recent corrosion research findings.
3. A cooler has been added to cool the fuel solution flowing from the dump tanks to the feed pump.

Its purpose is to prevent boiling of water and soup in the Pulsafeeder head during the suction stroke and to reduce the amount of gasses coming out of solution in the feed pump.

**Sampler.** Design layouts are nearing completion for a method of removing samples of fuel solution, and possibly gas, from the high-pressure circulating fuel system. The procedure planned for obtaining a sample is as follows:

1. A small high-pressure stream will be allowed to bypass through a 30-cc chamber until complete purge has been accomplished.
2. Valves will be closed, isolating the small volume in the chamber from the main system.
3. The chamber will be cooled to room temperature and vented to a pressure less than atmospheric.
4. By remote techniques the chamber will be opened, a 0.5-ml pipet will be inserted and filled, and the pipet will be placed in a shielded carrier for removal. The chamber will be closed immediately after the pipet is placed in the carrier.

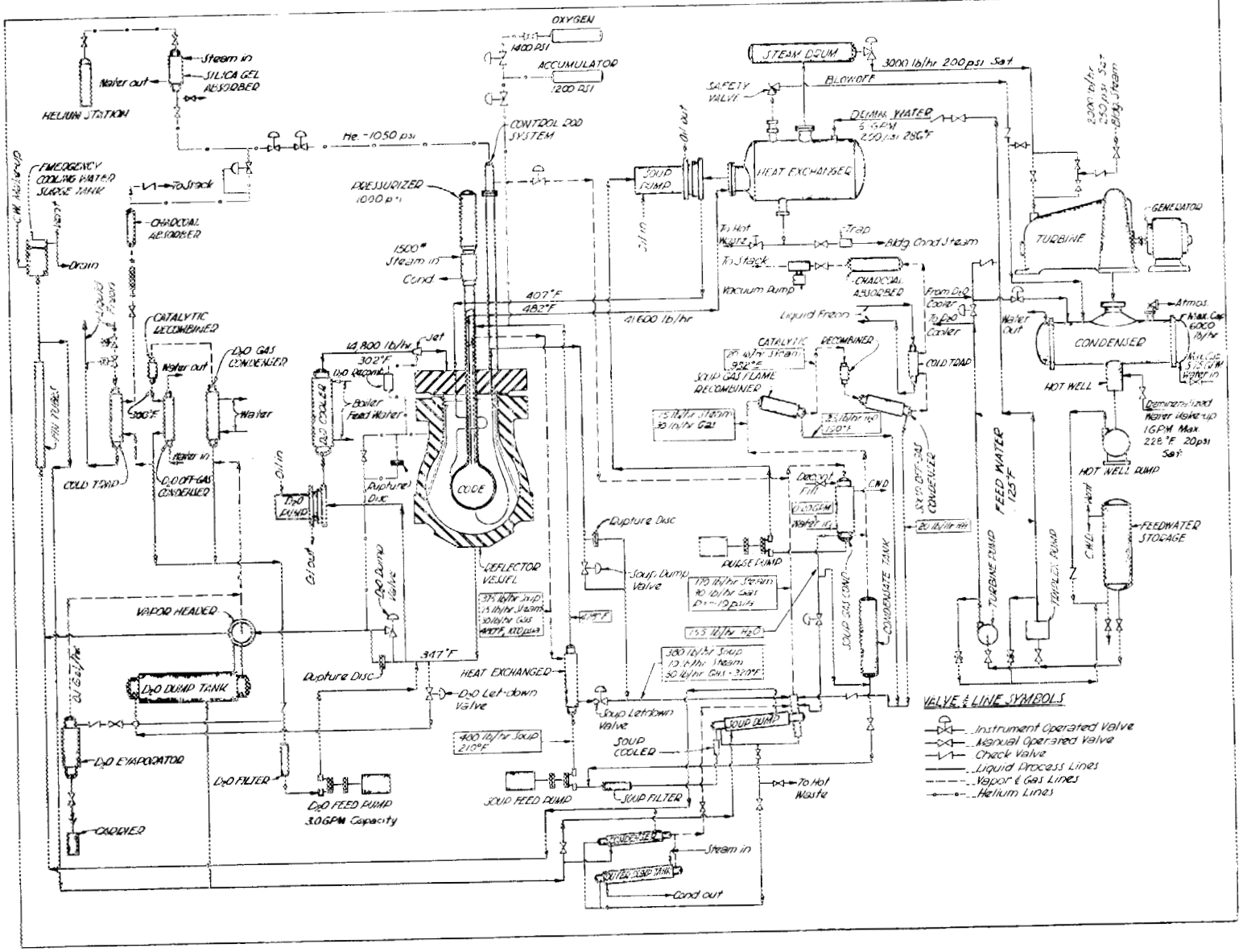


Fig. 2.1 - HRE Simplified Flow Diagram at 1000-kw Operation.

FOR PERIOD ENDING AUGUST 15, 1951

Access to the sampler will be from above, through the roof of the main heat-exchanger compartment. All handling of the pipet, carrier, and chamber cover will be done by remote handling tools permanently installed in a shield plug. Special double valves are being developed which are hydraulically operated from a remote location. If a valve leaks during the sampling process, leakage will be into a space between valves which is vented to the dump tanks. Figure 2.2 illustrates schematically the arrangement of equipment for the sampling process.

**Insulation.** Insulation of high-temperature and refrigeration equip-

ment and lines inside the reactor shield has been selected. In the fuel, reactor, and heat-exchanger compartments Foamglas as produced by Pittsburgh Corning Corporation will be used. This is a rigid cellular glass insulating material containing minute separate hermetically sealed cells, each filled with dead air. In the event of spills of radioactive materials on this insulation the amount absorbed will only be that in the cells at outer surfaces of the material which may be decontaminated by washing.

Equipment and lines in the reflector compartment and on outer surfaces of the shield will be insulated with 85% magnesia, except refrigeration equipment which will be covered with cork in these locations.

NOT CLASSIFIED  
DWG. 12989

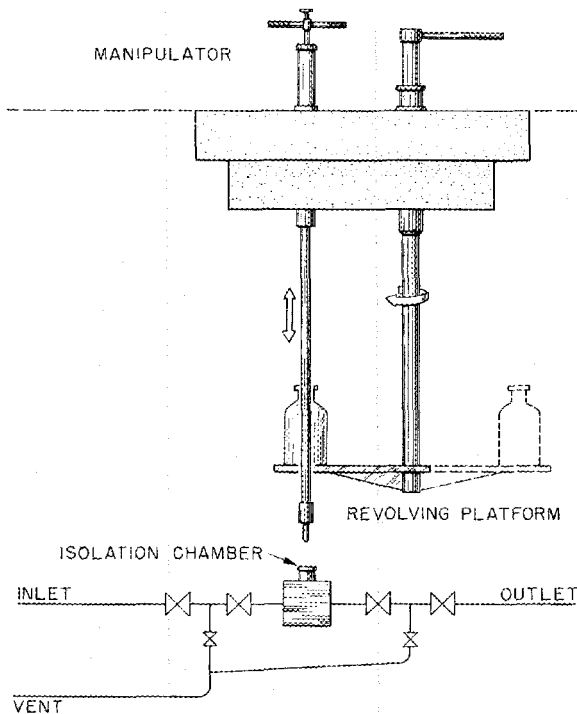


**Fig. 2.2 - Sampling Equipment Arrangement.**

**Pressure Drop in Soup Circulating System.** Calculations made on the soup circulating system indicate a total pressure drop which is below the available head of the soup circulating pump at an assumed flow rate of 100 gpm. The largest single pressure drop (~61% of the total) occurs in the soup heat exchanger. An experimental determination of the pressure drop in the heat exchanger was made with water at 70°F. When this value was corrected for the difference between this temperature and the operating temperature it agreed well with calculated values previously obtained.

Inasmuch as the total pressure drop in the system is less than the available head of the circulating pump at 100 gpm (assuming the experimental value of the pressure drop) it is likely that flows in excess of 100 gpm will be obtained.

## HRP QUARTERLY PROGRESS REPORT

**Removal of Heat from Core After Shutdown.** Calculations have been performed to determine the possibility of dissipating the heat generated in the core after shutdown if the soup remains in the core both with and without the soup pump or D<sub>2</sub>O pump in operation.

For long periods of shutdown during which it is desired to leave the soup in the core, the heat exchanger will be allowed to function and the steam generated will be bled off to the main condenser.

For shutdown periods which are less than 1.6 hr it is safe to utilize the heat capacity of the exchanger and the water which it contains to absorb the heat being generated in the soup. This requires soup circulation but allows the steam valve to be closed.

In the case of any shutdown which makes the soup circulation pump inoperative, the soup will be dumped and not be allowed to remain in the core. This requirement is a result of a study of the steady-state heat transfer through the core wall, D<sub>2</sub>O reflector vessel, and insulation. The value obtained was of the order of 1500 Btu/hr, which is 40 to 50 times smaller than the rate of heat generation. This indicates that the heat generated would be used to first heat the soup and then to vaporize it if the soup were left in the core with no circulation of the soup. The increase in pressure that would result from this vaporization was calculated and found to be prohibitive. Calculations indicated that 43 min after shutdown 10% of the soup would be vaporized and the pressure would be ~3000 psi in the core. The neces-

sary steps have been taken to insure that this situation can never occur.

**Pressure Drop in D<sub>2</sub>O Circulating System.** The calculated value of the pressure drop in the D<sub>2</sub>O circulating system is 57 psi at 30 gpm, which checks well with some experimental runs made on the system. The performance curve of the pump indicates ~22 gpm. This is somewhat lower than previous estimates, which were based on the assumption of a somewhat lower pressure drop in the D<sub>2</sub>O cooler. This flow rate is not at all critical, however, and a flow of 22 gpm is quite adequate. If, at any time, larger flow rates should be desired this can be easily accomplished by split flow in the D<sub>2</sub>O cooler or reduction of the D<sub>2</sub>O cooler size since its heat-transfer area is at least four times as large as the minimum required for the desired amount of cooling.

**Stress Analysis of Core Tank.** An estimate has been made of stresses induced in the shell of the core tank due to forces exerted by pipe connections to it when differential thermal expansion occurs. Without any reinforcement at pipe connections, a stress of 24,600 psi may be induced. It is planned to add reinforcement around these connections to reduce this stress to a safe value.

**Low-Pressure D<sub>2</sub>O Catalytic Re-combiner.** For design purposes, operating conditions of the reflector are assumed to be 1000 psia and 175°C, with a 5% by volume maximum concentration of dissociated D<sub>2</sub> and O<sub>2</sub> gas mixed with helium and D<sub>2</sub>O vapor above the reflector. It is also assumed that all dissolved gases will come out of solution when the reflector

[REDACTED]

FOR PERIOD ENDING AUGUST 15, 1951

is dumped. From solubility curves correlated by Smith, Katz, *et al.*, the amount of each gas may be computed as

0.286 ft <sup>3</sup> of He	} at STP
1.02 ft <sup>3</sup> of O <sub>2</sub>	
2.015 ft <sup>3</sup> of D <sub>2</sub>	

Assume all the recombinable gases are recombined in 10 min, as this is

the basis of the design of the D<sub>2</sub>O off-gas condenser. Therefore the rate of recombination is fixed as 0.3 ft<sup>3</sup>/min. The catalyst bed is made approximately 5 in. deep with a velocity of 1.5 ft/sec through the recombiner. This fixes the cross-sectional area necessary for the desired flow. A 2-in. Schedule 40 pipe will be sufficient for the recombiner. The pressure drop across the catalyst is negligible.

# HRP QUARTERLY PROGRESS REPORT

## 3. CORROSION

E. G. Bohlmann, Leader

J. C. Griess	J. H. Gross
J. L. English	C. G. Heisig
J. Reed	R. A. Lorenz
A. R. Olsen	H. C. Savage
S. H. Wheeler	M. H. Lietzke

### SCOUTING STUDIES

**Anodic and Cathodic Treatment of Type 347 Stainless Steel During Passivation with Nitric or Chromic Acid Solutions** (M. H. Lietzke). The type 347 stainless steel to be used in the homogeneous reactor experiment can be passivated by heating in either 1%  $\text{HNO}_3$  or 2%  $\text{CrO}_3$  solution at  $250^\circ\text{C}$  for 24 hr. Since either treatment is believed to produce a passive oxide film on the surface of the steel it seemed of interest to determine whether anodic treatment of the steel during either of the passivation processes might not produce a superior passive film. In addition, cathodic treatment during passivation was also investigated.

Specimens of type 347 stainless steel freshly passivated in either the  $\text{HNO}_3$  or  $\text{CrO}_3$  solutions show a potential greater than 700 mv more positive than the saturated calomel electrode (S.C.E.) when immersed in a 0.13 f  $\text{UO}_2\text{SO}_4$  solution (corresponding to 30 g/liter uranium). The potential becomes somewhat less positive when the passivated steel specimen is maintained at  $100^\circ\text{C}$  in the  $\text{UO}_2\text{SO}_4$  solution under reflux conditions. As long as the film is intact, the curve obtained by plotting potential vs. time does not show any sudden breaks. However, if sufficient

KCl is added to the uranyl sulfate solution, the potential of the passivated steel with respect to the S.C.E. may suddenly become much less positive, indicating failure of the passive film. The length of time before sudden breaks are observed in the potential vs. time curve when the uranyl sulfate solution at  $100^\circ\text{C}$  is made 0.2 M in KCl is taken as a measure of the quality of the passivated film being studied. The potential is measured using a vibrating reed electrometer and recorded by a Brown recording potentiometer.

It was observed in the first experiments that  $\text{HNO}_3$ -passivated specimens failed almost immediately when placed directly in uranyl sulfate solution 0.2 M in KCl. However, the passive films appeared much more resistant to the Cl when they were maintained in contact with the  $\text{UO}_2\text{SO}_4$  solution at  $100^\circ\text{C}$  for 48 hr prior to the addition of the KCl. Hence all specimens used in subsequent experiments were subjected to this preliminary treatment before KCl was added to the solution. The actual changes that occur in this film during this "conditioning" period are being investigated further.

Figure 3.1 shows the potential vs. time curves obtained with specimens of nitrate-passivated type 347

FOR PERIOD ENDING AUGUST 15, 1951

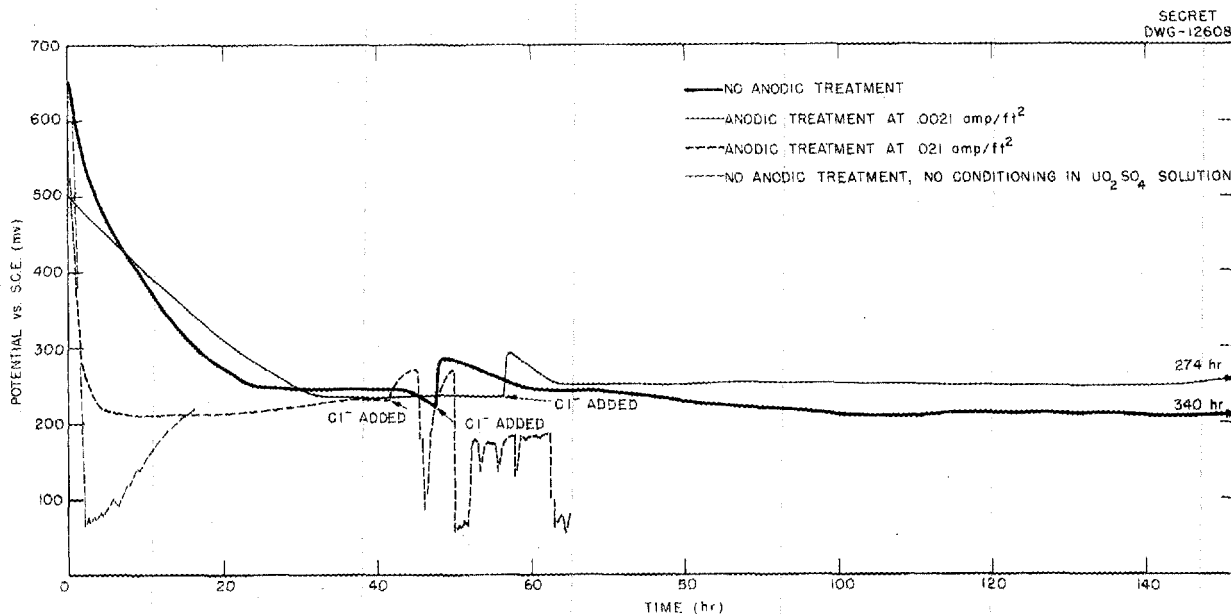


Fig. 3.1 - Effect of Anodic Treatment of Type 347 Stainless Steel at Various Current Densities During Passivation in 1% HNO<sub>3</sub>.

stainless steel. The initial decrease in potential probably corresponds to the removal of oxygen from the passive film. When the Cl<sup>-</sup> was added (as KCl dissolved in a small amount of UO<sub>2</sub>SO<sub>4</sub> solution), some oxygen was also introduced into the system which caused the sudden humps in the curve. As far as the curves were followed after the addition of the KCl no breaks were observed in the case of the specimens given no anodic treatment or anodized at 0.0021 amp/ft<sup>2</sup> during passivation. However, these specimens failed immediately if they were not "conditioned" in the UO<sub>2</sub>SO<sub>4</sub> solution before the addition of the chloride. The specimen given anodic treatment at 0.021 amp/ft<sup>2</sup> failed 3 hr after the addition of the KCl, even though it was previously "conditioned" in the UO<sub>2</sub>SO<sub>4</sub> solution.

Figure 3.2 shows the effect of anodic treatment of type 347 stainless steel at various current densities during passivation in 2% CrO<sub>3</sub> solution. The specimen that received no anodic treatment lasted for over 62 hr before it failed. The length of time the anodized specimens remained "good" decreased with increasing anodic current density during passivation. Hence it appears from these experiments that the passive film produced on type 347 stainless steel anodized in 2% CrO<sub>3</sub> at 250°C is inferior to that produced under the same conditions but without anodic treatment. The potential of a specimen passivated in 2% CrO<sub>3</sub> solution without anodic treatment was followed for 426 hr while the specimen was immersed in refluxing UO<sub>2</sub>SO<sub>4</sub> solution. During this time the potential decreased to +80 mv vs.

## HRP QUARTERLY PROGRESS REPORT

SECRET  
DWG-12609

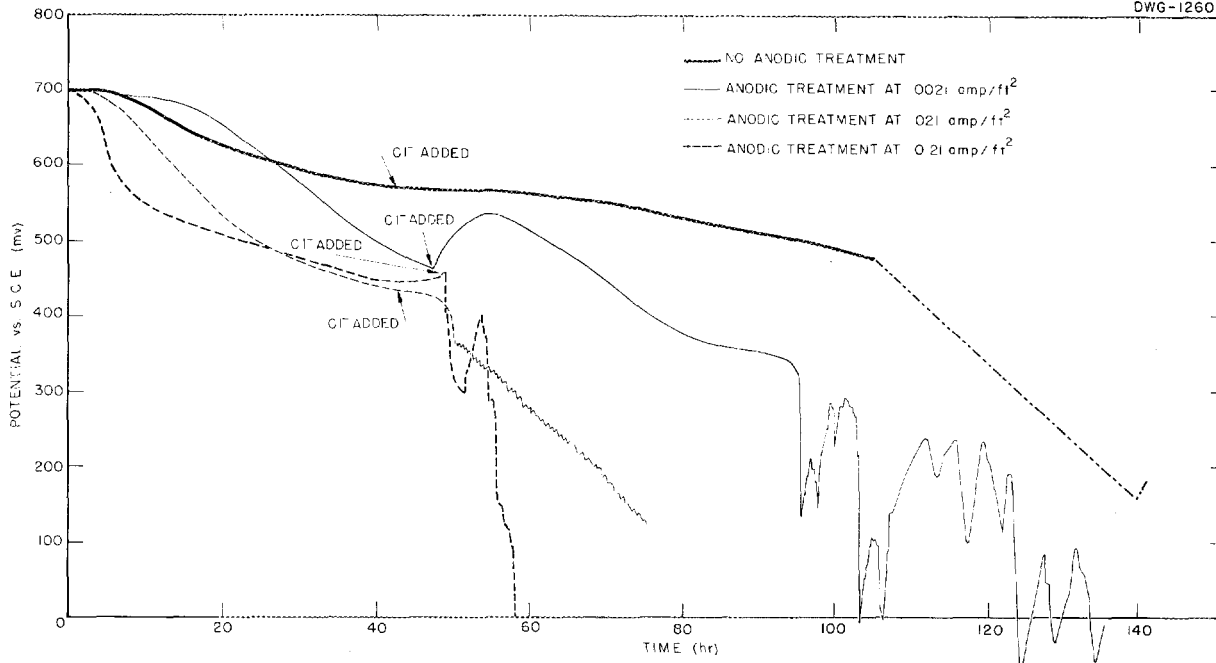


Fig. 3.2 - Effect of Anodic Treatment of Type 347 Stainless Steel at Various Current Densities During Passivation in 2%  $\text{CrO}_3$  Solution.

S.C.E. The potential dropped to +80 mv in about 300 hr, then maintained this value for the duration of the experiment.

Cathodic treatment of the steel was also tried in both the nitric acid and chromic acid solutions. Even though the specimens were "conditioned" in  $\text{UO}_2\text{SO}_4$  solution they failed immediately upon the addition of KCl to the solution.

From these experiments it appears that the passive films produced without anodic or cathodic treatment are superior to those produced with the treatment. The film produced in nitric acid suffers a much sharper initial decrease in potential than

does the chromic acid film. However, after 300 hr the film produced in nitric acid still has a value of +200 mv vs. S.C.E., while the film produced in chromic acid shows a potential of only +80 mv. The film produced by the nitric acid is more resistant to chloride attack than is the film produced by the chromic acid. If resistance to chloride attack is taken as a criterion of the protective character of a film, then the film produced by the nitric acid appears superior to the film produced by the chromic acid.

**Electrochemical Corrosion Studies** (J. C. Griess). A series of experiments designed to obtain information concerning the mechanism of the corrosion encountered in the HRE has been

[REDACTED]

FOR PERIOD ENDING AUGUST 15, 1951

completed. While the experiments are not conclusive, they do tend to substantiate the hypothesis that oxygen stabilizes uranyl sulfate solutions by being reduced in preference to uranyl ions.<sup>(1)</sup>

*Experimental Work.* Since it has been suggested that oxygen is consumed during the corrosion process, the following experiment was designed to determine the rate at which oxygen was reduced: A valve was connected by means of steel pressure tubing to the head of an Aminco bomb so that the gas volume could be determined inside the bomb before and after a run. To run an experiment a given volume of solution was placed in the bomb and the head of the bomb was closed with the valve open. The entire bomb was then placed in a constant temperature bath, and, after equilibrium was reached, the valve was closed at a known barometric pressure. After the bomb had been heated at a given temperature for a predetermined length of time, the bomb was cooled and again placed in the constant temperature bath. The outside end of the valve was then connected by means of rubber tubing to a measuring pipet, the tip of which was under water. The valve was opened and the volume of water that entered the pipet was measured at a known barometric pressure.

Before using the bomb the entire assembly was passivated with 1% nitric acid at 250°C for 24 hr. The inside volume of the assembly was 120 ml, and 65 ml of nitric acid was used.

---

(1) "Electrochemical Corrosion Study," *Homogeneous Reactor Project Quarterly Progress Report for Period Ending May 15, 1951*, ORNL-1057, p. 64 (Oct. 10, 1951).

After passivation the bomb was thoroughly rinsed, and 60 ml of a standardized uranyl sulfate solution was added (the gaseous portion contained air). The bomb was closed and the assembly was heated at 250°C for a given length of time. The bomb was cooled and the change in volume was measured in the manner described above. Table 3.1 gives the results of three such experiments. After each run was made, the solution in the bomb was replaced with a fresh solution. The original solution was analyzed for uranium, iron, chromium, and nickel.

Table 3.2 summarizes the results that were obtained when the solution contained 0.01 *M* potassium chloride in addition to uranyl sulfate.

On three occasions the gas in the bomb at the completion of a run was analyzed. All three samples showed a decrease in the oxygen content corresponding to the observed volume change. One of the gas samples contained 1.6% hydrogen. In no case was there a decrease in the uranium content of the solution.

On one occasion the bomb was half filled with uranyl sulfate solution containing 0.01 *M* potassium chloride, and the air above the solution was removed. The method of removing the air consisted of reducing the pressure in the bomb by means of the laboratory vacuum line. Then a nitrogen pressure, slightly greater than atmospheric pressure, was placed in the bomb. The entire procedure was then repeated three times. The assembly was heated at 250°C for 16 hr. At the end of this time the bomb was cooled, and the solution was analyzed. The analyses are given in Table 3.3.

HRP QUARTERLY PROGRESS REPORT

TABLE 3.1

Analyses of  $UO_2SO_4$  Solutions Heated in Type 347  
Passivated Steel Bomb at 250°C

SAMPLE	TIME OF RUN (hr)	pH OF SOLUTION	SOLUTION ANALYSES				OXYGEN CONSUMED (cc)
			URANIUM (g/liter)	IRON (ppm)	CHROMIUM (ppm)	NICKEL (ppm)	
Original		2.50	30.7	<5	<1	<5	
1 <sup>(a)</sup>	16						1.2
2	64	2.50	30.7	<5	3	11	2.7
3	160	2.50	30.9	<5	1	13	7.0

<sup>(a)</sup>Solution not analyzed.

TABLE 3.2

Analyses of  $UO_2SO_4$  Solutions Containing KCl Heated in a Type 347  
Passivated Steel Bomb at 250°C

SAMPLE	TIME OF RUN (hr)	pH OF SOLUTION	Cl MOLARITY	SOLUTION ANALYSES				OXYGEN CONSUMED (cc)
				URANIUM (g/liter)	IRON (ppm)	CHROMIUM (ppm)	NICKEL (ppm)	
Original		2.43		35.8	3	<2	<5	
C-1	16	2.44	0.0098	35.8	<3	<2	10	6.3
C-2	20	2.45	0.0095	35.7	1	1	10	6.6
C-3	29	2.42	0.0100	35.7	23 <sup>(a)</sup>	<3	20 <sup>(a)</sup>	7.0
C-4	4	2.43	0.0101	36.2	<3	<3	5	0.9
C-5	45	2.49	0.0100	35.8	<3	<3	10	6.3
C-6	20	2.45	0.0106	35.7	<3	<3	11	5.0

<sup>(a)</sup>No explanation for the relatively high iron and nickel concentrations.

*Discussion.* The results of all the experiments reported are open to question for two reasons: (1) The uranyl sulfate used to prepare the solutions contained at least a small amount of organic matter; and (2) the ratio of sulfate to uranium was  $1.016 \pm .003$ . The pH values of the

solutions used were the same as those reported by Helmholtz and Friedlander<sup>(2)</sup> for the given concentrations of uranyl sulfate. Recently, however, some

<sup>(2)</sup>L. Helmholtz and G. Friedlander, *Physical Properties of Uranyl Sulfate Solutions*, LAMS-30 (Dec. 15, 1943).

[REDACTED]

FOR PERIOD ENDING AUGUST 15, 1951

TABLE 3.3

Analyses of a  $UO_2SO_4$  Solution Containing KCl Heated 16 hr in a Type 347  
Passivated Steel Bomb at 250°C in the Absence of Oxygen

SAMPLE	pH OF SOLUTION	CHLORINE MOLARITY	SOLUTION ANALYSES			
			URANIUM (g/liter)	IRON (ppm)	CHROMIUM (ppm)	NICKEL (ppm)
Original	2.37		30.5	<3	<3	<3
Final	2.22	0.0099	29.4	99	<3	28

uranyl sulfate was prepared by reacting stoichiometric amounts of uranium trioxide and sulfuric acid. At a given concentration the pH of this solution was higher than the value given by Helmholtz and Friedlander.

While the results are such that no definite conclusions can be drawn, certain preliminary generalizations can be made. In all of the experiments carried out where the solution was in contact with air during heating, there was no change in the uranium, chromium, iron, or hydrogen ion concentrations. In each case there was a small amount of nickel in solution, but the amount of nickel was related neither to the time of heating nor to the amount of oxygen reduced. That corrosion had taken place was evident by the fact that there was a very fine red precipitate in all solutions. This precipitate was very unreactive and appeared to be ferric oxide. Furthermore at the completion of the runs in which the solution contained potassium chloride, the interior of the bomb showed definite pits.

When a uranyl sulfate solution was heated in a passivated steel

bomb in the absence of oxygen, some uranium was precipitated from solution. At the same time the amount of iron and nickel in solution was greater than in any other run. The iron in solution was present as ferrous iron which explains why the iron was not precipitated. This phenomenon was discussed in the last quarterly report.<sup>(1)</sup>

Further analysis of the data is not justified at this time because of the uncertainty about the uranyl sulfate. At present the above work is being repeated with uranyl sulfate of known purity.

#### STATIC TESTS

J. L. English                      A. R. Olsen  
J. Reed                                S. H. Wheeler

Stagnant corrosion studies for the Homogeneous Reactor Project continued on a somewhat restricted scale during the past quarter owing to unavailability of uranyl sulfate of desired chemical purity. The material used for corrosion studies was found to contain impurities which could well influence the true evaluation of corrosion test results. The major

## HRP QUARTERLY PROGRESS REPORT

contaminant was ammonium ion with small amounts of nitrate ion also present. The bulk of corrosion studies were abandoned for the period required to procure uranyl sulfate of the desired purity. This situation has now been greatly alleviated, and the corrosion program is continuing on an unabated scale. A portion of the effort is being directed to the repetition of tests in which the impure uranyl sulfate was used as the corrosion medium.

**Pretreatment Films.** An expanded program has been initiated for the study of nitric and chromic acid films formed on stainless steels at elevated temperatures. The objectives of this program will include: (1) the determination of the basic constituents of the films by optical and electron-diffraction examination; chemical analyses of films stripped from metal surfaces will be made also; (2) the determination of the film thicknesses; (3) the determination of the effects of metal surface condition and temperature on the characteristics of pretreatment films; (4) the determination of the effect of chemical variations in the stainless steel on the properties of the pretreatment films; (5) the determination of an "accelerated test" for measuring film effectiveness to correlate with corrosion behavior in uranyl sulfate at elevated temperatures.

*Effect of Metal Surface Condition and Exposure Time on Nitric Acid Pretreatment Films Formed at 250°C.* An experiment was run using type 347 stainless steel specimens which were prepared by machining and abrading on Nos. 80 and 120 grit papers and exposed for periods of 1, 4, 8, and

24 hr in 1% by weight of 70%  $\text{HNO}_3$  at 250°C. The test bombs had two types of metal surface conditions: (1) newly machined, and (2) chemically cleaned bombs which had been used numerous times for routine corrosion tests. The conclusions from the series of tests were:

- a. The physical appearance of nitric acid pretreatment films formed at 250°C is influenced by the surface condition of the test bombs in which the pretreatment is conducted. Newly machined surfaces resulted in specimens exhibiting highly lustrous surfaces with brilliantly colored interference patterns. Old chemically cleaned bomb surfaces resulted in specimens showing dull gray colored surfaces with greater film thicknesses than those obtained in the newly machined bombs. These thicker films, however, were equally as resistant to uranyl sulfate at 250°C as the thinner films.
- b. The magnitude of corrosion attack by the 1% nitric acid at 250°C was generally greater on specimens exposed in old bombs, compared to attack obtained on specimens exposed in newly machined bombs.
- c. The amount of dissolved nickel found in nitric acid solutions taken from the newly machined bombs was greater than the amount determined in solutions taken from the old bombs. Test data indicate selective attack on newly machined surfaces by nitric acid; the magnitude of

this attack was less pronounced with old bombs.

- d. The metal thickness losses for new bombs, calculated from dissolved nickel concentrations in the nitric acid solutions, were greater than losses determined by decrease in specimen weights, assuming corrosion attack to be uniform. Good agreement between actual and calculated metal thickness losses was obtained from nickel analyses on solutions removed from the old bombs. Actual thickness losses, based on weight losses, for both old and new bombs after 24 hr were 0.003 mil. The calculated thickness loss for new bombs for the same exposure time was 0.025 mil; for old bombs the calculated thickness loss was 0.002 mil for 24 hr.

After the pretreatment tests, the specimens were submitted to the Optical and Electron Microscopy Group for examination and study. Work was done by T. E. Willmarth and is fully reported in ORNL CF-51-7-10.<sup>(3)</sup> Results indicated that  $\alpha\text{-Fe}_2\text{O}_3$  was the basic film constituent in all cases, although a possibility existed that  $\text{Cr}_2\text{O}_3$  was present. Other results were:

- a. The film thickness ( $1\ \mu$ ) measured on the specimen from the old bomb after 1 hr was the same as that measured on the specimen from the new bomb after 24 hr.
- b. The film thickness on the old bombs increased from  $1$  to  $3\ \mu$

<sup>(3)</sup>T. E. Willmarth, *Microscopic Examination of Oxide Layers on Stainless Steel 347 Which Has Been Passivated with 1%  $\text{HNO}_3$  at  $250^\circ\text{C}$  for 1, 4, 8, and 24 Hours*, ORNL CF-51-7-10 (July 5, 1951).

during the first 8 hr. No additional increase occurred during the ensuing 16 hr of exposure. Film thickness on the new bombs remained practically constant at  $0.3\ \mu$  during the first 8 hr and then increased to  $1\ \mu$  during the remaining 16 hr.

- c. A two-layer effect was observed on all specimens. The substrate layer appeared almost structureless while the outer layer contained fairly large and uniform crystallites  $0.5$  to  $1.0\ \mu$  in diameter. This layer was not well-bonded to the substrate layer, as numerous areas were noted where the outer layer had sloughed off, exposing the substrate layer.

This last observation may offer additional support to the possibility that the protective nature of the pretreatment film is not entirely (and perhaps not at all) due to the formation of a bulk oxide film. Some other mechanism, as yet not established, may be the major contributing cause for the "passivity effect" obtained by pretreating stainless steel.

*A Comparison Between Nitric Acid Pretreatment Films Formed on Polished and on Etched Stainless Steel Surfaces.* Test specimens of type 347 stainless steel were abraded on Nos. 80 and 120 grit papers. A portion of these samples were then etched for 10 min at  $60^\circ\text{C}$  in a  $10\%\ \text{HNO}_3$ — $4\%\ \text{HF}$ — $1\%\ \text{HCl}$  solution (by volume). Both sets of samples, etched and unetched, were then exposed to  $1\%\ \text{HNO}_3$  at  $250^\circ\text{C}$  for 24 hr in newly machined bombs.

## HRP QUARTERLY PROGRESS REPORT

Samples were submitted to the Optical and Electron Microscopy Group for examination. Studies were made by T. E. Willmarth and reported in ORNL CF-51-7-67.<sup>(4)</sup> Results were as follows:

- a. Both types of films were reddish yellow to red in color by reflected light. The basic constituent in the films appeared to be  $\alpha\text{-Fe}_2\text{O}_3$ .
- b. The etched specimens exhibited pits ranging from 2 to 8  $\mu$  in depth. The pits were lined with a dark crystalline material of 1  $\mu$  particle size. Bands of this material were observed also along polishing lines. The unetched samples were relatively free of pits. Some bands of dark crystalline material were observed with crystallite size ranging on the order of 0.5  $\mu$ .
- c. The film layers on both samples followed the contours of the metal surface very closely. However, films stripped from the etched samples contained numerous holes which were originally sites for pits.
- d. Both films measured approximately 1  $\mu$  in thickness in this case.
- e. A preliminary examination disclosed that the film from the etched sample exhibited a greater degree of ferromagnetism than the unetched specimen.

<sup>(4)</sup>T. E. Willmarth, *A Microscopic Study of Oxide Films Formed on Etched and Unetched Stainless Steel 347 During Pretreatment with 1% HNO<sub>3</sub> at 250°C*, ORNL CF-51-7-67 (July 16, 1951).

Nitric acid pretreatment films were also stripped from type 347 stainless steel specimens by M. G. Fontana at Ohio State University using a mixture of bromine and ethanol. These films will be submitted to the W. B. Coleman Company in Philadelphia, Pennsylvania for chemical analyses.

**Uranyl Sulfate Corrosion Studies.** Studies of the corrosion behavior of nitric acid—pretreated type 347 stainless steel in uranyl sulfate solutions and the results of a series of stagnant corrosion tests with uranyl sulfate solution are reported in detail below.

*Corrosion Behavior of Nitric Acid—Pretreated Type 347 Stainless Steel in Concentrated Uranyl Sulfate Solutions.* Concentrated aqueous solutions of uranyl sulfate were prepared for use in determining the corrosion behavior of nitric acid—pretreated type 347 stainless steel at 250°C. The solutions were made 0.44 and 0.86 M, containing 103.8 and 203.8 g of uranium per liter, respectively.

The pretreatment consisted of exposing abraded specimens in 1% HNO<sub>3</sub> for 24 hr at 250°C in chemically cleaned stainless steel bombs. The corrosion tests in uranyl sulfate were run for 11 weeks with weekly sample inspection, using the same solutions throughout the total testing time. The chemical analyses on the uranyl sulfate solutions are included in Table 3.4.

Corrosion data for the nitric acid—pretreated type 347 stainless steel specimens are tabulated in Table 3.5. No reduction of uranyl

TABLE 3.4  
Chemical Analyses of Uranyl Sulfate Solutions

	SOLUTION ANALYSES (g/liter)	
	0.44 M UO <sub>2</sub> SO <sub>4</sub> ; INITIAL pH, 1.95; FINAL pH, 1.90	0.86 M UO <sub>2</sub> SO <sub>4</sub> ; INITIAL pH, 1.55; FINAL pH, 1.52
Initial uranium	103.8	203.8
Final uranium	103.0	200.0
Final dissolved iron	0.015	0.009
Final dissolved chromium	0.001	0.001
Final dissolved nickel	0.005	0.018
Final uranium(IV)	0.236	0.346

TABLE 3.5  
Corrosion Rates of Nitric Acid—Pretreated Type 347 Stainless Steel

EXPOSURE (weeks)	CORROSION			
	0.44 M (mdd)	UO <sub>2</sub> SO <sub>4</sub> (mpy)	0.86 M (mdd)	UO <sub>2</sub> SO <sub>4</sub> (mpy)
1	-1.40	0.25	-1.96	0.35
2	-0.29	0.05	-0.73	0.13
3	-0.14	0.03	-0.56	0.10
4	-0.13	0.02	-0.47	0.08
5	-0.32	0.06	-0.56	0.10
6	-0.25	0.05	-0.43	0.08
7	-0.42	0.08	-0.38	0.07
8	-0.22	0.04	-0.35	0.06
9	-0.19	0.03	-0.31	0.06
10	-0.18	0.03	-0.29	0.05
11	-0.20	0.03	-0.31	0.06

sulfate solutions was evident by physical appearance, chemical analyses, and pH measurements. The concentration of dissolved nickel was very low at the end of the test, indicating negligible corrosion attack on the stainless steel.

The corrosion resistance of 1% nitric acid—pretreated type 347 stainless steel appears to be a straight line function of uranyl sulfate concentration in the range 0.17 to 0.86 M. The magnitude of corrosion attack in all cases studied thus far is extremely low. Corrosion rates from stagnant tests at 250°C for 11 weeks in three different concentrations of uranyl sulfate were:

CONCENTRATION	CORROSION RATE (mpy)
0.17 M	0.01
0.44 M	0.03
0.86 M	0.06

The corrosion behavior of nitric acid and chromic acid pretreated stainless steels is being determined in uranyl sulfate solutions containing as high as 500 g of uranium per liter.

*Results of a Series of Stagnant Corrosion Tests with Uranyl Sulfate at 250°C.* This series of corrosion studies was conducted in a 750-ml capacity, electrically heated autoclave which was equipped with sample withdrawal cells to permit removal of the uranyl sulfate solution while the test was operating at 250°C. The apparatus was constructed entirely of type 347 stainless steel. The sample cell had a liquid volume of approximately 12 ml. The entry tube to the cell was positioned ¼ in. from the bottom of the solution chamber.

## HRP QUARTERLY PROGRESS REPORT

The procedure employed for sampling was to first flush the sample cell with the test solution. This operation also removed uranyl sulfate from the sample tube extending from the solution chamber to the sample cell so that subsequent withdrawal of uranyl sulfate from the main body of the liquid resulted in a more representative sample. The sample cell was re-filled immediately after flushing and this solution was used for the analytical sample. A description of the test runs with results follows.

### Run S194: Nitric Acid Pretreatment

Since the autoclave had been used previously for uranyl sulfate corrosion studies, it was decided to remove old surfaces by a machining operation on all areas which were exposed to uranyl sulfate. After this operation the same surfaces were etched for 15 min in a mixture of 10%  $\text{HNO}_3$  - 4%  $\text{HF}$  - 1%  $\text{HCl}$  (by volume) at  $60^\circ\text{C}$ . The system was then washed with hot distilled water until a qualitative check showed a negligible concentration of chloride iron, <1 ppm.

The autoclave was filled with 750 ml of 1% by weight of 70% nitric acid and sealed. The unit was operated at  $250^\circ\text{C}$  for 16 hr during which period solution samples were taken periodically. Results of the chemical analyses on the nitric acid solution appear in Table 3.6. At the end of the test, a solution deficit of 40 to 50 ml was observed which indicated a slow leak in the autoclave assembly.

The analyses show the general trend previously noted in pretreatment solution behavior. The dissolved iron content increased gradually during

TABLE 3.6

### Chemical Analyses of Nitric Acid Pretreatment Solution After Use at $250^\circ\text{C}$

EXPOSURE TIME (hr)	SOLUTION pH	DISSOLVED METALLIC IONS ( $\gamma/\text{ml}$ )		
		IRON	NICKEL	CHROMIUM
0	1.1			
2	1.0	13	6	<1
4	1.0	17	43	1
6	1.0	6	20	10
8	1.1	4	25	8
12	1.1	4	22	7
16	1.0	4	33	13

the first 4 hr, after which it decreased to a steady value of 4  $\gamma/\text{ml}$  as a result of precipitation from solution as ferric oxide. The nickel increased rapidly during the first 4 hr to 43  $\gamma/\text{ml}$  and then decreased to between 20 and 35  $\gamma/\text{ml}$  during the balance of the test. Dissolved chromium concentration progressively increased to 10  $\gamma/\text{ml}$  during the initial 6 hr and remained fairly constant for the remaining 16 hr.

The solution was clear and water-white in color at the end of the test. No visible precipitates were observed although a smut of brown-colored oxides was wiped from the walls of the autoclave. Sufficient sample of this residue could not be collected for X-ray examination to determine whether or not any chromium had been precipitated from the nitric acid solution and entered this film along with iron.

Inasmuch as a solution leak occurred in this run, the nitric acid pretreatment was repeated in run S196.

Run S196: Second Nitric Acid Pretreatment

The autoclave was washed with distilled water at the end of run S194 and again filled with 750 ml of 1% by weight of c.p. reagent grade nitric acid. The test was run for 43 hr at 250°C with periodic sampling while at temperature. Results of chemical analyses are listed in Table 3.7.

TABLE 3.7

Chemical Analyses of Nitric Acid—Pretreatment Solution After Use at 250°C

EXPOSURE TIME (hr)	SOLUTION pH	DISSOLVED METALLIC IONS (γ/ml)		
		IRON	NICKEL	CHROMIUM
0	1.0			
2	1.0	6	5	30
4	1.0	6	9	2
6	1.0	3	7	8
10	1.0	2	6	12
14	0.9	4	13	18
18	0.9	3	8	18
22	0.9	5	10	15
26	1.0	8	10	19
43	0.9	4	12	18

Sampling during the test was accomplished by discarding the first sample for flushing the sample tube and collecting a second sample for solution analyses. The total volume removed by this operation was 22 ml. The final solution volume in the autoclave was 550 ml: the total

volume of solution removed by sampling was 198 ml. The initial and final solution volume balance showed essentially no loss due to leakage.

The nickel analyses were considerably lower than those obtained in run S194 on newly machined and etched surfaces. These results again illustrate the fact that selective attack of nickel from the stainless steel is lessened after repeated exposure to the nitric acid medium. The nickel concentration essentially leveled off after 14 hr during this exposure to nitric acid solution.

The dissolved iron analyses exhibited no initial increase as was encountered in run S194 but remained fairly constant between 3 and 8 γ/ml throughout the run. A slight brown-colored precipitate was observed in the bottom of the autoclave at the end of the test, indicating that iron had been precipitated from solution during the exposure at 250°C.

The behavior of chromium was markedly different in this run as compared to run S194. A concentration of 30 γ/ml was obtained after 2 hr as compared to <1 γ/ml during the same time in run S194. Chromium apparently precipitated from solution since the value at the end of 4 hr had decreased from 30 to 2 γ/ml. During the remainder of the test, the chromium concentration ranged steadily between 12 and 19 γ/ml. The initial rapid dissolution of chromium, after "leaching out" of nickel has occurred in previous exposures, may be a function of the oxidizing capacity of the fresh nitric acid solution before thermal decomposition takes place.

Run S197: Uranyl Sulfate Test

Immediately after the nitric acid pretreatment for 43 hr, the autoclave

**[REDACTED]**

**HNP QUARTERLY PROGRESS REPORT**

was rinsed thoroughly with distilled water to remove precipitated iron oxides. The autoclave was filled with 750 ml of uranyl sulfate solution containing 38.0 g of uranium per liter. The temperature was raised to 250°C and maintained for 42.5 hr. The pressure reading during this run remained consistently around 595 psig. Samples were withdrawn periodically at temperature. A solution deficit of 20 ml was found at the end of the test.

The results of chemical analyses on the solution samples are listed in Table 3.8. The uranium results were fairly consistent during the first 30 hr but then decreased to 35.2 g/liter after 42.5 hr. The pH behavior followed a trend almost identical with that of the uranium

vs. time curve. Reduction in total uranium content was accompanied by a lowering of the pH value. A significant increase in both total uranium concentration and solution pH occurred after the test was cooled to room temperature and exposed to air for 1.5 hr. The uranium concentration changed from 35.2 to 37.2 g/liter, and the solution pH increased from 1.6 to 1.9 for the same period. The accuracy of the analytical method for determining uranium lies between ± 1 to 2% which may account for a portion of the variation in uranium analyses but does not explain the above increase.

The test samples of uranyl sulfate were clear and yellow as removed from the run during operation. No black residues were observed in the solution

**TABLE 3.8**

**Chemical Analyses of Uranyl Sulfate Solutions in Run S197**

EXPOSURE TIME (hr)	SOLUTION pH	TOTAL URANIUM (g/liter)	DISSOLVED METALLIC IONS (γ/ml)		
			IRON	NICKEL	CHROMIUM
0	2.4	38.0	<1	<1	<1
2	2.2	37.1	54	4	<1
4	2.3	38.9	38	5	<1
6	2.3	38.1	52	6	<1
10	2.2	38.0	74	11	<1
14	2.1	37.6	91	16	<1
18	2.0	37.7	71	13	<1
22	2.0	37.2	82	17	<1
30	1.7	37.2	100	20	<1
42.5	1.6	35.2	137	35	<3
45.5 (after cooling)	1.9	37.2	27	14	<1

remaining in the autoclave at the end of the test although some brown-colored residues of ferric and perhaps chromic oxides were observed. The condition of the autoclave inner walls was excellent with the original metallic luster and brilliantly colored interference patterns predominant.

The dissolved iron concentration increased steadily during the 42.5 hr of test to a maximum value of 137  $\gamma$ /ml. During the cooling-down period, the concentration dropped to 27  $\gamma$ /ml as a result of precipitation. The nickel concentration increased slightly to a maximum value of 35  $\gamma$ /ml and decreased to 14  $\gamma$ /ml during the cooling-down and air-exposure period. The dissolved chromium concentrations remained almost negligible throughout the entire test.

#### Run S198: Uranyl Sulfate Test

Since the physical appearance of the autoclave walls remained unchanged during run S197, it was decided to operate a second uranyl sulfate test without additional nitric acid pretreatment. The test objective was to study more closely the fluctuations in total uranium concentration exhibited by run S197 during the first 4 hr. The test procedure was planned so that samples were taken every 15 min from the time that the solution temperature just exceeded 100°C.

A 750-ml volume of uranyl sulfate solution containing 38.0 g of uranium per liter was placed in the autoclave. Samples were started when the autoclave temperature reached 106°C and were taken at 15-min intervals thereafter for the entire run. Arrangements were made to flush the sample cell

with distilled water prior to the introduction of sample solution into the cell. The first 11 to 12 ml of sulfate solution was discarded, and a second sample, taken immediately after the first, was used for the analytical sample. Results appear in Table 3.9.

The uranyl sulfate samples withdrawn during the test were free of insoluble residues; all samples were clear and yellow in color. The volume of solution measured in the autoclave at the end of the run was 230 ml. The total volume of solution removed by sampling was 504 ml for a solution deficit of 16 ml.

Analytical uranium results, included in Table 3.9, were consistently higher in value than the initial content of 38.0 g of uranium per liter. A portion of these increases could be attributed to a concentration effect caused by the loss of 16 ml of solution during the test. If this loss occurred during the initial phase of the test, the increase in uranium content was 0.8 g/liter. Most of the reported analyses, however, were 1.0 to 2.0 g/liter high. Data obtained later in run S199 which was a nitric acid pretreatment indicate the probable source of the excess uranium content. After analyzing the nitric acid solution from run S199, it was found to contain 2.1 g of uranium per liter. Thus, although a high uranium material balance was obtained in run S198, there still was additional uranium deposited on the bomb walls. The somewhat low uranium analyses obtained at the end of run S197 suggest this as the probable source of the

HRP QUARTERLY PROGRESS REPORT

TABLE 3.9

Chemical Analyses of Uranyl Sulfate  
Solutions in Run S198

SAMPLE NO.	EXPOSURE TIME (hr)	TEMP. (°C)	PRESSURE (psig)	SOLUTION pH	TOTAL URANIUM (g/liter)	DISSOLVED METALLIC IONS (γ/ml)	
						IRON	NICKEL
0	0	25	0	2.4	38.0	1	<1
1	0.25	106	0	2.3	38.3	9	1
2	0.50	165	100	2.3	39.4	2	1
3	0.75	194	150	2.3	38.4	3	1
4	1.00	238	400	2.3	39.6	10	1
5	1.25	260	600	2.3	40.1	13	1
6	1.50	256	525	2.2	40.1	11	1
7	1.75	245	450	2.3	39.8	12	1
8	2.00	255	510	2.3	40.2	13	1
9	2.25	249	470	2.3	40.2	13	1
10	2.50	254	510	2.3	38.6	10	1
11	2.75	246	450	2.4	39.4	10	1
12	3.00	253	505	2.3	41.0	9	1
13	3.25	251	490	2.3	40.5	12	1
14	3.50	249	480	2.3	40.2	10	1
15	3.75	253	505	2.4	41.1	12	1
16	4.00	245	455	2.3	40.7	13	1
17	4.25	253	505	2.3	40.2	12	1
18	4.50	247	450	2.3	40.2	14	1
19	4.75	253	505	2.4	40.0	12	1
20	5.00	246	455	2.3	40.8	16	1
21	5.25	247	460	2.3	40.2	17	1
Final	7.75	25	0	2.5	39.3	24	1

additional uranium. Partial solution of uranium deposited in run S197 could account for the high concentrations encountered in run S198.

The dissolved metallic ion concentrations reported for run S198 indicate that corrosion attack was very slight. The dissolved nickel concentration remained less than 1 γ/ml during the entire run. The dissolved iron contents were con-

siderably lower than those observed in run S197 in which partial solution reduction appeared to have occurred. Dissolved chromium concentrations, although not included in Table 3.9, were less than 1 γ/ml also. These results, plus the consistency of pH measurements between 2.3 and 2.4, serve as reliable criteria for the absence of solution reduction. From previous experience, it has been observed that when reduction of uranyl sulfate takes place, there is

an increase in the dissolved nickel, chromium, and iron contents as well as a decrease in the solution pH.

Run S199: Nitric Acid Pretreatment

Although the data from run S198 were not indicative of uranyl sulfate reduction, the autoclave was thoroughly rinsed with distilled water and pretreated for 24 hr at 250°C in 1% by weight of reagent grade 70% nitric acid. A volume of 750 ml was used which had a pH of 0.9. The pH at the end of the 24 hr was 1.0. Chemical analyses of the nitric acid solution gave the following results:

Total uranium	2.1 g/liter
Dissolved iron	1 $\gamma$ /ml
Dissolved nickel	10 $\gamma$ /ml
Dissolved chromium	5 $\gamma$ /ml

Examination of the autoclave at the end of the pretreatment disclosed a small amount of brown-colored smut on portions of the walls.

Run S201: Nitric Acid Pretreatment

Since uranium was found in the run S199 nitric acid pretreatment, the autoclave, including all component parts which had been contacted by uranyl sulfate solution, was cleaned twice using a mixture of HNO<sub>3</sub> and H<sub>2</sub>O<sub>2</sub> at room temperature. After this cleaning operation to remove adhering uranium oxides from the metal surfaces, the parts were then subjected to an etch treatment in 10% HNO<sub>3</sub>—4% HF—1% HCl (by volume) for 15 min at 60°C. Hot distilled water rinses with vigorous scrubbing followed until a qualitative check disclosed a chloride concentration of less than 1 ppm.

The autoclave was filled with 750 ml of 1% HNO<sub>3</sub> (c.p. reagent grade) and

heated at 250°C for 24 hr. The initial pH of this solution was 0.9; the final pH was 1.0. Chemical analyses of the solution at the end of the run showed a slight trace of uranium. The dissolved nickel, chromium, and iron concentrations analyzed 10, 31, and 2  $\gamma$ /ml, respectively. These results again indicate that previously exposed stainless steel surfaces undergo a slight selective attack of chromium by nitric acid at 250°C. No loss of solution was found at the end of the test, and the pretreatment was considered to be successful.

Run S203: Uranyl Sulfate Test

A 750-ml volume of uranyl sulfate solution containing 38.0 g of uranium per liter was placed in the autoclave immediately after the pretreatment. The test was run at 250°C, and samples were removed in the manner already described.

The total uranium concentration dropped to 25.0 g/liter 18 hr after the start of the test. The solution pH decreased from 2.4 to 1.9 during this period. The test was shut down and cooled to room temperature without opening. The autoclave was then pressurized with 50 psig of oxygen and reheated to 250°C. A solution sample taken as soon as the 250°C temperature was reached, a period of 1.5 hr, analyzed 38.8 g of uranium per liter. This result was within analytical accuracy of the initial content of 38.0 g/liter. The test was continued for an additional 43 hr, after which time the uranium content analyzed 39.8 g/liter. The results of solution analyses appear in Table 3.10.

The first part of Table 3.10 shows an increase of 4.2 g of uranium per

HRP QUARTERLY PROGRESS REPORT

TABLE 3.10

Chemical Analyses of Uranyl Sulfate Solutions  
from Run S203

SAMPLE NO.	EXPOSURE (hr)	TEMP. (°C)	SOLUTION pH	TOTAL URANIUM (g/liter)	DISSOLVED METALLIC IONS (γ/ml)	
					IRON	NICKEL
0	0	25	2.4	38.0	1	1
1	1.75	250	2.4	42.2	11	2
2	17.75	245	1.9	25.0	70	192
(The test was shut down, cooled, and 50 psig oxygen was added)						
3	1.5	253	2.3	38.8	62	23
4	19.0	254	2.1	40.0	116	69
5 <sup>(a)</sup>	19.1	254	2.5	40.3	1	20
6	27.1	245	2.6	40.0	4	23
7	43.1	250	2.5	39.8	2	22
(The test was shut down, cooled, and opened to air for 1 hr)						
8	3.5	25	2.4	39.8	1	20

<sup>(a)</sup> Sample No. 4 was removed from the autoclave containing a moderate quantity of brown precipitate. Sample No. 5 was taken 5 min after No. 4 and was clear and yellow in color. The brown-colored precipitate in No. 4 appeared to be ferric oxide.

liter after 1.75 hr at 250°C. At the end of 17.75 hr, the concentration had dropped to 25.0 g/liter. The solution pH dropped to 1.9, and an abrupt increase in the concentrations of dissolved iron and nickel was obtained as a result of increased corrosion attack during the solution reduction.

The addition of 50 psig of oxygen after cooling to room temperature in the closed system resulted in a return of uranium content to 38.8 g/liter during the 1.5 hr required for heating to 250°C. The solution pH increased to 2.3; the nickel concentration decreased from 192 to 23 γ/ml. Uranium analyses were consistently

2.0 g/liter higher than the initial 38.0 g/liter for the balance of the test, 43.1 hr. The dissolved iron precipitated from solution as iron oxide over this period, as evidenced by a reduction in concentration from 116 to 2 γ/ml. Approximately 172 γ/ml of dissolved nickel disappeared from the uranyl sulfate medium by some mechanism or other.

The measured solution volume remaining in the autoclave was 550 ml. The amount of samples withdrawn totaled 192 ml so that a solution deficit of 8 ml resulted from the operation of this test. This loss increased the total uranium concentration by 0.4 g/liter.

[REDACTED]

FOR PERIOD ENDING AUGUST 15, 1951

**Corrosion of Reflector Materials.** Corrosion studies with materials concerned with the reflector system of the Homogeneous Reactor Project were continued with emphasis placed upon a duplication of tests run previously. The materials considered in this investigation were SAE 1030 carbon steel and type 347 stainless steel. The test conditions were changed somewhat from those used in former tests. The general practice in stagnant tests was to replace the solution weekly. In the present series of tests, the test solutions were replaced twice weekly. Other tests which will be run in the near future include a study to determine the effect of corrosion product contamination in the same test solution on the corrosion behavior of the materials. Also to be run are tests using the same solution in which hydrogen peroxide additions will be made on a daily basis in order to approach conditions in the reflector where  $D_2O_2$  will be produced continuously. Tests using  $D_2O$  have been started to compare corrosion behavior with results obtained in ordinary water. Large autoclaves are being fabricated which will have a solution volume of approximately 1500-ml capacity. These autoclaves will be equipped with sample cells to permit solution sampling while at operating temperature. To be included in studies with these autoclaves will be the effect of oxygen, hydrogen, and mixtures of the two gases on the corrosion resistance of mild carbon steel and type 347 stainless steel.

In the present series of tests, newly machined stainless steel autoclaves of 150-ml capacity were used. The initial test results, especially those from tests using trisodium

phosphate as a corrosion inhibitor, were not in good agreement with results from previous tests. Corrosion rates were actually obtained in the inhibited tests as compared to slight weight gains exhibited by similar tests run earlier. The discrepancy was finally traced to the metal surface condition of the stainless steel autoclaves. The first corrosion tests with reflector materials were operated in stainless steel autoclaves which previously had been used for nitric acid pretreatments at  $250^\circ C$ . The difference between these "conditioned" surfaces and the newly machined surfaces resulted in a loss of inhibitor effectiveness due to the quantity of trisodium phosphate necessary to condition the newly machined surfaces. This effect was substantiated when new tests were run in the "conditioned" autoclaves. The corrosion behavior of the carbon steel specimens was then very similar to the behavior obtained originally.

*Corrosion of SAE 1030 Carbon Steel Uncoupled and Coupled with Type 347 Stainless Steel in Distilled Water Containing 0.005 M Hydrogen Peroxide at  $200^\circ C$ .* Tests were run with SAE 1030 carbon steel uncoupled and coupled with type 347 stainless steel in distilled water containing 0.005 M hydrogen peroxide at  $200^\circ C$ . The results from these tests were intended to serve as a basis of comparison with the results obtained from inhibited tests. The samples were removed twice weekly for inspection and measurement of corrosion damage. The test solutions were replaced twice weekly also.

Table 3.11 includes the corrosion data for these tests. The weight

**HRP QUARTERLY PROGRESS REPORT**

**TABLE 3.11**

**Corrosion of SAE 1030 Carbon Steel Uncoupled and Coupled with Type 347 Stainless Steel in 0.005 M Hydrogen Peroxide at 200°C**

EXPOSURE (hr)	UNCOUPLED		COUPLED	
	FINAL SOLUTION pH	WEIGHT LOSS (mg/cm <sup>2</sup> )	FINAL SOLUTION pH	WEIGHT LOSS (mg/cm <sup>2</sup> )
0	5.1		5.1	
64	6.5	1.08	6.7	0.67
155	5.8	1.39	6.3	1.02
221	5.5	1.63	6.5	1.16
317	5.8	1.71	6.5	4.55
385	5.8	1.81	6.4	4.85
478	6.9	1.87	6.5	5.08
548	5.7	1.96	5.2	5.18
640	6.3	3.15	5.5	5.22
730	6.3	4.64	5.6	5.32
797	6.2	5.42	5.4	5.45
888	5.4	7.25	5.3	5.63

losses reported are cumulative losses as removed from the corrosion media. The samples will be defilmed at the conclusion of the tests to determine actual metal loss.

The corrosion rate on the uncoupled specimen was 3.6 mils/year at the end of 888 hr. The sample was black in color with some small deposits of flaky brown-colored iron oxide scattered over the surfaces. Numerous pits were apparent, ranging in depth from 5 to 10 mils. The coupled carbon steel specimen showed a corrosion rate of 2.8 mils/year after 888 hr. Rather bulky adherent corrosion products covered the outside surface while the area in contact with the stainless steel was black with spotty corrosion products. Some pitting attack was observed along the outer edge of the area contacted by the stainless steel (the carbon steel

area to stainless steel surface area exposed was 1.2 to 1.0 cm<sup>2</sup>). A weight gain of 0.6 mg/cm<sup>2</sup> was reported for the stainless steel specimen, and its condition was excellent. The contact area was black in color as compared to a lustrous pink color on the uncontacted areas.

Examination of the data in Table 3.11 shows a more rapidly progressing increase in weight loss on the coupled specimen for 548 hr as compared to the uncoupled sample. However, during the last 91 hr, the weight loss on the latter was greater by 1.62 mg/cm<sup>2</sup> than on the coupled specimen. A rather dormant period of weight loss occurred after 548 hr on the single specimen; weight losses ranged from 1.08 to 1.96 mg/cm<sup>2</sup>. This period was followed by rapid corrosion attack for the remaining

340 hr. The dormant period may have been the result of formation of a protective film of hydrous iron oxide during the initial corrosion reactions. The film underwent a breakdown after 548 hr as evidenced by the rapid increase in corrosion attack. The diffusion of oxygen through the protective oxide layer could cause such increased corrosion attack.

The most pronounced variation in corrosion attack on the coupled specimen was observed during the 221- to 317-hr exposure period. The weight loss increase was from 1.16 to 4.55 mg/cm<sup>2</sup> during the 96-hr period.

The corrosion rates on the coupled and uncoupled SAE 1030 carbon steel under the described test conditions are not excessive for the test period, slightly over 5 weeks. Although some bulky corrosion products were observed, localized attack was not intense even with excess oxygen present for short periods before being consumed in corrosion product formation. Tests will be run to determine the effect of the rate of oxygen addition on corrosion behavior.

*Effect of Trisodium Phosphate Concentration on the Corrosion Behavior of Coupled and Uncoupled SAE 1030 Carbon Steel.* Tests were run at 200°C in which the trisodium phosphate concentrations ranged from 100 to 400 ppm. The test solutions (150 ml) were distilled water containing 0.005 M hydrogen peroxide. The solutions were replaced twice weekly. The carbon steel specimens were etched in dilute sulfuric acid containing Rodine 77 as an inhibitor.

The weight loss data appear in Table 3.12. The average surface area of the specimens was 18.5 cm<sup>2</sup>. The pH values in the table were determined after the specific exposure time at 200°C.

The trisodium phosphate concentration for minimum corrosion attack was 300 ppm with these test conditions. Increasing the concentration to 500 ppm raised the pH to 11 with resultant increase in corrosion attack, due perhaps to the formation of soluble sodium ferrate. Concentrations of trisodium phosphate below 300 ppm did result in an improvement of corrosion resistance as compared with the results from similar tests in uninhibited solutions.

The initial corrosion rates in solutions containing 300 and 400 ppm of the phosphate were greatly retarded in comparison with rates obtained in 100 and 200 ppm trisodium phosphate. The condition of all specimens as removed at the end of 888 hr was somewhat similar with the exception that in the 200-ppm test, the carbon steel exhibited a more gray, slightly etched appearance. The other specimens were of a semi-lustrous nature, pink in color, with a few black stains. No bulky scale formation existed on any of the samples.

Similar tests as described for the uncoupled samples were run in which the carbon steel was coupled to type 347 stainless steel. The diameter of the stainless steel samples was approximately 6 mm less than that of the 1030 carbon steel so that the surface area ratio of carbon steel to stainless steel was 1.2 to 1.0 cm<sup>2</sup>. The concentration of trisodium

HRP QUARTERLY PROGRESS REPORT

TABLE 3.12

Effect of Trisodium Phosphate Concentration on Corrosion Behavior of  
Uncoupled SAE 1030 Carbon Steel in 0.005 M  
Hydrogen Peroxide at 200°C

EXPOSURE TIME (hr)	WEIGHT LOSS (mg/cm <sup>2</sup> )			
	TRISODIUM PHOSPHATE CONCENTRATION			
	100 ppm	200 ppm	300 ppm	400 ppm
64	1.01	2.04	0.02	0.20
155	1.47	1.01	0.01	0.74
221	1.89	1.11	0.15	0.80
317	1.89	1.10	0.14	0.81
385	2.65	1.58	0.16	0.82
478	2.72	1.60	0.25	0.91
548	2.78	1.67	+0.01	0.87
640	2.89	1.86	0.55	0.87
730	2.91	1.88	0.57	0.88
797	2.92	1.92	0.57	0.75
888	2.96	1.94	0.59	0.92
Initial solution pH	9.2	10.3	10.7	11.0
Average final solution pH	8.3	8.8	9.8	9.1
Initial corrosion rate (64 hr) (mpy)	6.9	14.0	1.4	1.3
Final corrosion rate (888 hr) (mpy)	1.5	1.0	0.3	0.5

phosphate in these tests ranged from 100 to 400 ppm. Corrosion data on the 1030 carbon steel specimens are included in Table 3.13. The data on type 347 stainless steel are not included because the behavior of this material was exceptionally good in all tests. The specimens showed weight gains from 0.2 to 0.8 mg/cm<sup>2</sup> after 888 hr, and the surface areas not contacted by the carbon steel remained lustrous in appearance with light yellow color gradations. The contact areas were generally stained or dull black in color.

The requirement for sufficient trisodium phosphate to minimize cor-

rosion attack on coupled 1030 carbon steel increased to 400 ppm as compared to 300 ppm for uncoupled carbon steel. Some inhibiting effect was apparent in all concentrations of trisodium phosphate since the range of corrosion rates, 0.4 to 1.8 mils/year, was well below the 2.8 mils/year obtained in similar uninhibited systems. In the case of the 100-ppm solution, the initial corrosion attack for 64 hr was very high, 17.1 mils/year. However, the cumulative weight loss was relatively constant throughout the balance of the test and no tendency towards progressive increase in attack was observed. This was not the case in

[REDACTED]

FOR PERIOD ENDING AUGUST 15, 1951

TABLE 3.13

**Effect of Trisodium Phosphate on the Corrosion Behavior of  
SAE 1030 Carbon Steel Coupled to Type 347  
Stainless Steel in 0.005 M Hydrogen  
Peroxide at 200°C**

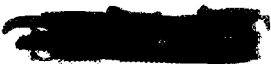
EXPOSURE TIME (hr)	CARBON STEEL WEIGHT LOSS (mg/cm <sup>2</sup> )			
	TRISODIUM PHOSPHATE CONCENTRATION			
	100 ppm	200 ppm	300 ppm	400 ppm
64	2.49	0.48	0.83	0.19
155	2.39	1.04	0.91	0.23
221	2.44	1.62	1.17	0.31
317	2.50	1.94	1.25	0.49
385	2.60	2.25	2.39	0.54
478	2.65	2.87	2.72	0.75
548	2.73	3.30	2.83	0.97
640	2.71	3.26	2.91	0.81
730	2.72	3.27	2.91	0.84
797	2.78	3.27	2.92	0.80
888	2.82	3.57	3.02	0.80
Initial solution pH	9.2	10.3	10.7	11.0
Average final solution pH	6.7	8.5	8.8	9.1
Initial corrosion rate (64 hr) (mpy)	17.1	3.3	5.7	1.3
Final corrosion rate (888 hr) (mpy)	1.4	1.8	1.5	0.4

the 200- and 300-ppm solutions. Here the initial rates of attack were low, 3.3 and 5.7 mils penetration per year, respectively, but corrosion attack was progressive to the end of the tests. The 400-ppm sample showed a low initial rate of 1.3 mils/year. The weight loss increased slightly for 548 hr but then leveled off at a fairly constant value of 0.81 mg/cm<sup>2</sup> for the remaining 340 hr.

The results from the 100-ppm test indicate that an initial conditioning of carbon steel surfaces with trisodium phosphate solution at 200°C would be beneficial in two

ways: (1) The initial corrosion reaction could be eliminated before the introduction of D<sub>2</sub>O by using ordinary distilled water as the solvent for the inhibitor; and (2) after preconditioning, it may be possible to operate the D<sub>2</sub>O system with a minimum concentration of trisodium phosphate, say 100 ppm, rather than the 400 ppm required to inhibit corrosion as determined by these tests.

The condition of the test samples was good as removed from the solutions. Although the contact areas with the type 347 stainless steel



## HRP QUARTERLY PROGRESS REPORT

discolored and stained black, there was no localized corrosion attack. The outer areas of the samples were progressively more lustrous in appearance as the trisodium phosphate concentration increased from 100 to 400 ppm.

Summarizing this group of tests, it appears that the minimum concentration necessary to reduce corrosion attack on SAE 1030 carbon steel, uncoupled and coupled to type 347 stainless steel, lies within the range of 300 to 400 ppm. This conclusion is based entirely upon the evaluation of data from stagnant laboratory tests and may be only an approximation of results obtained in the operation of the D<sub>2</sub>O reflector system where two additional variables are introduced, solution movement and continual production of D<sub>2</sub>O<sub>2</sub>.

*Effect of K<sub>2</sub>HPO<sub>4</sub> on the Corrosion Behavior of SAE 1030 Carbon Steel in 0.005 M Hydrogen Peroxide at 200°C.* A stagnant test was run in which 300 ppm of potassium hydrogen phosphate were added to the 0.005 M hydrogen peroxide solution to determine its effect as a corrosion inhibitor. The initial pH of the test solution was 7.6; the average pH value of the final solutions was 7.3. The test solution was replaced twice weekly. A corrosion rate of 1.0 mil/year was obtained for an exposure of 888 hr at 200°C, which was comparable to the rate obtained in the 200-ppm trisodium phosphate test and three times greater than the corrosion rate of carbon steel in 300-ppm trisodium phosphate solution.

The specimen exhibited a slightly metallic color with blue and red interference tints. No corrosion

scale deposition was observed, and localized corrosion attack was absent.

### DYNAMIC CORROSION STUDIES

E. E. Bohlmann            C. G. Heisig  
J. H. Gross                R. A. Lorenz  
                                 H. C. Savage

The presence of ammonium sulfate in the uranyl sulfate, which produced some unexpected results in early runs, has now been eliminated. This ammonium sulfate impurity in the uranyl sulfate resulted in the disappearance of uranium with a lowering of the pH of the solution (as measured on cold samples) during operation at 250°C. An equilibrium seemed to be reached at a concentration of uranyl sulfate somewhat lower than the starting concentration and dependent on the uranyl sulfate concentration, ammonium sulfate concentration, and temperature. It seems likely that the precipitation of a complex ammonium uranium sulfate on the walls of the system was the mechanism of the uranium disappearance. It was shown that the uranium disappearance could be prevented by lowering the pH of the uranyl sulfate solution through the addition of sulfuric acid. With a uranyl sulfate solution containing 30 g of uranium per liter a pH of 1.6 was shown to be adequate for this purpose, and solution stability was quite satisfactory. Corrosion also did not seem to be unusually severe, based on nickel concentration increase, but the run was not long enough to give more than an indication.

Since the presence of the ammonium sulfate was a side issue, no attempt was made to investigate its effects

FOR PERIOD ENDING AUGUST 15, 1951

further. The work of this quarter has emphasized the investigation of the effect of oxygen on solution stability and corrosion in the uranyl sulfate solution—type 347 stainless steel system.

**Loop A, Runs A-7 and A-8.** Additional runs totaling 852 hr have been made with  $\text{UO}_2\text{SO}_4$  containing 30 to 40 g of uranium per liter under varying partial pressures of  $\text{O}_2$  on pump loop A. This loop had previously operated for a total of 422 hr with a similar solution.<sup>(5)</sup>

The loop consisted of a Westinghouse Model 100A canned-rotor pump circulating a nominal 100 gpm through approximately 7 ft of 1½-in. Schedule 80 pipe made of type 347 stainless steel. Loop line temperature was held at 250°C, and super-pressure for the system was obtained by holding a side reservoir, the "pressurizer," at 285°C. At the nominal flow rate calculated mean velocity of fluid in the loop was 15 ft/sec. The pump bearings consisted of Stellite journals running in graphitar blocks at temperatures well below that of the system. To preserve proper pump loading, a machined flow restrictor was welded into the loop. At no time had this loop been given any pretreatment. The latest runs, designated A-7 and A-8, are summarized sequentially as follows:

- a. 26 hr:  $\text{O}_2$  cold partial pressure fell from 500 to 210 psig; no precipitation.
- b. 21 hr:  $\text{O}_2$  cold partial pressure fell from 100 to 75 psig; no precipitation.
- c. 18 hr:  $\text{O}_2$  cold partial pressure fell from 100 to 60 psig; no precipitation, although downward trend in cold pH indicated that precipitation was imminent.
- d. Decrement in system volume was made up with fresh solution.
- e. 78 hr:  $\text{O}_2$  cold partial pressure fell from 500 to 25 psig; no precipitation, although precipitation appeared imminent as the  $\text{O}_2$  pressure fell below ~50 psig. During all of this time, uranium had shown a tendency to concentrate in the line samples. A brief series of simultaneous line and pressurizer samplings showed that concentration of uranium in the line was at the expense of the pressurizer. Accordingly a bypass line from the pressurizer vapor space to the pump motor housing was installed, and about 1 gph of  $\text{H}_2\text{O}$  with accompanying  $\text{O}_2$  was permitted to re-enter the loop by leakage through the pump bearings.
- f. 51 hr:  $\text{O}_2$  cold partial pressure fell from 250 to ~0 psig. During the last 10 hr onset of precipitation was indicated by falling pH and rising dissolved iron values.

<sup>(5)</sup>" Pump Loop Studies," ORNL-1057, *op. cit.*, p. 52.



[REDACTED]

FOR PERIOD ENDING AUGUST 15, 1951

- c. 10 hr: Beginning run B-1 with  $\text{UO}_2\text{SO}_4$ , 200 psig  $\text{O}_2$ ; precipitation took place suddenly after 9 hr; 190 psig  $\text{O}_2$  remained.
- d. Cleaned with  $\text{H}_2\text{O}_2$ - $\text{H}_2\text{SO}_4$ ; charged new  $\text{UO}_2\text{SO}_4$  solution.
- e. 412 hr:  $\text{O}_2$  cold partial pressure varied between 500 and 300 psig. System was shut down regularly to replace sampling losses in the solution and to restore  $\text{O}_2$  to 500 psig. No sign of precipitation at any time. Two out of three qualitative tests for  $\text{CO}_2$  were positive.
- f. Beginning run B-2; new  $\text{UO}_2\text{SO}_4$  solution charged.
- g. 105 hr:  $\text{O}_2$  cold partial pressure fell from 50 to 40 psig; no indication of precipitation. All samples contained a brown-black powder which spectrographic analysis indicated was chiefly iron (oxide) with only traces of nickel and chromium.
- 919 hr Total time on all  
Stellite bearings
- 527 hr Total time on  
 $\text{UO}_2\text{SO}_4 + \text{O}_2$
- At this time the pump was torn down for inspection, the flow restricting orifice was cut out and sectioned, and a holder for three corrosion specimens was installed at a corner of the pumping circuit. The pump impeller had rubbed the balancing pads in its housing and had undergone severe corrosive attack; it was replaced with a new impeller. Stellite-Graphitar bearings were installed. A new flow restrictor was installed. Results of inspection of the system are discussed below.
- h. Etched with  $\text{HNO}_3$ -HF-HCl (except pump).
- i. 12 hr: Run B-3. 2%  $\text{CrO}_3$  solution,  $250^\circ\text{C}$ . Corrosion specimens of types 347, 316, and 316 ELC stainless steels removed; impeller removed, inspected, replaced. See discussion of observed corrosion below.
- j. 5 hr: New corrosion specimens of types 347, 316, 316 ELC stainless steels installed after etching. Ran on  $\text{H}_2\text{O}$ ; charged 1%  $\text{HNO}_3$ .
- k. 48 hr: Run B-4. 1%  $\text{HNO}_3$ ,  $250^\circ\text{C}$ . Removed corrosion specimens and impeller for inspection.
- l. 36 hr: Run B-5. 1%  $\text{HNO}_3$ ,  $250^\circ\text{C}$ . Annealed specimens of types 347, 316, and 316 ELC stainless steels. Inspected system as before.
- m. 6 hr: Beginning run B-6. Corrosion specimens from run B-4 reused. 6-hr pretreatment with  $\text{HNO}_3$ ; rinsed; charged  $\text{UO}_2\text{SO}_4$  solution.
- n. 205 hr:  $\text{O}_2$  cold partial pressure fell from 50 to 25 psig. Interrupted by 22-hr total power failure. One corrosion specimen broke

## HRP QUARTERLY PROGRESS REPORT

loose and lodged in the pump impeller for an undetermined period. The pump was not damaged. System inspected as before.

**Thermal Loops.** One thermal loop has been reworked to improve mixing of  $O_2$  with the solution, and several runs have been made with  $UO_2SO_4$ . Results have been erratic, and it is apparent that further reworking will be necessary to improve reliability of the information obtained from these devices.

**Results and Discussion.** The effects of oxygen on solution stability and corrosion and the effects of pretreatments during the runs of loops A and B are discussed below.

*Effect of Oxygen on Solution Stability.* There was one rapid precipitation in the first few hours of run B-1 under a 200-psig cold partial pressure of  $O_2$ . Aside from this single failure, all evidence indicates that the  $UO_2SO_4$  solution remains stable at  $O_2$  cold partial pressures approaching 0. In all cases except that mentioned above and one other, the system was leak-tested at 500 psig of  $O_2$  before proceeding at the same or lower  $O_2$  pressure. The importance of this point must be investigated further.

During all successful operations free  $O_2$  content of the system decreases, while corrosion, as indicated by dissolved nickel values, proceeds at an appreciable rate. Uranium content meanwhile remains sensibly constant (except for fluctuations due to poor mixing). On the other hand, in earlier experiments without oxygen, uranium precipi-

tated as oxide, with greatly accelerated generation of corrosion products, after brief periods of operation. Evidently oxygen may serve as a substitute corrosive and/or rapidly reoxidize uranium reduced in corrosion. Possibly, also, the corrosion reaction involves iron(II), and the oxygen limits corrosion by keeping all the iron oxidized to iron(III). The necessity of maintaining some concentration of  $O_2$  in the dynamic system is now considered to be established. Laboratory studies on the relation between corrosion and  $O_2$  utilization in the uranyl sulfate solution—type 347 stainless steel system were described in a previous section of this report.

*Corrosion.* By following the rate of increase of nickel in solution, it is possible to estimate a rate of corrosion in the total system under study. In most of the runs made to date there is an initial period of a few hours of fairly high corrosion rate, followed by a reasonably steady slower corrosion rate. Final rates have been estimated graphically for all of the runs described in the experimental section, except run A-7 ( $UO_2SO_4$ ) and run B-3 ( $CrO_3$ ). In run A-7 the rate was too erratic to estimate more than a continuous upward trend; in run B-3, the operation lasted only 12 hr. In all other runs the corrosion rate was in the range 0.2 to 0.3 mils/1000 hr for the whole system with  $UO_2SO_4$ , and an order of magnitude higher with 1%  $HNO_3$ .

These general penetration rates are based on average system volumes and submerged areas and include the contribution of localized accelerated corrosion. Their accuracy, therefore,

[REDACTED]

FOR PERIOD ENDING AUGUST 15, 1951

cannot be high. However, it appears that the order of magnitude of general corrosion rate is one that will be acceptable for the massive smooth-flow sections of the HRE.

Detailed inspection of pump parts, corrosion specimens, and pipe interiors in the pump loops has shown the existence of regions of moderate to severe corrosive attack apparently associated with high local flow rates.

At the end of run B-2, after loop B had run 392 hr on H<sub>2</sub>O and 527 hr on UO<sub>2</sub>SO<sub>4</sub>, the pump impeller was removed for inspection. During operation it had become slightly misaligned and had drifted forward so that an extensive portion of one-half of the front face had rubbed against the hydraulic positioning pads in the impeller housing. The outer part of the face was severely pitted all around. Welds were preferentially attacked. The inner lower velocity parts of the face were not so heavily pitted. This impeller was photographed and sectioned and has been the subject of rigorous examination, not yet complete, by different groups of investigators.

The flow restrictor was removed from loop B at this time also. The restrictor had consisted of an 1/8-in. thick orifice plate machined as part of a short length of tubing from bar stock. The short piece containing the plate had then been welded into the system. The upstream edge of the orifice was attacked with the removal of a fairly large amount of metal rather irregularly, as in the impeller. This attack progressed at one point completely through the plate as a small channel barely covered by

the blackened original inner surface of the orifice. Downstream from the orifice plate pitting had begun in the tool marks on the wall of the machined section and was also found in and on either side of the weld region where the machined section joined the system pipe. The weld upstream from the orifice plate also showed pitting. In both of these welds, considerable weld metal projected into the flow stream as berry-like blobs. Precautions taken in construction should preclude the occurrence of such welds in the HRE.

A few inches downstream from the orifice plate in loop B, a cooling jacket had been welded to the outside of the pipe. A ring of pits was found inside the pipe at this point. This section of the loop is still in use.

Other sections of the pipe, in which flow was presumably relatively smooth, did not display pitting. Rather, they were covered with a fairly thick black deposit, easily removed in flakes, after drying, to reveal a thinner and more adherent film.

At the end of run A-8, after loop A had operated for a total of 1700 hr, 1300 hr on UO<sub>2</sub>SO<sub>4</sub> and O<sub>2</sub>, the entire loop was sectioned and the pump was disassembled for inspection.

The impeller here was more generally attacked than in the case of loop B, but it did not display the small deep pits found in the loop B impeller. Instead, the appearance of the front face was scaly, with random high and low areas. Welds appeared to be somewhat more deeply penetrated than the rest of the metal.

## HRP QUARTERLY PROGRESS REPORT

In the impeller housing some pitting of the weld metal of the positioning pads was found. The outer (higher pressure) wall of the entry of the discharge channel was heavily attacked in an irregular pattern extending a short distance into the discharge line.

The flow restrictor in loop A was machined from bar stock and welded into the loop as in loop B. The throat was  $\frac{3}{4}$  in. in diameter,  $\frac{1}{2}$  in. long, and had conical approaches on each side. The upstream edge was heavily attacked, and the downstream half of the restriction was severely pitted.

The welds in loop A in which full penetration had not been obtained showed extension of the remaining fissures by pitting.

In straight runs of pipe, slight pitting was found in a number of areas. Moderate pitting occurred at points where apparatus had been welded to the outside of the pipe.

A new impeller was installed for run B-3, 2% chromic acid at 250°C. After 12 hr this run was ended because of a leak. The impeller had been badly pitted and dimpled, particularly on the front face, although the weld spots were not pitted at all (compare previous impeller, loop B). Corrosion specimens of stainless steels 347, 316, and 316 ELC were all pitted in the same fashion as the impeller.

The impeller was reinstalled and remains in use for lack of a replacement. Runs B-4 and B-5 with 1% HNO<sub>3</sub> were then conducted as outlined in the operational summary.

The as-machined specimens of run B-4 each suffered a weight loss of about 300 mg (exposed area approximately 0.8 in.<sup>2</sup>). The loss was patterned, apparently being most severe in the highest flow regions. A few irregular "islands" of relatively little attack remained. These islands were covered with a black deposit. Regions in which appreciable amounts of metal had been removed were of a sandy appearance; some area was blackened, and some had no visible coating. In run B-4 the pits in the impeller increased in number and size.

In run B-5 the annealed specimens of the three steels were stripped of metal over their entire areas, except for a very few small blackened "islands." The weight loss here was about 600 mg on each specimen. The stripped areas had no black coating; bare metal of sandy texture appeared everywhere except in the small protected islands. The increase in size and number of impeller pits continued about as before.

As shown in the operational summary, run B-6 was a 200-hr UO<sub>2</sub>SO<sub>4</sub> plus O<sub>2</sub> run following a 6-hr 1% HNO<sub>3</sub> pretreatment. The corrosion specimens were those of run B-4, 48-hr 1% HNO<sub>3</sub> pretreatment. Very definite flow patterns of attack were found on these specimens. Extensive bare metal areas were bordered by steep undercut walls up to 0.020 in. high; past the borders of the bare areas considerably less metal had been removed, and the rough new surface was blackened. In still less severely attacked areas tool marks from the original machining were well defined through the protecting black layer. The impeller showed a considerably increased number of pits after this

[REDACTED]

FOR PERIOD ENDING AUGUST 15, 1951

run, some of the shallow smooth "dimples" of the previous inspection having become rough red-bottomed "pits." At some time during the run, at least 50 hr before the end, the specimen of 316 ELC stainless steel broke out of the pedestal and lodged in the impeller for the rest of the run. It is of interest to note that the pump was not damaged by this treatment.

Three degrees of corrosive attack appear on all of these specimens. Evidently in the beginning a protective film of some kind is laid down, at least in some areas. The first degree of attack is then shown by those areas (the "islands") in which the original film is able to resist removal because of a low local flow rate or because of an unknown local surface condition, with the result that little or no metal is removed. The second degree of attack is represented by the areas which are blackened, although considerable metal has been removed. Apparently in those areas the black film is removed by erosion and re-established by chemical action at comparable rates, so that metal is consumed at less than the maximum possible rate. The third degree of attack is unretarded removal of metal from a bare surface on which no protective film can be maintained, probably because of rapid erosion, or possibly because these sections of the surface become anodic in an electrolytic process.

From examination of the pipe interiors and pumps it appears that the first degree of attack takes place in the smooth-flow moderate velocity sections of straight pipe, and that the second and third degrees

of attack take place in regions of high fluid velocity and turbulence, and perhaps in and near welds.

*Pretreatment.* The long successful runs with  $\text{UO}_2\text{SO}_4$  plus  $\text{O}_2$  in loops A and B were made without benefit of any conventional pretreatment. The general corrosion rate was not excessive, although severe local corrosion took place. Runs B-3, B-4, and B-5 were made with conventional pretreating solutions to investigate the pretreatment effect. The general corrosion rate (dissolved nickel increase) was about 10 times the rate with  $\text{UO}_2\text{SO}_4$ , and regions subject to accelerated corrosion were very badly attacked. The rate of dissolved nickel increase in the  $\text{UO}_2\text{SO}_4$  run immediately following the pretreatment runs was somewhat larger than in previous nonpretreated runs.

These results suggest that  $\text{UO}_2\text{SO}_4$  solution bearing  $\text{O}_2$  quickly establishes at least as good a protection of the system as do the conventional pretreatments, and with less removal of metal from the system. Thus the results to date indicate that pretreatment in the dynamic system is useless. It is to be emphasized, however, that this deduction is not yet based upon sufficient information to be conclusive.

*Future Work.* Present plans for dynamic pump loop operation include a run with a new loop at  $150^\circ\text{C}$ . This run will be made with no pretreatment and no added oxygen, if this is feasible, to investigate solution stability and corrosion at this lower temperature. Comparison of results obtained in specific high-flow areas will also be of interest.

██████████

## HRF QUARTERLY PROGRESS REPORT

A loop is being prepared for operation in the presence of mixtures of hydrogen and oxygen. The effect of fission products (simulated by the addition of a "representative" group of sulfates) will also be investigated. Ultimately the combined effects of stoichiometric quantities of hydrogen and oxygen and fission products will be investigated in a single loop with the objective of

simulating HRE conditions as nearly as possible.

In view of the favorable results obtained in static corrosion tests with titanium, specimens of this metal will be compared with type 347 stainless steel specimens in high-flow areas where the attack on the stainless steel specimens has been very great.

#### 4. RADIATION STABILITY

H. F. McDuffie, Leader

J. W. Boyle	J. F. Manneschildt
F. J. Fitch	D. M. Richardson
T. H. Handley	J. Ruth
K. A. Hub	F. H. Sweeton

**Radiation Experiments in the Graphite Pile.** During the past quarter a set of three bombs previously irradiated for a short period (5 days) in hole 12 of the graphite pile was opened and the contents were analyzed. A set of five bombs was removed from hole 60 of the graphite pile after a very long period of irradiation [2280 hr (95 days)], allowed to decay for 6 weeks and then opened for analyses of the solutions. Residual solutions from two untreated bombs, irradiated in hole 12 at much earlier dates for 7 and 14 days, were analyzed for nickel in connection with the corrosion situation. The results of all these analyses are presented as Table 4.1, together with some information concerning a set of bombs now under irradiation in hole 60.

The outstanding conclusion which might be drawn on the basis of these experiments is that the longer irradiation has apparently not produced deterioration of the solution. The clear yellow solutions removed from the bombs correlate well with the observed maintenance of residual gas pressure during the experiment (evidence for fission fragment decomposition of water, from which it is inferred that uranium was in solution). The relatively low concentrations of nickel found in the solutions (when compared with other

solutions which had been heated out of radiation and in the absence of oxygen, the test given these bombs before they were subjected to irradiation) are encouraging and indicate that radiation is not increasing the corrosion problem. Furthermore, the nickel concentrations are not higher than those found in corresponding irradiation tests of short duration.

With respect to corrosion it should be emphasized that experience during the past two quarters has led to greater knowledge concerning solution stability. Accordingly, the experiments now in progress are being carried out in bombs which were *not* heated for long periods of time in the absence of radiation and added oxygen. Moreover, the temperature of the bombs is lowered whenever the neutron flux of the pile goes down; thus the present tests are effectively tests of radiation corrosion and radiation stability rather than tests of both radiation and nonradiation conditions.

**Out-of-Pile Bomb Experiments.** The experiments, reported in the last quarterly,<sup>(1)</sup> directed to the use of oxygen both as a pretreating agent and as a stabilizer during

(1) "Out-of-Pile Studies of Stainless Steel Bomb-Fitting-Tubing Assemblies," *Homogeneous Reactor Project Quarterly Progress Report for Period Ending May 15, 1951*, p. 73 (Oct. 10, 1951).

TABLE 4.1

## In-Pile Radiation Experiments with HRE Constituents

BOMB NUMBER	PRETREATMENT		URANIUM CONTENT OF SOLUTION AFTER SUCCESSIVE OUT-OF-PILE HEATING PERIODS (mg/ml)	HOLE FLUX	LENGTH OF RADIATION (days)	INITIAL URANIUM (mg)	FINAL URANIUM IN SOLUTION (mg)	URANIUM RECOVERED IN SOLUTION (%)	NICKEL (mg/ml)	pH
	TYPE	TEMP. (°C)								
316	Nitrate	250	42.4, 42.8, 40.9, 42.9	12-full	5	253	235	92.9	1.29	2.45
324	Nitrate	290	42.8, 43.4	12-full	5	252	233	92.5	0.49	2.55
325	Nitrate	290	42.4, 44.2	12-full	5	252	216	85.7	1.04	3.67
321	Nitrate	275	41.6, 44.2, 43.4, 40.6, 40.4, 28.7	60-full	95	253	206	81.5	0.75	2.9
328	Chromate	275	44.0, 66.4, 36.0	60-full	95	265	200	75.5	0.25	3.0
330-D	Chromate	275	38.0, 36.0	60-full	95	209	170	81.5	0.62	3.7
330-S	Chromate	275	36.0	60-full	95	215	175	81.5	0.93	2.85
331-D	Nitrate	275	39.4, <1.0	60-full	95	208	148	71	0.95	3.35
283	None			12-full	7	330	282 ± 14	85.5	0.33	
304	None (etched)			12-half	14	181	158 ± 8	87	0.20	4.0
357	Chromate	275	(Inserted 7-23-51)			239				
358	Chromate	275				241				
359	Oxygen, 400 psi	275				242				
361	Oxygen, 400 psi	275				233				
362	None					235				

heating with uranyl sulfate have been carried forward during the past few months. A repeat set of type 347 stainless steel bombs pretreated with oxygen in the presence of water was compared with bombs having no pretreatment, both being tested with uranyl sulfate solution containing 40 g of uranium per liter under varying oxygen pressures. The results are presented as Table 4.2. There is no evidence from these results that the oxygen pretreatment added significantly to the protection afforded by the use of oxygen during the test run.

When solution instability occurs after a short heating period, there is usually formed a black precipitate in a water-white solution of low pH. This suggests partial reduction of the uranyl ion and hydrolysis to  $U_3O_8$ . In order to test the reversibility of this situation, bomb number 347 (reported in previous quarterly, ORNL-1057, page 75, as bad after 24 hr heating; no pretreatment and no oxygen present during heating) was placed under 400 psi oxygen pressure and heated overnight at

275°C, after which the solution was found to be clear yellow. The uranium content had risen from less than 2.0 to 52.2 mg/ml. The oxidation of reduced uranium back to the hexavalent state may have been followed or accompanied by oxidation of the ferrous ion to the ferric state, after which the ferric sulfate was hydrolyzed while the  $UO_3$  was reconverted into uranyl sulfate. This chemical reaction proceeds with iron or chromium compounds; nickel, however, does not hydrolyze and remains in solution, tying up sulfate ions. Presumably if a stoichiometric amount of nickel were removed from the bomb wall by corrosion the sulfate would remain unavailable, and the uranium could be oxidized to  $UO_3$  without coming back into solution.

**Experiments at Higher Fluxes.**  
During the quarter a second exploratory experiment in a vertical hole in the LITR was carried out. Using uranyl sulfate containing 40 g of uranium per liter and 93% enrichment, an equilibrium pressure of 7500 psi (steam +  $2H_2$  +  $O_2$ ) was reached at 280°C using a 500-kw power level

TABLE 4.2

Effect of Oxygen on Stability of HRE System

RUN NO.	OXYGEN PRESSURE (psi)		CONDITION OF SOLUTION AFTER HEATING AT 275°C	
	PRETREATMENT	TEST	75 hr	240 hr
349	200	200	Precipitated	Precipitated
350	400	400	Clear yellow	Clear yellow
351	600	600	Clear yellow	Clear yellow
352	None	200	Clear yellow	Clear yellow
353	None	400	Clear yellow	Clear yellow
354	None	600	Clear yellow	Precipitated

~~SECRET~~

# HRP QUARTERLY PROGRESS REPORT

TABLE 4.3

G Values for HRE Reflector Solutions

SOLUTION	G VALUE	REMARKS
500 ppm Na <sub>3</sub> PO <sub>4</sub>	0.7 - 0.8	All determinations were at less than atmospheric pressures and at pile-ambient temperatures
250 ppm Na <sub>3</sub> PO <sub>4</sub>	0.7 - 0.8	
0.005 N NaOH	0.7 - 0.8	
Saturated Mg(OH) <sub>2</sub>	0.6 - 0.7	

(half flux). Data were obtained at power levels up to 1000 kw, temperatures up to 280°C, and pressures up to 8000 psi. After the experiment was terminated because of mechanical difficulties the apparatus was re-designed in the interests of greater safety and convenience of operation. The modified apparatus is now being finished in the shops and is nearly ready for assembly and testing.

For long-term irradiations in horizontal holes of the LITR careful calculations have been carried out with respect to gamma heating, heat transfer, temperature control, and shielding. Apparatus for these irradiations has been designed, and the critical parts are now being tested in the laboratory.

**Radiation Effects on the HRE Reflector System.** An estimation of the gas evolution to be expected in the reflector has been made by irradiating quartz ampoules filled with light water containing 500 ppm of trisodium phosphate (Na<sub>3</sub>PO<sub>4</sub>), 250 ppm of trisodium phosphate, 0.005 N NaOH, or saturated with Mg(OH)<sub>2</sub>. Bombs made of SAE 1030 carbon steel

containing solutions of 500-ppm trisodium phosphate or saturated Mg(OH)<sub>2</sub> gave indications of the steady-state pressures to be expected in gamma and neutron fluxes comparable to those of the graphite pile and at temperatures of 100 to 140°C.

Estimations of the G values for the above solutions have been made on the basis of ampoule studies and are presented as Table 4.3. G is calculated as the number of hydrogen molecules produced in the solution per 100 ev of energy input. The energy input was determined from the value for water given by D. M. Richardson in ORNL-129.<sup>(2)</sup> The energy from the n-p reaction on phosphorus was neglected.

It appears that oxygen over the solution increases the decomposition rate slightly, whereas hydrogen over the solution decreases the decomposition rate slightly.

---

<sup>(2)</sup>D. M. Richardson, *Calorimetric Measurement of Radiation Energy Dissipated by Various Materials Placed in the Oak Ridge Pile*, ORNL-129 (Oct. 1, 1948).

[REDACTED]

FOR PERIOD ENDING AUGUST 15, 1951

Instrumental troubles have limited the accuracy of the determination of the steady-state pressures in metal bomb systems under irradiation. The first 3 or 4 days of the test showed a gradual pressure increase with a tendency to level off. After an irradiation of 3.5 weeks at 100 to 140°C there was 30-psi residual gas pressure ( $2H_2 + O_2$ ) over the  $Mg(OH)_2$  system and 90-psi residual gas pressure over the 500-ppm  $Na_3PO_4$  system.

Further work is in progress using  $D_2O$  instead of  $H_2O$  as a final check on the gas production by the reflector system.

**Plans for Next Quarter.** Examination of the heavy-water reflector system will be carried to a definite conclusion, using heavy water from the same containers and in the same

condition as that which will be used in the HRE.

Long-term irradiations in hole 60 will be continued, and shielded facilities will be provided so that bombs can be opened and solutions can be analyzed without the necessity for a long radioactive cooling period.

Apparatus for further exploratory experiments using a vertical hole in the LITR will be completed, and the experiments will be resumed. Particular attention will be given to studies of uranium peroxide precipitation under different combinations of flux and temperature.

Apparatus for long-term irradiations in the LITR using horizontal beam holes will be completed, and experiments will be initiated.

# HRP QUARTERLY PROGRESS REPORT

## 5. ENGINEERING COMPONENT STUDIES

C. B. Graham, Leader

J. O. Bradfute	C. W. Keller	H. C. Savage
J. S. Culver	H. I. Kraig	I. Spiewak
J. I. Gonzalez	R. A. Lorenz	R. Van Winkle
P. N. Haubenreich	J. A. Ransohoff	R. H. Wilson
C. G. Heisig	W. L. Ross	C. D. Zerby

### MECHANICAL ASPECTS OF SOUP RECIRCULATING TEST LOOPS

P. N. Haubenreich	C. G. Heisig
H. I. Kraig	R. A. Lorenz
W. L. Ross	H. C. Savage

Operation of the soup recirculating test loops has established the requirements necessary to maintain solution stability and minimize corrosion (see section on *Dynamic Corrosion Studies*, p. 42). The essential requirement appears to be an adequate supply of dissolved oxygen in the recirculated solution. An oxygen concentration as low as 20 ppm has maintained solution stability satisfactorily for periods as long as several hundred hours.

To maintain the required oxygen concentration the following two methods have been used.

1. Diffusion of oxygen gas at 300 to 500 psi\* from the pressurizer into the loop).
2. Oxygen gas at 50 psi in the pressurizer and with a bypass of approximately 0.5 gph of condensate from the top of the pressurizer to the rear of the pump rotor cavity and into the loop through the pump.

\*All He and/or O<sub>2</sub> pressures are those measured with the system at room temperature.

Test loop A has been run ~800 hr (runs A-7 and A-8) with uranyl sulfate, and solution stability has been satisfactorily maintained using an oxygen partial pressure in the steam pressurizer. In run A-7 a total gas pressure (oxygen + helium or oxygen) of 300 to 500 psi\* was necessary to maintain solution stability. The system consisted of a vapor space of approximately 4 liters above 9 liters of solution. With lower gas pressures it was necessary to operate the pressurizer at substantially 285°C to maintain the system pressure of 1000 psi. Under these conditions the pressurizer very effectively stripped the oxygen out of solution. With oxygen pressures of 300 to 500 psi, the pressurizer could be operated at lower temperatures (~250°C) and still maintain the required system pressure. Under these conditions an adequate amount of oxygen was present in the solution to prevent uranium reduction. This condition had one disadvantage in that all undissolved gas accumulated in the rear of the Westinghouse pump and periodic venting was required. In addition to endangering the pump bearings, the gas was soon vented off so that the required pressure was lost and frequent shutdowns were required for oxygen additions. One additional fact which emerged from the above tests was that the oxygen and/or helium gas and steam stratified, i.e., the oxygen and/or helium remained in

FOR PERIOD ENDING AUGUST 15, 1951

the topmost part of the pressurizer vapor space and the steam in the lower part. This was verified by pressure measurements and by a temperature survey through the vapor space. This same effect is found by the Argonne group in their work with a loop in the X-10 pile and by others.

These observations led to the installation of a bypass line connecting the top of the pressurizer to the rear of the pump rotor cavity. With the pump in operation, the pressure difference between these two points will maintain a flow of condensate and gas to the rear of the pump cavity and thus to the recirculating line. A condenser in this bypass keeps the fluid cool. A flow rate in the order of 0.5 gph or less will result in solution stability. Oxygen pressure in the pressurizer (measured cold) is not over 50 psi. In order to determine or estimate the amount of oxygen in solution required to maintain stability, samples of soup for analysis of dissolved gases are taken at operating conditions. Based on the method of sampling and analysis now in use, oxygen concentration as low as 20 ppm will maintain solution stability. Using the same procedures, a sample taken from a thermal loop in which precipitation of the uranium had started showed zero oxygen concentration in the solution.

**Examination of Loop After Operation.** At the conclusion of run A-8 on pump recirculating loop A, the pipe was removed and cut up for inspection and evaluation of corrosion and erosion in the loop. The loop operating time was 1750 hr. Corrosion in the form of pitting was evident at sections of the loop with reduced cross-sectional area and in highly turbulent areas (around welded pads in impeller

housing). Most of the interior of the 1½-in. Schedule 80 pipe (type 347 stainless steel) was in very good condition and had a smooth, tightly adhering, black coating. Corrosion was also noted at welded joints where excess metal had penetrated the joint. This loop had been subjected to numerous precipitations, etches, and passivations and was in relatively good condition considering these factors. The loop is now being rebuilt using 1-in. pipe and maintaining the same standard of welding in use on the HRE.

A second pump loop, designated as loop B, was completed and is now running. An operation time of 1400 hr has been accumulated on loop B, approximately 1000 hr with uranyl sulfate. Operating conditions have been 250°C in the recirculating line, 285°C and 1000 psi pressure in the pressurizer. Uranyl sulfate solution containing ~40 g of uranium per liter has been used entirely. The pipe in loop B is 1-in. pipe with average velocities of ~30 ft/sec.

A section of the pipe in loop B was removed after ~1000 hr operation (~500 hr with uranyl sulfate). The corrosion effects were approximately the same as in loop A. Pitting was observed at restricted sections and at welded joints where excess weld metal had penetrated the joints. This system had not been subjected to as wide a variety of conditions as loop A but had been attacked by 2% chromic acid during a passivation. Chromic acid is too corrosive for use in the loops and causes excessive pitting.

**Pretreatment of the Loops.** In regard to the pretreatments necessary in the HRE system for solution stability and/or reduced corrosion rates,

## HRP QUARTERLY PROGRESS REPORT

the following observations have been made in the pump loops:

1. Passivation with 1% HNO<sub>3</sub> or 2% CrO<sub>3</sub> does not appear to enhance solution stability. Solution stability is maintained only by a sufficient concentration of oxygen in solution.
2. Passivation does not appear to reduce corrosion rates as measured by nickel concentration in samples of solutions taken during operation.

In general the only requirement seems to be that the loops be clean and free of grease. This is only desirable to the extent of solution contamination and protection of pump bearings. In other words, no differences in solution stability or corrosion rates (although very little information is available as yet) is noted, whether the loop is run with a minimum cleaning (such as circulating a 3% solution of trisodium phosphate at ~150°C in the loop followed by thorough rinsing with distilled water) or whether the system is carefully etched with acid followed by passivation with 1% nitric acid at 250°C.

The above points are being investigated as thoroughly as possible, and just recently all loops were provided with openings and holders for corrosion samples.

A third pump recirculating loop, loop C, has been used only to test a Model 30A Westinghouse pump. This pump was run ~300 hr recirculating water and was sent to the HRE site for installation in the D<sub>2</sub>O system. A model 100A pump has been installed in loop C and test work will begin

in a few days. Present plans are for this loop, with corrosion samples, to be run with uranyl sulfate at 150°C to determine differences in solution stability and corrosion rates as compared to 250°C.

Long range plans include the construction of ~12 additional pump recirculating test loops. However, two or three additional loops will be constructed as soon as possible to be used as follows:

1. One loop to be used for mechanical test work on Model 100A pumps.
2. One loop to be constructed with a letdown system (heat exchanger, valve, etc.) and a Pulsafeeder pump. This system will be used to test corrosion rates and solution stability in this part of the HRE. It may be possible to do some of this work in the mock-up on the first floor of Bldg. 9204-1, Y-12 Area.
3. One loop will be constructed of steel and will have a Model 30A pump installed to check corrosion rates of the D<sub>2</sub>O system.

**Westinghouse Pump, Model 100A.** A recirculation pump bearing program to increase the reliability of the Westinghouse 100A pump has involved the proper selection of materials and design for the bearings.

At the present time the Model 100A Westinghouse pump as modified with Stellite 98M2 journals (and possibly Stellite 98M2 bearings), improved thrust pads, and tantalum seal rings

[REDACTED]

FOR PERIOD ENDING AUGUST 15, 1951

is believed reliable enough for installation in the HRE. It is believed that a minimum of 3000 to 4000 hr of trouble-free operation would be expected, providing the seal rings continue to operate satisfactorily. The metal bearings appear to be just as satisfactory but less operating experience has been accumulated. A new bearing design would possibly increase the life expectancy of the bearings and allow the elimination of the thrust pads. The pads are a source of concern from the corrosion standpoint.

**Bearings.** Several of the Stellite materials have been tried with excellent results. The pump in test loop A is equipped with Stellite No. 6 journals and Graphitar No. 14 bearings. After 1750 hr operation, wear was not measurable by the methods used ( $<0.0005$  in.), except for an initial wear of  $\sim 0.001$  in. resulting from oxide particles during a precipitation.

Since chemical results indicated that carbon was detrimental to solution stability, a metal to metal bearing was installed in the pump in test loop B. Stellite 98M2 was used and is now considered the best material tried to date. These bearings were operated for  $\sim 1000$  hr. At this point a routine shutdown revealed that wear on the thrust surface of the front bearing was excessive. This wear resulted from excessive thrust load which developed when the stainless steel seal rings corroded excessively. No wear of the radial surface could be detected. This pump is now operating with Stellite 98M2 journals and Graphitar No. 14 bearings. At the present stage, the Stellite 98M2 journal against Graphitar

No. 14 bearings appears to be the most reliable combination. This combination seems to give better service on the thrust surfaces as compared to the metal to metal bearing as presently designed. Operating time on Stellite 98M2 and Graphitar No. 14 is  $\sim 500$  hr in the pump.

Based on the approximate experimental evidence accumulated there is no apparent difference in solution stability or the amount of oxygen required in loops with and without the Graphitar pump bearings.

Investigation has shown that the bearings as designed are not capable of withstanding possible thrust loads developed by the pump. The present solution developed by Westinghouse is the addition of welded pads on the front and rear surfaces of the impeller housing. With these pads it is possible to eliminate the thrust load on the bearings by proper location of the impeller. However, there are two distinct disadvantages to this method: (1) The thrust pads are close to the impeller and areas of high velocity and turbulence are created with a resulting increase in the corrosion rate, and (2) there is no guarantee that the thrust load is permanently eliminated. Wear or corrosion around the impeller seal rings changes the hydraulic thrust balance. Thus, a pump initially balanced with respect to thrust may become unbalanced enough to cause bearing wear after a period of operation.

A bearing has been designed with an area large enough to take the maximum expected thrust loads. The design also features a self-aligning bearing face. This design is expected to permit elimination of the thrust

## HRP QUARTERLY PROGRESS REPORT

pads. When the pads have been removed, the pump will be tested for thrust load, and, if excessive, the diameter of the seal rings will be changed. In this way, the magnitude of the thrust load may be reduced to a satisfactory value.

One method of correcting the difficulties resulting from the thrust pads is to refine the pads and install more reliable seal rings. Since the pads on the pumps received are unfinished weld metal applied with the electric arc welder and are of non-uniform height, a rework is mandatory to minimize corrosion if the pads are retained. On one pump, the original pads have been removed and new pads applied with the Heliarc welder. These new pads were carefully machined to a uniform height and polished. No operating data on these pads are available to date. With respect to the seal rings, several different types are under trial. However, no conclusive results have been obtained. At present, rings of tantalum show the best corrosion resistance.

**Double-Discharge Pump.** To minimize the radial load on the bearings a double-discharge pump was tested on the radial load tester. Tests showed the radial load with open discharge to be 1/2 to 1/3 that of the single-discharge pump. Unfortunately, this saving is negated by a vibration condition which is induced in the pump by the new flow conditions. There is, however, some optimum operating point where throttling of one discharge will present the most mutually desirable condition of radial load and vibration. The vibration may also be reduced or eliminated by reducing the diameter of both discharge throats. This was not tested, and no further work is contemplated on the double-

discharge pump since other corrections have reduced the wear on the radial bearing faces to a satisfactory value.

**Pulsafeeder Pumps.** A Model 5-100 Lapp Pulsafeeder pump has been under test for some time. This pump is rated at 1 gpm at 1000 psi. As received, this pump contained stainless steel diaphragms in bolted heads. Diaphragm failure was noted after 1000 hr of operation with uranyl sulfate at  $\sim 80^{\circ}\text{C}$  and pumping at rated head and flow. Cause of the failure is unknown. Studies of the diaphragm are under way, but no specific reason for failure has been found as of now.

The diaphragm in the intermediate head was replaced, and a new remote head of all welded construction was installed. To date these two heads have been in operation  $\sim 1700$  hr ( $\sim 1300$  hr on soup) with no apparent failure. A sample of water is taken from between the heads at regular intervals to check for any leakage of either oil or soup.

### OPERATION OF THE HRE MOCK-UP

J. S. Culver	C. W. Keller
J. A. Ramsohoff	R. Van Winkle
R. H. Wilson	C. D. Zerby

The problem of removing gas from the core of the HRE has been studied in two steps. Early work centered around development of a geometry for the core itself to provide a means of removing the gas as rapidly as possible from the critical volume. Once the gas was removed from the critical volume. Once the gas was removed from the core there still remained the problem of reducing its pressure to essentially atmospheric

where it could be handled by the recombiner system. The latter problem has occupied a good portion of the effort expended on the HRE mock-up.

The capacity of the Pulsafeeder pump has been increased resulting in improvement in the performance of the letdown system. The 10- and 40-kw boilers are operating satisfactorily, although some improvement in controls is desirable.

The recombiner system is being tested and is fundamentally satisfactory. A number of improvements are required, and an operating technique is being developed.

**Letdown System.** Previous quarterly reports have covered early developments of the gas and liquid letdown system in some detail, so this report will be confined to the system which is now proposed for the reactor.

The system as tested with water and helium operates satisfactorily with the limitation that the liquid flow from the Pulsafeeder must be kept greater than 0.8 gpm. Since the normal output is 1.5 to 1.6 gpm, the condition is met except in case of gas binding of the pump. Several relatively minor details must be checked before the letdown system can be considered to be completely satisfactory. These include: (1) the effect of recommended changes in the inlet and discharge connections to the exchanger, (2) final adjustment of the pressurizer level control (discussed elsewhere in this report), and (3) the severity of corrosion under operating conditions.

Since approximately 1gpm of liquid is removed with the gas, the principal problem studied was the inherent

tendency for slugging found in two-phase flow systems. Under certain conditions, this slugging would initiate a continuous series of large rhythmic pressure surges or oscillations at the letdown valve. The effect of these surges was transmitted back to the core and pressurizer, causing a change in volume of the vortex void and a continually changing pressurizer level. Since the letdown valve is controlled by the pressurizer level, such surges would make smooth automatic control impossible.

A satisfactory system is one in which the letdown system is discharged surge free under all normal conditions of gas flow and temperature to be encountered in reactor operation. All efforts have been directed to this end, and the resulting system and its limitations are described below.

**Apparatus.** Referring to Fig. 5.1, it is seen that the entire mock-up flow sheet duplicates the reactor soup system in all details except for the main soup heat exchanger which has already been installed at the reactor site. The critical items such as the pressurizer, letdown heat exchanger, and letdown valve are all identical to those to be used in the reactor. The core itself is geometrically identical to the reactor core, and a 100A Westinghouse pump is used to provide circulation of the main soup stream. Water was used in all tests, and helium was injected into the soup inlet port to simulate the  $H_2$  and  $O_2$  expected to be generated in the reactor.

A small constriction in the letdown stream close to the core and a surge tank in the system adjacent to

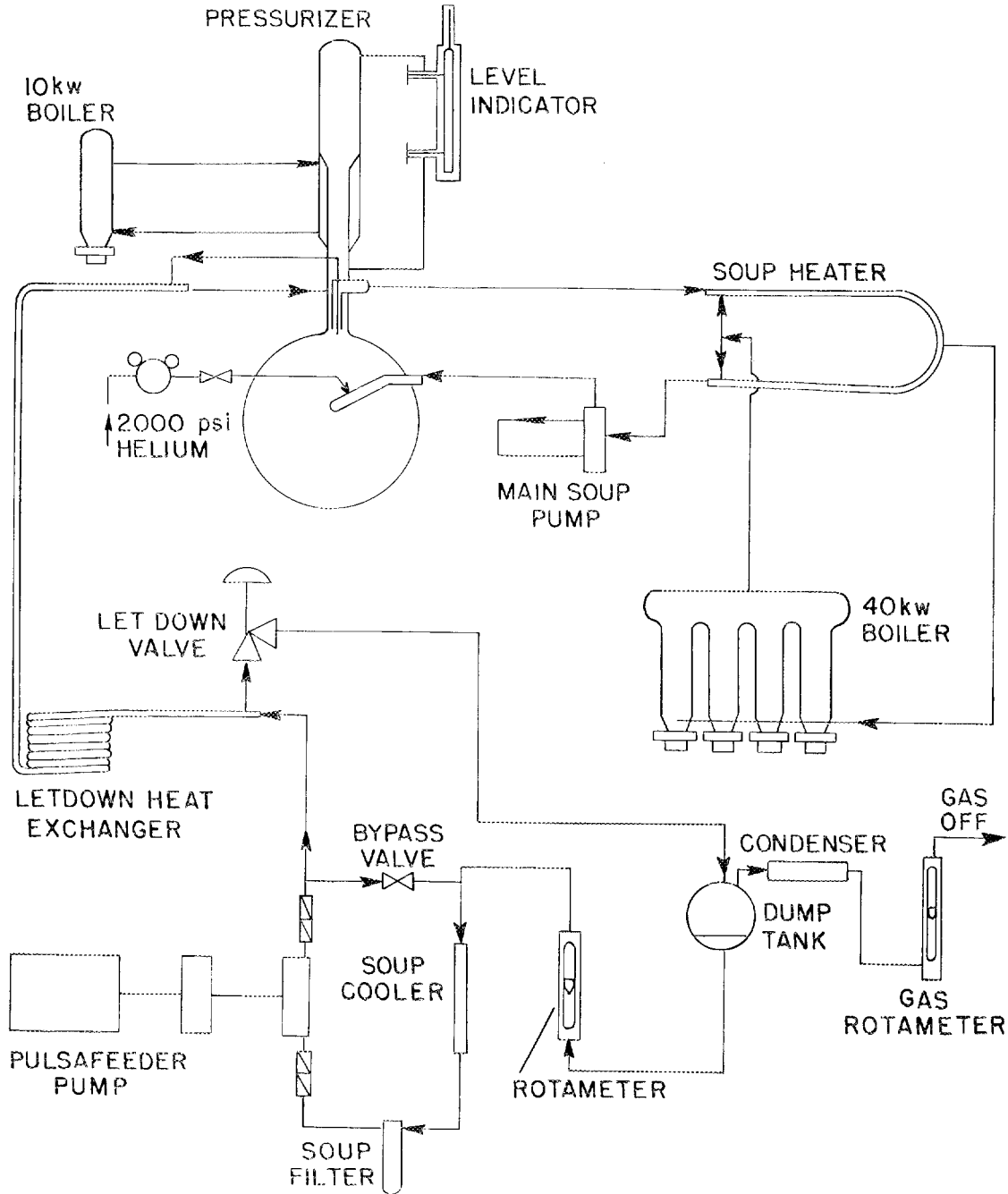


Fig. 5.1 - Flow Diagram of the HRE Mock-up.

the letdown valve were removed from the original system to provide as clean a system as possible with a minimum of high-velocity passages which might promote cavitation or corrosion. Although this simplified system is not stable over as wide a range of conditions as the original, it is deemed satisfactory for all expected operating conditions.

**Performance of the Letdown System.**  
All tests show that when the soup output of the Pulsafeeder pump (1.6 gpm) is flowing through the letdown valve with the gas stream, the system will not oscillate at operating temperatures between 100 and 250°C. Gas flow was varied from 0 to 1000 cfh, which is equivalent to the expected gas flow at 1000 kw based on 50 ev per molecule of H<sub>2</sub>O dissociated.

In an effort to understand better the nature of the conditions producing the oscillation, the liquid flow rate was progressively reduced and the gas rate was continually varied over a wide range. This investigation revealed a minimum liquid flow which will give steady operation. This

minimum liquid flow varies with the temperature of the system entering the letdown heat exchanger. The results are shown in Fig. 5.2.

From the standpoint of the reactor design, one can feel reasonably sure that if the system is identical to the one tested and the liquid flow exceeds the minimum indicated on the curve, no oscillation will occur. Any small change in geometry must be thoroughly tested since such seemingly unimportant details as the small constriction in the letdown stream, direction of approach to the letdown valve, and accidental constrictions in the letdown heat exchanger have profound effect on the stable range of the system. A device will be developed to measure the flow to the Pulsafeeder pump and to give a signal if it drops to 1 gpm.

**Development of Pulsafeeder Pump.**  
Tests of the Pulsafeeder pump as received, but installed with piping to simulate the reactor arrangement (i.e., distance of oil and water piping and location of water and soup heads), showed the maximum reliable output to be 0.6 gpm at 1000 psi. Based on experience with the letdown system, this was known to be insufficient to prevent oscillation of the high-pressure system. Consultation with the manufacturer of the pump established a maximum safe displacement in the heads for reasonable diaphragm life. This maximum displacement was more than the displacement required to pump 1.6 gpm. A larger diameter piston and cylinder for the oil pump was ordered from Vickers Company.

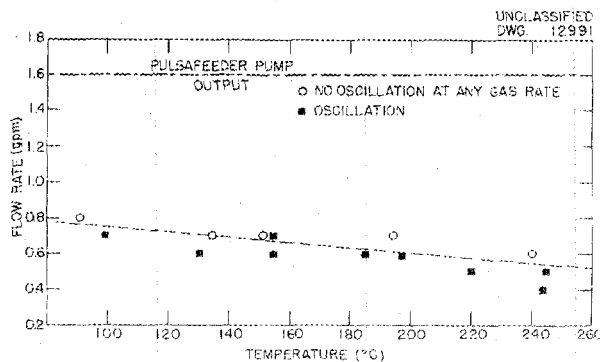


**Fig. 5.2 - Liquid Flow Rate vs. Temperature Entering Letdown Heat Exchanger.**

To allow immediate testing with the Pulsafeeder pump, a brass cylinder and steel piston fitted with cup

## HRP QUARTERLY PROGRESS REPORT

leathers was designed and built. It has operated quite successfully, but it has an expected life of only a few months. This oil cylinder has the same displacement as the one ordered from Vickers and delivers 1.5 to 1.6 gpm at 1000 psi.

The effect of heating the inlet water is small and the pump is apparently capable of handling a relatively large volume of gas in the water. Quantitative studies of the ability of the pump to handle liquid with gas are planned for the immediate future.

**40- and 10-kw Boilers.** The two electrically heated boilers have operated quite satisfactorily. The 10-kw boiler heats the pressurizer and is controlled by a pressure switch on the soup pressure. In general, the pressure in the pressurizer can be held at 1000 psi  $\pm$  20 psi by this device. The boiler operating pressure is from 1000 to 1300 psi.

The 40-kw boiler serves to heat the soup stream and gives good control of the soup temperature considering the large changes in load when liquid flow and gas flow into the system are changed. A maximum temperature of 260°C has been obtained in the circulating system. This is limited by the 750 psi safety valve on the boiler which starts to leak slightly at 675 psi or above. Since no means of filling the boiler at high pressure has been provided, the level drops as soon as the safety valve leaks, causing shutdown of the boiler.

**Soup Pressurizer.** The pressurizer in the mock-up is a duplicate of the one to be used in the reactor and operates quite well. Considerable

pressure variation has been observed with level changes corresponding to the compression of the steam (and gas, if present). Level changes may be produced by closing the letdown valve or by the introduction of gas into the core. Pressure changes as high as 300 psi have been noted over a period of several minutes. No ill effects are anticipated or observed as a result of these changes, particularly since they are believed to be negligible under normal operation.

Some difficulty has been experienced in maintaining smooth pressure control in the pressurizer. This is believed to be due to the sluggish, slow response of the steam generator to changes of pressure in the pressurizer.

**Recombiner System.** The HRE flow sheet for the soup off-gas recombiner system operates satisfactorily at steady flows between 1 and 15 scfm; however, when the gas flow is rapidly reduced from the maximum flow rate of 15 to 1 scfm, gas and steam flow from the first condenser to the burner chamber is stopped momentarily, long enough to cause flashbacks from the burner nozzle to the first condenser. Several minutes are required to heat the first condenser enough to allow sufficient steam and gas to flow through the burner nozzle to prevent flashbacks. All flashbacks have been quenched in the first condenser, for the gas and steam mixture entering the first condenser is noncombustible at all times. The soup evaporator produces enough steam by itself to dilute the gas entering the first condenser to 28% gas and 72% steam at a flow of 15 scfm of dry gas. This dilution has been found by the pilot plant group to cause all flashbacks to be quenched in the condenser.

Some changes in the flow sheet have been proposed in an attempt to eliminate the flashbacks when gas flow is rapidly reduced and to allow the burner to recombine all the gas down to flows as low as  $\sim 0.03$  scfm. By injecting about 5 lb/hr of steam into the gas line from the first condenser to the burner, and into the line between the burner and the catalytic recombiner, the pilot plant group has been able to affect smooth burning at the nozzle at gas flows as low as 0.025 scfm. Equipment has been installed to test these changes and tests are under way.

Excessive erosion has been observed on the spark plug electrode used in the pilot plant tests. It has been recommended that a magneto driven by a variable speed motor (to get 5 to 10 sparks per second) be used in place of the 10,000-volt 60-cycle a-c ignition transformer, and that a platinum electrode be substituted for the tantalum electrode to minimize electrode erosion.

Preliminary tests using an airplane magneto, obtained from the Power Plant Laboratory at Wright Field, indicate that frequency of sparking influences the smoothness of burning at the nozzle at low flows of gas ( $H_2 + O_2$ ). This matter is being investigated in conjunction with the tests on burner operation at low gas flows (ranges between  $\sim 0.3$  and 0.5 scfm).

#### MIXING IN THE HRE CORE

J. O. Bradfute    J. I. Gonzalez  
I. Spiewak

A study has been made to evaluate the mixing characteristics of the HRE core and to improve the mixing

in the regions which normally are partially stagnant. This work has been carried on in a transparent, full-scale plastic sphere. Data are obtained by introducing dye into the model and measuring variation of concentration with time. Observations are made at various points in the vessel by means of movable probes.

It has been found that liquid rotates in a relatively stable orbit in the body of the sphere and mixes with liquid bypassing along the walls of the vessel. In the northern hemisphere, which includes the inlet and outlet connections, this bypass goes rapidly from the inlet to the outlet. In the southern hemisphere the stream finds a vertical path through the central axis of the core to the outlet.

As a result of the flow mechanism, there is a region which is mixed poorly with respect to the average in the sphere. This region is located in a cylinder of about 6-cm inside radius and 11-cm outside radius. The sphere radius is 22.9 cm. A more complete description of the flow pattern is found in ORNL-990.<sup>(1)</sup>

Quantitatively, mixing in the stagnant area requires about six times as long as the average for the entire vessel, with no density gradients in the liquid. This relation does not change appreciably with changes in the Reynolds number in the sphere. The Reynolds number was varied by a factor of 8 by means of changes in flow rate and viscosity.

---

<sup>(1)</sup>I. Spiewak and J. O. Bradfute, "Mixing in the HRE Core," *Homogeneous Reactor Experiment Quarterly Progress Report for Period Ending February 28, 1951*, ORNL-990, p. 31 (May 18, 1951).

## HRP QUARTERLY PROGRESS REPORT

Presence of density variations in the sphere improves the mixing of the stagnant region by virtue of centrifugal effects. Introduction of cold water into a sphere containing hot water with accompanying density variance up to 0.9% produced no observable difference in the rate of mixing. However, introduction of methanol solution, with density differences of up to 6%, showed there was considerable improvement in the mixing rate.

The density variation of the soup flowing out to the soup flowing into the reactor operating at 1000 kw will probably amount to about 5%. If this density variation along is relied upon to cool the stagnant area, indications are that the effectiveness of the mixing may be marginal at 250°C and 1000-kw operation. Overheating could be avoided at lower temperatures or lower power levels.

Should HRE operating experience show that stagnant regions in the core will prevent satisfactory operation up to 250°C and 1000 kw, it will become necessary to employ mechanical obstructions which distribute the flow properly. These core baffles will be required to strike the proper balance between: (1) effect on mixing, (2) effect on gas removal, (3) effect on reactivity, and (4) structural strength and resistance to fatigue.

ORNL-1057<sup>(2)</sup> describes the preliminary development on baffles. Cylindrical cantilever rods were found to be the most promising type

(2) "Mixing in the HRE Core," *Homogeneous Reactor Project Quarterly Progress Report for Period Ending May 15, 1951*, ORNL-1057, P. 104 (Oct. 10, 1951).

of baffle with respect to the criteria indicated in the previous paragraph. These rods were mounted along radii in the horizontal equatorial plane of the sphere. The optimum length was 7 in., bringing the rods out from the sphere wall, through the stagnant layer, and just into the updraft going to the outlet. The rotational flow is normal to these rods, producing a turbulent pressure loss behind them. Liquid flows toward the center in this low-pressure area and greatly improves the mixing in the stagnant region.

Further work has since been carried on to optimize the rod design. If baffles are necessary for the HRE, the following arrangement is proposed:

1. A stainless rod 7 in. long, tapered from 1/8 in. at the tip to 1/4 in. at the base, is welded to the sphere wall in a radial position in the horizontal equatorial plane. This rod is displaced 90° from the inlet connection.
2. A similar rod is welded to the wall in a radial position in a horizontal plane 4 in. below the equator. This rod is displaced 270° from the inlet.
3. A rod 4 in. long, tapered from 3/16 in. at the tip to 1/4 in. at the base, is welded in a radial position in a horizontal plane 4 in. above the equator. This rod is also displaced 270° from the inlet.

The taper has been introduced to make the rods less susceptible to resonance vibrations and to increase the strength of the rods at the base, where the maximum stress occurs. The

[REDACTED]

FOR PERIOD ENDING AUGUST 15, 1951

number of rods specified is believed to be the minimum to bring about effective destruction of the stagnant region, and their arrangement was the most effective obtainable by trial and error in the plastic model.

Using these rods the maximum observed residence time in the sphere was 15% above the theoretical average. The rate of bubble removal into the central vortex is close to the rate without baffles. However, the vortex suffers from increased precession and irregularities. These are not great enough to introduce serious fluctuations in reactivity, but they will contribute slightly to the gas holdup.

There is no resonance vibration in the baffles between 50 and 140 gpm which might be considered the extreme limits of flow in the HRE recirculating system. There is a condition of resonance somewhere below 50 gpm, but the amplitude of the vibrations at very low flows is quite small.

There is present at all flow rates a forced vibration stemming from turbulence in the flow through the sphere. The maximum observed amplitude of this vibration has been 1/32 in. at the tip of the rods. This leads to a repeated bending stress of 5400 psi near the root of the rods. The dynamic bending stress is at right angles to a static bending stress of 4700 psi produced by the velocity pressure of the rotating fluid.

For purposes of evaluating the possibility of fatigue, only the dynamic stress need be considered. The endurance limit of type 347 stainless steel at 250°C is approximately 30,000 psi. Thus the safety factor on the rods is 5.5. Because of the possibility of corrosion fatigue, this safety factor is not necessarily adequate. Dynamic tests will be made of tapered rods in the test loops and in the mock-up to examine further the possibility of failure when operating in soup.

**HRP QUARTERLY PROGRESS REPORT**

**6. RECOMBINATION OF HYDROGEN AND OXYGEN**

H. M. McLeod, Leader  
 D. W. Kuhn                      M. J. Fortenberry  
 A. D. Ryon                      D. Phillips  
 A. A. Palko                      T. S. Mackey

Work during the past quarter was concentrated on a continuation of the pilot plant testing of the HRE recombiner system and on small-scale tests to (1) investigate the feasibility of recombining undiluted electrolytic gas by means of massive metal catalysts, (2) complete the development of a high-pressure recombination method for the HRE reflector system, and (3) complete the studies of removal of iodine from the gas stream prior to its introduction to the catalytic recombiner.

**LABORATORY SCALE STUDIES**

D. W. Kuhn                      A. A. Palko  
 A. D. Ryon                      M. J. Fortenberry

**100% Conversion.** Upon passing a mixture of hydrogen, oxygen, and steam through a platinum catalyst, one may readily convert greater than 99% of the hydrogen to water. If conversions greater than 99.99% are desired, however, it would appear that a two-stage catalytic unit would be most advantageous. That is, the off-gas from the first catalytic unit

would be cooled to condense and remove steam; this would greatly reduce the gas volume to be handled and also allow the concentration of hydrogen-oxygen to be increased to any desired level. This small volume of gas mixture containing perhaps 2 to 10% electrolytic gas in steam could be passed through a small secondary catalyst bed and react to the extent of greater than 99%, giving an over-all conversion of greater than 99.99%. Such performance is to be expected based on single-stage catalytic tests. In order to demonstrate that this could actually be carried out, an experimental two-stage catalytic recombiner has been operated in the laboratory. The results, as given in Table 6.1, show that 100% conversion is closely approximated in a two-stage catalytic unit.

It should be pointed out that the gas passing out of the second catalytic unit was not electrolytic gas, since it contained excess hydrogen and carbon dioxide and very little

**TABLE 6.1**  
**Two-Stage Catalytic Recombination**  
**0.3% Pt on Al<sub>2</sub>O<sub>3</sub>**

REPORT NO.	STAGE 1				STAGE 2				OVER-ALL PERCENT CONVERSION	
	CATALYST (g)	ELECTROLYTIC GAS (cc/min)	WATER (cc/min)	PERCENT CONVERSION	WEIGHT OF CATALYST (g)	ELECTROLYTIC GAS (cc/min)	WATER (cc/min)	PERCENT CONVERSION		
379	12.0	60	60	99.30	15	60	3790	0.957	99.89	99.9950
42	9.0	60	73.5	99.20	15	72.5	2000	0.54	99.3	99.994

\* Hydrogen removed from off-gases and also (H<sub>2</sub>) gas sample was analyzed to determine amount of unreacted electrolytic gas.

oxygen. Hence it was necessary to have gas samples analyzed and to base the conversion data on the amount of recombinable mixture passing through uncombined.

**Conversion Inside Tubes.** The interesting possibility of recombining electrolytic gas catalytically on metal surfaces without the necessity for diluting the reactants has been considered. The principal requirement to be met in such experiments is that means must be provided for the removal of the heat of reaction at a rate sufficient to maintain every part of the system below the ignition temperature of the gas mixture. This has been accomplished by completely immersing metal tubing in a fused  $\text{KNO}_3$ - $\text{NaNO}_2$  salt bath. Copper, silver, and nickel have each been

found to exhibit catalytic activity which improves markedly with increasing temperature. All of the experiments except one were run using unpacked tubes. In one case, a 5-ft length of  $\frac{1}{2}$ -in. copper tubing (0.41-in. i.d.) was packed with copper pellets. The results of this work are shown in Fig. 6.1 and in Table 6.2.

The results of this work show that a large-scale catalytic conversion of  $\text{H}_2 + \text{O}_2$  on copper may be entirely feasible. For example, a surface area of approximately 15 sq ft of copper is capable of converting 1 cfm of electrolytic gas at an operating temperature of  $440^\circ\text{C}$ . It is planned to continue these studies, covering a wider range of flow rates, temperatures, and tube diameters in order to

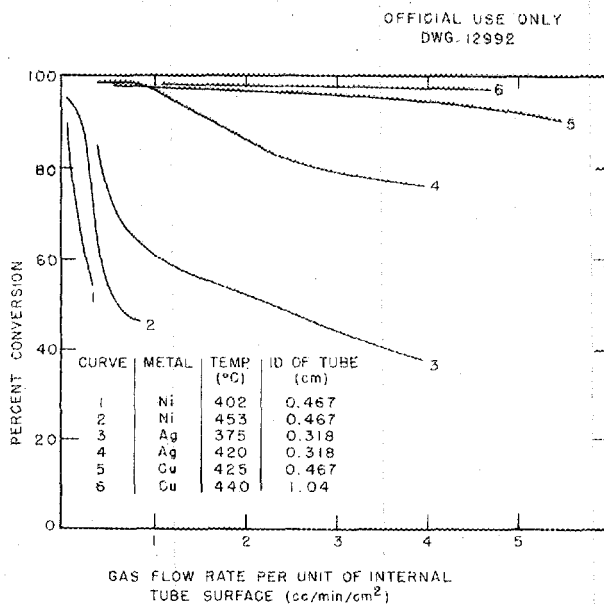


**Fig. 6.1 - Recombination of Undiluted Electrolytic Gas in Metal Tubes.**

**TABLE 6.2**

**Conversion of Undiluted Electrolytic Gas in Copper Tube**

Gas flow rate, 588 cc/min  
Copper tube, 5 ft long,  
0.41 in. i.d.

SALT BATH TEMPERATURE (°C)	PERCENT CONVERSION	
	UNPACKED TUBE	PACKED TUBE <sup>(a)</sup>
250	4.7	
285	17	61
300	32	82
320	53	95
342	80	100
368	96	

<sup>(a)</sup> 10 to 18 mesh size.

**[REDACTED]**

## HRP QUARTERLY PROGRESS REPORT

provide sufficient data to permit design of large-scale units of this type.

**Catalysts Other than Platinum.** A catalyst containing 35%  $V_2O_5$ -65%  $Al_2O_3$  was tried out with mixtures of electrolytic gas and steam and also with undiluted electrolytic gas. Using 7.9% electrolytic gas in steam at 430°C, the conversion was 22% complete. The steam flow rate was 5.5 liters/min, and the space velocity was about 7000  $hr^{-1}$ . Thus the performance of this catalyst is rather poor. When used with undiluted electrolytic gas, the percentage conversion was better, but flashbacks were encountered at apparent catalyst temperatures of 350 to 360°C. At a flow rate of 360 cc of undiluted electrolytic gas per minute, the percentage conversion was 62% at 325°C.

**Pressurizer Tests.** A typical test loop pressurizer (3-in. Schedule 80 stainless steel pipe, 36 in. long)

has been subjected to a series of four explosions in order to determine how well a loop component would withstand explosions at various initial pressures and gas compositions. In all of the tests, water was contained in the bottom of the pressurizer to a depth of about 12 in., leaving 3½ liters of free space within the pressurizer. A summary of the data for the first three tests is given in Table 6.3.

In the fourth test, with the pressurizer at room temperature, electrolytic gas was admitted to the system until the pressure read 300 psi. The system was then closed off and heated until the total pressure (steam +  $H_2$  +  $O_2$ ) read 1000 psi. It was evident from temperature measurements that steam did not mix with the hydrogen and oxygen in the top section of the pressurizer, so that partial pressures and percent composition in any given section of the pressurizer were unknown. Upon ignition of this

TABLE 6.3

Summary of Pressurizer Test Data

TEST NO.	TEMPERATURE (°C)	TOTAL PRESSURE (psia)	PARTIAL PRESSURES (psia)			RESULT UPON EXPLOSION
			H <sub>2</sub>	O <sub>2</sub>	He	
1	25	30	20	10	0	No damage
2	25	90	60	30	0	No damage
3	25	984	204	102	678	A section of 1/4-in. o.d. stainless steel tubing (0.032 in. wall) was ruptured and twisted; two small, jagged fragments of torn steel tubing were found

mixture by a hot wire at the top of the pressurizer, a violent explosion occurred which ripped open the bottom of the pressurizer and slammed the lower end of the pipe through a 3/4-in. thick plywood wall.

It is evident that both the pressurizer pipe and connecting tubing are vulnerable to explosions which might occur if mixtures of hydrogen and oxygen are introduced into a test loop. Such installations should be enclosed by sand bags, sheets of boiler plate, or other means to prevent injury to personnel. Small tubes used as pressure taps from the system to instrument panels may also be hazardous should they become filled with an explosive gas mixture, since explosions can travel through such tubes and burst a pressure gauge, for example.

**High-Pressure Recombination-Reflector System.** Two experiments have been completed in which the high-pressure recombination of hydrogen and oxygen mixed with helium and steam has been carried out using a platinum-on-alumina catalyst. Conditions of temperature, pressure, and composition corresponding to those expected in the reflector system were employed. The catalyst was suspended above water in a heated pipe with the water temperature about 200°C and the partial pressure of steam about 225 psi. The total pressure was then brought to 1000 psi by addition of helium, after which electrolytic gas was bubbled into the reactor through the water in the bottom section. During a 45-min period, 10 liters (STP) of electrolytic gas was admitted to the reactor. If no recombination had occurred, the final pressure would have been

about 1450 psi. Actually there was no pressure rise at any time, indicating that the reaction proceeded as rapidly as the electrolytic gas was admitted. The necessary information to permit design of a recombiner for the D<sub>2</sub>O system was transmitted to the Reactor Experimental Engineering Division.

**Removal of Iodine from the Gas Stream.** An exploratory test indicated that iodine could be quantitatively removed from the gas stream by passing the vapor through a tube packed with type 316 stainless steel turnings prior to its introduction into the catalytic recombiner. A second test was carried out in which the length of the run was 900 hr instead of 480 hr, and the rate of flow of iodine was 43 mg/hr instead of 19 mg/hr. Means for periodic removal of the liquid from the trap also were provided. The conditions under which the test was carried out are as follows:

Flow Rates	
Steam	11 liters/min
Electrolytic gas	0.27 liter/min
Iodine to steel trap	43 mg/hr
Temperature of	
Catalyst	240°C
Space Velocity	12,000 hr <sup>-1</sup>
Percent Conversion	
At start	97.8%
After 340 hr	93.2%
After 900 hr	92.6%

After 900 hr, it was found that 9.4 g of stainless steel had been dissolved. Chemical analysis of the trap liquid showed it to be a mixture of FeI<sub>2</sub>, NiI<sub>2</sub>, CrI<sub>3</sub>, and water.

## HRP QUARTERLY PROGRESS REPORT

To point out the effectiveness of the stainless steel as a trap for iodine, another test was made identical to the one above in all respects except that no stainless steel trap was included. In this case, the iodine very rapidly reached the catalyst and poisoned it. After 2 hr the percentage conversion for the reaction was 45%, and after 7¼ hr the conversion had fallen to 18%.

### PILOT PLANT TESTS

Don Phillips    T. S. Mackey  
M. J. Fotenberry

**Pilot Plant Runs with Low Gas Flow Rates.** Following the initial operation of the pilot plant as described in the previous report,<sup>(1)</sup> the follow-up catalytic recombiner was installed and runs were made with gas flow rates (electrolytic) of 0.5 to 0.025 cfm. These runs were for the purpose of determining the efficiency of recombination and the temperature distribution over the catalyst bed with and without steam in the inlet stream. In carrying out the tests, the electrolytic gas flow was started at 0.4 to 0.5 cfm; after about 15 min the gas flow was adjusted to the desired rate and from 30 to 60 min additional time, depending on the flow rate, was allowed to permit the system to reach equilibrium prior to the start of the run. Other conditions were: 1.5 cfm steam to the burner orifice inlet and either full or no flow of cooling water to the burner chamber jacket. The gases entering the burner chamber were preheated to about 110°C and the cata-

lytic recombiner jacket was heated with steam at about 75 lb. Temperatures at the inlet, midpoint, and exit of the catalyst bed as well as the magnitude of the pressure surges were averaged over a 30-min interval. Product water from the second condenser was withdrawn at 30-min intervals and examined for evidence of catalyst breakdown (milky appearance). For purposes of comparison, a 4-hr run was made under the conditions previously used except that for the first 2 hr there was a gas flow of 0.1 cfm of N<sub>2</sub> instead of electrolytic gas and there was no gas flow during the last 2 hr, and a second run of 2.5-hr duration was made with .05 cfm gas which was not permitted to burn in the combustion chamber. The data are given in Table 6.4.

The results show that the effect of variables on recombination in the burner chamber and follow-up recombiner at low gas flow rates is as follows:

1. With the full flow of cooling water on the burner chamber shell, recombination by burning was complete at all of the gas flows employed. This is shown by a comparison of runs 38, 36, and 31, employing a full flow of coolant, with runs 28b, 27, and 26, using no flow; in runs 38, 36, and 31 there was no measurable off-gas, and the maximum temperature in the catalyst bed remained constant at about 165°C (the ambient value), while in runs 28b, 27, and 26 the off-gas averaged about .004 cfm, and the maximum temperature in the catalyst bed increased from 118°C at a gas flow of .05 to 382°C at .25 cfm.

<sup>(1)</sup> "Pilot Plant Tests," *Homogeneous Reactor Project Quarterly Progress Report for Period Ending May 15, 1951*, ORNL-1057, p. 82 (Oct. 10, 1951).

FOR PERIOD ENDING AUGUST 15, 1951

TABLE 6.4

Effect of Variables on Recombination in the Burner Chamber and Follow-up Recombiner at Low Gas Flow Rates

RUN NO.	ELECTROLYTIC GAS FLOW (cfm)	STEAM TO CATALYTIC RECOMBINER (cfm)	MAXIMUM TEMPERATURE IN CATALYST ( $^{\circ}$ C) <sup>(a)</sup>	OFF-GAS (cfm)	MAXIMUM PRESSURE SURGE (lb)	EVIDENCE OF CATALYST BREAKDOWN	FLASH-BACKS
38	.025	0	165	0	.50	No	No
29 <sup>(b)</sup>	.05	0	270-450	.017	6	Yes	Yes
36	.05	0	166	0	1.5	No	No
31	.35	0	164	0	1	No	No
37	.05	.55	114	0	1	No	No
37	.10	.55	112	0	2.5	No	No
37	.15	.55	102	0	3.0	No	No
35	.05	1.0	103	0	1.5	No	No
34	.10	1.0	98	0	2	No	No
34	.15	1.0	100	0	2	No	No
39	0	1.5	102	0	1.25	No	No
28	.05	1.5	108	0	3	No	No
33	.10	1.5	103	0	4	No	No
33	.35	1.5	100	0	1	No	No
32	.50	1.5	118	0	.5	No	No
39	.1(N <sub>2</sub> )	1.5	112	.1	.25	No	No
28b <sup>(c)</sup>	.05	1.5	118	.007	2.5	No	No
27 <sup>(c)</sup>	.15	1.5	295	.003	4	No	No
26 <sup>(c)</sup>	.25	1.5	382	.004	4	Slight	Yes

(a) Ambient temperature inside recombiner about 165 $^{\circ}$ C.

(b) No combustion in burner chamber (spark off).

(c) No cooling water through burner chamber jacket.

- The addition of steam to the catalytic recombiner served only to reduce the temperature in the catalyst bed.
- The only evidence of catalyst breakdown occurred during run 29, in which recombination was

carried out in the catalytic recombiner (by stopping the spark coil), and run 26. In run 29, the full flow of coolant was employed in the burner chamber shell and no steam was added to the follow-up catalytic recombiner, conditions which

## HRP QUARTERLY PROGRESS REPORT

insured a low percentage of water vapor in the gas entering the catalyst bed; in run 26 there was no coolant flow and steam was added to the catalytic recombiner; nevertheless, the catalyst bed temperature indicated that the inlet mixture was rich in gas. The results indicate, therefore, that the catalyst breakdown was due to explosions originating in the catalyst bed while recombination in the bed was in progress. It appears desirable to add a small flow of steam to the gas entering the catalytic recombiner to minimize the possibility of flashbacks at that point.

Conclusions were that the full flow of cooling water to the burner chamber shell should be maintained at all gas flow rates and that about 0.5 cfm of steam at a constant rate should be added on the inlet side of the catalytic recombiner. Under these conditions breakdown of the catalyst should no longer occur.

**Pilot Plant Runs with High Gas Flow Rates.** The pilot plant test runs were completed with three runs in which the gas flow rate was approximately 16, 19, and 28 cfm.

The run at 16 cfm was made to determine the pressure drops and temperatures at various important points in the system, including the catalytic recombiner. The runs at 19 and 28 cfm were made with the follow-up recombiner and second condenser removed from the system and were carried out for the purpose of determining if the flame recombiner was capable of operating in a satisfactory manner with the higher gas

flow rates. Other conditions and procedures were the same as those described in the previous section. The data are summarized in Table 6.5.

The results show that the performance of the recombiner system with a gas flow rate of 16 cfm was satisfactory in all respects; with gas flow rates of 19 and 28 cfm, operation of the flame recombiner was satisfactory although the vapor temperature in the off-gas line was 774°C at the higher flow.

A final report on this phase of the work is now in progress and after its completion work will be started on the design of a recombiner pilot plant using the data obtained in the small-scale work with copper tubes.

TABLE 6.5

Summary of Results of Pilot Plant  
Runs with Gas Flow Rates of 16,  
19, and 28 cfm

Gas flow rates (cfm)	16	19	28
Duration of runs (hr)	3	0.6	1
Pressure at top of first condenser (lb)	3.8	4.9	9.25
Pressure drop across burner orifice (lb)	2.2	1.5	3.6
Pressure drop across catalyst recom- biner (lb)	0.56		
Temperature of vapor leaving burner chamber (°C)	340	658	774
Maximum temperature in catalyst bed (°C)	206		

[REDACTED]

FOR PERIOD ENDING AUGUST 15, 1951

## 7. CHEMICAL CONTROL

W. H. Davenport, Leader

R. H. Powell                      W. H. Brand

The determination of density using the electromagnetic densitometer, although time consuming, appears to be feasible on the basis of laboratory testing which was concluded in the past quarter. A variation of this method, whereby the electromagnet is eliminated and float movement is effected by control of the temperature of the solution, shows some promise. Neither of these methods give continuous measurement of the density and both require a static solution.

The first of three Princo Densitrol instruments has been received. Since these instruments record continuously and their development is more advanced than the work on other methods, most of the effort is now being directed towards the completion of the testing of the Princo Densitrol units so that they may be included in the present design program for the HRE.

Developmental work on Q coil ceramics, glazes, and gasketing is continuing. K. Kline of the ORNL Instrument Department is developing a remote control measuring instrument.

Optical spectra of slow-neutron absorbing optical glasses have been measured before and after ORNL graphite reactor exposure. A radiation and chemically stable glass could be very useful as a window to view soup solution in the HRE and to follow certain physical properties of the soup.

### ELECTROMAGNETIC DENSITOMETER

W. H. Davenport and R. H. Powell

In the previous quarterly report<sup>(1)</sup> a description of the electromagnetic densitometer and the procedure used in calibrating the instrument were given. It was reported that poor reproducibility was obtained between calibration curves made on separate days and also that the average deviation of the points from a given calibration curve was as high as  $\pm 0.001$  g/cc. On all of the runs reported, both coil current and temperature were changing while measurements were being made.

It has been found that by holding the current constant at the appropriate settings and increasing the temperature until movement of the float is indicated on the oscilloscope reproducible calibration curves may be obtained. The average deviation of any point from the calibration curve obtained in this manner was  $\pm 0.0004$  g/cc over a density range 0.864 to 0.924 g/cc.

Experimental runs were made using uranyl sulfate solutions containing 30.915 mg of uranium per milliliter instead of water. The data were plotted as temperature vs. coil current. The density of uranyl sulfate

<sup>(1)</sup>W. H. Davenport, Jr., and R. H. Powell, "Analytical Chemical Control of the Homogeneous Reactor Solution," *Homogeneous Reactor Project Quarterly Progress Report for Period Ending May 15, 1951*, ORNL-1057, p. 86 (Oct. 10, 1951).

## HRP QUARTERLY PROGRESS REPORT

at any temperature on the curve could then be determined from an expression which was set forth by A. R. Richards<sup>(2)</sup> and gives the relationship of coil current to the density of the float and the solution as  $p = Ri^2 + P$ .

In Richards' expression,  $p$  is the density (g/cc) of the solution,  $i$  is the coil current (amp),  $P$  is the float density (g/cc), and  $R$  is a constant which is a function of the configuration of the system, size and shape of magnet, susceptibility of armature, etc.

In this case  $R$  was determined from the data obtained on the water runs, in which the density of water at the temperatures measured was taken as a standard.

The uranyl sulfate data, after correction for temperature gradients in the bomb and for thermal expansion of the float, was substituted into Richards' expression. The density of the uranyl sulfate was found to average 0.0421 g/cc higher than the density of water at the corresponding temperatures over the range 183 to 232.5°C. The density of another aliquot of the same uranyl sulfate solution (30.915 mg of uranium per milliliter) had been determined previously at 25°C using a pycnometer and was also found to be 0.0421 g/cc higher than that of water.

Due to the corrections which are required, the present apparatus is not considered reliable for accurate density determinations, but, when calibrated, is reproducible and

(2) A. R. Richards, "An Electromagnetic Densitometer," *Ind. Eng. Chem., Anal. Ed.* 14, 595 (1942).

should permit measurements of uranium concentration with an accuracy of 1%.

The apparatus has several disadvantages. It is difficult to thermostat uniformly since the principle requires that the large magnet be placed immediately below the sample chamber. In addition, the chamber has a small reservoir at the base into which the iron core of the float extends. It would be impossible to drain the liquid from this trap or to get satisfactory circulation into this section.

Another difficulty may be encountered when the iron cores of the electromagnet and the float are placed in a radiation field. Changes in permeability of the cores due to radiation would change the calibration of the instrument.

A modified densitometer in which float movement is achieved by temperature control of the density of the solution would eliminate some of the disadvantages of the electromagnetic method such as uneven thermostating, draining difficulties, and loss of susceptibility of iron cores if the latter should occur. The modified densitometer would be calibrated for uranium concentration vs. temperature required to sink the float.

The electromagnetic densitometer apparatus, minus the electromagnet, was used to investigate the possibilities of this modified method. For distilled water the apparent sinking temperature was 205.3°C and for a concentration of uranyl sulfate equal to 30 mg of uranium per milliliter the temperature was 240.9°C. A check using a solution containing 15 mg of uranium per milliliter of

solution indicated that a linear interpolation of temperature may be made for sinking points between the sinking points for 0 and 30 mg of uranium per milliliter.

Since a 35.6°C span in temperature is required to cover the uranium concentration range 0 to 30 mg of uranium per milliliter, a change of 0.1°C in sinking temperature represents about 0.1 mg of uranium per milliliter in uranium concentration. With proper thermostating the temperature could probably be determined to 0.2°C.

It was also found that satisfactory sinking points could be obtained when the rate of change of temperature was as great as 2°C per minute. This would mean that the maximum time consumed in adjusting temperature (concentration change of 30 mg of uranium per milliliter) would be 20 min.

#### PRINCO DENSITROL

W. H. Davenport and R. H. Powell

The Princo Densitrol instruments ordered from Precision Thermometer and Instrument Co., Philadelphia, Pa., are all of the design shown in Fig. 7.1 with the exception that the 600-lb ring joint flange facings and lap joint backing flanges have been replaced with 900-lb members.

The plummet in the center of the sampling chamber contains an iron core (not shown). The position of the plummet, determined by the density of the solution being measured, is translated into an indication of specific gravity on a Brown Recorder by means of a differential trans-

former (shown as a coil in the drawing) wound on an insulator on the outside of the sampling chamber. The travel of the plummet is decreased, and the specific gravity range is increased by the chains attached to the plummet and to a fixed reference point on the wall of the chamber. As the plummet rises with an increase in density it must support a greater weight of chains; as it sinks, the walls support a greater weight of chains. The plummet assembly and the differential transformer are so designed that the measured electrical output is linear with respect to density.

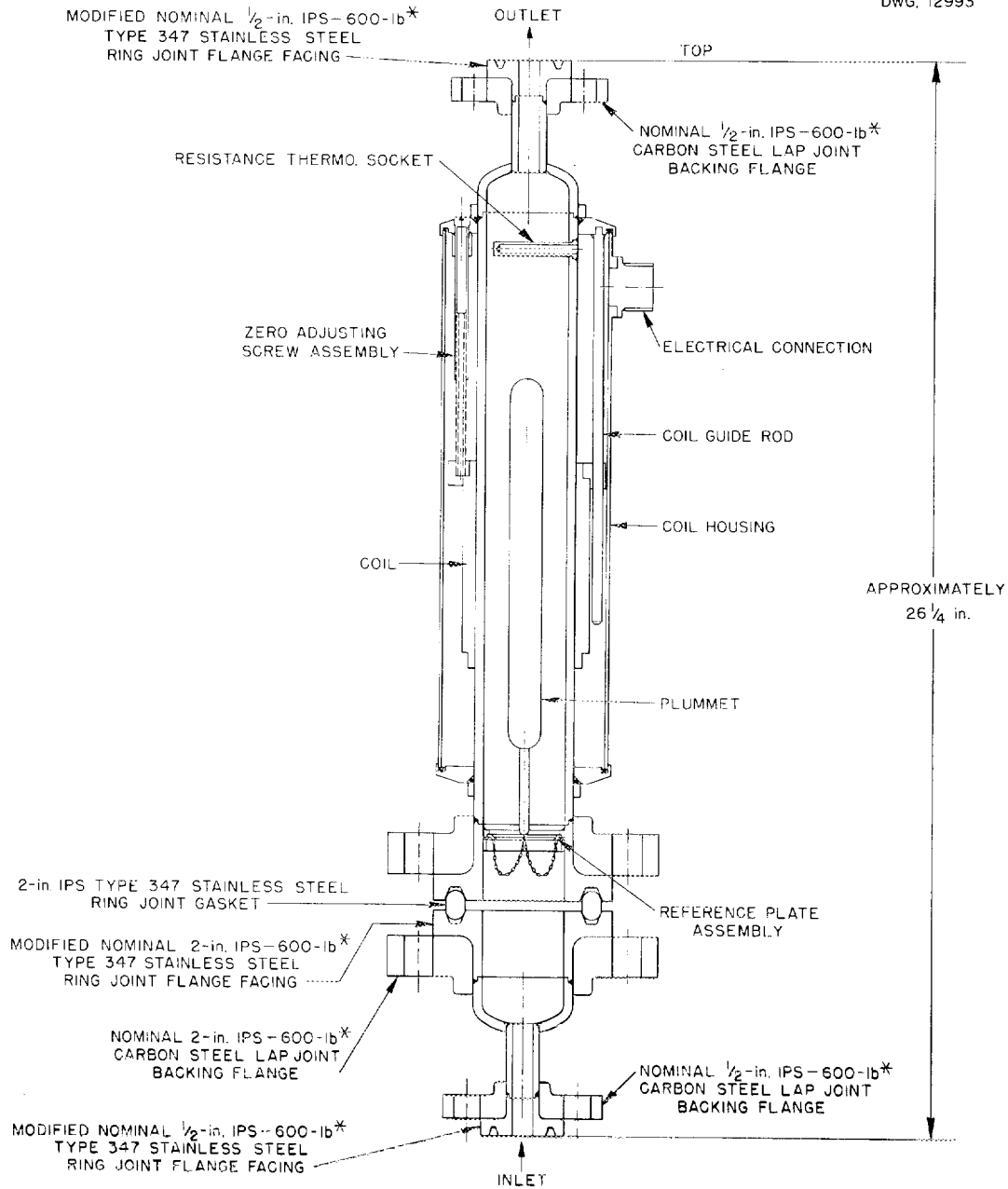
The instrument also contains an automatic temperature compensator. The temperature is measured by a resistance thermometer and corrected to the base temperature for which the instrument is calibrated by means of a balanced bridge circuit which applies a factor determined by the temperature density coefficient of the solution being measured.

The first instrument which was received measures specific gravity in the range 1.033 to 1.053,  $t/4^{\circ}\text{C}$ . Several components are not suitable for use in the high-radiation field of the HRE, e.g., the coil is wound on a Bakelite form, but the next two instruments will contain what are believed to be satisfactory replacements. In the case of the coil the Bakelite insulation will be replaced with Lava.

The choice of a suitable plummet material for all HRE conditions is still in question. Three materials are being considered, pyrex, type 347 stainless steel, and titanium.

**HRP QUARTERLY PROGRESS REPORT**

NOT CLASSIFIED  
DWG. 12993



\*600-lb ring joint flange facings and lap joint backing flanges have been replaced with 900-lb members;  
All piping to be 1/2-in. and 2-in. IPS type 347 stainless steel Schedule 80 pipe.

**Fig. 7.1 - Pipeline Model Densitrol Assembly with Modified 600-lb Ring Joint Flanges.**

[REDACTED]

FOR PERIOD ENDING AUGUST 15, 1951

**Pyrex.** Pyrex has shown good radiation resistance<sup>(3)</sup> and pressure stability. Four plummets representative of those under consideration for the Princo Densitrol were found to be pressure stable to hydraulic pressures of 4100 psi or better. The corrosion stability of pyrex in uranyl sulfate at 250°C is not good, however, and for this reason pyrex is only being considered for a plummet which will be in a low-temperature HRE line.

**Stainless Steel.** The stainless steel plummets will have radiation and corrosion stability equal to the rest of the reactor, but, due to the fact that the wall thickness is limited by permissible float weight to 0.015 in., the pressure stability is borderline. The Precision Thermometer and Instrument Co. is submitting stainless steel plummets which, it is believed by their Mr. Boonschaft, will withstand 150 psi external and 1100 psi internal working pressures. These plummets are to be pressurized internally to 900 psi with nitrogen. This should permit their use at normal operating conditions of the HRE but would give no margin of safety in the event of external pressure increases without accompanying temperature increases.

**Titanium.** A design for a titanium plummet has been decided upon which provides for a 0.025-in. wall thickness and also permits final adjustment to the required weight by the addition of a known volume of two collars of different specific gravity materials, namely type 347 stainless steel and titanium.

---

<sup>(3)</sup>J. C. Horsman, *Summary of NRX Pile Irradiations*, NP-1922, p. 6 (Dec. 8, 1950).

The construction of such a plummet is dependent upon the successful welding of two sets of three titanium rims. The Heliarc welding of three such rims has been undertaken experimentally by R. J. Fox of Research Shops. All materials for construction are on hand. The plummet is to be internally pressurized to 900 psi at 25°C with argon. A final small Heliarc well is to be made at the gas fill point after the plummet and argon gas have been frozen in liquid helium. The first of such titanium plummets is designed for low-temperature use.

It is hoped that if one or more of the plummet materials proves satisfactory Princo Densitrol instruments can be provided for measurement of soup solutions at 250°C as well as at lower temperatures. In either case a bypass line from either the 1.4-gpm line or the 100-gpm line will be necessary since the flow through the Densitrol must be controlled within the range 0.1 to 0.5 gpm. Suspended solids smaller than 1/32 in. in mean diameter may be passed, but solid particles as well as bubbles will affect the density of the solution being measured. Since the Densitrol measures the average density of all material in the sampling chamber, the extent of error introduced by solids or bubbles is equal to the difference between the average density and the density of the liquid alone. The instrument cannot operate satisfactorily when violent intermittent gas surges are present in the measuring line.

Rigid temperature control will not be necessary. Temperature fluctuations to the extent of ±3°C

## HRP QUARTERLY PROGRESS REPORT

at 250°C or  $\pm 10^\circ\text{C}$  at 50°C are compensated for by means of the automatic compensator.

The testing program for these instruments includes a study in the laboratory of the variables temperature, pressure, concentration, and flow rate, and installation for further studies of one unit in a test loop now being constructed by C. Heisig at Y-12.

### Q MEASUREMENT

W. H. Davenport and R. H. Powell

A major problem in the measurement of the Q of a high-frequency coil as affected by changes in concentration of uranium soup solution is the introduction of an electrically insulated coil directly into the high-pressure high-temperature soup solution.

Recently consideration has been directed to the fabrication of powdered, compressed, fired Lava grade 1137 ceramics, which encase copper coils, following the general procedure of E. S. Cantrell and R. J. Fox,<sup>(4)</sup> but fired with the added precaution of protecting the copper leads by use of powdered graphite and a hydrogen atmosphere. Such copper Q coil ceramics have been glazed using the American Lava Corp. glaze and a glaze devised by E. S. Cantrell. Both glazes have cracked when the ceramic was gasket tested

---

<sup>(4)</sup>W. H. Davenport, Jr., and R. H. Powell, "Analytical Chemical Control of the Homogeneous Reactor Solution," *Homogeneous Reactor Experiment Quarterly Progress Report for Period Ending November 30, 1950*, ORNL-925, p. 260, esp. p. 269 (Jan. 30, 1951).

in a bomb.<sup>(1)</sup> However, these ceramics and glazes have not been eliminated for use, since good gasketing tests have not yet been achieved. Irregular surfaces and overloading from the pressure of the gold gaskets contributed to each of the two failures of glazed copper Q coil ceramics.

E. S. Cantrell of Chemistry Research Shop is currently attempting to build up a thicker glaze, capable of being machined and polished. This attempt is being confined to Lava grade 1137 collars.

Disks of pyrex, fire polished and carefully annealed, are being prepared for gasket testing in the bomb.

If such ceramic forms or pyrex cannot be gasketed in the conventional manner, use of a pressurized air or gas lock will be attempted.

One of the two powdered, compressed, fired Lava grade 1137 ceramics cracked on the collar during gasketing. It is noted that the rupture strength of the ceramic collar could be increased about three times by use of natural grade 1137 Lava for the collar, into which collar a plug hole for the thimble could be machined. The collar and thimble could then be bonded by the glaze.

Specific measurement of the effect of temperature and pressure on Q of various concentrations of HRE soup solutions have not been accomplished yet due to gasketing difficulties.

The instrumental work necessary for remotely measuring Q of the uranyl sulfate fuel solution is progressing satisfactorily.

FOR PERIOD ENDING AUGUST 15, 1951

TABLE 7.1

Composition of Glass Samples

ELEMENT	GLASS SAMPLE NUMBER			
	1-M	2-M	3-M	4-M
Al	Moderate	Moderate	Moderate	Moderate
B	Very strong	Trace	Strong	Moderate
Bi	?	Faint trace	Faint trace	Faint trace
Ca	Very strong	Very strong	Very strong	Very strong
Cd	Moderate	Strong	Strong	Strong
Cu	Very weak	Very weak	Very weak	Very weak
Fe	Weak	Weak	Weak	Weak
Mg	Very weak	Very weak	Very weak	Very weak
Mn	Trace	Trace	Trace	Trace
Na	Moderate	Weak	Moderate	Moderate
Ni	Faint trace	Faint trace	Faint trace	Faint trace
Pb	Very weak	Very weak	Very weak	Very weak
Si	Very strong	Very strong	Very strong	Very strong

Film 3171: 2/1/51

**RADIATION RESISTANT GLASSES**

W. H. Davenport and R. H. Powell

The neutron absorbing glasses from A. Silverman<sup>(5)</sup> were removed from the ORNL graphite reactor after exposure in hole 60 at 250°C at an average flux of  $7.3 \times 10^{11}$  for a total exposure of  $5.4 \times 10^{18}$  nvt.

The optical spectrum of the pre-polished  $1 \times 1 \times 0.5$  cm specimens was measured by a Model DU Beckman Quartz Spectrophotometer before and after irradiation. The glasses were kept in the dark at all times except during short periods of visual

examination and during optical measurement. Optical measurements were made 7 days after removal from the pile.

The ORNL Analytical Chemistry Spectrographic Laboratory identifies the composition of each glass as listed in Table 7.1. Graphs showing the spectrum before and after radiation are given in Figs. 7.2 - 7.5.

It is to be especially noted that these glasses were made using common boron and that the damage to the glass is greatest when the boron content is greatest. A possible explanation is that the large  $B^{10}$  (na) thermal-neutron capture cross-section results in the greatest

<sup>(5)</sup>ORNL-925, op. cit., p. 275.

**HRP QUARTERLY PROGRESS REPORT**

damage to the glass when the  $B^{10}$  content is greatest.

However, damage to any of the slow-neutron absorbing glasses is only moderate in the 585- $m\mu$  region, and use of the glasses in this region offers some possibility if the glasses prove to be chemically stable, and providing a saturation point has been reached in damage. To explore the latter question the glasses have been returned to hole 60 to 250°C for further pile radiation.

A new approach to the problem of obtaining a suitable glass for HRE use, the possibility of a glass relatively transparent to gamma and neutron radiation, is being considered in cooperation with Penberthy Instrument Co.,<sup>(1)</sup> Seattle, Washington. It will attempt to develop a glass of such properties by using components of low atomic number and low cross-section for neutron capture.

This approach is opposite to that of developing a neutron and gamma absorbing glass.

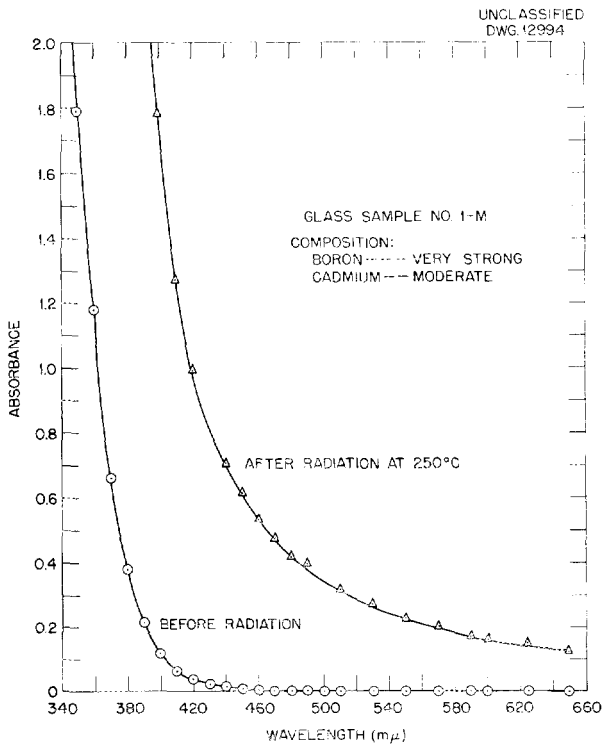


**Fig. 7.2 - Irradiated Glass Sample No. 1-M.**

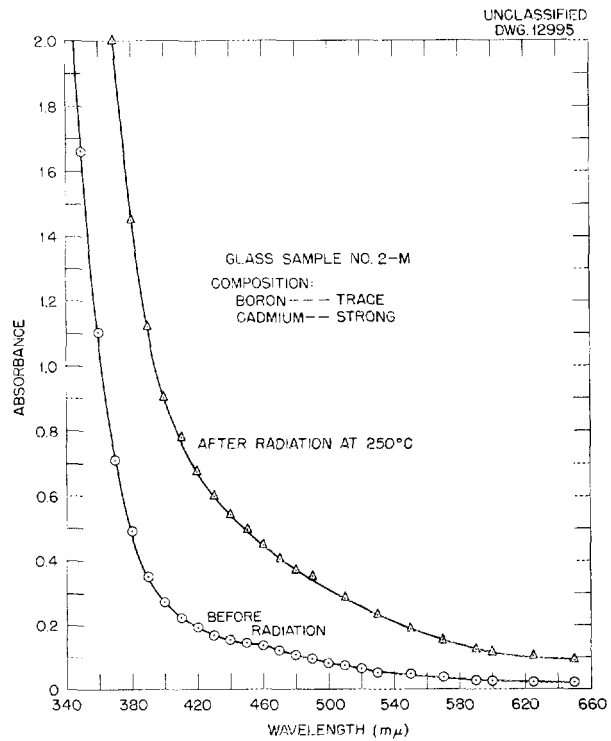


**Fig. 7.3 - Irradiated Glass Sample No. 2-M.**

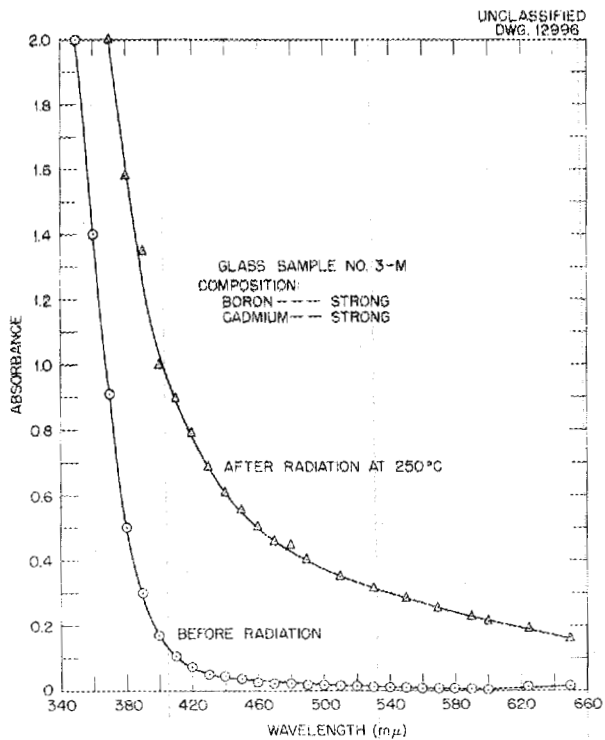


Fig. 7.4 - Irradiated Glass Sample No. 3-M.

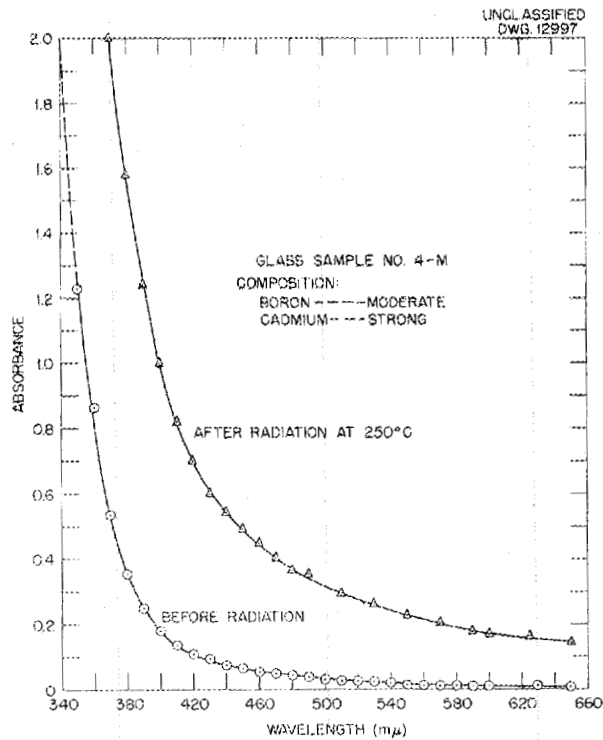


Fig. 7.5 - Irradiated Glass Sample No. 4-M.

# HRP QUARTERLY PROGRESS REPORT

## 8. PHYSICS

T. A. Welton, Leader

L. H. Thacker	W. C. Sangren
H. T. Williams	R. E. Aven
P. M. Wood	P. R. Kasten
G. T. Trammell	L. C. Biedenharn

### CRITICALITY CALCULATIONS

T. A. Welton	L. H. Thacker
H. T. Williams	P. M. Wood

A number of more or less routine neutron-diffusion calculations were made to answer safety questions and questions concerning operating procedures, and to give some check of numbers previously obtained by others. The method used was the standard two-group approximation. The answers are somewhat undependable, but it is felt that valid comparisons of various configurations can often be made in this way. All predictions of critical concentrations, temperature coefficients, etc. must be regarded merely as plausible estimates. Limits of error are now being established by further work, and some refinements of the values here given probably will be available before any critical experiments are done.

Even the full two-group method is somewhat cumbersome, and a very large amount of time was saved (with apparently negligible sacrifice on an already doubtful accuracy) by the use of an approximate method for the solution of the two-group equations. This method was developed and thoroughly tested at Los Alamos in connection with other types of problems.<sup>(1)</sup> Its application is straight-

forward, and no discussion will be given here.

**Constants.** The macroscopic two-group constants used for light water were those given in ORNL-933,<sup>(2)</sup> while those used for heavy water are from ORNL CF-50-10-97.<sup>(3)</sup> If  $T_0$  refers to room temperature (293°K) the constants for absolute temperature  $T$  were obtained from

$$L^2(T) = L^2(T_0) \frac{\rho^2(T_0)}{\rho^2(T)} \sqrt{\frac{T \sigma_s(T_0)}{T_0 \sigma_s(T)}}$$

$$\tau(T) = \tau(T_0) \frac{\rho^2(T_0)}{\rho^2(T)}$$

$$D_1(T) = D_1(T_0) \frac{\rho(T_0)}{\rho(T)}$$

and

$$D_2(T) = D_2(T_0) \frac{\rho(T_0) \sigma_s(T_0)}{\rho(T) \sigma_s(T)}$$

<sup>(1)</sup>LA-524.

<sup>(2)</sup>F. J. Sisk, *Transport Parameters for Thermal Neutrons in Water*, ORNL-933 (Mar. 15, 1951).

<sup>(3)</sup>J. M. Stein, *Constants for Two Group Calculations of Uranium-D<sub>2</sub>O Reactors*, ORNL CF-50-10-97 (Oct. 20, 1950).

where

- $L$  = thermal diffusion length,
- $\tau$  = age from fission to thermal,
- $D_1$  = fast diffusion constant,
- $D_2$  = thermal diffusion constant,
- $\rho$  = density of water, and
- $\sigma_s(T)$  = microscopic scattering cross-section of water at energy  $kT$ .

The values used for these constants are given for H<sub>2</sub>O and D<sub>2</sub>O at various temperatures in Table 8.1. The microscopic capture cross-sections used are given in Table 8.2 for a neutron energy of 0.025 ev.

The type 347 stainless steel core tank was assumed to disturb only the thermal flux. A modified boundary condition at the core-reflector interface was used to take into account this absorption. Essentially, the current was made discontinuous by the amount required to account for the tank absorption. The macroscopic capture cross-section of type 347 stainless steel was taken to be 0.24 cm<sup>-1</sup>.

**Light-Water Reflector.** An investigation has been made of the feasi-

bility of using a light-water reflector for the HRE. A solution of 93.4% enriched UO<sub>2</sub>SO<sub>4</sub> was assumed for the core. Criticality calculations were made for a cold reactor with core and reflector both at 20°C and for a hot reactor with the core at 250°C and the reflector at 175°C. (This core temperature is actually higher than the average core temperature for 250°C outlet temperature. A figure of 230°C would be better.)

The concentrations required for criticality under various conditions are given in Table 8.3.

In Fig. 8.1 is plotted the effective multiplication (called  $k$  below, it is equal to unity for criticality and is the number of fissions produced directly by one fission) as a function of concentration for the four conditions of Table 8.3. It should be noticed that a reflector dump at operating temperature drops  $k$  by about 0.20. Such a dump, if not followed by some other operation, would result in criticality again being reached somewhat above room temperature (about 45°C). If, however, about 3 kg of water were to be added to the soup during the cooling process, no trouble would arise.

TABLE 8.1

Values of Macroscopic Two-Group Constants

	$T$ (°C)	$L^2$ (cm <sup>2</sup> )	$\tau$ (cm <sup>2</sup> )	$D_1$ (cm)	$D_2$ (cm)
H <sub>2</sub> O	20	7.068	33.00	1.143	0.1611
	175	12.773	41.345	1.279	0.2104
	250	18.435	52.158	1.437	0.2502
D <sub>2</sub> O	20	1.513 × 10 <sup>4</sup>	120.00	1.127	0.910
	175	2.532 × 10 <sup>4</sup>	152.95	1.271	1.103

# HRP QUARTERLY PROGRESS REPORT

TABLE 8.2

Microscopic Capture Cross-Sections

ELEMENT	CAPTURE CROSS-SECTION (barns)
H <sub>2</sub> O (per molecule)	0.69
D <sub>2</sub> O (per molecule)	0.00182
O	0.001
S	0.40
U <sup>235</sup>	644 ( $\sigma_f = 546$ )
U <sup>238</sup>	2.9

TABLE 8.3

Concentrations Required for Criticality Under Various Conditions

TEMPERATURE	REFLECTOR LEVEL	CRITICAL CONCENTRATION (g U/kg H <sub>2</sub> O)
Cold	Full	34.1
Hot	Full	59.6
Cold	Empty	56.7
Hot	Empty	>300

For the purpose of calculating reactor kinetics, three derivatives of  $k$  were obtained. These were

$$\left(\frac{\partial k}{\partial \rho}\right)_T, \left(\frac{\partial k}{\partial T}\right)_\rho, \text{ and } \frac{\partial k}{\partial \Sigma}$$

The first is calculated with respect to core density, holding core temperature, reflector temperature, and density constant. The second is calculated with respect to core temperature, holding the other quantities constant. The third is the variation

of  $k$  with macroscopic thermal capture cross-section added uniformly over the core and reflector. All derivatives are taken around the operating condition. The values are

$$\left(\frac{\partial k}{\partial \rho}\right)_T = 0.81 \text{ cm}^3/\text{g},$$

$$\left(\frac{\partial k}{\partial T}\right)_\rho = -5.3 \times 10^{-5}/^\circ\text{C},$$

and

$$\frac{\partial k}{\partial \Sigma} = 12.33 \text{ cm}.$$

From these quantities can be calculated the temperature coefficient

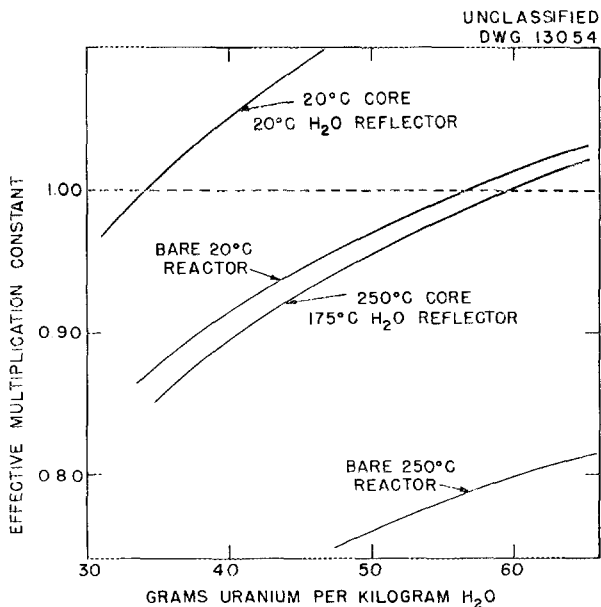


Fig. 8.1 - Effective Multiplication Constant of HRE with Light-Water Reflector, 93.4% Enriched Uranium.

of reactivity at constant pressure and the prompt generation time. These are

$$\left(\frac{\partial k}{\partial T}\right)_p = \left(\frac{\partial k}{\partial T}\right)_\rho + \left(\frac{\partial k}{\partial \rho}\right)_T \left(\frac{\partial \rho}{\partial T}\right)_p$$

and

$$\tau = \frac{1}{\bar{v}} \frac{\partial k}{\partial \Sigma}$$

where  $(\partial \rho / \partial T)_p$  is available from the steam tables,  $\bar{v}$  is the mean thermal neutron velocity at the operating temperature =  $3.22 \times 10^5$  cm/sec. The results are

$$\left(\frac{\partial k}{\partial T}\right)_p = -0.00130/^\circ\text{C}$$

and

$$\tau = 0.372 \times 10^{-4} \text{ sec.}$$

Finally, the composite result which is of direct interest for the kinetics is the quantity  $\omega_N^2$ , given by

$$\omega_N^2 = -\frac{\epsilon P_0}{\tau} \left(\frac{\partial k}{\partial T}\right)_p$$

where  $\epsilon$  is the reciprocal heat capacity of the reactor core and  $P_0$  is the reactor power. Taking

$$\epsilon = 0.00571 \text{ } ^\circ\text{C}/\text{kw-sec}$$

and

$$P_0 = 10^3 \text{ kw, } \omega_N^2 \text{ becomes } 200 \text{ sec}^{-2}.$$

There seems to be no strong reason why a light-water reflector should not be used. The most obvious disadvantage is the higher critical mass

(greater than 5 kg for the complete system). The margin of only 20% in  $k$  available from reflector changes seems to be adequate since, at the worst, small concentration changes can be made easily. A better argument probably is that passage from a mean reactor temperature of 230 to 20°C can be more than compensated for by dropping the reflector. The most obvious advantage of the light-water reflector is the great saving of complication in handling such a cheap material. Probably the strongest disadvantage of the system lies in the high value of  $\omega_N^2$ , which is about four times the corresponding quantity for a heavy-water reflector at the same reactor power. This means essentially that if the HRE with D<sub>2</sub>O reflector is so designed that all instabilities of the type discussed later are removed at all power levels below 1mw, then with an H<sub>2</sub>O reflector smooth operation will be possible only to ¼ mw.

#### Operation with Low-Enrichment Fuel.

With 300 g of uranium per liter of H<sub>2</sub>O at 250°C and a D<sub>2</sub>O reflector at 175°C, the HRE should be critical with an enrichment of 13.6%. At 20°C, a uranium concentration of 223 g per liter is required, so that a dilution ratio of 300/223 = 1.345 is needed to keep the system critical in going from hot to cold. The figure is in terms of grams per liter. A more convenient figure is the ratio on the basis of grams of uranium per kilogram of water. This ratio is 1.761.

#### KINETICS OF THE HRE

Further work has been done on the kinetic behavior of the HRE. Previous

## HRP QUARTERLY PROGRESS REPORT

work has consisted largely of extensive study of a somewhat simplified model in which thermal expansion of the core was assumed to take place at constant pressure. It was further assumed that heat is removed from the core at a steady rate. In the absence of delayed neutrons, this model exhibited steady oscillations about the equilibrium power, while the presence of delayed neutrons gave rise to a strong damping effect. Calculation of the power surges produced by steps in  $k$  of various sizes has given reasonable assurance that a violent nuclear accident is impossible in the HRE.

Before the actual operation of the HRE is begun, it is planned to investigate, with some care, the kinetics of a reactor which includes all the essential features of the HRE. Some preliminary work on this program has been started and is reported in a later section, but the main work on kinetics of the last quarter has still been concerned with a more or less idealized reactor. Only the assumption of expansion at constant pressure has been improved, but a considerable number of results have been obtained, some interesting from the practical point of view and others from the theoretical point of view only.

The simplest kinetic calculations are those in which the change with time of small deviations from equilibrium conditions is calculated by linearizing the equations of motion. These calculations are very useful for obtaining information on the stability of the system, and have, in fact, revealed that the proposed HRE design contained some unsuspected instabilities.

For the study of large power variations, it is essential that the

true nonlinear equations be solved. Some exploratory and approximate work of this type has been performed (and is described following the report of the work on the linearized equations). Two important conclusions result from this work:

1. The simple assumption of expansion at constant pressure is in fact very good for the calculation of any achievable power surges.
2. The delayed neutrons exert a tremendous damping effect which apparently removes all danger of sustained violent oscillation. Some instabilities, of a relatively nonviolent nature, enter as noted previously under the linearized calculations.

**Linearized Treatment of HRE with Pressurizer (G. T. Trammell).** In the present treatment the influence of gas is not considered; nor is correct account taken of the heat exchanger as the cooling agent, but instead a constant rate of cooling with no delay is assumed. A treatment dealing with these two additional factors will appear shortly. With these assumptions the linearized equations of motion of the system are:

$$\ddot{\rho} + \alpha \dot{\rho} + \frac{\omega_H^2}{C^2} \rho = 0, \quad (1)$$

$$\begin{aligned} \dot{P} = & \frac{P_0}{\tau} \left[ \frac{\partial k}{\partial \rho} \right]_S (1 - \beta) \rho - \frac{\beta}{\tau} P \\ & + \frac{\beta P_0}{\tau} \left[ \frac{\partial k}{\partial \rho} \right]_S \int_0^{\infty} K(s) \rho(t - s) ds \\ & + \frac{\beta}{\tau} \int_0^{\infty} K(s) P(t - s) ds, \quad (2) \end{aligned}$$

$$\rho = \left[ \frac{\partial \rho}{\partial S} \right]_p S + \frac{p}{c^2}, \quad (3)$$

and

$$\dot{S} = \epsilon P. \quad (4)$$

These equations are identical with those derived in ORNL-630<sup>(4)</sup> when the latter have been linearized, except for notation and trivial changes of form.

$\rho$ ,  $p$ ,  $P$ , and  $S$  are deviations from the equilibrium values of density, pressure, fission power, and reactor entropy. These symbols with subscript 0 (e.g.,  $P_0$ ) refer to the equilibrium values of density, pressure, etc.  $K(s)$  is the normalized delayed neutron kernel. The quantity  $c$  is the velocity of sound in the soup.  $\omega_H/2\pi$  is the frequency of the Helmholtz resonator (composed of core vessel plus pressurizer pipe) at zero power, and  $\alpha$  is the damping coefficient for this resonator.

A simplification which has been made in the past to study certain aspects of the system is to neglect the inertia of the fluid in the pressurizer and thereby to assume that as the fluid is heated the density of the fluid decreases immediately in accordance with Eq. (3), with  $p$  set equal to zero. The resulting motion, in response to a  $\delta k$  added say, is then given by Eqs. (2), (3), and (4), with  $p = 0$  in Eq. (3). The result is an oscillation with frequency given by

$$\omega_N^2 = \epsilon \frac{P_0}{\tau} \frac{\partial k}{\partial \rho} \left[ \frac{\partial \rho}{\partial S} \right]_p = 48 \text{ sec}^{-2},$$

<sup>(4)</sup> "Physics," *Homogeneous Reactor Experiment Report for the Quarter Ending February 28, 1950*, ORNL-630, p. 21 (Apr. 21, 1950).

which (as has been shown previously) is strongly damped because of the presence of delayed neutrons ( $\beta \neq 0$  would result in pure undamped oscillation with angular frequency  $\omega_N$ ). The actual motion in response to an added  $\delta k$ , as given by the full set of Eqs. (1) through (4), differs from the above simplified motion by the superposition of a rapid oscillation corresponding to the frequency of the pressurizer which has been shocked into oscillation, the amplitude of this "pressurizer" oscillation diverging exponentially with time unless (as shown below)

$$\frac{\beta}{\tau \alpha} \cdot \frac{\omega_N^2}{\omega_H^2}$$

is less than a certain number. The main purpose of this linearized treatment of the HRE motion is to uncover these possible diverging oscillations and to determine the conditions necessary to eliminate them. If Eqs. (3) and (4) are substituted into Eqs. (1) and (2), the following are obtained:

$$\ddot{y} + \alpha \dot{y} + \omega_H^2 y = -\omega_N^2 \omega_H^2 P, \quad (5)$$

and

$$\begin{aligned} \ddot{P} = & y - \beta \left[ y - \int_0^\infty K(s)y(t-s)ds \right] \\ & - \frac{\beta}{\tau} \left[ \dot{P}(t) - \int_0^\infty K(s)\dot{P}(t-s)ds \right], \quad (6) \end{aligned}$$

where

$$y = \dot{P} \frac{P_0}{\tau} \frac{\partial k}{\partial \rho}$$

## HRP QUARTERLY PROGRESS REPORT

has been taken as a convenient new variable, and

$$\omega_N^2 = \frac{\epsilon P_0}{\tau} \frac{\partial k}{\partial \rho} \left| \frac{\partial \rho}{\partial S} \right|_p$$

The general solution of Eqs. (5) and (6) will be a sum of terms of the form  $e^{\gamma t}$  ( $\gamma = \text{constant}$ ). Substituting  $y = c_1 e^{\gamma t}$  and  $P = c_2 e^{\gamma t}$  into Eqs. (5) and (6), the following equation for  $\gamma$  is obtained:

$$\gamma^2 [\gamma^2 + \alpha\gamma + \omega_H^2] [\gamma + \lambda + (\beta/\tau)] + \omega_N^2 \omega_H^2 (\gamma + \lambda) - \beta \omega_N^2 \omega_H^2 \gamma = 0, \quad (7)$$

where in Eq. (6) the approximation  $K(s) = \lambda e^{-\lambda s}$  has been made, which amounts to replacing all of the delay groups by one group with decay period =  $\lambda$ ; this approximation with  $\lambda = .1$  will not affect the validity of the results.

For the case that  $\alpha = 0$  (no damping of the hydrodynamical system) and  $\beta = 0$  (no damping of the nuclear system) Eq. (7) becomes

$$\gamma^2 [\gamma^2 + \omega_H^2] + \omega_N^2 \omega_H^2 = 0; \quad (8)$$

this has the solutions

$$\gamma^2 = -\frac{\omega_H^2}{2} \left[ 1 \pm \sqrt{1 - \frac{4\omega_N^2}{\omega_H^2}} \right], \quad (9)$$

and for  $\omega_N^2 \ll \omega_H^2$  this becomes

$$\gamma^2 = -\omega_H^2, -\omega_N^2; \quad \gamma = \pm i\omega_H, \pm i\omega_N. \quad (10)$$

This means that for the case  $\omega_H \gg \omega_N$  if an impulse is given to the fluid in the pressurizer, the resulting density vibrations in the core will be of such high frequency as to make negligible the effect on the pressure of the resulting heating due to the induced-power vibration. And in case of an added  $\delta k$ , the temperature rises so slowly that the inertia effect of the fluid in the pressurizer is negligible and the density of the fluid is that appropriate to the temperature with  $p = 0$ . As  $\omega_H/\omega_N$  becomes smaller, the effect of the nuclear power production on the pressurizer motion and pressurizer inertia on the nuclear power motion become larger, making the frequencies of these two motions depart from Eq. (10) in accordance with Eq. (9). Finally, as has been pointed out in the H. K. Ferguson Report 109,<sup>(5)</sup> if  $\omega_H^2 < 4\omega_N^2$  it is seen from Eq. (9) that there are solutions of Eq. (10) corresponding to  $\gamma$ 's with a positive real part which represent diverging oscillations.

For the HRE operating at a power  $P_0 = 1000$  kw,  $T = 250^\circ\text{C}$ , and  $p = 1000$  psi,  $\omega_N^2 = 48 \text{ sec}^{-2}$  and  $\omega_H^2 = 2.5 \times 10^4 \text{ sec}^{-2}$  (see end of this section for the derivation of these numbers).

Therefore, in the absence of fluid friction and delayed neutrons, pure sinusoidal oscillations with frequencies  $\approx \omega_H$  and  $\omega_N$  are obtained. The possibility of diverging oscillations arises when the delayed neutron and fluid friction effects are retained in Eq. (7). The delayed neutron terms tend to make the lower root ( $\approx \pm i\omega_N$  for  $\beta = \alpha = 0$ ) move to

<sup>(5)</sup>H. K. Ferguson Co., *Homogeneous Reactor for Subsonic Aircraft*, HKF-109 (Dec. 15, 1950).

the left in the complex plane, indicating a damped oscillation, as might be expected. On the other hand, the delayed neutron terms in Eq. (7) tend to make the upper root ( $\approx \pm i\omega_H$  for  $\beta = \alpha = 0$ ) move to the right in the complex plane, indicating an *antidamped* oscillation. The fluid friction terms in Eq. (7) tend to damp the higher frequency motion and antidamp the lower frequency. This will be found to be general: An effect (e.g., the delayed bubble production effect) which tends to damp one of the motions will tend to antidamp the other.

In order to demonstrate the validity of these statements, rewrite Eq. (7), separating out the terms in  $\beta$  and  $\alpha$ :

$$\begin{aligned} &(\gamma + \lambda) \{ \gamma^2(\gamma^2 + \omega_H^2) + \omega_N^2 \omega_H^2 \} \\ &+ (\beta/\tau) \gamma^2(\gamma^2 + \omega_H^2) - \beta \omega_N^2 \omega_H^2 \gamma \\ &+ \alpha \gamma^3(\gamma + \lambda) + \alpha \gamma^3(\beta/\tau) = 0. \quad (11) \end{aligned}$$

To exhibit semiquantitatively the behavior of the roots for  $\alpha \neq 0$ ,  $\beta \neq 0$ , call the left side of Eq. (11)  $F(\gamma, \beta, \alpha)$ . Let  $\gamma_1$  satisfy

$$F(\gamma_1, 0, 0) = 0$$

and let  $\delta\gamma$  satisfy

$$F[\gamma_1 + \delta\gamma(\beta), \beta, 0] = 0.$$

Then

$$\frac{\partial F(\gamma_1, 0, 0)}{\partial \gamma} \delta\gamma(\beta) + \frac{\partial F(\gamma_1, 0, 0)}{\partial \beta} \beta = 0$$

for small  $\beta$ ; therefore,

$$\begin{aligned} \delta\gamma &= -\beta \frac{\frac{\partial F(\gamma_1, 0, 0)}{\partial \beta}}{\frac{\partial F(\gamma_1, 0, 0)}{\partial \gamma}} \\ &= -\beta \frac{\frac{\gamma_1}{\tau} (\gamma_1^2 + \omega_N^2) - \omega_N^2 \omega_H^2}{2(2\gamma_1^2 + \omega_H^2) (\gamma + \lambda)}. \quad (12) \end{aligned}$$

Now from Eq. (11)

$$\begin{aligned} \gamma_1^2 &= -\frac{\omega_H^2}{2} \left[ 1 \pm \sqrt{1 - \frac{4\omega_N^2}{\omega_H^2}} \right] \\ &\approx -\omega_H^2 + \omega_N^2, \quad -\omega_N^2 \end{aligned}$$

Therefore,

$$\delta\gamma_1(\beta) \approx + \frac{\beta}{2\tau} \frac{\omega_N^2}{\omega_H^2} \quad (13)$$

for the upper root ( $\gamma_1 \approx \pm i\omega_H$ ), where small terms have been dropped, and

$$\delta\gamma_1(\beta) \approx -\frac{\beta}{2\tau} \quad (14)$$

for the lower root ( $\gamma_1 \approx \pm i\omega_N$ ), where again small terms have been dropped. Proceeding in the same manner to find the effect on the roots for  $\alpha \neq 0$ ,

HRP QUARTERLY PROGRESS REPORT

$$\delta\gamma(a) = -a \frac{\frac{F(\gamma_1, 0, 0)}{\partial a}}{\frac{\partial F(\gamma_1, 0, 0)}{\partial \gamma}}$$

$$= -a \frac{\gamma_1^2}{2(2\gamma_1^2 + \omega_H^2)}, \quad (15)$$

$$= -\frac{a}{2} \text{ at upper root } (\gamma_1 \approx \pm i\omega_H), \quad (16)$$

$$= +\frac{a \omega_N^2}{2 \omega_H^2} \text{ at lower root } (\gamma_1 \approx \pm i\omega_N). \quad (17)$$

In the above formulas  $\delta\gamma$  has been assumed small, and the formulas have been simplified by dropping small terms. It is to be noticed that an effect which causes damping of one of the oscillations causes antidamping of the other and that this "transfer effect" is  $\omega_N^2/\omega_H^2$  as large as the "direct" effect. From Eqs. (13) and (16) it is seen that the condition that the upper root have a negative real part is

$$\frac{\beta \omega_N^2}{2\tau \omega_H^2} < \frac{a}{2} \quad (18)$$

and that the lower root have negative real part is

$$\frac{\beta}{2\tau} > \frac{a \omega_N^2}{2 \omega_H^2}. \quad (19)$$

Actually  $\beta/\tau \approx 10^2$  is too large to make the results of Eqs. (12) through (19) more than suggestive. In particular Eq. (14) does not hold for this large  $\beta/\tau$ . These roots ( $\pm i\omega_N$  for  $\beta = 0$ ) go over into two negative real roots corresponding to overdamped "oscillation." The antidamping of the fluid friction will not affect appreciably this condition for the lower root. At the upper root the approximation is better, but since this will turn out to be a fairly crucial point a more precise stability condition than Eq. (18) must be obtained. The Nyquist stability criterion gives for stability, instead of Eq. (18),

$$\left[ 1 + \frac{\lambda a}{\omega_H^2} + \frac{\beta a}{\tau \omega_H^2} \right] + \sqrt{\left[ 1 + \frac{\lambda a}{\omega_H^2} + \frac{\beta a}{\tau \omega_H^2} \right]^2 - \frac{4\omega_N^2}{\omega_H^2}}$$

$$> \frac{\left[ \frac{\beta}{\tau} + \lambda \right] + \sqrt{\left[ \lambda + \frac{\beta}{\tau} \right]^2 - 4 \left[ \lambda + \frac{\beta}{\tau} + a \right] \frac{\omega_N^2}{\omega_H^2}}}{\lambda + \frac{\beta}{\tau} + a}, \quad (20)$$

which simplifies (taking  $\lambda \approx 0.1$ ) to

$$a > \frac{\beta \omega_N^2}{\tau \omega_H^2} \cdot \left( 1 + \frac{\beta^2}{\tau^2 \omega_H^2} \right) \quad (21)$$

For the HRE ( $P_0 = 1000$  kw,  $T_0 = 250^\circ\text{C}$ ,  $p_0 = 1000$  psi),

$$\begin{aligned} \omega_N^2 &= - \frac{\epsilon P_0}{\tau} \frac{\partial k}{\partial \rho} \left[ \frac{\partial \rho}{\partial S} \right]_P \\ &= \frac{1}{\tau} P_0 \frac{1}{\rho_0 V C_p} \frac{1}{K_c} \frac{\partial K_c}{\partial T} \\ &= \frac{10^4}{.837} 1000 \times (.00571) \times \frac{.0011}{1.56} \\ &= 48 \text{ sec}^{-2}. \end{aligned}$$

These numbers are given in ORNL-630,<sup>(4)</sup> except that  $\tau$  is taken as  $0.837 \times 10^{-4}$  sec from an earlier section of this report. Take  $\beta = .007$  and  $\omega_H^2 = 2.56 \times 10^4 \text{ sec}^{-2}$ , as given in a later section. This latter figure refers to the HRE design with separated main and pressurizer flows.

To agree with other work<sup>(6)</sup> in notation, multiply both sides of Eq. (21) by  $2\pi/\omega_H$ ,

$$\begin{aligned} \frac{2\pi}{\omega_H} a &\equiv \mu_f > \mu \\ &= \frac{2\pi}{\omega_H} \frac{\beta}{\tau} \frac{\omega_N^2}{1 + \frac{\beta^2}{\tau^2 \omega_H^2}} \quad (\text{for stability}) \quad (22) \\ &= 4.05 \times 10^{-3}. \end{aligned}$$

In Eq. (22)  $\mu_f$  represents the fractional loss of oscillation energy per cycle due to fluid friction, and  $\mu$  represents the fractional gain per cycle due to the antidamping arising from the delayed neutrons. In a later section  $\mu_f$  is calculated for the present design, and it is found that for laminar flow in the pressurizer (which corresponds to fluctuating pressure  $\sim 2.5$  psi)  $\mu_f \approx 9 \times 10^{-5}$ . For larger amplitudes the flow becomes turbulent and  $\mu_f$  increases about linearly with amplitude.  $\mu_f = 4 \times 10^{-3}$  will be reached at  $\Delta p \approx 65$  psi. This then will be the limiting amplitude of these oscillations. Other effects such as bubbles, expansibility of the core tank and heat exchanger, etc. may change this result appreciably so that no final conclusion on the magnitude of limiting oscillation can be made yet.

Some work (not yet final) has been done attempting to specify a pressurizer arrangement which will be stable against small oscillations.

<sup>(6)</sup>T. A. Welton to C. E. Winters, *Pressurizer Design*, ORNL CF-51-8-31 (Aug. 6, 1951); N. H. Woodruff to C. E. Larson, *Review of Idaho Operations Office Assistance Program at ORNL*, ORNL CF-51-4-114 (Apr. 24, 1951).

**Nonlinear Mechanics of HRE with Pressurizer** (G. T. Trammell and T. A. Welton). Consider first the

# HRP QUARTERLY PROGRESS REPORT

model represented by the following simplified set of equations:

$$\left. \begin{aligned} \dot{P} &= \frac{1}{\tau} \left[ \delta + \frac{dk}{d\rho} \right] P \\ \dot{S} &= \epsilon(P - P_0) \\ \frac{1}{\omega_H^2} \ddot{\rho} + \rho &= \left[ \frac{\partial \rho}{\partial S} \right]_p S, \end{aligned} \right\} (1)$$

$$\left. \begin{aligned} \ddot{Q} &= \frac{\dot{\delta}}{\tau} + \frac{1}{\tau} \frac{dk}{d\rho} \dot{\rho} \\ \dot{S} &= \epsilon P_0 (e^Q - 1) \\ \left[ \frac{1}{\omega_H^2} \frac{d^2}{dt^2} + 1 \right] \dot{\rho} &= \left[ \frac{\partial \rho}{\partial S} \right]_p \dot{S} \\ &= \epsilon P_0 \left[ \frac{\partial \rho}{\partial S} \right]_p (e^Q - 1). \end{aligned} \right\} (2)$$

where

- $P$  = reactor power,
- $\tau$  = prompt generation time,
- $\delta$  = excess reactivity under external control,
- $S$  = excess entropy of core,
- $\rho$  = excess density of core,
- $P_0$  = heat removed per second,
- $\epsilon$  = factor for conversion from excess power to rate of change of entropy,
- $\omega_H$  = frequency (radians per second) of oscillation of fluid into and out of the core, and
- $p$  = core pressure.

A convenient treatment of these equations is obtained by the introduction of a logarithmic power variable,  $Q = \log P/P_0$ . Equations (1) then become

A little further work yields

$$\left[ \frac{1}{\omega_H^2} \frac{d^2}{dt^2} + 1 \right] \left[ \ddot{Q} - \frac{\dot{\delta}}{\tau} \right] + \left[ -\frac{\epsilon P_0}{\tau} \frac{dk}{d\rho} \left[ \frac{\partial \rho}{\partial S} \right]_p \right] (e^Q - 1) = 0 \quad (3)$$

or

$$\frac{1}{\omega_H^2} \ddot{\ddot{Q}} + \ddot{Q} + \omega_N^2 (e^Q - 1) = \left[ \frac{1}{\omega_H^2} \frac{d^2}{dt^2} + 1 \right] \frac{\dot{\delta}}{\tau}, \quad (4)$$

with

$$\omega_N^2 = - \frac{\epsilon P_0}{\tau} \frac{dk}{d\rho} \left[ \frac{\partial \rho}{\partial S} \right]_p$$

In this model delayed neutrons are ignored, which assumption will be seen to be completely unrealistic in some respects, but is reasonable for the study of power surges. In this case,  $\delta$  is the excess prompt reactivity.

Consider first the case  $\delta = 0$ . Equation (4) is then equivalent to an energy equation,

$$\frac{d}{dt} \left[ \frac{1}{\omega_H^2} \left( \dot{Q} \ddot{Q} - \frac{\ddot{Q}^2}{2} \right) + \frac{\dot{Q}^2}{2} + \omega_N^2 (e^Q - Q) \right] = 0 \quad (5)$$

If  $1/\omega_H^2 = 0$ , the previously extensively studied case is obtained. In this case, evaluation of the energy constant yields an expression for  $\dot{Q}$  as a function of  $Q$ , and the motion is therefore periodic, as has been previously pointed out by J. M. Stein. It is further obvious that since  $\dot{Q}^2$  increases monotonically as  $|Q|$  increases and since  $(e^Q - Q)$  likewise increases monotonically as  $|Q|$  increases, any motion must be contained in a finite region of the  $Q, \dot{Q}$  space.

If  $1/\omega_H^2$  is not zero, then it is not possible to show rigorously that

the solution of Eq. (5) remains finite for all time. The trouble arises from the term

$$\left[ \dot{Q} \ddot{Q} - \frac{\ddot{Q}^2}{2} \right],$$

which is not positive definite and may actually decrease strongly as  $\dot{Q}$ ,  $\ddot{Q}$ , or  $\ddot{Q}^2$  become large in magnitude. It is therefore to be suspected that the motion described by Eq. (5) goes arbitrarily far from  $Q = 0$  after sufficiently long times. This possibility is difficult to verify formally, but a simple examination of possible mechanisms suffices to make it clear that this diverging motion would actually occur.

Qualitatively, the motion described by Eq. (5) can be regarded as a superposition of two nearly independent motions. This is strictly true for small amplitudes, in which case (if  $\omega_H^2 \gg \omega_N^2$ , as is actually the case) one motion is a rapid sinusoidal variation with frequency nearly equal to  $\omega_H$ , and the other motion is a slow sinusoidal variation with frequency nearly equal to  $\omega_N$ . No divergence occurs in the linear approximation.

Assume, however, that a sudden variation in  $k$  is made, so that a large power surge is initiated. If the initial rise rate of the power is comparable with  $\omega_H$ , the pressurizer flow lags initially behind that required for expansion at constant pressure. This lag persists until the rapid increase of pressure has stopped, and the pressurizer flow then overshoots. The net result is that because of the nonlinearity of

## HRP QUARTERLY PROGRESS REPORT

the system, one type of motion generates the other type. That is, a single power surge generates an undamped train of density oscillations (frequency  $\omega_H$ ). These persist during the recovery (or cooling) period, and, as the reactor again rises through prompt critical, the density variation may have such a phase that the rate of rise of reactivity from cooling is augmented by that due to fluid rushing in from the pressurizer. The next power surge will then be more violent than the first. It is apparently possible to find one or more stationary motions ("limit cycles," in not quite the correct sense) in which the thermal oscillation repeats, shifting the phase of the mechanical oscillation properly each time a power surge occurs. A more usual type of motion would involve a steady increase of the average level of the mechanical oscillations, with a corresponding increase in the amplitude of the power surges.

It is clear that a small amount of frictional damping of the mechanical oscillations, combined with some heat transfer or delayed neutron damping of the thermal oscillations will prevent a true divergent motion, but may make possible one or more stable or unstable limit cycles involving a periodic sequence of large power surges.

The precise restrictions which must be made on the operating procedures to avoid the initiation of such limit cycles are very difficult to determine, although there is some reason to believe that the existence of the actual delayed neutron fraction may render this type of motion impossible. Some numerical calculations on this point are in progress.

**Effect of Pressurizer on Limiting Power Surges** (T. A. Welton). The simplest application of the foregoing is to the question of calculating the magnitude of the power and pressure surge resulting from a sudden change in  $k$ . For the simple (constant pressure) model, the power calculation is extremely simple and has been given in a previous quarterly report (ORNL 630).<sup>(4)</sup> The pressure calculation (also given there) is more complicated since the pressurizer mechanism must be taken into account in estimating the deviation from the constant pressure condition. The influence of the pressurizer system on the maximum power has, on the other hand, not previously been given, and this is of considerable interest in the design of a suitable pressurizer.

The result for the constant pressure model is obtained by the use of the previously given energy expression ( $1/\omega_H^2 = 0$ ) and is

$$\omega_N^2(e^Q - Q) = \frac{\delta^2}{2\tau^2}, \quad (1)$$

where  $Q$  is the value of logarithmic power ratio at maximum and  $\delta$  is the initial excess prompt reactivity. For large  $\delta$ ,  $e^Q \gg Q$  and Eq. (1) becomes

$$P = \frac{P_0 \delta^2}{\omega_N^2 2\tau^2}. \quad (2)$$

A standard method for solving such problems approximately is to assume that the system exponentiates at the

initial rate ( $\delta/\tau$ ) until the rate suddenly drops to zero a time  $\Delta$  after the beginning of the "accident." This time  $\Delta$  is determined by calculating the expansion on the assumption of a steady exponentiation. On the constant pressure model

$$\left. \begin{aligned} \dot{Q} &= \frac{1}{\tau} \left[ \delta + \left[ \frac{\partial k}{\partial S} \right]_p S \right] \\ \dot{S} &= \epsilon P_0 (e^{\delta t} - 1) \end{aligned} \right\} (3)$$

According to the simple procedure outlined,

$$\left. \begin{aligned} \dot{Q} &= \frac{\delta}{\tau} \\ Q &= \frac{\delta}{\tau} t \\ \dot{S} &= \epsilon P_0 (e^{(\delta/\tau)t} - 1) \\ S &= \epsilon P_0 \left[ \frac{e^{(\delta/\tau)t} - 1}{\delta/\tau} - t \right] \end{aligned} \right\} (4)$$

Finally, set  $t = \Delta$  and equate the total reactivity to zero. An equation is thereby obtained for  $\Delta$ ,

$$\delta = - \left[ \frac{\partial k}{\partial S} \right]_p \frac{\epsilon P_0 \tau}{\delta} \left[ e^{(\delta/\tau)\Delta} - 1 - \frac{\delta}{\tau} \Delta \right] (5)$$

If  $(\delta/\tau)\Delta$  is somewhat larger than unity, only the exponential term is important, so that

$$P_0 e^{(\delta/\tau)\Delta} = P = \frac{\delta^2}{\epsilon \tau \left[ \frac{\partial k}{\partial S} \right]_p} = \frac{P_0 \delta^2}{\omega_N^2 \tau^2} (6)$$

It is seen that the peak power is overestimated by a factor of two only.

The same procedure can be used in the model with pressurizer and may then be expected to be of comparable accuracy. Consider Eqs. (1) of the previous section,

$$\left. \begin{aligned} \dot{Q} &= \frac{1}{\tau} \left[ \delta + \frac{dk}{d\rho} \rho \right] \\ \dot{S} &= \epsilon P_0 (e^{\delta t} - 1) \\ \frac{1}{\omega_H^2} \ddot{\rho} + \rho &= \left[ \frac{\partial \rho}{\partial S} \right]_p S \end{aligned} \right\} (7)$$

Using a similar procedure and making similar neglections,

HRP QUARTERLY PROGRESS REPORT

$$\dot{Q} = \frac{\delta}{\tau}$$

$$Q = \frac{\delta}{\tau} t$$

$$\dot{S} = \epsilon P_0 e^{(\delta/\tau)t}$$

$$S = \frac{\epsilon P_0}{\delta/\tau} e^{(\delta/\tau)t}$$

$$\rho = \frac{\frac{\epsilon \tau}{\delta} P_0 \left[ \frac{\partial \rho}{\partial S} \right]_P e^{(\delta/\tau)t}}{1 + \frac{\delta^2}{\omega_H^2 \tau^2}} \quad (8)$$

In obtaining the final line of Eq. (8), only the dominant exponential dependence has been kept.

The analog of Eq. (5) is

$$\delta = \frac{-\frac{dk}{d\rho} \epsilon \left[ \frac{\partial \rho}{\partial S} \right]_P}{\frac{\delta}{\tau} \left[ 1 + \frac{\delta^2}{\omega_H^2 \tau^2} \right]} P_0 e^{(\delta/\tau)\Delta} \quad (9)$$

The maximum power  $P$  is then given by

$$P = P_0 e^{(\delta/\tau)\Delta}$$

$$= \frac{\delta^2}{\epsilon \tau \frac{dk}{d\rho} \left[ -\frac{\partial \rho}{\partial S} \right]_P} \left[ 1 + \frac{\delta^2}{\omega_H^2 \tau^2} \right]$$

$$= \frac{P_0}{\omega_N^2 \tau^2} \frac{\delta^2}{\tau^2} \left[ 1 + \frac{\delta^2}{\omega_H^2 \tau^2} \right] \quad (10)$$

This is identical with the corresponding result for the constant pressure model except for an increase by a factor

$$\left[ 1 + \frac{\delta^2}{\omega_H^2 \tau^2} \right]$$

This factor obviously takes into account the fact that the reaction now progresses further before the acceleration of the pressurizer flow allows criticality to be reached. It is clear that the size of the parameter  $\delta/\omega_H\tau$  determines the size of the departure from the previously obtained constant pressure results.

For orientation, take  $\omega_H = 160 \text{ sec}^{-1}$  and  $\tau = 10^{-4} \text{ sec}$ . Then the correction factor is approximately

$$1 + (60\delta)^2 \quad (11)$$

which is seriously greater than unity for all values of  $\delta$  larger than 0.01. It is therefore clear that previous calculations seriously underestimate the maximum power and pressure to be

expected from various steps in  $k$ , for all steps larger than 1%. This statement holds only for the present pressurizer design, and various simple modifications are under consideration which would increase  $\omega_H^2$  by a factor of as much as ten and thereby greatly alleviate the situation.

**Damping Produced by Delayed Neutrons (T. A. Welton).** As noted in the treatment of the system with pressurizer and constant power removal, but no delayed neutrons, dangerous self-sustained power oscillations can be set up whenever information concerning the past of the reactor is fed back into the reactivity. These oscillations do not have the character of antidamped solutions of the linearized equations, but are rather "limit-cycle" types of motion. In the simple cases studied the existence of a reasonable delayed neutron fraction seems to insure that such limit cycles will be very difficult to set up. Some work has been done in attempting to understand the mechanisms involved, so that fairly general criteria for stable operation can be formulated.

Consider the model with expansion at constant pressure and constant power removal. The equations are

$$\left. \begin{aligned} \dot{P}(t) &= \frac{1}{\tau} [\delta - \alpha S - \beta] P(t) \\ &+ \frac{\beta}{\tau} \int_0^{\infty} ds K(s) P(t-s) \\ \dot{S} &= \epsilon(P - P_0) \end{aligned} \right\} (1)$$

In these equations a slight modification has been made of the usual definition of prompt generation time, and this modified quantity is assumed to be independent of the state of the reactor ( $\tau$  independent of  $S$ ). The kernel  $K(s)$  is the time distribution of delayed neutron emission following fission at  $s = 0$  [ $K(s)$  has unit integral], and  $\beta$  is the fraction of delayed neutrons. Introducing the logarithmic power variable ( $Q = \log P/P_0$ ) previously defined,

$$\left. \begin{aligned} \dot{Q} &= \frac{1}{\tau} [\delta - \alpha S \\ &- \beta] \frac{\beta}{\tau} e^{-Q(t)} \int_0^{\infty} ds K(s) e^{Q(t-s)} \\ \dot{S} &= \epsilon P_0 (e^Q - 1) \end{aligned} \right\} (2)$$

or

$$\ddot{Q} + \omega_N^2 (e^Q - 1) = \frac{\dot{\delta}}{\tau} - \frac{\beta}{\tau} \int_0^{\infty} ds K(s) e^{Q(t-s) - Q(t)} \left[ \dot{Q}(t) - \dot{Q}(t-s) \right]. \quad (3)$$

similar to those given previously with  $1/\omega_H^2 = 0$  and a "memory" term inserted to account for delayed neutrons.

It is desired to show that solutions of this equation are always damped. For this purpose, multiply by  $\dot{Q}$  and rewrite the equation as

[REDACTED]

## HRP QUARTERLY PROGRESS REPORT

$$\frac{d}{dt} \left[ \frac{\dot{Q}^2}{2} + \omega_H^2 (eQ - Q) \right] = \frac{\dot{\delta}}{\tau} \dot{Q} - \frac{\beta}{\tau} \int_0^{\infty} ds K(s) e^{Q(t-s)-Q(t)} \left[ \dot{Q}^2(t) - \dot{Q}(t)\dot{Q}(t-s) \right]. \quad (4)$$

The term on the left is the rate of change of a positive definite "energy." The first term (involving  $\dot{\delta}$ ) on the right is the work done per unit time by an external "force," while the second term (proportional to  $\beta$ ) is the work done per unit time by the damping "force" due to the delayed neutrons. Consider the linearized equation (small motion about  $Q = 0$ ). The above equation becomes

$$\frac{d}{dt} \left[ \frac{\dot{Q}^2}{2} + \frac{\omega_N^2}{2} Q^2 \right] = \frac{\dot{\delta}}{\tau} \dot{Q} - \frac{\beta}{\tau} \int_0^{\infty} ds K(s) \left[ \dot{Q}^2(t) - \dot{Q}(t)\dot{Q}(t-s) \right]. \quad (5)$$

With this equation the delayed neutrons always cause damping. This can be shown by imagining that the "force"  $\dot{\delta}/\tau$  is such as to maintain any steady motion of  $Q$ . Under these conditions, the average value of the left-hand side is zero, and the average work done per unit time on the system by the external "force" is

$$\overline{\frac{\dot{\delta}}{\tau} \dot{Q}} = \frac{\beta}{\tau} \int_0^{\infty} ds K(s) \left[ \overline{\dot{Q}^2(t)} - \overline{\dot{Q}(t)\dot{Q}(t-s)} \right]. \quad (6)$$

There exists an obvious theorem that for any periodic function

$$\overline{\dot{Q}^2(t)} \geq \overline{\dot{Q}(t)\dot{Q}(t-s)}, \quad (7)$$

so that the function  $K(s)$  in the integrand is multiplied by a positive function of  $s$ . Since  $K(s)$  must also be positive (from its meaning), the average work done on the system per unit time by the external force is

positive. Without the force, the energy of the system would therefore decrease with time, and damping is assured.

Such a theorem cannot be proven when the linearized equation is invalid. It is in fact a simple matter to obtain a counter-example. Suppose all the delayed neutrons are emitted a definite time after fission and that this time is of the order of magnitude of the cooling time required by the reactor for some particular size power pulse. It will then clearly be possible for a steady motion to occur which consists of a regular succession of power surges separated by cooling periods. The fission fragments

[REDACTED]

FOR PERIOD ENDING AUGUST 15, 1951

generated in each surge release their neutrons during the last portion of the heating phase of the following surge. In this way, each surge can reinforce the next, and the losses in the system can be canceled.

Such a pathological delayed neutron law does not actually hold, and a simple consideration of the mechanism of damping indicates that probably for a law with  $K(s)$  decreasing monotonically, no real trouble can occur. Systems of this type have been solved numerically in several instances (one such solution is described in a later section of this report), and the HRE simulator has, of course, given many such solutions during its use. With a delayed neutron law resembling the correct one even in a rough way, nothing but a single overdamped power surge has ever been found to result from a single disturbance of reactivity. The presence of a delay fraction larger than 1/2% with a mean delay time in the range from 1 sec upward then seems absolutely certain to render all power surges overdamped.

It is of some interest that the assumption of a large mean delay time makes it possible to prove the damping property rigorously. Under this condition, the memory term in Eqs. (1) can obviously be calculated by setting  $P(t - s)$  equal to its average value  $P_0$ . This is actually a fair approximation to the true situation when it is remembered that  $\omega_N \simeq 7 \text{ sec}^{-1}$ , while a mean decay constant for the delayed neutrons might be  $0.1 \text{ sec}^{-1}$ . The first of the two Eqs. (2) then becomes

$$\dot{Q} = \frac{1}{\tau} [\delta - \alpha S - \beta] + \frac{\beta}{\tau} e^{-Q}, \quad (8)$$

and Eq. (3) becomes

$$\ddot{Q} + \omega_N^2 (e^Q - 1) = \frac{\dot{\delta}}{\tau} - \frac{\beta}{\tau} e^{-Q} \dot{Q}. \quad (9)$$

The analog of Eq. (4) is

$$\frac{d}{dt} \left[ \frac{\dot{Q}^2}{2} + \omega_N^2 (e^Q - Q) \right] = \frac{\dot{\delta}}{\tau} \dot{Q} - \frac{\beta}{\tau} e^{-Q} \dot{Q}^2. \quad (10)$$

If  $\dot{\delta} = 0$  (no applied "force"), then the rate of change of the positive definite "energy" is equal to the negative definite "dissipation function"

$$-\frac{\beta}{\tau} e^{-Q} \dot{Q}^2,$$

and any motion must therefore become smaller and eventually cease.

A similar situation holds when a simple heat transfer lag (Newton's law for cooling, rather than constant heat removal) is assumed. For the second of Eqs. (1), substitute

$$\dot{S} + \eta S = \epsilon P_0 (e^Q - 1), \quad (11)$$

where a shift in the origin of  $S$  (and hence of reactivity) has been made. Combined with the assumption of an average delayed neutron level, Eq. (11) leads to

## HRP QUARTERLY PROGRESS REPORT

$$\ddot{Q} + \omega_N^2 \left[ e^Q - 1 + \frac{\beta\eta}{\omega_N^2\tau} (1 - e^{-Q}) \right] = \frac{\dot{\delta} + \eta\delta}{\tau} - \left[ \frac{\beta}{\tau} e^{-Q} + \eta \right] \dot{Q}. \quad (12)$$

Here again Eq. (12) gives the time derivative of a positive definite energy equal to a negative definite function, and damping is assured. Such simple calculations give some reason to believe that the much more complicated heat transfer effects in the HRE will likewise contribute to the damping of power surges. Unfortunately, it is fairly certain (from a preceding section) that such damping is necessarily accompanied by a tendency to antidamp the pressurizer motion.

**Numerical Calculation of a Power Surge** (W. C. Sangren, L. H. Thacker, H. T. Williams, and P. M. Wood). The results of some numerical calculations are given in ORNL-925.<sup>(7)</sup> Similar calculations have been carried out for a simplified set of equations with a  $\delta k$  equal to 0.01. The calculations were performed in order to obtain a better concept of the role that delayed neutrons play in the damping of large power oscillations and in order to obtain data for comparison with analytical results. The equations of motion under consideration are

$$(1) \quad \dot{P} = \frac{1}{\tau} \left[ -\alpha(T - T_0) + \delta k - \beta \right] P + \lambda C,$$

$$(2) \quad \dot{T} = S(P - P_0),$$

$$(3) \quad \dot{C} = -\lambda C + \frac{\beta}{\tau} P,$$

where

$P$  = power level of reactor,  $P_0 = 10^3$  kw,

$T$  = temperature,  $T_0 = 250^\circ\text{C}$ ,

$C$  = lumped concentration of delayed neutron emitters,

$\tau$  = prompt generation time =  $10^{-4}$  sec,

$\alpha$  = temperature coefficient of reactivity =  $10^{-3}/^\circ\text{C}$ ,

$\lambda$  = decay constant for assumed single group of delayed neutron emitters =  $.08 \text{ sec}^{-1}$ ,

$\beta$  = fraction of delayed neutrons =  $7.5 \times 10^{-4}$ , and

$S$  = reciprocal heat capacity of reactor =  $5.73 \times 10^{-3} \text{ }^\circ\text{C/kw-sec}$ .

The same results are obtained whether one assumes a given  $\delta k$  and the initial temperature equal to the equilibrium temperature or one assumes  $\delta k = 0$  and the initial temperature equal to the equilibrium temperature minus  $\delta k/\alpha$ . The Runge-Kutta method of numerical integration was used.

The results of the calculations are displayed in Figs. 8.2 - 8.4.

<sup>(7)</sup>"Dynamics," *Homogeneous Reactor Experiment Quarterly Progress Report for Period Ending November 30, 1950*, ORNL-925, p. 78 (Jan. 30, 1951).

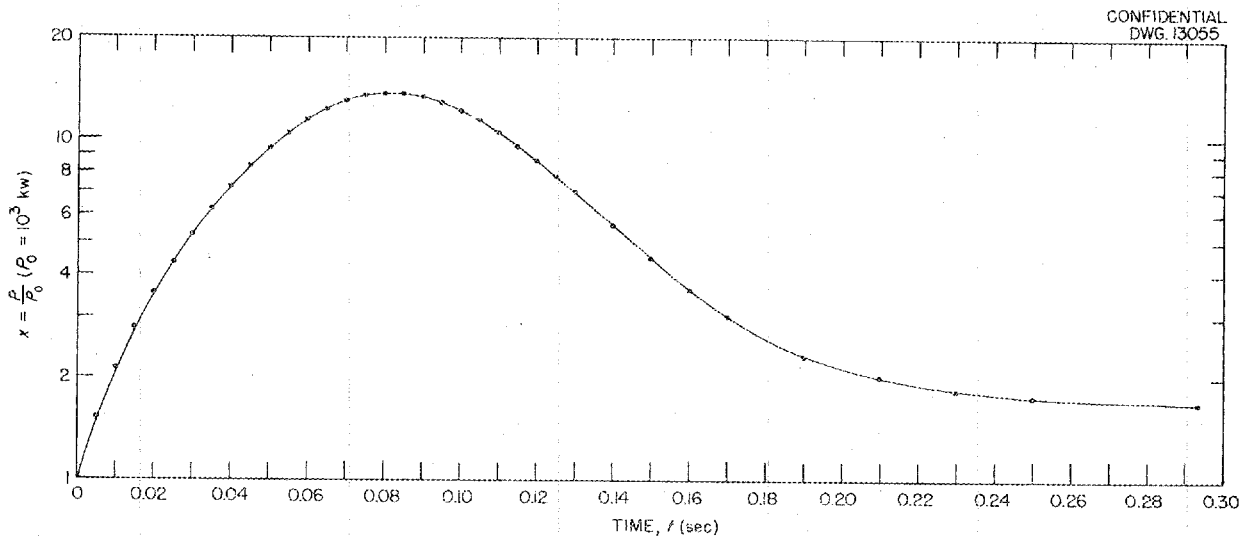


Fig. 8.2 - Power as a Function of Time Following a Step in  $k$ .

These results agree fairly well with those obtained in ORNL-925<sup>(7)</sup> when allowance is made for the differences in the constants used. It is apparent from the graphs that the power is overdamped. Assuming at  $t = .29$  that the power is proportional to the concentration of delayed neutron emitters, i.e.,

$$P_{.29}^d = \frac{\lambda r}{[\beta + \alpha T_{.29}]} C_{.29} ,$$

one obtains

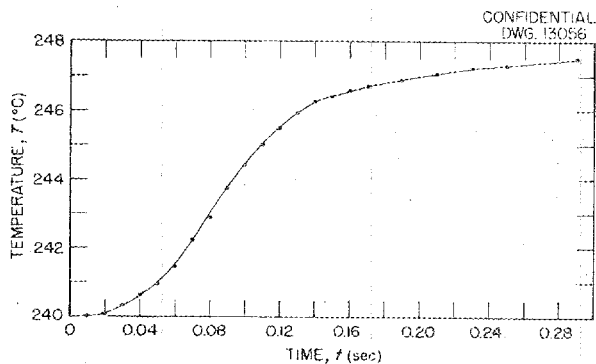


Fig. 8.3 - Temperature as a Function of Time Following a Step in  $k$ .

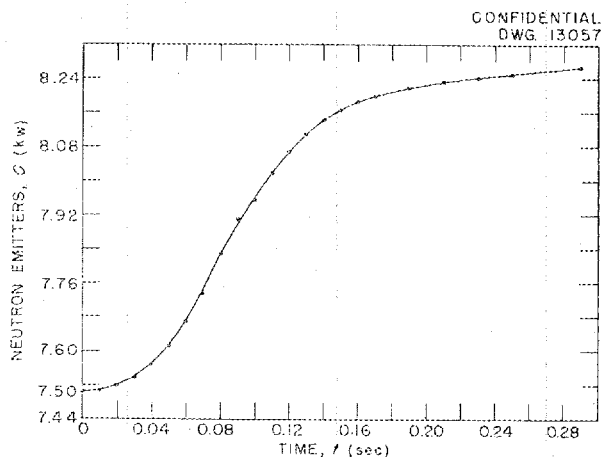


Fig. 8.4 - Number of Delayed Neutron Emitters Present as a Function of Time Following a Step in  $k$ .

~~XXXXXXXXXX~~

## HRP QUARTERLY PROGRESS REPORT

$$P_{.29}^d = 1.65 \times 10^3 \text{ kw ,}$$

This may be compared to the calculated value

$$P_{.29} = 1.70 \times 10^3 \text{ kw ,}$$

which perhaps makes it clear that the role of the delayed neutrons is to provide a slowly decaying power level. This slow decay interferes with the recovery process, which, in the absence of delayed neutrons, would begin at about  $t = 0.16$  sec. In this case, the temperature rises monotonically to the equilibrium value. If  $\beta$  were smaller, the temperature could rise above equilibrium, but only at a slower rate than the first time, so that damping of a prompt power surge seems inevitable in any event.

**Possibility of Slow, Undamped Power Excursions** (W. C. Sangren and T. A. Welton). Although it seems unlikely that any rapid, undamped power variations (with reactivity at times exceeding prompt critical) can occur when a reasonable delayed neutron fraction is present, the absence of a rigorous theorem on this point raises the possibility that slow power variations may exist which can be steady and which never involve passage above prompt critical. This possibility can be ruled out, or at least rendered very unlikely, by use of the method of isoclines. Consider the model with constant pressure expansion, constant power removal, and one group of delayed neutrons. The equations are

$$\left. \begin{aligned} \dot{P} &= \frac{1}{\tau} (\alpha S + \beta)P + \lambda C \\ \dot{C} &= -\lambda C + \frac{\beta}{\tau} P \\ \dot{S} &= \epsilon(P - P_0) . \end{aligned} \right\} \quad (1)$$

If no excursions above prompt critical are made and all variations with time are small in a time  $\tau/\beta$  ( $\approx 10^{-2}$  sec), an excellent approximation to Eqs. (1) is obtained by dropping  $\dot{P}$ . This corresponds to calculating the power level by simple instantaneous multiplication of the delayed neutron source.

Choose  $1/\lambda$  as the unit of time and define

$$\left. \begin{aligned} x &= \frac{P}{P_0} \\ \frac{\lambda S}{\epsilon P_0} &= Q \\ y &= \frac{\lambda \tau}{\beta P_0} C \\ \frac{\beta}{\lambda \tau} &= \mu \\ \frac{\alpha \epsilon P_0}{\lambda \tau^2} &= \nu . \end{aligned} \right\} \quad (2)$$

With these definitions and neglect of  $\dot{P}$  the Eqs. (1) are equivalent to

$$\left. \begin{aligned} x\dot{y} - y\dot{x} &= \frac{\nu}{\mu} x^2 (x - 1) \\ \dot{y} &= -y + x . \end{aligned} \right\} \quad (3)$$

Finally, substitution of the second into the first yields

$$\left. \begin{aligned} \dot{x} &= \left(1 + \frac{\nu}{\mu}\right) \frac{x^2}{y} - \frac{\nu}{\mu} \frac{x^3}{y} - x \\ \dot{y} &= x - y \end{aligned} \right\} (4)$$

Division of the second equation by the first yields

$$\frac{dy}{dx} = \frac{y(x - y)}{\left(1 + \frac{\nu}{\mu}\right)x^2 - xy - \frac{\nu}{\mu}x^3} \quad (5)$$

Taking  $\alpha P_0/\tau = 50 \text{ sec}^{-2}$  for the HRE,  $\beta = 0.01$ ,  $\lambda = 0.1 \text{ sec}^{-1}$ , the constants become

$$\nu = 5 \times 10^3,$$

$$\mu = 10^3,$$

$$\nu/\mu \equiv K = 5.$$

Figure 8.5 represents the solutions in the phase plane of the equation

$$\frac{dy}{dx} = \frac{y(x - y)}{(1 + K)x^2 - xy - Kx^3}.$$

The equation has three singular points:  $y = 0, x = 0$ ;  $y = 1, x = 1$ ; and  $y = 0, x = (1 + K)/K$ . The singular point  $y = 1, x = 1$  is a stable node while the singular point  $y = 0, x = (1 + K)/K$  is a saddle point. The usual plot in the phase plane is somewhat complicated by the fact that the isocline curves are not easily drawn. It is clear from the graph that a stable situation exists, i.e., starting from any point except  $y = 0, x = 0$  the motion will always end at  $y = 1, x = 1$ . This behavior is assured by the "im-

penetrable" line extending from the stable node to the saddle point.

A Method for Treating Certain Second-Order Nonlinear Differential Equations (W. C. Sangren). Many second-order nonlinear differential equations, including some of interest in the treatment of reactor kinetics, fall into one of the following three classes:

$$(1) \left[ \frac{d}{dx_1} + f(x_1) \right] [h(x_1, x_2, x_3)] = 0,$$

$$(2) \left[ \frac{d}{dx_1} + g(x_1, x_2, x_3) \right] [G\{g(x_1, x_2, x_3)\}] = 0,$$

and

$$(3) \left[ \frac{d}{dt} + k(t, y) \right] \left[ K\left\{k, \frac{dk}{dt}, t\right\} \right] = 0,$$

where  $x_1, x_2, x_3$  represent  $t, y, dy/dt$  in any order. Equations in classes (1) and (2) may be solved by solving in sequence two first-order equations, while equations in class (3) may be solved by solving a simpler second-order equation. Further details concerning the technique of obtaining the solutions will appear in the next quarterly progress report of the Mathematics Panel.<sup>(8)</sup>

<sup>(8)</sup>W. C. Sangren, "A Method for Treating Certain Second-Order Nonlinear Differential Equations," *Mathematics Panel Quarterly Progress Report for Period Ending October, 31, 1951*, ORNL-1151 (to be issued).

HRP QUARTERLY PROGRESS REPORT

NOT CLASSIFIED  
DWG. 13058

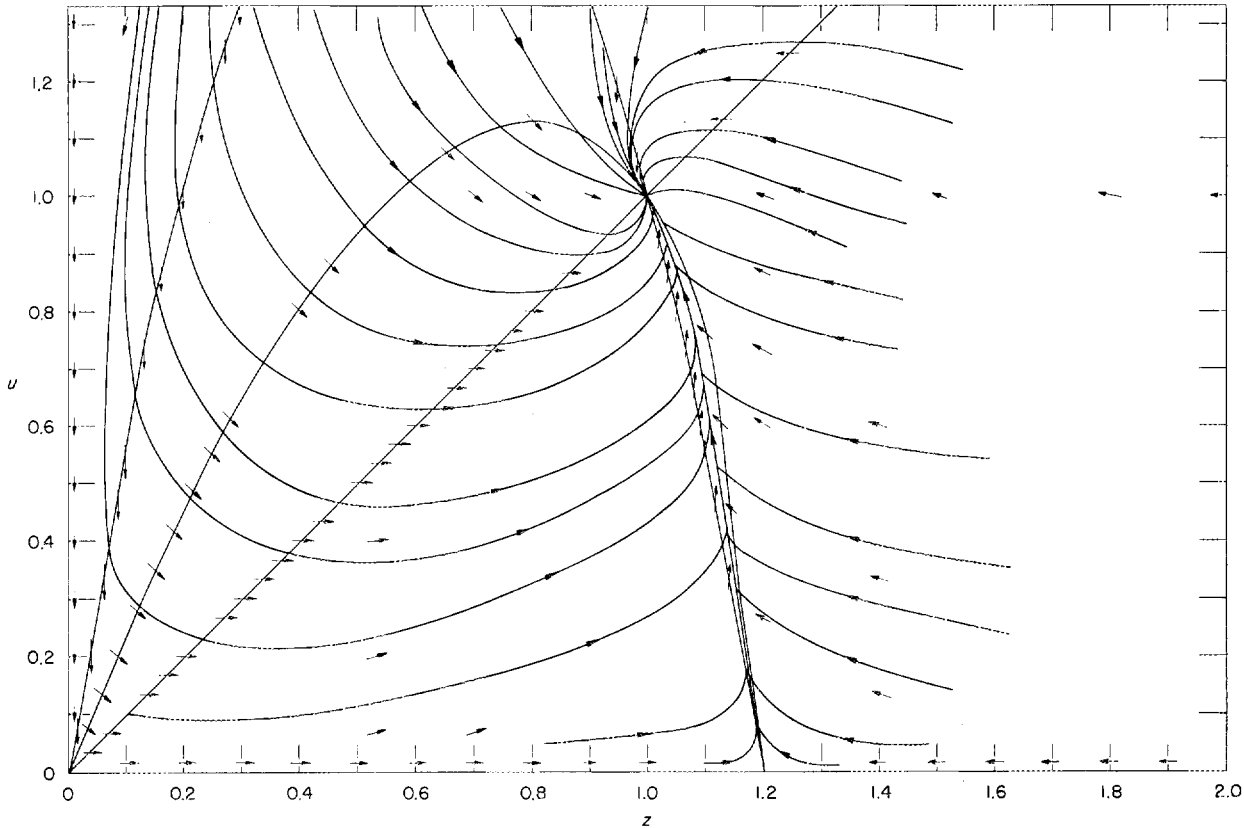


Fig. 8.5 - Paths in a Phase Plane Given by

$$\frac{dn}{dz} = \frac{u(z - u)}{z^2 - uz - az^3 + az^2}, \quad a = 5.$$

An elementary application may be made to the equation

$$\frac{\ddot{P}}{P} - \frac{\dot{P}^2}{P^2} = -\alpha S(P - P_0),$$

which results from the elimination of  $T$  between the equations  $T = S(P - P_0)$  and  $\dot{P} = -(\alpha T + S)P$ . Let  $P/P_0 = y$  and multiply by  $y$ . One then obtains

$$\ddot{y} - \frac{1}{y}\dot{y}^2 + \alpha SP_0 y(y - 1) = 0.$$

This equation takes the factored form

$$\left[ \frac{d}{dy} - \frac{2}{y} \right] \left[ \frac{1}{2} \dot{y}^2 + \alpha SP_0 y^2 (y - \log y) \right] = 0.$$

Consequently,

$$\frac{1}{2} y^2 + \alpha SP_0 y^2 (y - \log y) = Ky^2,$$

where  $K$  is an integration constant. This result can also be obtained by using Eqs. (3) and (4), page 24, ORNL-630.<sup>(4)</sup> From the last equation it follows that

$$t = \int_{y(0)}^{y(t)} [2K - 2\alpha SP_0 (z - \log z)]^{-1/2} z^{-1} dz.$$

The equations

$$\ddot{y} = \left[ \frac{dh}{dy} \right] \frac{\dot{y}^2}{h(y)} + F \left[ \frac{y}{h} \right] G(y) = 0$$

and

$$\ddot{y} + f \left[ \frac{\dot{y}}{h} \right] \frac{dh}{dy} h(y) = 0$$

can be replaced by two first-order equations which may be integrated by quadrature in the phase plane since the variables are separable. The above two equations prove to be the most general equations of the type  $\ddot{y} = H(y, \dot{y})$ , which can be integrated in such a fashion. This result is of interest as demonstrating explicitly when many second-order equations can be transformed by change of dependent variables to a form where an "energy" constant of the motion exists.

**FLUID FRICTION COEFFICIENTS IN THE PRESSURIZER TUBE AND THEIR EFFECTS ON THE REACTIVITY OF THE CORE MATERIALS**

R. E. Aven

Changes in the reactor core density are caused by reactor temperature

changes and are essential for stability. These changes are actually affected by the flow of core liquid into or out of the pressurizer, and it is necessary to know the natural frequency and damping coefficient of the resulting pressurizer oscillations. The frequency is 24 cycles per second at 500°F and 31 cycles per second at 400°F. By using a modified form of the Fanning equation for the turbulent flow region and a modification of Poiseuille's law for the streamline flow region, and by assuming that the flow in the pressurizer tube is essentially that due to the core acting as a Helmholtz resonator, it is possible to derive the equation for the friction decay coefficient of mechanical oscillation.

$$\mu = [16/3]FB = \text{fraction of energy of oscillation lost per cycle,}$$

where

$$\mu = \text{friction decay coefficient,}$$

$$F = 0.0621f \sum_{i=1}^3 \frac{L_i V^2 \omega^2}{D_{e_i} A_i^2 P c^2},$$

$$B = \Delta\rho = \text{excess density of solution,}$$

$$f = \text{friction factor,}$$

$$L = \text{length of pressurizer tube section,}$$

$$D_e = \text{equivalent diameter of tube,}$$

$$V = \text{volume of reactor core,}$$

$$A = \text{cross-sectional area of the pressurizer tube available to flow,}$$

$$\rho = \text{density of liquid in reactor,}$$

**HRP QUARTERLY PROGRESS REPORT**

$c$  = velocity of sound through the liquid,

$$\omega = \frac{c}{\sqrt{V \int_0^L \frac{dx}{A}}} = \text{frequency of oscillation,}$$

and

$x$  = distance along pressurizer, measured from core edge.

The relation between the pressure amplitude in the core and the change in reactivity is given by

$$[\Delta k]_{\max} = 2.46 \times 10^{-6} \text{ @ } 500^\circ\text{F}$$

or

$$[\Delta k]_{\max} = 1.44 \times 10^{-6} \text{ @ } 400^\circ\text{F,}$$

where  $[\Delta k]_{\max}$  is the maximum change of reactivity and  $\Delta p$  is the pressure amplitude in psi.

Figure 8.6 shows the decay factor,  $\mu$ , plotted vs. the change of reactivity and the pressure amplitude. For further information on this subject see ORNL CF-51-7-114. <sup>(9)</sup>

**HEAT TRANSFER COEFFICIENTS FOR THE STEAM GENERATOR**

R. E. Aven

Reactivity changes in the core materials produce certain effects on the heat generator and its ability

<sup>(9)</sup>R. E. Aven, *Calculation of Fluid Friction Coefficients in the Pressurizer Tube and Their Effects on the Reactivity of the Core Materials*, ORNL CF-51-7-114 (July 25, 1951).

to deliver steam at the desired power level. To make an analytical study of the reactor vessel--heat exchanger system, particular fluid and heat transfer coefficients of the heat exchanger are needed. The coefficient,  $K$ , which determines the temperature drop per unit time of a slug of fluid passing through the heat exchanger tube, is defined as

$$K = \frac{UA}{C_p}$$

where

$K$  = thermal coefficient in lb/hr,

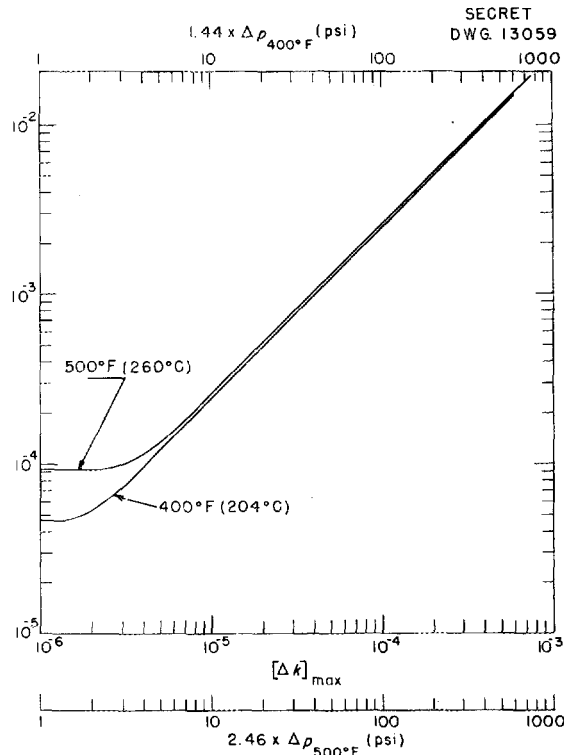


**Fig. 8.6 - Fractional Energy Loss Per Cycle of Pressurizer Oscillation as a Function of Amplitude.**

FOR PERIOD ENDING AUGUST 15, 1951

- $A$  = area of heat transfer in  $\text{ft}^2$ ,  
 $C_p$  = heat capacity of fluid flowing in the tubes in  $\text{Btu/lb-}^\circ\text{F}$ , and  
 $U$  = over-all heat transfer coefficient of the heat exchanger in  $\text{Btu/hr-ft}^2\text{-}^\circ\text{F}$ .

By using the equation

$$U = \frac{1}{\frac{1}{h_i(D_i/D_o)} + \frac{k}{x_w D_{\text{avg}}/D_o} + \frac{1}{h_o} + \frac{1}{h_f}}$$

where

- $h_i$  = inside fluid film coefficient of heat transfer,  
 $h_o$  = outside fluid film coefficient of heat transfer,  
 $h_f$  = fouling coefficient (assumed 5000),  
 $k$  = thermal conductivity of metal in tubes,  
 $x_w$  = thickness of tube wall,  
 $D_o$  = outside diameter of the tubes,  
 $D_{\text{avg}}$  = arithmetic average diameter of the tubes, and  
 $D_i$  = inside diameter of the tubes,

the value of the heat transfer coefficient can be calculated.

It is necessary also to know the value of the coefficient

$$L \frac{dW}{dT_s}$$

at various power levels of operation. The latent heat of vaporization,  $L$ ,

is found from the steam tables and the variation of the weight of stored steam with temperature is found from the equation

$$\frac{dW}{dT_s} = \frac{MV}{R} \left[ \frac{1}{T_s} \frac{dp_s}{dT_s} + \frac{p_s}{T_s^2} \right],$$

where

- $W$  = weight of stored steam in the steam generator,  
 $V$  = volume of steam in the steam generator,  
 $M$  = molecular weight of the steam,  
 $R$  = gas constant,  
 $T_s$  = temperature in absolute units, and

$\frac{dp_s}{dT_s}$  = variation of the vapor pressure of steam with temperature, which is found from the steam tables.

The coefficients

$$K, U, \text{ and } L \frac{dW}{dT_s}$$

are plotted vs. the power level in Figs. 8.7 and 8.8.

The time required for a particle of fluid to pass through each tube varies due to the varying length of the tubes and the resulting variation of the velocity in each tube. By assuming an equal pressure drop across each tube, the velocity in each tube can be calculated and consequently

HRP QUARTERLY PROGRESS REPORT

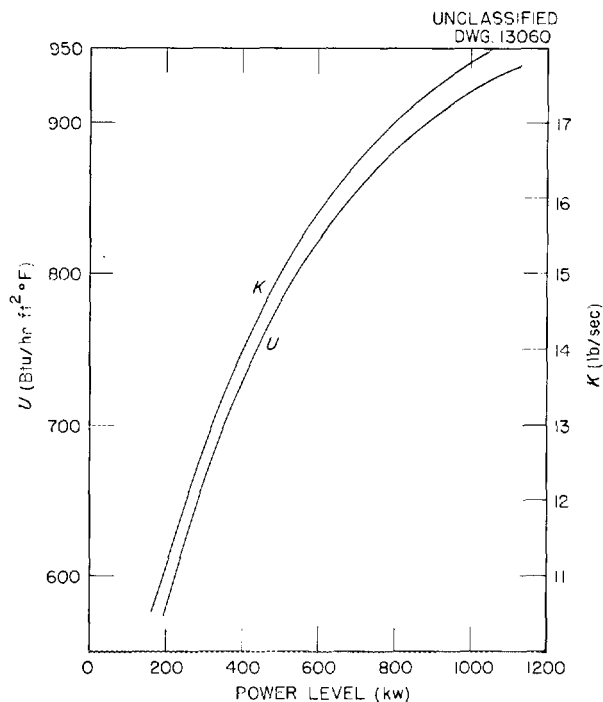


Fig. 8.7 - Heat Transfer Coefficients for the HRE Boiler.

the time of passage through each tube may be found. Table 8.4 shows the results of such calculations.

For further information on the heat transfer coefficients see ORNL CF-51-8-116.<sup>(10)</sup>

SAFETY CALCULATIONS FOR THE HRE

R. E. Aven and P. C. Zmola

The generation of hydrogen and oxygen from the decomposition of water by fission fragments in the core tank of the HRE presents a

<sup>(10)</sup>R. E. Aven, *Heat Transfer Coefficients for the Heat Exchanger*, ORNL CF-51-8-116 (Aug. 17, 1951).

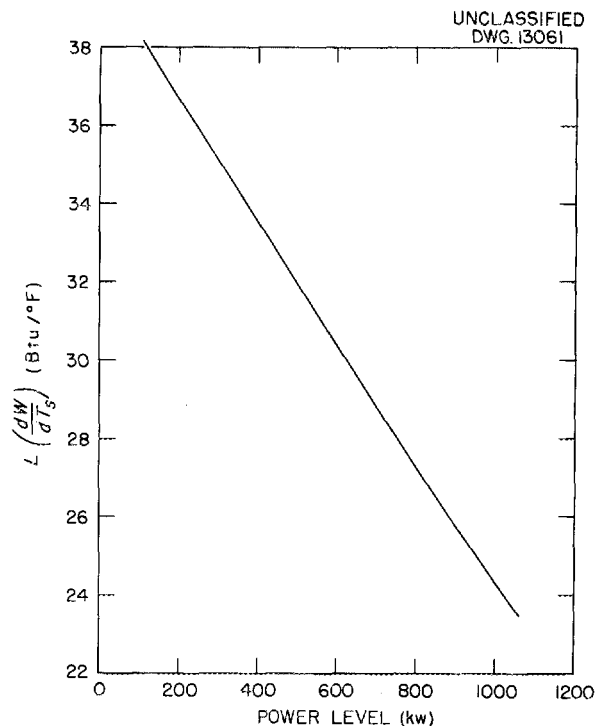


Fig. 8.8 - Heat Required to Change the Steam Temperature in the Boiler by Unit Amount with No Efflux of Steam.

possible hazard from a chemical explosion should the gas mixture become ignited. A similar hazard exists from the possible accumulation of deuterium and oxygen in the gas space above the reflector as a result of radiation decomposition of the reflector.

Calculations for the core tank explosion were performed for a mean core temperature and pressure of 250°C and 1000 psi, respectively.<sup>(11)</sup> The gas volume geometry in the core may be idealized in a number of ways.

<sup>(11)</sup>P. C. Zmola and T. A. Welton, *Effects of Possible Chemical Explosions in the Core Tank of the HRE*, ORNL CF-51-7-3 (July 3, 1951).

TABLE 8.4

Calculated Values of Velocity and Time of Passage Through Steam Generator Tubes

ROW	NUMBER OF TUBES	TIME IN EACH ROW (sec)	FRACTION OF FLUID THROUGH EACH ROW OF TUBES
1	14	0.619	0.127
2	16	0.629	0.143
3	15	0.639	0.135
4	16	0.651	0.143
5	15	0.660	0.134
6	12	0.671	0.107
7	11	0.683	0.097
8	8	0.691	0.070
9	5	0.701	0.044

The idealizations which appeared most realistic were:

1. The explosive mixture occupies a 200-cc spherical volume concentric with the core shell.
2. The explosive mixture occupies a 200-cc cylindrical volume at the axis of the core vortex and extends across the entire diameter of the core. For this geometry the core vessel could fail in two ways,
  - a. Failure in tension as a result of a radial shock wave,
  - b. Failure in shear as a result of localized shock at either end of the gas core.

Results of the calculations indicated that an explosion in the gas core would not be of sufficient violence to rupture or deform the core tank.

A similar calculation<sup>(12)</sup> was carried out for the reflector tank at a number of temperatures. Deuterium and oxygen resulting from decomposition of the reflector material by radiation can collect in the gas space above the reflector. Should ignition take place, an explosion could result which might (1) rupture the reflector tank, (2) blow off the reflector tank cover, (3) crush or buckle the core tank, and (4) crush or buckle the pressurizer tube.

Results indicate that the reflector tank and cover would not fail in this type of explosion. On the other hand, the core tank and pressurizer pipe might be crushed. However, inertia effects, which were neglected, would probably enable the liquid-filled core tank to withstand somewhat greater pressures than indicated by the calculations.

The rates of diluent addition required to keep combustibles at nonexplosive concentrations are given in Table 8.5. The gas generation was calculated on the basis of one molecule of H<sub>2</sub> per 100 ev absorbed in the reflector. Approximately 5% of the total power was taken as absorbed in the reflector on the basis of a calculation made by estimating the quantity of primary gamma radiation, neutrons, and secondary gamma radiation absorbed in the reflector. Convenient diluent gases might be hydrogen, deuterium, or helium.

<sup>(12)</sup>R. E. Aven and P. C. Zmola, *Effects of Possible Chemical Explosions in the Reflector Tank of the HRE*, ORNL CF-51-7-105 (July 24, 1951).

HRP QUARTERLY PROGRESS REPORT

TABLE 8.5

Rate of Diluent Addition To Keep  $2H_2 + O_2$  Above Reflector at Nonexplosive Concentration (15%) for a Reflector Pressure of 1000 psi and Reactor Power of 1000 kw

REFLECTOR TEMPERATURE (°C)	GAS GENERATION RATE (ft <sup>3</sup> /hr)	TIME REQUIRED FOR ACCUMULATION OF EXPLOSIVE MIXTURE		DILUENT REQUIRED FOR STEADY-STATE OPERATION (%)	MINIMUM RATE OF DILUENT ADDITION	
		REFLECTOR AT HIGH LEVEL (hr)	REFLECTOR AT LOW LEVEL (hr)		AT REFLECTOR CONDITIONS (ft <sup>3</sup> /hr)	STP (ft <sup>3</sup> /hr)
100	0.38	1.9	5.4	84	2.12	107
150	0.43	1.7	4.7	78	2.25	97
200	0.48	1.6	4.3	62	2.01	77
250	0.54	1.6	4.3	27	0.97	34
274	0.56	∞	∞	0	0.0	0

9. CONTROLS

L. R. Quarles, Leader

D. G. Davis	E. E. Mason
J. R. Hart	C. A. Mossman
L. P. Howland	J. E. Owens
L. P. Inglis	V. K. Pare
E. R. Mann	W. P. Walker

B. P. White

More complete calculations on heat generation and loss in the reactor indicate that the shutdown operation must be modified. Accordingly, the soup circulating pump must be left running or the soup must be dumped on any shutdown. Any signal indicating a soup leak must, of course, dump the soup, but other emergency signals or manual operation will not dump the soup unless the circulating pump stops.

The pressurizer control has been changed to permit partial oxygen pressurization. The flow sheet for this is shown in Fig. 9.1. The vapor pressure is maintained at the desired value by temperature control of the 10-kw boiler. The total pressure is maintained at the desired value by admitting oxygen under control of the total pressure instrument. The double valving system shown is used to prevent any possibility of active gas backing up in a line to the outside of the shield. Oxygen pressure is maintained in the intermediate reservoir at a value above that in the pressurizer space. Interlocks prevent both valves opening at the same time.

The soup circulating system instrumentation has been changed. The instrument which formerly gave soup average temperature has been recon-

nected to measure temperature drop across the heat exchanger and will be calibrated in terms of extracted power. This instrument and the neutron level instrument will be supplied with integrators to provide a direct indication of total energy.

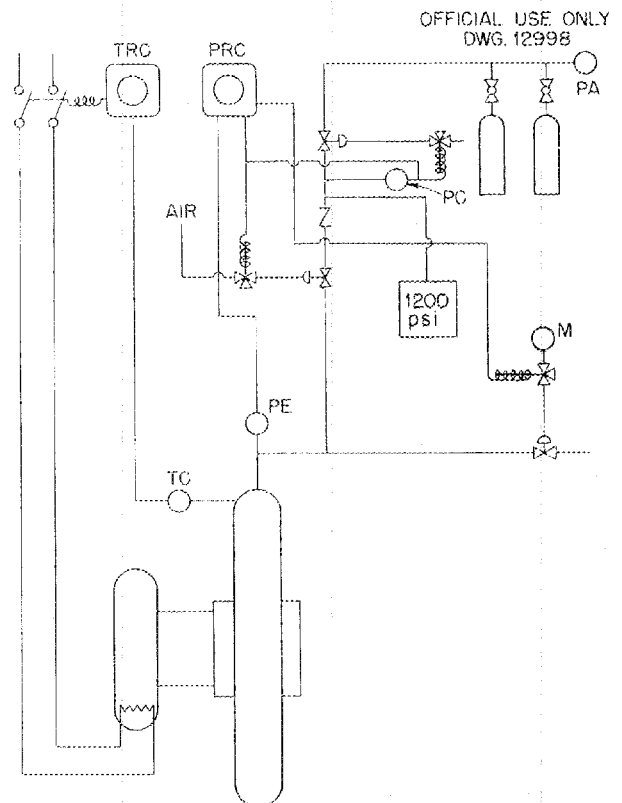


Fig. 9.1 - Flow Sheet for Pressurizer Control.

## HRP QUARTERLY PROGRESS REPORT

Development work on a deuterium detector has given promising results. This device is intended for use in the  $D_2O$  off-gas system (and possibly elsewhere) to detect any decrease in efficiency of the recombiners. The specifications call for operation over a wide range of flow rates and for the detector to be as sensitive as is consistent with reliable operation. A survey of available methods of detecting hydrogen with a simple instrument failed to show anything which was suitable but did show a promising approach. The work therefore has been concentrated on modifying a commercially available device, the Davis Hydrogen Detector, for this purpose. This detector uses an activated platinum filament, electrically heated, with an attached thermocouple. Hydrogen and oxygen passed over the filament recombine and heat the filament still more, the increase of temperature being determined with the thermocouple. To compensate for variations in cooling by changing flow rates, a second unit, similar in construction but using a noncatalytic filament, is inserted in the gas stream and the thermocouples of the two are connected in opposition. Tungsten and chromel have been used for this second filament, the latter being somewhat the better. An output which is approximately 2.5 times the noise level signal can be obtained for a 0.25% stoichiometric mixture of hydrogen and oxygen in helium with flow rates from 10 to 5000 cc/min.

A liquid-level transmitter has been developed for use on the pressurizer. This consists essentially of a restrained float and inductance transmitter as shown in Fig. 9.2.

The float is Schedule 40 pipe supported by a double cantilever structure of stainless steel rods. These are placed at the top of the chamber so they are in a gas bound space and hence not subject to large temperature variations and resulting errors. A motion of the magnetic core of approximately 0.03 in. for a

OFFICIAL USE ONLY  
DWG. 12999

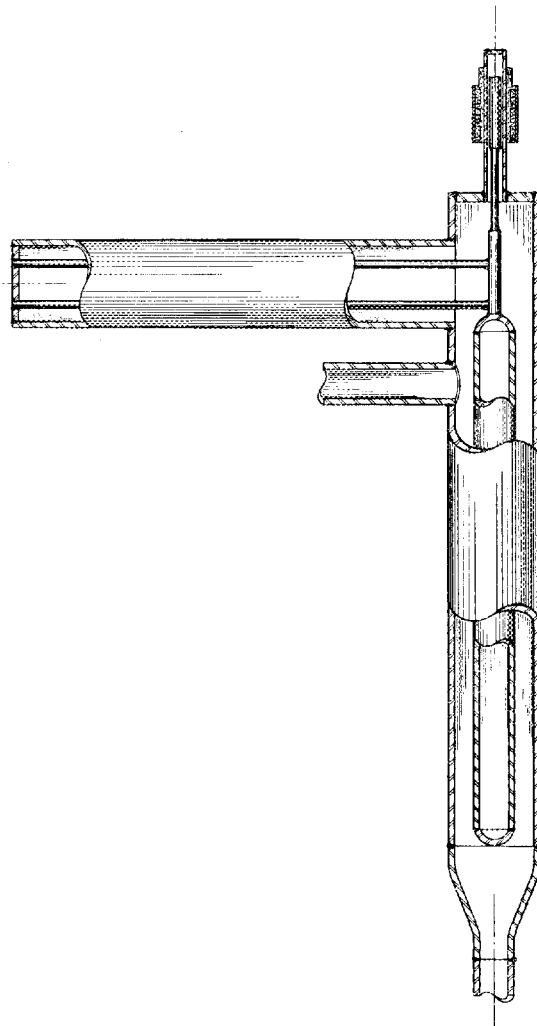


Fig. 9.2 - Pressurizer Liquid-Level Float.

~~SECRET~~

FOR PERIOD ENDING AUGUST 15, 1951

10-in. change of level produces full-scale deflection on the recorder. Present work is directed toward suitable damping means to remove

high-frequency fluctuations while still permitting the instrument to follow level changes due to power changes.

1000

1000

[REDACTED]

**Part II**

**ALTERNATE SYSTEMS**

[REDACTED]



## 10. SOLUTION CHEMISTRY

W. L. Marshall, Leader  
W. B. Bunger                      J. S. Gill  
H. O. Day, Jr.                    E. V. Jones  
H. W. Wright

### THE URANIUM TRIOXIDE—PHOSPHORIC ACID—WATER SYSTEM

J. S. Gill      W. L. Marshall  
H. W. Wright

During the past four months a study has been made of the uranium trioxide—phosphoric acid—water system to determine its potentialities as a reactor fuel. As a result, the phase solubility relationships of uranium trioxide in phosphoric acid have been determined at 250°C from dilute concentrations to 350 g of uranium per liter of solution. These data have been coupled with the preliminary work<sup>(1)</sup> in order to present a more complete picture of the system.

Much uncertainty has existed in using the synthetic method for the study of this particular system because of the apparent slow approach to equilibrium. Consequently, effort has been concentrated in devising methods which rely on final analyses of the solutions after equilibrium is attained.

**Experimental.** A rotator was devised which could hold ten silica tubes (4-in. length, 4-mm i.d.) containing appropriate solutions and solids and which operated in a small oven equipped with quartz windows for

observation. However, the temperature control was not better than  $\pm 5^\circ\text{C}$ ; therefore, a second rotator was devised which operated in a liquid salt bath thermostated to  $250 \pm 0.5^\circ\text{C}$ . All reported analytical data were obtained using the liquid salt rotator; the oven rotator was used only for exploratory purposes.

Appropriate concentrations of Mallinckrodt water-washed uranium trioxide and c.p. Baker and Adamson orthophosphoric acid were sealed in 4-mm-i.d. silica tubing. Dissolved air was not removed before sealing. These tubes were placed in the liquid salt unit and rotated at 250°C for 72 hr. Each tube was removed, cooled rapidly in an ice mush, centrifuged, and broken, and the solution was pipeted from the solid phase. Approximately 1½ min elapsed from the time of removal to final separation. The assumption, based on previous observations,<sup>(1)</sup> is that solubility equilibrium is not sufficiently altered during this operation to affect the analyses.

Both phosphate and uranium were analyzed by colorimetric methods<sup>(2,3)</sup> accurate to  $\pm 3\%$ .

(1) "The Uranium Trioxide-Phosphorus Acid-Water System," *Homogeneous Reactor Project Quarterly Progress Report for Period Ending May 15, 1951*, ORNL-1057, p. 112 (Oct. 10, 1951).

(2) J. E. Currah and F. E. Beamish, "Colorimetric Determination of Uranium with Thiocyanate," *Anal. Chem.* 19, 609 (1947).

(3) P. B. Fisk *et al.*, "Microdetermination of Phosphate," *Chemical Research — Analytical, Metallurgical Project*, A. H. Compton, Director, CN-1792, p. 18 (June 1, 1944).

**HRP QUARTERLY PROGRESS REPORT**

The solubility of uranium trioxide at 250°C as a function of phosphoric acid concentration is given in Table 10.1 and Fig. 10.1. Two of the points obtained previously<sup>(1)</sup> by the synthetic method are shown on the figure and agree approximately with the analytical values.

**TABLE 10.1**

**Solubility of Uranium Trioxide in Orthophosphoric Acid Solutions at 250°C**

SAMPLE NO.	MOLARITY OF H <sub>3</sub> PO <sub>4</sub>	MOLARITY OF UO <sub>3</sub>	MOLE SOLUBILITY RATIO, PO <sub>4</sub> /U
1	2.77	0.23	12.
2	3.57	0.42	8.5
3	4.86	0.78	6.2
4	5.05	0.84	6.0
5	5.95	1.26 (?)	
6	6.05	1.13	5.35
7	6.69	1.30	5.15
8	6.95	1.43	4.86

From these data, then, at 300 g of uranium per liter, a mole ratio, PO<sub>4</sub>/U = 5.2, will be necessary for this solubility. At 40 g of uranium per liter, the ratio is 13.

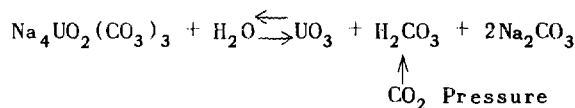
**Conclusions.** At 250°C aqueous phosphoric acid solutions of approximately 300 g of uranium per liter or more apparently are feasible for reactor fuels from a phase solubility and neutron economy standpoint.

No additional work will be done on this system unless future developments warrant a more extensive study.

**THE EFFECT OF CARBON DIOXIDE ON THE SODIUM URANYL CARBONATE-WATER SYSTEM**

H. W. Wright and J. S. Gill

This study was undertaken to ascertain the feasibility of sodium uranyl carbonate in water and under carbon dioxide pressure as an alternate fuel for a homogeneous reactor. Previous studies<sup>(4)</sup> at temperatures up to 90°C indicated that this salt might prove an acceptable fuel for operation at 250°C if the forward hydrolysis equilibrium could be sufficiently inhibited by carbon dioxide pressure according to the following reaction:



Aliquots of approximately 1 cc of a saturated (0.24 M) Na<sub>4</sub>UO<sub>2</sub>(CO<sub>3</sub>)<sub>3</sub> solution prepared from an aqueous reaction of uranium trioxide and sodium bicarbonate were sealed in silica tubes, heated to 250°C and observed. A "blank" containing a saturated solution of sodium bicarbonate was run at 250°C in order to note any reaction which might be due to sodium or bicarbonate. In addition, tubes with the Na<sub>4</sub>UO<sub>2</sub>(CO<sub>3</sub>)<sub>3</sub> solution saturated with carbon dioxide and other tubes containing solution in which small amounts of dry ice were added before sealing were run.

No precipitation was observed in the "blank" after 24 hr at 250°C.

(4) W. E. Bunce, N. H. Furman, and R. J. Mundy, *The Solubility of Sodium Uranyl Carbonate in Water and in Solutions of Various Salts*, M-4238 (May 1947).

UNCLASSIFIED  
DWG. 13000

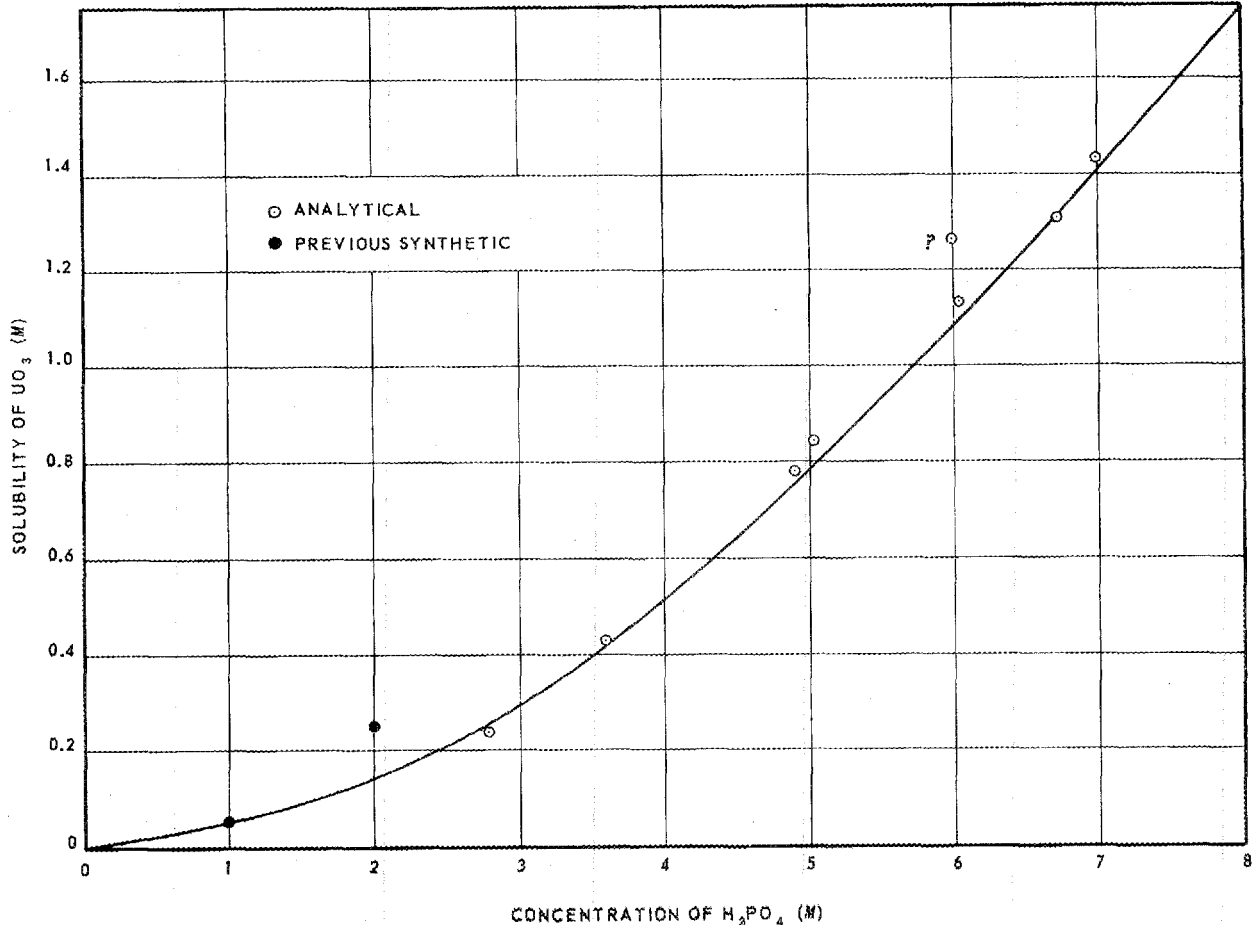


Fig. 10.1 - The Solubility of Uranium Trioxide in Phosphoric Acid at 250°C.

However, upon cooling, a cloudiness did appear and remain on the walls of the tube indicating that a definite but slow decomposition had occurred. In all runs involving the  $Na_4UO_2(CO_3)_3$  solutions, uranium compounds (evidently hydrolysis products) precipitated from solution. These yellow precipitates were first observed at 190°C in the tubes containing no carbon dioxide. Precipitation occurred to a lesser degree and at a slower

rate in those tubes containing carbon dioxide but only after remaining at 200°C for 1 hr.

A sodium uranyl carbonate-carbon dioxide-water system, therefore, appears unfeasible at 250°C both from a hydrolytic instability and low-solubility standpoint. Further study could indicate hydrolytic stability if high carbon dioxide pressure were applied to the system; however,

## HRP QUARTERLY PROGRESS REPORT

it is doubtful whether the uranium solubility could be increased sufficiently.

### VAPOR PRESSURES OF URANYL SALT SOLUTIONS

H. O. Day, Jr.

The compound manometer system which had been designed for measurement of vapor pressures below 10 atm has been completed. The utilization of this apparatus has been postponed temporarily in favor of measurements of vapor pressures at the higher temperatures (150 to 350°C) and corresponding higher pressures.

In preparation for the measurement of these pressures a Leeds and Northrup thermohm unit with a resistance of 25 ohms was selected to measure the temperature. This platinum resistance thermometer was carefully calibrated against a Bureau of Standards calibrated platinum resistance thermometer at 100, 130, and 160°C. The values obtained together with the ice point provided sufficient data to assign values to the constants in the Callendar equation.

An a-c type Brown recorder and Baldwin pressure gage (strain gage) was obtained and very carefully calibrated against a dead weight piston gage. The pressures were measured at temperatures from 25 to 35°C at 50-psi intervals from 35 to 200 psi and at 100-psi intervals from 200 to 5000 psi. Reproducibility seems to be within 1 to 2 lb/sq in. at any particular temperature and pressure.

A thermostat containing the molten eutectic mixture of  $\text{KNO}_3$ ,  $\text{LiNO}_3$ , and  $\text{NaNO}_3$  was built for use at the higher

temperatures. Apparatus for gently shaking the pressure bomb mounted inside the thermostat was constructed. Temperature control is attained by use of a nickel resistance thermometer in conjunction with a Leeds and Northrup Duration Adjusting Type Controller. The thermostat fluid is stirred by means of a centrifugal pump.

The first measurements of vapor pressure will be made on solutions of uranyl sulfate with concentrations of approximately 30 g of uranium per liter and 300 g of uranium per liter. The solutions will not be degassed but will contain practically equilibrium quantities of dissolved air. Later measurements of vapor pressure will be made on pure distilled water both degassed and saturated with air. This will determine whether degassing of the uranyl salt solutions is a necessary step and will also check the over-all accuracy of temperature and pressure measurements. It is, of course, realized that air introduces an error in the vapor pressure measurements, but if it is less than 1 to 2 lb/sq in. it can be ignored.

Apparatus for sampling the vapor phase from the bomb together with connecting lines for degassing purposes is being designed.

### STUDIES OF ELECTRICAL CONDUCTIVITIES OF AQUEOUS URANYL SULFATE SOLUTIONS

W. B. Bungler

The investigation of electrical conductivities of solutions of uranyl salts in water has been broken down into two series of measurements. The first series will consist of measurements made with a conductivity cell

[REDACTED]

FOR PERIOD ENDING AUGUST 15, 1951

of conventional design covering the temperature range of 15 to 100°C. A second series of measurements over the temperature range of 100 to 300°C presents a more difficult problem, for in this case the cell must be capable of withstanding corrosion and high pressures (up to 100 atm).

Equipment for the measurement of conductivities in the lower temperature range has been assembled and is expected to be in operation soon. The bridge chosen for this work was a modification of the bridge of Jones and Josephs<sup>(5)</sup> described by Dike.<sup>(6)</sup> This bridge is capable of giving results having an over-all accuracy of  $\pm 0.009\%$ . For the present we expect a somewhat lower accuracy,  $\pm 0.02\%$ , since no effort has been made to control the temperature and humidity of the room, and the bridge resistors have not been calibrated.

The source of alternating current will be a Hewlett Packard audio-oscillator. Measurements are planned using several different frequencies at each temperature so that correction can be made for the resistance at the electrodes of the cell due to polarization.<sup>(7)</sup> These data may also be

used as criteria for sufficient platinization of the electrodes.<sup>(8)</sup> The output of the bridge will be fed into a tuned amplifier and an oscillograph will be used as the detector.<sup>(9)</sup>

The temperature of the cell will be controlled by a thermostat constructed in our laboratory. Temperature measurements will be made by a platinum wire resistance thermometer whose resistance is measured with a Muller bridge.

A still has been constructed for the production of conductivity water. It is essentially a modification of the still described by Thiessen and Hermann<sup>(10)</sup> which was redesigned so as to occupy less laboratory space.

For measurements in the higher temperature range (100 to 300°C) a cell similar to that described by Noyes and Coolidge<sup>(11)</sup> is being constructed. This cell may be subject to a large Parker effect<sup>(12)</sup> which will not be conducive to results of high precision.

---

<sup>(5)</sup>G. Jones and R. C. Josephs, "The Measurement of the Conductance of Electrolytes. I. An Experimental and Theoretical Study of Principles of Design of the Wheatstone Bridge for Use with Alternating Currents and an Improved Form of Direct Reading Alternating Current Bridge," *J. Am. Chem. Soc.* 50, 1049 (1928).

<sup>(6)</sup>P. H. Dike, "A Bridge for the Measurement of the Conductance of Electrolytes," *Rev. Sci. Instruments* 2, 379 (1931).

<sup>(7)</sup>G. Jones and S. M. Christian, "The Measurement of the Conductance of Electrolytes. VI. Galvanic Polarization by Alternating Current," *J. Am. Chem. Soc.* 57, 272 (1935).

---

<sup>(8)</sup>G. Jones and D. M. Bollinger, "The Measurement of the Conductance of Electrolytes. VII. On Platinization," *J. Am. Chem. Soc.* 57, 280 (1935).

<sup>(9)</sup>G. Jones, K. J. Mysels, and W. Juda, "The Measurement of the Conductance of Electrolytes. IX. The Use of the Cathode-Ray Oscillograph as a Detector," *J. Am. Chem. Soc.* 62, 2919 (1949).

<sup>(10)</sup>P. A. Thiessen and K. Herrmann, "Eine Einfache Methode zur Herstellung von Leitfähigkeitswasser Hochstein Reinheitsgrades," *Z. Elektrochem.* 43, 66 (1937).

<sup>(11)</sup>A. A. Noyes and Coolidge, Carnegie Institute of Washington Publication No. 63 (1905).

<sup>(12)</sup>H. C. Parker, "The Calibration of Cells for Conductance Measurements. II. The Inter-comparison of Cell Constants," *J. Am. Chem. Soc.* 45, 1366 (1923).

## HRP QUARTERLY PROGRESS REPORT

### PREPARATION OF PURE URANYL SULFATE FOR EXPERIMENTAL PURPOSES

M. H. Lietzke and J. C. Griess

A very pure uranyl sulfate solution has been prepared for experimental purposes by combining stoichiometric amounts of uranium trioxide and sulfuric acid. The uranium trioxide (Mallinckrodt) was first washed four times by decantation to remove any contaminating uranyl nitrate. A conductimetric titration of a slurry of the oxide in water was then made with 4 M sulfuric acid. Since an excess of acid was used, the back titration was effected with uranium trioxide of known uranium content. Analysis showed that the uranium to sulfate ratio on the final product was  $1.003 \pm .003$ .

A preliminary pH curve has been run for various concentrations of this uranyl sulfate and has been found to differ from the one given by Helmholtz and Friedlander.<sup>(13)</sup> The pH curve will be investigated further and a density vs. concentration curve will be obtained.

### URANYL SULFATE PRODUCTION - ACIDITIES, REFRACTIVE INDICES, AND DENSITIES OF URANYL SULFATE SOLUTIONS

M. H. Lietzke      H. W. Wright  
W. L. Marshall

A production procedure for uranyl sulfate involving the direct addition of sulfuric acid to uranium trioxide has been written and distributed to the proper groups. For analytical control purposes, acidities, refrac-

tive indices, and densities of uranyl sulfate solutions near room temperature have been determined. pH values as a function of concentration at 20.0, 25.0, 30.0, and  $35.0 \pm 0.1^\circ\text{C}$  are shown in Fig. 10.2. Values interpolated from these data differ somewhat from previous values at  $22^\circ\text{C}$ .<sup>(13)</sup> The refractive indices and densities at  $25 \pm 0.2^\circ\text{C}$  are given in Table 10.2 and shown in Figs. 10.3 and 10.4. By assuming a temperature correction factor the densities at  $25^\circ\text{C}$  are in agreement with previous data<sup>(13)</sup> at  $20^\circ\text{C}$ .

**Experimental.** Uranyl sulfate was prepared according to the production procedure mentioned above by J. C. Griess and M. H. Lietzke. The molar ratio of sulfate to uranium after final adjustment was  $1.003 \pm 0.003$ .

Acidities were measured using a Beckman pH meter, and a 10-ml picnometer was used for the density determinations. Refractive indices

TABLE 10.2

Refractive Indices and Densities of Aqueous Uranyl Sulfate at  $25.0 \pm 0.2^\circ\text{C}$

MOLARITY OF $\text{UO}_2\text{SO}_4$	DENSITY (g/cc)	REFRACTIVE INDEX
0.0	0.9970	1.3320
0.4196	1.1295	1.3452
0.8455	1.2668	1.3583
1.2597	1.4002	1.3705
1.6755	1.5298	1.3844
2.0939	1.6610	1.3973
2.3249	1.7260	1.4024
2.5635	1.7994	1.4089
2.7244	1.8573	1.4145
2.8718	1.9076	1.4189
3.3309	2.0484	1.4312

<sup>(13)</sup>L. Helmholtz and G. Friedlander, *Physical Properties of Uranyl Sulfate Solutions*, LAMS-30 (Dec. 15, 1943).

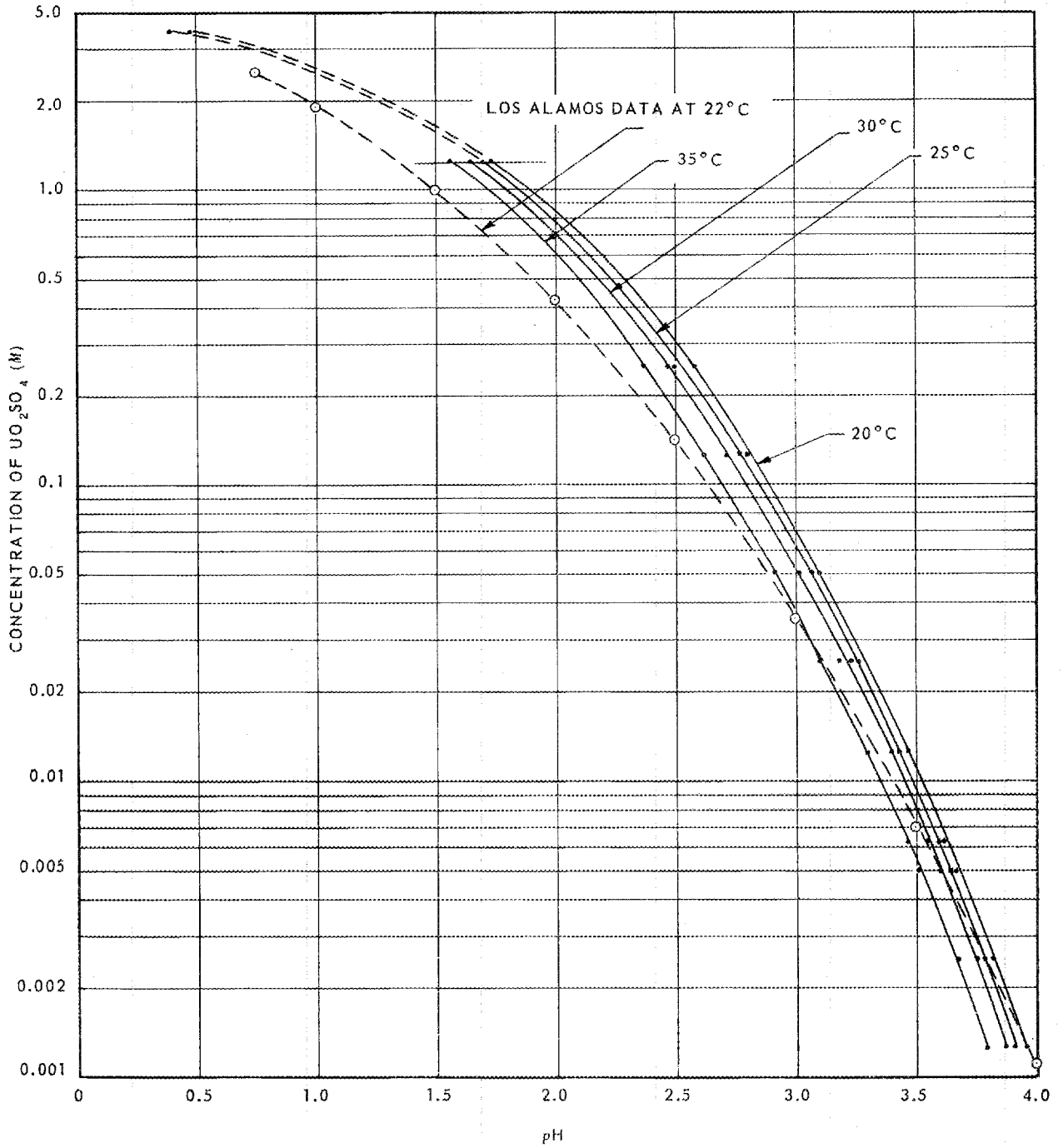


Fig. 10.2 - pH of Uranyl Sulfate Solutions as a Function of Temperature and Concentration.

HRP QUARTERLY PROGRESS REPORT

UNCLASSIFIED  
DWG. 13002

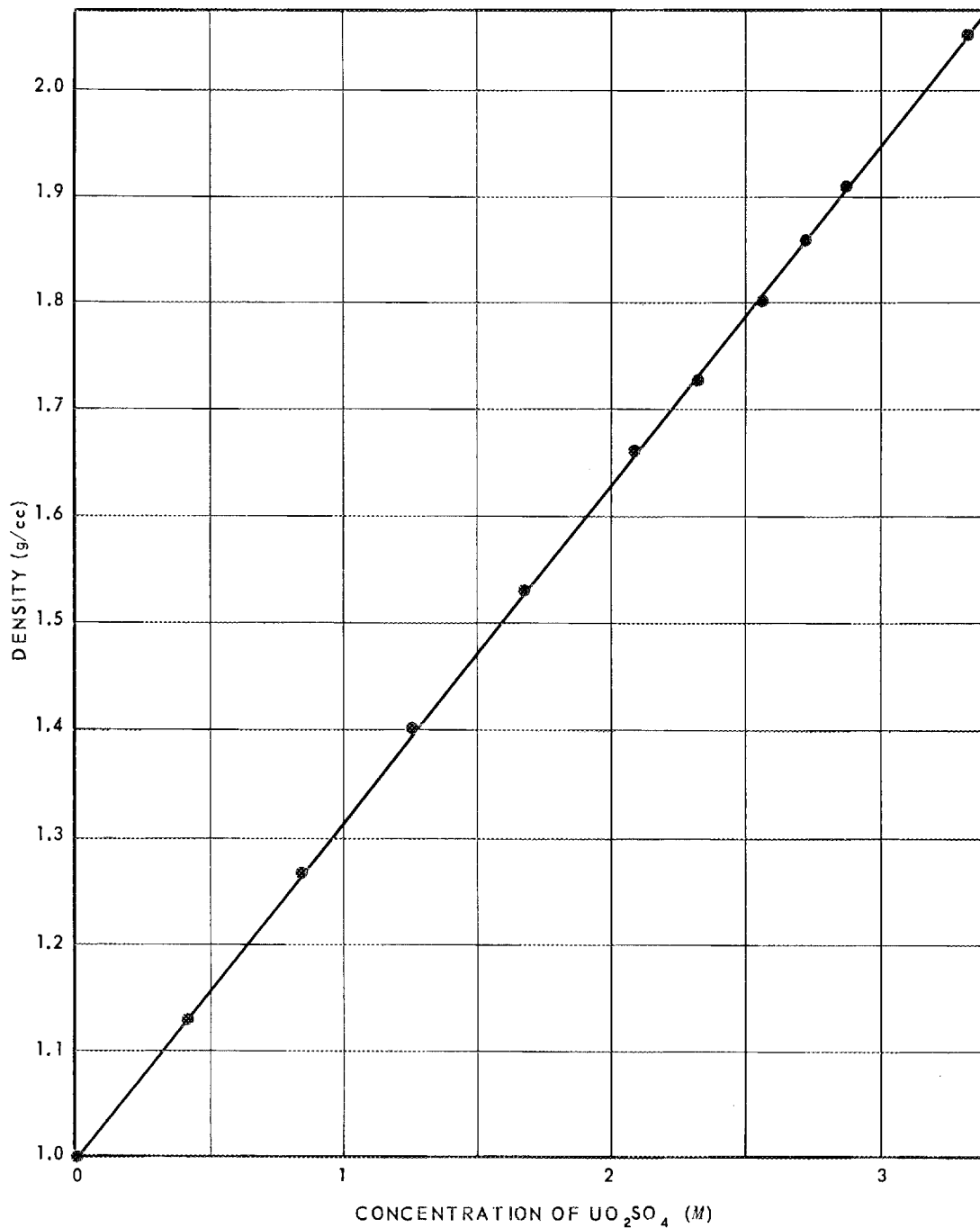


Fig. 10.3 - Density of UO<sub>2</sub>SO<sub>4</sub> Solutions at 25°C.

FOR PERIOD ENDING AUGUST 15, 1951

UNCLASSIFIED  
DWG. 13003

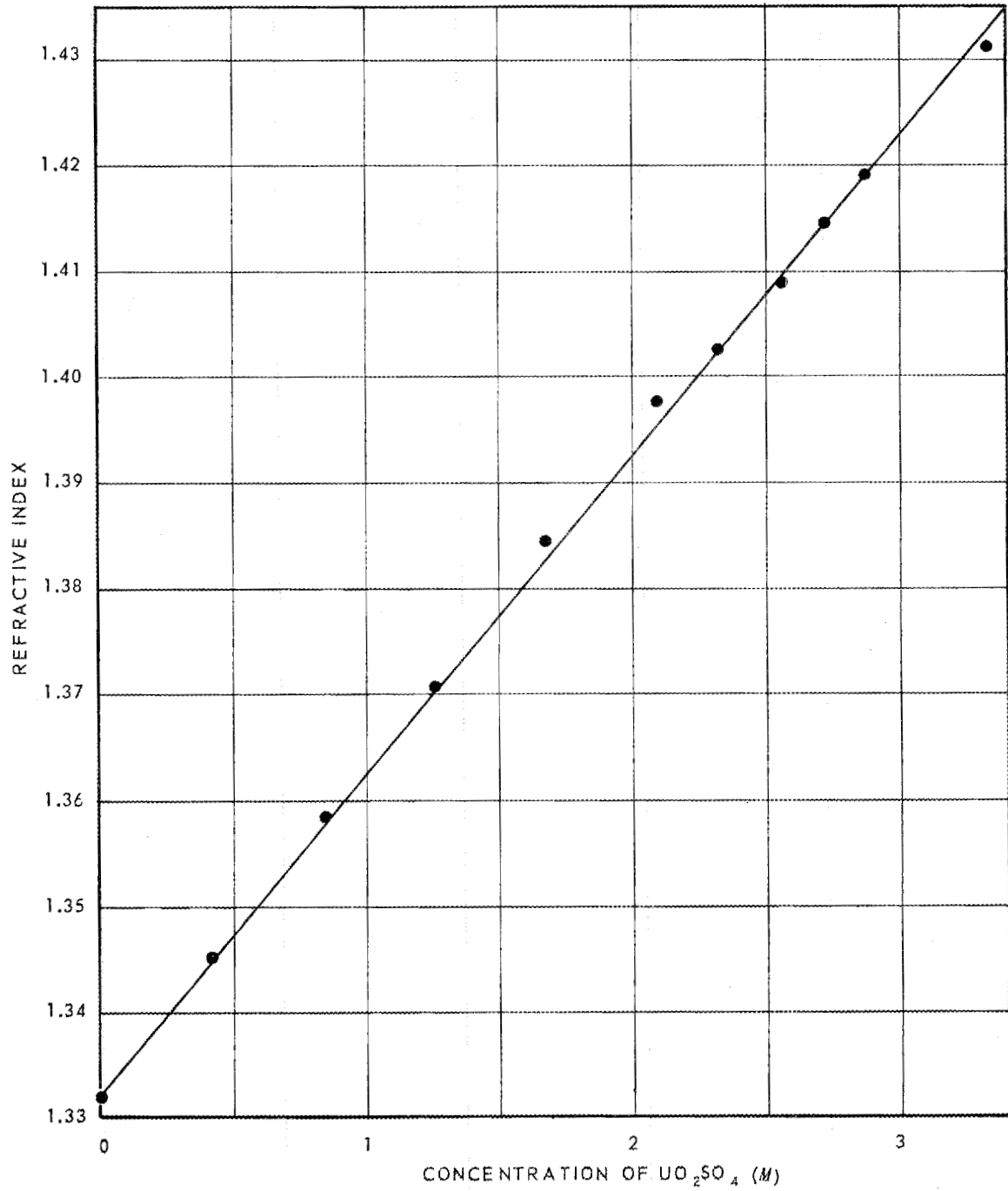
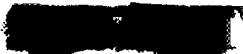


Fig. 10.4 - Refractive Index of  $SO_4$  Solutions at 25°C.



## HRP QUARTERLY PROGRESS REPORT

were obtained using both an Abbe and a thermostated Bausch and Lomb refractometer. These data were averaged for a given solution.

Concentrations were determined gravimetrically by ignition at 900 to 1000°C to  $U_3O_8$ . Concentrations are accurate to  $\pm 0.3\%$ .

## 11. CORROSION

J. L. English, Leader

J. L. Olsen                      J. Reed  
S. H. Wheeler

### CORROSION OF TITANIUM

Stagnant corrosion tests using various types of titanium metal have been run during the past quarter. These tests were operated in stainless steel autoclaves which initially received a pretreatment in either 1% HNO<sub>3</sub> or 2% CrO<sub>3</sub> for 24 hr at 250°C. The test medium was 0.17 M UO<sub>2</sub>SO<sub>4</sub>, and solutions were replaced weekly when the samples were examined for corrosion damage. The results of these investigations appear below.

**Corrosion of Rem-Cru Titanium Sheet and Plate.** Two samples of titanium metal obtained from Rem-Cru Titanium, Inc. for corrosion testing are described as follows:

**Sheet:**

Material designation RC 70; 1/8 in. thick; rolled and annealed; carbon content 0.17%; tensile strength, 94,000 psi; yield strength, 86,000 psi; elongation, 22% in 2 in.

**Plate:**

1/4 in. thick; high-purity material produced by Kroll process; low in carbon, oxygen, and nitrogen.

The samples were run for 8 weeks in uranyl sulfate at 250°C and the results are listed in Table 11.1. Weight changes are cumulative.

TABLE 11.1

**Corrosion of Rem-Cru Titanium  
in 0.17 M UO<sub>2</sub>SO<sub>4</sub> at 250°C**

EXPOSURE TIME (hr)	CORROSION			
	TITANIUM SHEET		TITANIUM PLATE	
	(mg/cm <sup>2</sup> )	(mpy)	(mg/cm <sup>2</sup> )	(mpy)
168	-0.058	0.26	-0.041	0.18
336	-0.032	0.07	+0.007	
504	-0.013	0.02	-0.020	0.03
672	-0.065	0.006	-0.020	0.02
840	-0.019	0.02	+0.041	
1008	-0.039	0.03		

Both samples were characterized by a highly lustrous golden-yellow color. Corrosion attack was of negligible magnitude as evidenced by the data in Table 11.1. Although the chemical analyses of the test solutions are not complete, a preliminary inspection showed that no reduction of uranyl sulfate had occurred. Little change in solution pH between initial and final values was determined.

**Corrosion of Welded Titanium Tubing.** Samples of 3/8- and 1/2-in.-o.d. welded titanium tubing were obtained from Rem-Cru for corrosion studies. The tubing was fabricated by welding into a larger diameter tube, grinding the outside of the weld on a belt, and drawing to size. The tubing was tested in an annealed

**HRP QUARTERLY PROGRESS REPORT**

**TABLE 11.2**

**Corrosion of Welded Titanium Tubing in 0.17 M UO<sub>2</sub>SO<sub>4</sub> at 250°C**

Sample 1: 3/8-in. o.d.; not annealed; degreased before testing.  
 Sample 2: 3/8-in. o.d.; annealed; descaled.  
 Sample 3: 1/2-in. o.d.; annealed; degreased before testing.

EXPOSURE TIME (hr)	CORROSION					
	SAMPLE 1		SAMPLE 2		SAMPLE 3	
	(mg/cm <sup>2</sup> )	(mpy)	(mg/cm <sup>2</sup> )	(mpy)	(mg/cm <sup>2</sup> )	(mpy)
168	-0.19	0.86	-0.058	0.26	-0.079	0.35
336	-0.24	0.54	-0.051	0.11	-0.105	0.23
504	-0.29	0.43	-0.043	0.07	-0.095	0.14
672	-0.25	0.28	-0.101	0.11	-0.089	0.10
840	-0.30	0.26	-0.072	0.07	-0.095	0.09
1008	-0.31	0.23	-0.101	0.07		

condition (annealed at 1200°F) and in the as-fabricated condition. The annealed tubing was descaled in a molten salt bath. Corrosion results are included in Table 11.2.

All samples showed the lustrous golden-yellow color as found on previous specimens. The difference in corrosion behavior in Samples 1 and 2 may be due to a combination of the annealing operation and the removal of surface contaminants by the molten salt bath descaling operation. The corrosion attack on the unannealed specimen was three times greater than that on the annealed and cleaned sample.

The 1/2-in.-o.d. welded tubing, although possessing good corrosion resistance, showed numerous small fissures in the weld zone which would be sufficient basis for rejection of the material. The 3/8-

in.-o.d. tubing samples showed no such signs of defective welding.

**Corrosion of Welded Titanium.** A sample of commercial sheet-titanium which had been Heliarc-welded under an inert atmosphere was obtained from Wright Field. Thin strips of titanium, cut from the same sheet, were used for filler metal. Before testing, the sample was etched for 15 min in a HNO<sub>3</sub>-HF solution at 60°C. It was then exposed for weekly periods in 0.17 M uranyl sulfate at 250°C, using a nitric acid—pre-treated stainless steel bomb. Test data appear in Table 11.3 based on cumulative weight loss.

The corrosion resistance of this material was comparable to that of the welded tubing, Sample 2, in Table 11.2. The major portion of the surfaces were a dull yellow color. The weld zone and adjacent

FOR PERIOD ENDING AUGUST 15, 1951

TABLE 11.3

Corrosion of Welded Titanium Sheet  
in 0.17 M UO<sub>2</sub>SO<sub>4</sub> at 250°C

EXPOSURE TIME (hr)	WEIGHT LOSS (mg/cm <sup>2</sup> )	CORROSION RATE (mil/year)
168	0.073	0.33
336	0.073	0.16
504	0.073	0.11
672	0.044	0.11
840	0.105	0.09
1008	0.098	0.07

heat-affected areas were of a darker yellow color. The weld area was smooth in appearance; no cracks or localized corrosion attack were found by microscopic examination. The sample will be sectioned and examined further microscopically at the conclusion of the test.

Chemical analyses of the uranyl sulfate test solution disclosed no reduction in total uranium content. The titanium content of these solutions averaged <1 γ/ml.

Corrosion of Titanium Coupled to Type 347 Stainless Steel. The galvanic corrosion behavior of annealed titanium sheet and titanium plate with type 347 stainless steel was investigated in 0.17 M uranyl sulfate at 100°C. The couple consisted of a flat square of the titanium bolted to a disk of stainless steel by means of a type 347 stainless steel bolt and nut. The couples were removed weekly, dismantled, weighed, and examined for indications of corrosion attack. Data appear in Table 11.4.

No evidence of galvanic or crevice corrosion was observed on any of the specimens; all exhibited their original high degree of metallic

TABLE 11.4

Corrosion of Annealed Titanium—Type 347 Stainless Steel  
Couples in 0.17 M UO<sub>2</sub>SO<sub>4</sub> at 100°C

EXPOSURE TIME (hr)	MATERIAL	TEMPERATURE (°C)	CUMULATIVE WEIGHT GAIN (mg/cm <sup>2</sup> )
168	Titanium (sheet)	100	0.060
	Type 347 stainless steel		0.074
336	Titanium (sheet)	100	0.042
	Type 347 stainless steel		0.035
168	Titanium (plate)	250	0.110
	Type 347 stainless steel		0.089
336	Titanium (plate)	250	0.082
	Type 347 stainless steel		0.079

## HRP QUARTERLY PROGRESS REPORT

luster. No reduction in total uranium content was found by chemical analyses. The couple tests will be repeated at 250°C in uranyl sulfate solutions.

### Corrosion of Sintered Titanium.

Two samples of titanium produced by powder metallurgy techniques were obtained from the Brush Laboratories in Cleveland, Ohio.

#### Sample 1:

Produced from average, 30 mesh, Bureau of Mines titanium powder containing 0.5% Mg before consolidation.

#### Sample 2:

Produced from Du Pont sponge of very high purity.

It was very probable that a small amount of impurity segregations existed in both of the compacts.

The samples were exposed to 0.17 M  $UO_2SO_4$  at 250°C for 7 weeks with weekly examination. Stainless steel bombs, pretreated in nitric acid, were used to contain the samples and solutions at this temperature. Corrosion data are listed in Table 11.5.

No significant variation in the corrosion behavior of the two specimens was evident, although both did show a slight corrosion attack as the test time increased to 672 hr. A period of weight gain followed on both specimens. Both samples were colored a brilliant golden yellow at the end of the first week. This color gradually changed to a deep, lustrous golden brown as the testing time increased.

TABLE 11.5

### Corrosion of Sintered Titanium in 0.17 M $UO_2SO_4$ at 250°C

EXPOSURE TIME (hr)	CUMULATIVE WEIGHT GAIN (mg/cm <sup>2</sup> )	
	SAMPLE 1	SAMPLE 2
168	0.143	0.111
336	0.099	0.116
504	0.074	0.101
672	0.049	0.015
840	0.059	0.082
1008	0.123	0.155
1176	0.113	0.140

Uranium analyses available show no reduction in concentration. The titanium content in the uranyl sulfate solutions was less than 1  $\gamma$ /ml throughout the test.

### CORROSION OF ZIRCONIUM

Corrosion studies have continued with zirconium-tin alloys and crystal bar zirconium in uranyl sulfate solutions at 250°C. No recent samples of regular Bureau of Mines zirconium have been received; therefore, corrosion data on this type are not included in this report.

Since previous studies disclosed that the zirconium-tin alloys showed superior corrosion resistance to the regular Bureau of Mines metal in uranyl sulfate at 250°C, the major effort on the zirconium corrosion investigation has been devoted to a more intensive study of these alloys.

Stagnant corrosion tests were conducted in pretreated stainless steel bombs containing 0.17 M uranyl sulfate. The test samples were examined weekly for general appearance and weight change. The uranyl sulfate solutions were replaced weekly with new solution. The results of the corrosion studies on zirconium appear in the following sections.

**Corrosion of Bureau of Mines Resistance-Melted Zirconium-Tin Alloys.** Samples of Bureau of Mines resistance-melted zirconium containing 3 and 5% tin additions were run for 15 weeks in uranyl sulfate at 250°C. The samples were hot-forged and rolled after melting. Before exposing to uranyl sulfate, the specimens were abraded on Nos. 80 and 120 grit papers and etched for 3 to 5 min in 5% HF at room temperature. Results of these tests appear in Table 11.6.

A marked difference in the corrosion behavior of these two alloys is evident from an examination of the corrosion data. The 3% tin alloy exhibited a continuous weight gain throughout the 16 weeks of test. The 5% tin alloy, on the other hand, showed a continuous weight loss. The corrosion rate on this specimen for the total time of exposure was 0.05 mil penetration per year. Both samples were identical in appearance at the end of the first week, and little change occurred during the course of the test. A dark brown iridescent film covered both specimens; no dull gray film formation was observed as is generally encountered on regular Bureau of Mines specimens exposed under similar conditions.

TABLE 11.6

**Corrosion of BuMines Resistance-Melted Zirconium-Tin Alloys in 0.17 M UO<sub>2</sub>SO<sub>4</sub> at 250°C**

EXPOSURE TIME (weeks)	CUMULATIVE WEIGHT CHANGE (mg/cm <sup>2</sup> )	
	3% TIN ALLOY	5% TIN ALLOY
1	+0.031	-0.017
2	+0.052	+0.034
3	+0.062	+0.017
4	+0.072	-0.034
5	+0.103	-0.051
6	+0.134	-0.051
7	+0.113	-0.119
8	+0.144	-0.119
9	+0.124	-0.170
10	+0.134	-0.153
11	+0.144	-0.170
12	+0.175	-0.170
13	+0.196	-0.187
14	+0.206	-0.203
15	+0.155	-0.237
16	+0.206	-0.254

**Corrosion of Bureau of Mines Induction-Melted Zirconium-Tin Alloys.** Three samples of induction-melted Bureau of Mines zirconium containing a nominal addition of 5% tin were exposed to uranyl sulfate at 250°C for periods of 10 to 16 weeks (Table 11.7). A description of the fabrication techniques used for each specimen follows:

Sample 1:

Induction-melted Bureau of Mines sponge (BMI 302); forged and rolled at 1800°F; etched in 5% HF before test exposure.

Sample 2:

Same as Sample 1; uranyl sulfate corrosion test operated with no solution change.

**HRP QUARTERLY PROGRESS REPORT**

Sample 3:  
MIT induction-melted Bureau of Mines sponge; hot forged; polished and etched in 5% HF before test exposure.

**TABLE 11.7**

**Corrosion of Induction-Melted Zirconium Containing 5% Tin in 0.17 M Uranyl Sulfate Solution at 250°C**

EXPOSURE TIME (weeks)	CUMULATIVE WEIGHT CHANGE (mg/cm <sup>2</sup> )		
	SAMPLE 1	SAMPLE 2	SAMPLE 3
1	-0.044	-0.015	-0.021
2	0.0	-0.015	+0.021
3	-0.033	-0.015	+0.062
4	-0.022	-0.030	+0.144
5	-0.022	-0.015	+0.103
6		-0.044	+0.206
7	-0.033	-0.030	+0.062
8	-0.022	-0.015	+0.082
9	-0.022	-0.015	+0.062
10	+0.011	-0.015	+0.062
11	0.0		+0.082
12	-0.011		+0.082
13	0.0		+0.062
14			+0.062
15			+0.021
16			+0.041

The corrosion behavior of all three test specimens was excellent under the conditions of the test. The corrosion rate on Sample 2, the only specimen which showed a measured weight loss, was 0.005 mil penetration per year after 10 weeks at 250°C. This figure was obtained using the original uranyl sulfate test solution throughout the entire 10 weeks. The specimen did not lose any weight after the eighth week of

test. Sample 1 showed no measured weight change after 13 weeks; i.e., the cumulative weight changes totaled zero at the end of this time. Sample 3 was characterized by a weight gain during 16 weeks of exposure. The maximum gain reported was 0.206 mg/cm<sup>2</sup> at the end of 6 weeks. However, some corrosion attack or dissolution of surface films occurred later since the cumulative weight gain at the end of 16 weeks had decreased to 0.041 mg/cm<sup>2</sup>. The corrosion resistance of these materials was superior to that shown by the resistance-melted Bureau of Mines zirconium described in the preceding section. Where measured weight losses were reported, the corrosion resistance of induction-melted zirconium containing 5% tin was 10 times better than that of resistance-melted Bureau of Mines zirconium containing 5% tin addition. The physical appearance of the induction-melted specimens at the end of the tests was similar to that of the resistance-melted specimens in that dark brown iridescent films were found on the samples.

**Corrosion of Arc-Melted Crystal Bar Zirconium Containing 5% Tin.** A sample of arc-melted crystal bar zirconium containing a nominal addition of 5% tin was tested in uranyl sulfate at 250°C for 12 weeks. This material was forged and rolled at 1450°F after melting and was identified as BMI 927. The sample was etched in 5% HF before test exposure. Corrosion data are listed in Table 11.8.

The corrosion rate on this sample was less than 0.001 mil/year at the end of 12 weeks. The sample was

FOR PERIOD ENDING AUGUST 15, 1951

covered with a very thin film which was lustrous and brown in color.

TABLE 11.8

Corrosion of Arc-Melted Crystal Bar Zirconium Containing 5% Tin in 0.17 M  $UO_2SO_4$  at 250°C

EXPOSURE TIME (weeks)	CUMULATIVE WEIGHT CHANGE (mg/cm <sup>2</sup> )
1	-0.039
2	0.0
3	-0.039
4	-0.023
5	-0.023
6	-0.031
7	+0.047
8	-0.016
9	0.0
10	-0.016
11	0.0
12	-0.008

Corrosion of Bureau of Mines Zirconium Tubing Containing 5% Tin. Samples of the first Bureau of Mines zirconium tubing containing 5% tin were obtained from MIT. This material had proved very difficult to work, and the first product was considered far from being satisfactory. Higher quality tubing is now being produced. The fabrication of the tubing was as follows: The cast billet was clad in copper and extruded into a tube 0.650 in. o.d.; the tube was cold drawn to its present diameter, 0.480 in. o.d. and 0.376 in. i.d.; it was then heated to 1200°F for straightening. Corrosion data in uranyl sulfate at 250°C appear in Table 11.9. Sample 1 was degreased only before exposure while Sample 2 was etched for 3 min in 5% HF before testing.

TABLE 11.9

Corrosion of Extruded Zirconium Tubing Containing 5% Tin in 0.17 M Uranyl Sulfate at 250°C

EXPOSURE TIME (weeks)	CUMULATIVE WEIGHT LOSS (mg/cm <sup>2</sup> )	
	SAMPLE 1	SAMPLE 2
1	3.54	2.01
2	4.14	2.82
3	4.22	3.32
4	4.35	3.60
5	4.33	3.80
6	4.33	4.15
7	4.35	4.64

Both samples were dull gray in color with numerous dark spots at the end of the tests. A slight initial enhancement of the corrosion resistance appeared as a result of the etching operation. However, continued testing resulted in greater corrosion attack than obtained on the unetched specimen. The corrosion rates for Sample 1 and Sample 2 were 2.0 and 2.1 mils/year, respectively.

Corrosion of Crystal Bar Zirconium. A sample of Foote Mineral Co. crystal bar zirconium, Grade 1, was tested in uranyl sulfate at 250°C for 7 weeks. The bars had been cleaned initially and corrosion-tested in 600°F water for 2 weeks. The specimen showed a cumulative weight gain of 0.283 mg/cm<sup>2</sup> after the 7-week test period. After the first week, the sample had a highly lustrous surface which was brilliantly colored with green and violet interference tints. This appearance remained unchanged throughout the test period.

**HRP QUARTERLY PROGRESS REPORT**

**URANYL FLUORIDE STABILITY AND CORROSION STUDIES**

**Solution Stability of Uranyl Fluoride Contained in Untreated Type 347 Stainless Steel Bombs.** A group of tests was run with 0.13 and 1.26 M  $UO_2F_2$  contained in untreated type 347 stainless steel bombs which remained closed for periods of 24 to 168 hr. The object of these tests was to determine solution stability in untreated systems as a function of temperature and exposure time. The  $UO_2F_2$  solutions were placed in chemically cleaned bombs and heated in ovens to the desired temperature.

In one series of 12 tests, 0.13 M  $UO_2F_2$  (30 g of uranium per liter) was heated at 150°C in untreated bombs. One of the bombs was opened

at each 24-hr interval during the first 96 hr of exposure. The other eight bombs were opened after a total of 163 hr of continued exposure. The  $UO_2F_2$  was partially reduced in all the bombs exposed for more than 48 hr with the exception of one bomb exposed for 163 hr. In most of the tests, a decrease in pH occurred when the fluoride was reduced. Although the data are erratic, the dissolved nickel content generally increased with length of exposure. These data are given in Table 11.10.

Three tests of 376 hr duration were run at 150, 200, and 250°C using 0.13 M  $UO_2F_2$  contained in untreated bombs which were opened after 47 and 208 hr of exposure. The bombs were opened for solution

**TABLE 11.10**

**Solution Stability Data for 0.13 M  $UO_2F_2$  Exposed at 150°C in Untreated Type 347 Stainless Steel Bombs**

EXPOSURE TIME (hr)	TOTAL URANIUM (g/liter) <sup>(a)</sup>	SOLUTION ANALYSES (γ/ml)			pH <sup>(b)</sup>	SOLUTION APPEARANCE
		NICKEL	IRON	CHROMIUM		
24	29.6	28			3.70	Clear and yellow
48	30.4	6			3.35	Clear and yellow
72	24.8	14			3.70	Green-black precipitate
96	27.6	15		4	3.25	Green-black precipitate
163	21.1	78	106	19	2.85	Green-black precipitate
163	27.1	34	60	20	3.05	Green-black precipitate
163	21.8	51	115	26	2.80	Green-black precipitate
163	28.4	76	16	1	3.38	Green-black precipitate
163	22.7	24	117	3	2.80	Green-black precipitate
163	29.7	57	11	1	3.25	Clear and yellow
163	24.6	26	109	20	2.80	Green-black precipitate
163	21.6	64	125	29	2.70	Green-black precipitate

(a) Initial uranium concentration, 29.4 g/liter.

(b) Natural pH, 3.35.

[REDACTED]

FOR PERIOD ENDING AUGUST 15, 1951

sampling. No uranium precipitation occurred during the first 47 hr of exposure. During the two subsequent continuous exposure periods of 161 and 163 hr, no uranium precipitation occurred. This is contrary to the results obtained in untreated bombs exposed at 150°C for an initial period of 163 hr without opening. Possibly the oxygen introduced during the initial sampling period prevented uranium reduction. The dissolved nickel content was generally lower than in the tests run continuously for an initial period of 163 hr. Less than 1  $\gamma$ /ml of iron and chromium were present in the solutions. These data are given in Table 11.11.

Three tests of 168 hr duration were run at 150, 200, and 250°C

using 1.26 M  $UO_2F_2$  contained in untreated bombs. Partial uranium reduction occurred at all three temperatures. Solution analyses for these tests are as follows:

TEMP. (°C)	TOTAL U (g/liter)	U(IV) ( $\gamma$ /ml)	Ni ( $\gamma$ /ml)	FINAL pH
150	252.4	358	218	2.95
200	181.0	580	195	2.10
250	237.4	666	1339	1.98

The initial uranium concentration was 302.0 g/liter; the initial pH was 2.25.

An effort is being made to identify the precipitated compounds which occur when the uranyl fluoride is reduced. The following chemical analyses have been obtained for

TABLE 11.11

Solution Stability Data for 0.13 M  $UO_2F_2$  Exposed in Untreated Type 347 Stainless Steel Bombs

CUMULATIVE EXPOSURE TIME (hr)	TEMPERATURE (°C)	TOTAL URANIUM (g/liter) <sup>(a)</sup>	SOLUTION ANALYSES ( $\gamma$ /ml)			pH <sup>(b)</sup>
			NICKEL	IRON	CHROMIUM	
47	150	29.7	9	1	1	3.45
208	150	30.9	35	1	1	3.52
376	150	29.3	48	1	1	3.55
47	200	29.2	3	1	1	3.30
208	200	29.0	7	1	1	2.95
376	200	28.2	13	1	1	3.00
47	250	28.8	17	1	1	3.30
208	250	29.1	13	1	1	2.30
376	250	31.1	27	1	1	3.35

(a) Initial uranium concentration, 29.4 g/liter.

(b) Natural pH, 3.35.

[REDACTED]

## HRP QUARTERLY PROGRESS REPORT

precipitates formed under various conditions:

TEST CONDITIONS	U	F	ATOMIC
	(%)	(%)	RATIO, U/F
150°C, untreated bomb	68.3	5.61	1.03
150°C, CrO <sub>3</sub> -pretreated bomb	69.1	6.13	1.11
200°C, untreated bomb	68.9	5.52	1.00
200°C, CrO <sub>3</sub> -pretreated bomb	69.8	5.94	1.06
250°C, untreated bomb	72.2	8.63	1.50

X-ray-diffraction patterns are being obtained for these precipitates in a further effort to completely identify them.

**Effect of Pretreatment Films on Solution Stability.** Tests were run to determine if pretreatment films formed on stainless steel at elevated temperatures were effective in inhibiting corrosion and uranium reduction. The pretreatment films were formed on the steel by heating the metal surfaces for 24 hr at 250°C in 1% by weight of HNO<sub>3</sub> or 2% by weight of CrO<sub>3</sub>.

No detectable uranium reduction occurred in 0.13 M UO<sub>2</sub>F<sub>2</sub> contained in three HNO<sub>3</sub>-pretreated bombs after 168 hr of continuous exposure at temperatures of 150, 200, and 250°C. The solution analyses for these tests are as follows:

TEMP. (°C)	TOTAL U (g/liter)	Ni (γ/ml)	Fe (γ/ml)	Cr (γ/ml)	pH
150	29.4	2	10	1	2.80
200	29.5	1	1	1	3.20
250	28.1	8	1	1	2.95

The initial uranium concentration was 29.4 g/liter; the initial pH was 3.35. Two other HNO<sub>3</sub>-pretreated bombs containing samples of untreated type 347 stainless steel and Illium R have shown no uranium reduction after one month of continuous exposure under similar conditions.

Partial uranium reduction occurred in most of the tests at 150°C using 1.26 M UO<sub>2</sub>F<sub>2</sub> contained in bombs pretreated by either 1% HNO<sub>3</sub> or 2% CrO<sub>3</sub>. The exposure period varied from 24 to 167 hr. The pH of the solutions was erratic, but was usually higher than the initial value of 2.25. The soluble nickel content was usually high in solutions where precipitation occurred, reaching a maximum of 201 γ/ml in a HNO<sub>3</sub>-pretreated bomb after 167 hr of exposure. These data are given in Tables 11.12 and 11.13.

No detectable uranium reduction occurred in three tests of 96 hr duration at 200°C using 1.26 M UO<sub>2</sub>F<sub>2</sub> contained in 2% CrO<sub>3</sub>-pretreated bombs. The solutions were clear and yellow with no evidence of precipitation. The pH of the solution in one of tests increased from 2.25 to 2.30, while in the other two tests no change in pH occurred. The solution analyses for these tests are as follows:

TOTAL U (g/liter)	U(IV) (γ/ml)	Ni (γ/ml)	Fe (γ/ml)	Cr (γ/ml)	pH
302.9	207	72	31	16	2.30
303.6	466	38	36	16	2.25
302.5	338	74	18	35	2.25

The initial uranium concentration was 302.0 g/liter.

[REDACTED]

FOR PERIOD ENDING AUGUST 15, 1951

TABLE 11.12

Solution Stability Data for 1.26 M  $UO_2F_2$  Exposed at 150°C in  $HNO_3$ -Pretreated Type 347 Stainless Steel Bombs

EXPOSURE TIME (hr)	TOTAL URANIUM (g/liter) <sup>(a)</sup>	SOLUTION ANALYSES (γ/ml)		pH <sup>(b)</sup>	SOLUTION APPEARANCE
		URANIUM(IV)	NICKEL		
24	302.0	1665	127	2.92	Green
48	295.6	1069	115	3.00	Green-black precipitate
72	287.6	974	168	2.45	Clear and yellow
96	266.0	1171	176	2.55	Green-black precipitate
96	297.1	1473	115	2.65	Green-black precipitate
96	301.1	267	114	2.80	Green-black precipitate
96	299.7	1196	101	2.85	Green-black precipitate
96	295.5	297	22	2.40	Green-black precipitate
167	266.0		201	2.85	Green-black precipitate

<sup>(a)</sup>Initial uranium concentration, 302.0 g/liter.

<sup>(b)</sup>Natural pH, 2.25.

A group of 15 tests was run at 250°C using 1.26 M  $UO_2F_2$  contained in  $HNO_3$ - and  $CrO_3$ -pretreated bombs. One bomb pretreated by each method was opened every 24 hr for the first 72 hr of exposure; then the remaining 9 bombs were opened after 96 hr of continuous exposure. No detectable uranium reduction occurred in any of the tests except in one test of 24 hr duration run in a  $HNO_3$ -pretreated bomb. The dissolved nickel content of this precipitated solution was 439 γ/ml, while in the other tests where no precipitation occurred the maximum nickel content was 88 γ/ml in the solution exposed for 72 hr in a  $HNO_3$ -pretreated bomb. Precipitation of this solution may have been caused by a faulty pretreatment film. The pH of the solutions, in

most cases, was equal to or slightly greater than the initial value of 2.25. The solution analyses data for these tests are given in Tables 11.14 and 11.15. The accuracy of the analytical method used for determining uranium concentration is now ±1%; however, it has been shown that this accuracy was not attained for some of the analyses run during the first part of this quarter. This may account for some of the erratic results given in the above-mentioned tables.

Specimens of  $CrO_3$ -pretreated types 309, 316 ELC, 321, and 347 stainless steels were exposed at 250°C to 1.26 M  $UO_2F_2$  contained in  $CrO_3$ -pretreated bombs. The purpose of these tests was to obtain corrosion rates for the stainless

HRP QUARTERLY PROGRESS REPORT

TABLE 11.13

Solution Stability Data for 1.26 M UO<sub>2</sub>F<sub>2</sub> Exposed at 150°C in CrO<sub>3</sub>-Pretreated Type 347 Stainless Steel Bombs

EXPOSURE TIME (hr)	TOTAL URANIUM (g/liter) <sup>(a)</sup>	SOLUTION ANALYSES (γ/ml)		pH <sup>(b)</sup>	SOLUTION APPEARANCE
		URANIUM(IV)	NICKEL		
24	316.5	228	5	2.35	Clear and yellow
48	302.0	1058	64	2.90	Green-black precipitate
72	303.5	419	4	1.39	Green-black precipitate
96	291.7	1665	80	2.70	Green-black precipitate
96	281.2	1517	110	2.81	Green-black precipitate
96	291.2	1141	119	2.60	Green-black precipitate
122	294.0		275	2.95	Green-black precipitate
122	279.0		253	2.91	Green-black precipitate
122	291.0		173	2.95	Green-black precipitate
122	293.0		167	2.89	Green-black precipitate

<sup>(a)</sup>Initial uranium concentration, 302.0 g/liter.

<sup>(b)</sup>Natural pH, 2.25.

TABLE 11.14

Solution Stability data for 1.26 M UO<sub>2</sub>F<sub>2</sub> Exposed at 250°C in HNO<sub>3</sub>-Pretreated Type 347 Stainless Steel Bombs

EXPOSURE TIME (hr)	TOTAL URANIUM (g/liter)	SOLUTION ANALYSES (γ/ml)				pH	SOLUTION APPEARANCE
		URANIUM(IV)	NICKEL	IRON	CHROMIUM		
24	285.9		439	48	105	2.20	Green-black precipitate
48	301.6	257	7	13	3	2.25	Clear and yellow
72	296.9	678	88	92	7	2.00	Clear and yellow
96	304.0	508	19	7	5	2.30	Clear and yellow
96	302.5	619	25	8		2.25	Clear and yellow
96	295.6	260	59	9	22	2.28	Clear and yellow
96	301.1	285	42	7	20	2.28	Clear and yellow
96	302.6	36	16	4	5	2.25	Clear and yellow

FOR PERIOD ENDING AUGUST 15, 1951

TABLE 11. 15

Solution Stability data for 1.26 M  $UO_2F_2$  Exposed at 250°C in  $CrO_3$ -Pretreated Type 347 Stainless Steel Bombs

EXPOSURE TIME (hr)	TOTAL URANIUM (g/liter)	SOLUTION ANALYSES (γ/ml)				pH	SOLUTION APPEARANCE
		URANIUM(IV)	NICKEL	IRON	CHROMIUM		
24	300.2		3	4	5	2.35	Clear and yellow
48	305.4	365	14	5	1	2.10	Clear and yellow
72	301.9	284	18	19	10	2.30	Clear and yellow
96	305.2	417	21	29	5	2.30	Clear and yellow
96	305.5	580	25	15	7	2.50	Clear and yellow
96	304.1	239	51	16	8	2.50	Clear and yellow
96	303.6	417	9	16	8	2.25	Clear and yellow

steels as well as additional solution stability data. The solutions in the bombs were changed weekly at which time the specimens were inspected and weighed. No evidence of solution reduction occurred in these tests after a total exposure time of 21 days. The dark lustrous pretreatment films remained intact on all of the specimens. Corrosion rates, based on three weeks of exposure, were 0.0112, 0.0048, 0.0108, and 0.0349 mil/month for the types 309, 316, 321, and 347 stainless steel specimens, respectively. These data are given in Table 11.16.

At this time no explanation can be given to account for the anomalous phenomenon of uranium reduction occurring in 1.26 M  $UO_2F_2$  exposed at 150°C in pretreated systems, whereas no precipitation, in most

cases, occurred at 250°C. Furthermore, no precipitation, occurred at 150°C using 0.13 M  $UO_2F_2$  contained in pretreated systems. In order to study solution stability in pretreated systems where fewer variables are involved, larger bombs of 1500-ml capacity are now being fabricated with provisions for sampling test media at elevated temperatures. By varying the temperature from 100 to 250°C, accompanied by solution sampling, it can be established whether the uranium reduction is actually a function of temperature, concentration, or perhaps other as yet undetermined variables. The limited number of tests which have been run where many uncontrollable variables exist may not give a true indication of the solution stability with respect to temperature and uranium concentration.

HRP QUARTERLY PROGRESS REPORT

TABLE 11.16

Corrosion Data for CrO<sub>3</sub>-Pretreated Type 347 Stainless Steels  
Exposed to 1.26 M Uranyl Fluoride at 250°C

MATERIAL	CUMULATIVE EXPOSURE TIME (days)	WEIGHT CHANGE (mg/dm <sup>2</sup> /month)	CORROSION RATE (mils/month)	TOTAL URANIUM (g/liter) <sup>(a)</sup>	SOLUTION ANALYSES (γ/ml)				pH <sup>(b)</sup>
					U(IV)	Ni	Fe	Cr	
309 SS	7	0.0	0.0	302.9	215	7	25	11	2.1
309 SS	14	-3.26	0.0016	301.9	356	3	6	9	2.3
309 SS	21	-22.60	0.0112	297.5	297	9	13		2.3
316 SS	7	+1.81		302.3	195	23	12	12	2.1
316 SS	14	-0.90	0.0010	302.2	261	16	11	4	2.3
316 SS	21	-6.32	0.0048	302.7	408	16	16		2.4
321 SS	7	-1.47	0.0032	303.0	747	6	23	11	2.2
321 SS	14	-6.40	0.0070	301.9	264	12	10	4	2.3
321 SS	21	-14.30	0.0108	302.4	381	14	16		2.4
347 SS	7	+4.65		303.8	282	25	18	13	2.2
347 SS	14	-10.40	0.0052	301.9	318	12	7	2	2.3
347 SS	21	-70.50	0.0349	304.5	371	23	16		2.4

<sup>(a)</sup>Initial uranium concentration, 302.0 g/liter.

<sup>(b)</sup>Natural pH, 2.25.

## 12. RADIATION DAMAGE

H. F. McDuffie, Leader  
J. W. Boyle            C. J. Hochenadel  
S. F. Clark            W. F. Kieffer  
J. A. Ghormley        M. D. Silverman  
T. H. Handley        A. W. Smith  
T. J. Sworski

**Specific and Net Gas Production in Homogeneous Reactor Systems.** With the recent addition of four persons to the group of two already engaged in this problem, it is planned that during the next two quarters rather complete and fundamental information will be obtained with reference to the radiation chemistry of aqueous uranyl sulfate, uranyl fluoride, uranyl nitrate, and other proposed HRP solutions. Initial yields of decomposition products will be determined for pile-irradiated solutions containing 40 to 300 g of uranium per liter at several different enrichments. Irradiations will be made at temperatures from 100 to 250°C.

The previous studies on uranyl sulfate at 40 g of uranium per liter and 93% enrichment have been extended to higher concentrations (300 g of uranium per liter) and lower enrichment (0.7%) using ampoules and stainless steel bombs. In short-term irradiations using ampoules some production of acid gas has been noted, with the accompanying absence of oxygen. This gas has been identified as a mixture of CO<sub>2</sub> and acetone; the CO<sub>2</sub> presumably arises from the oxidative decomposition of acetone remaining from one of the steps in the purification of the uranyl sulfate. Considerable difficulty has been encountered in obtaining pure uranyl sulfate from the usual channels of

supply, but it is understood that other groups have made progress toward improving this situation. When longer irradiations of the concentrated uranyl sulfate were carried out in stainless steel bombs, the maintenance of considerable pressure in excess of steam pressure and a reduction of this pressure in the absence of neutrons (obviously from recombination) provided good evidence that both hydrogen and oxygen were being formed, i.e., the main course of the decomposition was not in the direction of hydrogen plus acid gas. This situation will, of course, be clarified as further work provides more data.

A preliminary study has been made of the formation of SO<sub>2</sub> from gamma-irradiated sulfuric acid and uranyl sulfate solutions. The technique involved sweeping a solution with helium gas during irradiation, bubbling the gas through dilute ceric sulfate solution, and estimating the SO<sub>2</sub> formed by measuring the change in transmission of the ceric sulfate solution at 3200 or 3800 Å. SO<sub>2</sub> was produced in 95% H<sub>2</sub>SO<sub>4</sub> and 11 M H<sub>2</sub>SO<sub>4</sub>, but none was detected from 0.4 M H<sub>2</sub>SO<sub>4</sub> or 1.24 M UO<sub>2</sub>SO<sub>4</sub> solutions.

From ampoule irradiations it appears that uranyl nitrate will be decomposed by attack on the nitrate ion.

## HRP QUARTERLY PROGRESS REPORT

The uranyl fluoride solutions under irradiation at high concentrations and low enrichment in ampoules and stainless steel bombs behave much like the above-mentioned uranyl sulfate solutions containing 300 g of uranium per liter.

**Survey of the Stability of HRP Systems.** Out-of-pile ampoule corrosion tests to determine the effects of numerous variables on the corrosion resistance of type 347 stainless steel in uranyl sulfate systems have been summarized in the previous homogeneous reactor quarterly report.<sup>(1)</sup> This report is concerned with an examination of the behavior of titanium and zirconium in addition to pretreated type 347 stainless steel in concentrated solutions (300 g of uranium per liter) of uranyl sulfate, uranyl nitrate, and uranyl fluoride.

The experimental techniques and procedures which have been previously described<sup>(1)</sup> consist of sealing a small volume of solution along with a short length of metal rod inside a silica ampoule and then heating the ampoule to 250°C for various periods of time. The onset of corrosion can frequently be observed visually without interrupting the course of the experiment. The concentration and pH of the tests solutions are listed in Table 12.1. The data and results are summarized in Table 12.2. The two main criteria previously used to determine whether a test run was successful have again been employed: (1) the appearance of the test specimen under the microscope, and (2) the condition of the solution at the end

(1) "Effect of Variables on Corrosion: Series II," *Homogeneous Reactor Project Quarterly Progress Report for Period Ending May 15, 1951*, ORNL-1057, p. 61 (Oct. 10, 1951).

TABLE 12.1

Possible HRP Fuel Solutions

SOLUTION	URANIUM CONCENTRATION (mg/ml)	pH
UO <sub>2</sub> SO <sub>4</sub>	307	1.95
UO <sub>2</sub> (NO <sub>3</sub> ) <sub>2</sub>	318	1.03
UO <sub>2</sub> F <sub>2</sub>	289	2.38

of the test (uranium concentration, pH, analyses for metal ions, etc). The results of these experiments are interpreted below.

*Uranyl Sulfate.* Titanium appears much more resistant than zirconium or pretreated stainless steel, both in the presence and absence of air. No microscopically evident change in the titanium surface was noted at the end of the runs. Zirconium forms a heavy layer of white oxide and, in degassed solutions, a heavy black crystalline layer of U<sub>3</sub>O<sub>8</sub>. Furthermore, with the passage of time (and air present in the samples) this white layer of zirconium oxide is flaked off and settles as a precipitate.

*Uranyl Nitrate.* Titanium appears much more resistant than zirconium or pretreated stainless steel, both in the presence and absence of air. No microscopically evident change in the titanium surface was noted at the end of the runs except for a very fine iridescent oxide layer on the surface of the metal. Both nitrate- and chromate-treated stainless steels were attacked with leaching of the nickel and chromium. This may possibly be

[REDACTED]

FOR PERIOD ENDING AUGUST 15, 1951

TABLE 12.2

Survey of the Stability of HRP Fuel-Metal Combinations

(Unless otherwise noted, all samples were heated for 160 hr at 250°C.)

SOLUTION	METAL	PRETREATMENT	OXYGEN	REMARKS
UO <sub>2</sub> SO <sub>4</sub>	Zirconium	None	Air	White oxide layer on metal; becomes flaky and deposits precipitate.
		None	Degassed	Black U <sub>3</sub> O <sub>8</sub> layer containing 60% uranium precipitated from solution over white oxide layer.
	Titanium	None	Air	Samples and solution excellent.
UO <sub>2</sub> (NO <sub>3</sub> ) <sub>2</sub>	Zirconium	None	Air	Fine layer of oxide present on metal.
			Degassed	Fine layer of oxide present; white precipitate deposit.
	Titanium	None	Air	Samples and solution excellent; very thin iridescent layer on surface, probably oxide.
	Stainless steel	Chromate	Air	Samples have peeled flaky oxide layer; 800 ppm chromium in solution.
			Degassed	~250 ppm chromium, 30 ppm nickel in solution; iron present as solid oxide.
Stainless steel	Nitrate	Air	Solution and samples look good; 50 ppm nickel in solution.	
		Degassed	300 ppm nickel, 50 ppm chromium in solution; iron present in solid state.	
UO <sub>2</sub> F <sub>2</sub>	Zirconium	None	Air	Samples blew up; gas evolved and precipitates formed even on standing at room temperature
			Degassed	
	Titanium	None	Air	~20 ppm titanium in solution; black layer dissolved in HNO <sub>3</sub> gave 10 mg uranium.
			Degassed	45 to 170 ppm titanium in solution.
	Stainless steel	Chromate	Air	Samples good; traces of black solid in solution; 20 to 60 ppm nickel, 30 ppm chromium in solution; iron present as solid oxide.
			Degassed	150 ppm nickel in solution; heavy oxide layer on samples.
Stainless steel	Nitrate	Air Degassed	Large amounts of black solid, U <sub>3</sub> O <sub>8</sub> and Fe <sub>2</sub> O <sub>3</sub> ; 300 to 700 ppm nickel in solution; 20% uranium precipitates.	

## HRP QUARTERLY PROGRESS REPORT

due to the higher acidity of the nitrate as compared to the sulfate solution.

*Uranyl Fluoride.* Zirconium is unstable even at room temperature. The titanium surface appeared good after the test, though a fine layer of  $U_3O_8$  was found as an overlay. Some titanium (45 to 170 ppm) was found in solution in the degassed samples. Nitrate-pretreated stainless steel does not stand up well, large amounts of nickel being leached out into the solution (250 to 770 ppm), along with the formation of considerable amounts of black solid (iron and uranium oxides). Chromate-pretreated stainless steel showed less attack on the nickel (18 to 190 ppm in solution).

**Hydrolysis of Iron, Chromium, and Nickel Salts in Uranyl Sulfate Solutions.** The purpose of this series of experiments was to determine whether analyses for nickel could be used as an indication of the amount of corrosion occurring in test loop solutions.

Definite quantities of iron, chromium, and nickel salts [ $Fe_2(SO_4)_3 \cdot (NH_4)_2SO_4 \cdot 24H_2O$ ,  $Cr_2(SO_4)_3 \cdot K_2SO_4 \cdot 24H_2O$ , and  $NiSO_4 \cdot 6H_2O$ ] were introduced into quartz tubes containing uranyl sulfate solution [307 g of uranium per liter, pH 1.95]. These tubes were sealed and heated for 60 hr at 250°C. Upon completion of the run the tubes were opened, and the solutions were centrifuged and analyzed for iron, chromium, and nickel; wherever visible, precipitates were washed free of the original solution, fused with sodium bisulfate, dissolved in hydrochloric acid, and analyzed for the appropriate species.

The data and results are listed in Table 12.3. From these, the following conclusions are evident:

1. Nickel remains in solution at this concentration and pH, even when iron and chromium, present in the solution at the start, hydrolyze and precipitate almost completely.
2. Chromium largely remains in solution unless iron is also present; in the latter case it is almost completely precipitated, probably indicating adsorption or occlusion of structurally similar chromium oxide with iron oxide.
3. Precipitation of iron from these solutions, regardless of the presence of chromium and nickel, is practically complete.

**Hydrogenation of Uranyl Sulfate Solutions.** The successful restoration of a uranyl sulfate solution by treatment of a slurry of reduced uranium oxide in a water-white solution of low pH with oxygen pressure at high temperature (reported elsewhere, p. 51) led to an investigation of the reaction of hydrogen with uranyl solutions. It was found that Gall and Manchot<sup>(2)</sup> had reported the catalytic reduction of uranyl sulfate by hydrogen using platinum black as the catalyst. The reduction appeared to go smoothly to the tetravalent state. Ipatiew and Muromtzev<sup>(3)</sup> reported the noncatalytic reduction

(2) H. Gall and W. Manchot, "Katalytische Hydrierung anorganischer Substanzen," *Ber.* 58, 482 (1925).

(3) W. Ipatiew and B. Muromtzev, "Die Einwirkung des Wasserstoffs auf Metallnitrate," *Ber.* 63, p. 160, esp. p. 164 (1930).

FOR PERIOD ENDING AUGUST 15, 1951

TABLE 12.3

Hydrolysis of Iron, Chromium, and Nickel Salts in Uranyl Sulfate Solution

CONCENTRATION IN INITIAL SOLUTION (ppm)			CONCENTRATION IN FINAL SOLUTION (ppm)			CONCENTRATION IN PRECIPITATE (ppm) <sup>(a)</sup>		
IRON	CHROMIUM	NICKEL	IRON	CHROMIUM	NICKEL	IRON	CHROMIUM	NICKEL
4500	1150	500	30	60	540	4300	1000	<2
4500	1150	500	40	75	480	5060	875	<2
4500		540	70		540	4190		<2
4500		540	70		550	4560		<2
	980	450		670	460		159	<2
	980	450		660	440		262	<2
		475			450			<2
		475			440			<2

<sup>(a)</sup> ppm referred to original solution.

of uranyl nitrate using a gold-lined bomb and 50 to 80 atm of hydrogen, measured at room temperature. At 300°C the reaction gave pure crystalline  $UO_3 \cdot H_2O$ , and the product contained no nitrogen. At higher temperatures and with longer time of contact they were able to obtain  $U_3O_8$  or mixtures of this compound with  $UO_3$ . Eventually they were able to reduce the uranium to  $UO_2$ . The significance of the first product to the homogeneous reactor program might be that the hydrogen, normally present in a reactor, can reduce the nitrate ion without reducing the uranium. Moreover, even in a uranyl sulfate solution the uranyl ion appears to be easily reduced (a fact known from solution stability studies). Gillies, reporting work of the SAM laboratories

in MDDC-647,<sup>(4)</sup> discusses the ability of hydrogen and oxygen to reduce or oxidize slurries of  $U_3O_8$  at temperatures of 100 to 300°C.

During the past quarter exploratory experiments have been carried out, under noncatalytic conditions using solutions in silica liners, which have shown conclusively that at temperatures of 250 to 290°C hydrogen alone can react with uranyl sulfate solutions to produce insoluble black oxides along with a drop in the pH of the solutions.

<sup>(4)</sup>D. M. Gillies, *Some Studies of the Reaction of Uranium with Hydrogen, Oxygen, and Water*, MDDC-647 (June, 1946).

## HRP QUARTERLY PROGRESS REPORT

At the present time an effort is under way to establish the kinetics of this reaction with hydrogen in order to facilitate interpretation of the high-pressure recombination studies and because of its obvious relationship to the stability of the reactor solution. The effect of various hydrogen-oxygen mixtures (particularly 2:1) will also be studied using noncatalytic (silica tube) conditions in order to ascertain the relative rates of the oxidation and reduction reactions and to establish the percentage of uranium in the reduced state at "equilibrium." From in-pile radiation experiments using stainless steel bombs it appears that this "equilibrium" is at or very near the hexavalent state since our recoveries of uranium in solution have been excellent. However, the dynamics of this balance point and the influence upon it of added catalytic materials are considered of great interest to the successful operation of the reactor.

**Recombination of Hydrogen and Oxygen at High Pressures.** In the previous quarterly<sup>(5)</sup> it was indicated that out-of-pile studies of the recombination of hydrogen and oxygen might be initiated because of the significance of this reaction in connection with the interpretation of in-pile pressure-temperature data. A thorough search of the literature preceding actual experimental work failed to disclose any references really pertinent to the problem but provided a good general background for the study of the hydrogen-oxygen reaction. Apparatus was designed and constructed for the generation of

high pressures of electrolytic gas, and this apparatus, together with suitable furnaces, pressure recorders, etc. has now been installed and tested behind the high-pressure barricade. Detailed experimentation will be carried out during the next quarter with particular study on the following questions:

1. What is the source of the temperature effect upon the recombination reaction? In our bombs under irradiation it is known that raising the temperature causes a lowering of the residual pressure. This could be due to an effect upon the gas-phase reaction, a liquid-phase reaction, a catalytic reaction with the walls of the stainless steel bomb, or a reaction with the uranyl ion. Ascertaining which of these is the controlling reaction is the main object of the study.
2. Do changes in uranium concentration or changes from uranyl sulfate to uranyl fluoride or phosphate affect the reaction?
3. Can good kinetic studies of this reaction be carried out which might be helpful in predicting net gas production under a variety of unexplored reactor conditions?
4. Is the uranium maintained in the hexavalent state under conditions of the recombination reaction? The answer to this question may explain the pressure "hump" sometimes obtained under irradiation.

---

(5) "Projected Work for the Next Quarter," ORNL-1057 *op. cit.*, p. 77.

5. Are metals other than stainless steel satisfactory for use under conditions of the recombination reaction? Specifically, is titanium converted to the hydride or the oxide under these conditions?

It is planned to bracket the temperature and pressure conditions likely to be encountered in the HRE in order to obtain as much information as possible of direct relevance to the operation of the HRE.

**Hydrogen Embrittlement.** The thin-walled capillary tubing (type 347 stainless steel) used in the radiation stability studies would be particularly vulnerable to hydrogen embrittlement if such a process were favored by the conditions of our experiments. In order to survey this situation a bundle of short capillary tubes was formed by sealing one end of each and joining the other ends to a common header. The tubes were then placed under 5000-psi pressure of hydrogen and held at 250°C for 15 days. A coil of the same tubing was also held at 250°C for 15 days. These tubes were subsequently tested by the Metallurgy Division. Lengths of tubing were gripped in a vise and given repeated 90° bends until fracture occurred. The results of this test are given in Table 12.4. There is obviously no significant difference between the two means and probably no significant difference between the two spreads. It does not, therefore, seem probable that our test conditions, as far as temperature, time, and hydrogen pressure are concerned, lead to serious weakening or embrittlement of the tubes. If further exploratory studies of hydrogen embrittlement are carried out by other groups it has been recommended that

samples of thin sheet, exposed to hydrogen on both sides, might give a more sensitive indication of embrittlement effects.

TABLE 12.4

**Results of Hydrogen Embrittlement Tests**

SPECIMEN	NUMBER OF BENDS BEFORE FRACTURE	
	EXPOSED TO H <sub>2</sub>	EXPOSED TO AIR
1	38	38
2	32	33
3	41	33
4	22	
Mean value	33-1/4	34-2/3

**Out-of-Pile Bomb Studies.** Using unenriched uranyl sulfate solution containing 307 g of uranium per liter, a few experiments have been carried out in stainless steel bombs to demonstrate solution stability prior to radiation tests. Both chromate-pretreated and oxygen-pretreated bombs were used, and a pressure of oxygen was maintained during the heating period of the test. Analyses of the solutions for uranium and nickel after different periods of heating were carried out to give evidence of solution stability and corrosion. The results are presented in Table 12.5. These results indicate clearly that the solution is stable under the conditions chosen. The nickel analyses and pH measurements indicate that the corrosion is of the same magnitude as that previously found with the uranyl sulfate solutions containing 40 g of uranium per liter in the same type of containers.

**HRP QUARTERLY PROGRESS REPORT**

**TABLE 12.5**

**Out-of-Pile Bomb Experiments with High Concentrations of Uranyl Sulfate**

(All tests were conducted with 400-psi O<sub>2</sub> pressure at 275°C; initial concentration was 307 g of uranium per liter.)

EXPERIMENT NUMBER	PRETREATMENT	HEATING PERIOD (hr)	SOLUTION ANALYSES			pH
			URANIUM (g/liter)	NICKEL (mg/ml)	CHROMIUM (mg/ml)	
355	2% CrO <sub>3</sub>	168	309	0.012		
		500	309	0.23		
364	2% CrO <sub>3</sub>	624	305	0.14	1.7	1.06
356	400-psi O <sub>2</sub>	168	314	3.3		
		500	325	0.59		
365	400-psi O <sub>2</sub>	624	301	0.26	0.24	1.35

**Plans for Next Quarter.** Fundamental work on specific and net gas production in uranyl sulfate, nitrate, fluoride, and other systems at various concentrations and enrichments will be continued using ampoules and bombs in hole 12 of the graphite pile.

Studies of various inhibitors of corrosion will be initiated using silica tubes and nonradiation conditions to determine whether there is any possibility of protection of various HRP systems by this method. If any materials of promise are found, studies in radiation will be attempted.

The kinetics of the recombination of hydrogen and oxygen at high pres-

ures in stainless steel bombs will be determined. In this connection, the suggested possible effect of ruthenium (a fission product which might "plate out" on the metal surfaces of the system) will be explored.

The studies of the interaction of hydrogen with uranyl solutions under noncatalytic conditions and the effect of the hydrogen-oxygen ratio upon the valence stage of the uranium will be continued.

Particular attention will be given to the use of titanium in radiation studies, since a supply of the metal suitable for making small bombs is available.

### 13. SLURRY FUEL STUDIES

F. R. Bruce, Leader  
J. O. Blomeke            J. M. Fulmer  
G. A. Eaton            C. P. Johnson  
L. E. Morse

A study is being made of uranium slurries which might serve as satisfactory homogeneous reactor fuel. Such a fuel should contain between 100 and 250 g of uranium per liter, with preference being given to the higher uranium concentration. It is desirable that the slurry should remain in suspension during its useful life in the reactor. For a plutonium producer, the longevity of a stable slurry is determined by the operating time required to increase the plutonium concentration to its maximum permissible value. From this it follows that the desired slurry should remain in suspension after being subjected to pile conditions for about 19 days and allowed to remain at rest for 24 hr. While the attainment of a stable slurry is desirable, it is not essential if the material may be easily resuspended after having settled out. Arbitrarily, a system having satisfactory nuclear properties has been defined as one in which the ratio of neutron cross-section of  $U^{238}$  to the cross-section of constituents other than uranium is greater than 20. In other words, less than 5% of the neutrons available for plutonium production should be lost by parasitic capture in the fuel.

The main advantage of a slurry fuel is visualized as being the elimination of the difficult corrosion problem which is inevitably present with solutions of uranium compounds. On the other hand, slurries may present a serious erosion problem in

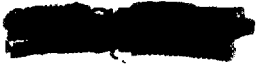
circulating systems, and the power required for pumping slurry fuels would undoubtedly be much greater than that required for circulating solutions.

In order to alleviate these difficulties, Dr. Harold C. Urey has suggested that the boiling reactor be considered as the ideal application for slurry fuels, thereby eliminating the erosion and pumping problems. Much of the slurry fuel development program has recently been realigned in this direction.

#### URANIUM TRIOXIDE STUDIES

A true chemical solution may be completely characterized by specifying its composition, concentration, and temperature. On the other hand, a solid-liquid system such as a slurry is unique in that still another property must be considered, namely, that pertaining to particle size and the solid-liquid interfacial area. Because of the extremely large interfacial area present in slurries of micron size particles, a relatively small variation in particle size may be expected to exert a very large influence on such properties as settling rate, viscosity, dispersibility, erosion rate, and boiling characteristics.

In order to study quantitatively the effect of particle size on slurries, it is necessary to have either



## HRP QUARTERLY PROGRESS REPORT

an efficient method of producing very uniformly sized particles of uranium trioxide over the size range of interest to the present slurry program, or the means of separating and classifying such particles from large mixtures containing a wide distribution in particle sizes.

At the present time, uranium trioxide is prepared either by thermal decomposition of uranyl nitrate or by the thermal decomposition of uranyl nitrate or by the thermal decomposition of uranium peroxide. Neither of these methods provides a uranium trioxide which is applicable directly to the slurry program; therefore, methods of reducing the particle size and classifying the resulting particle are being investigated.

An Eppenbach colloid mill which is capable of grinding uranium trioxide in water suspension to particle sizes in the range of 1 to 10  $\mu$  is now being used. The major limitations of this mill are: (1) It produces a nonuniformly sized product; (2) the product is contaminated with iron; and (3) the mill may be used only as a wet grinder, which necessitates a drying operation in the event that air classification is desirable.

To supplement the colloid mill, a laboratory scale fluid energy mill has been ordered from the Micronizer Company. This mill utilizes compressed air as a source of energy to reduce solid particles to the sub-sieve range and is expected to produce uranium trioxide particles of greater uniformity than those obtained from the colloid mill and with little or no iron.

Approximately 200 lb of Mallinckrodt uranium trioxide has been obtained as

starting material for the slurry program. This material, formed by the thermal decomposition of uranyl nitrate, was received as the uranium trioxide monohydrate and was washed eight times with water to remove soluble nitrate. It was then ground batchwise for 45 min in a colloid mill, and a Dorco water classifier was employed to separate the material into five size ranges. Approximately 80% of the material was separated out with a particle size of less than 5  $\mu$ . The remainder of the material comprises particles within the size range of 5 to 50  $\mu$ . Further classification into smaller size ranges will be carried out using laboratory air and water classifiers.

Utilizing the experiences gained in the work on concentrations of 40 g of uranium per liter, an attempt was made to prepare slurries containing 300 g of uranium per liter using anhydrous uranium trioxide prepared by the thermal decomposition of uranyl peroxide. However, due to the adsorption of water in the hydration of oxide the consistency of the dispersion became so high that it was impossible to prepare uniform suspensions in a Waring Blender. The addition of an organic dispersant or polyphosphate increased the fluidity of the suspension, but on heating at 250°C either reduction of the uranium trioxide in the case of the organic dispersant or formation of a uranyl phosphate with the polyphosphate occurred. In order to alleviate these difficulties, work was initiated using uranium trioxide monohydrate as a starting material.

A slurry containing 300 g of uranium per liter as uranium trioxide monohydrate of particle size between 1 and 4  $\mu$  and stabilized with 13 g of

electrodialyzed bentonite per liter was prepared. This slurry, though showing some thixotropy, was readily prepared in a Waring Blendor in contrast to the slurries prepared from the anhydrous oxide. After heating for 24 hr in a sealed quartz tube at 250°C, the slurry became unstable and settled very rapidly at room temperature. In this behavior it resembled the heated dispersion of uranium trioxide in water alone. From this, it is apparent that the preparation of high concentration uranium slurries is difficult. In the future, slurries containing 100 g of uranium per liter will be investigated.

#### URANIUM DIOXIDE STUDIES

Stability of uranium dioxide slurries under an atmosphere of oxygen was investigated by boiling and periodically stirring a slurry for 7 days at atmospheric pressure under an atmosphere of oxygen. Colloidal yellow material resembling uranium trioxide formed in the slurry, and it is apparent that uranium dioxide is oxidized by oxygen at the boiling temperature.

#### MAGNESIUM URANATE AND MAGNESIUM DIURANATE STUDIES

Slurries of uranium oxides are objectionable in that they have a low pH in solution, thus they present somewhat of a corrosion problem. In order to overcome this difficulty, Dr. Harold C. Urey has suggested that magnesium uranate and magnesium diuranate be considered as possible slurry material. Magnesium uranate was prepared by adding ammonia to a solution of magnesium chloride and uranyl chloride to form the yellow solid. A suspension of this material

in water was heated in a sealed pyrex tube at 250°C for 20 hr. At the end of this time the color of the slurry had changed from orange to yellow, and the suspension had a silky appearance when agitated. Magnesium diuranate was prepared by the ignition of magnesium uranyl acetate at 750°C. This material formed as a brownish-yellow solid. The suspension of this brownish-yellow solid in water when heated in a sealed pyrex tube at 250°C for 20 hr gave a lemon-colored yellow material. This color change also occurred on boiling the material at 100°C.

Magnesium uranate and magnesium diuranate slurries exhibit instability on being heated at 250°C. The magnesium diuranate slurries settled and packed very badly, resisting dispersion.

#### SLURRY CIRCULATORS AND BOILERS

A slurry circulator system is being set up to study the fundamental aspects of slurry dynamics. The effect of pumping on particle size as well as generalized observations on erosion, power requirements, and heat transfer will be made employing a simple circulating loop. The circulator which is now under construction has a total holdup of only 2 liters and will operate between room temperatures and 90°C. A second circulator has been designed for operation at higher temperatures, and a pump capable of performance in such a system at temperatures up to 200°C has been ordered. A small stainless steel boiler of 1-liter capacity and equipped with a 4-kw resistance heater has been designed for operation at 250°C and 600 lb/sq in. pressure. The



## HRP QUARTERLY PROGRESS REPORT

purpose of this equipment is to demonstrate that slurries may be made to boil in a controllable and even

fashion at power levels and temperatures and pressures of interest in proposed reactor operation.



14. SLURRY PUMPING STUDIES

A. S. Kitzes, Leader

R. B. Gallaher  
R. V. Bailey

W. Q. Hullings  
C. A. Gifford

A literature survey has resulted in the tentative conclusion that slurries in general have a turbulent viscosity which is not changed by the Reynolds number in turbulent flow.

The particle size of hydrated  $UO_3$  is reduced rapidly to less than  $100 \mu$  by 100 ft/sec circulation at room temperature.

Metallic iron in the slurry after the test indicates abrasion of the iron fittings in the system.

Tests indicate that dry hydrated  $UO_3$  abrades types 347 and 321 stainless steel. Using a number of rather broad assumptions, an equation has been developed which indicates qualitatively the rate of abrasion by a slurry at a pipe bend.

A temperature cycle circulating system is now in operation with an upper temperature of  $150^\circ C$ . Heat-transfer coefficients for the slurry will be compared with those obtained using water in the same system.

**Heat Transfer and Apparent Viscosity of  $UO_3$  Slurries.** A literature survey has shown that in turbulent flow a value for the so-called turbulent viscosity of a slurry can be obtained from pressure-drop data. This is done by finding the Reynolds number which corresponds to the measured friction factor and solving for viscosity, knowing the tube diameter and the density and velocity of the slurry. In the cases re-

ported, the turbulent viscosity appeared to be independent of the Reynolds number, so long as the slurry was in turbulent flow. Unfortunately, however, calculation of the viscosity in this way uses the fifth power of the friction factor and the tenth power of the velocity, so that the final figure for turbulent viscosity is subject to considerable error. In the standard heat-transfer equation for fluids in turbulent flow, viscosity enters to the 0.47 power.

Since the turbulent viscosity of most slurries appears to be independent of the Reynolds number, there is reason to believe that heat transfer in turbulent  $UO_3$  slurries can be predicted by the usual relationships.

In viscous flow, most concentrated slurries change in apparent viscosity as the shear rate in the fluid changes. Flowing through a tube the shear rate varies as a function of distance from the center of the tube, and the normal paraboloid associated with viscous flow of true fluids may not be present in flowing slurries. For this reason new equations are required to predict heat transfer to slurries in viscous flow. For circular tubes the new equation has been found to be

$$\frac{h_{am}D}{k} = 1.615 \left[ \frac{V\rho CD^2}{kz} \right]^{1/3} \left[ 1 + \frac{g\tau_0 D}{24\eta V} \right]^{1/3}$$

## HRP QUARTERLY PROGRESS REPORT

where

$h_{am}$  = the average heat-transfer coefficient over the length of the tube,

$D$  = tube diameter,

$k$  = thermal conductivity of the slurry,

$V$  = mean velocity of the slurry,

$\rho$  = density of slurry,

$C$  = specific heat of slurry,

$z$  = heated length of the tube,

$g$  = gravitational constant,

$\tau_0$  = yield stress of the slurry, and

$\eta$  = coefficient rigidity of the slurry.

The development of the above equation is presented in ORNL-1071.<sup>(1)</sup>

Equipment has been designed, and construction has been started for measuring the viscosity of various  $UO_3$  slurries, both in turbulent flow and in viscous flow.

**$UO_3$  Abrasion Tests.** One of the major problems in pumping a slurry is erosion (abrasion). An experiment was therefore set up to determine qualitatively the abrading action of  $UO_3 \cdot H_2O$  as it falls freely between a stationary metal plate specimen and a softer metal rotating disk separated a known distance (Fig. 14.1).

Preliminary results indicated that  $UO_3 \cdot H_2O$  abraded types 321 and 347

<sup>(1)</sup>R. V. Bailey, *Erosion Due to Particle Impingement upon Bends in Circular Conduits*, ORNL-1071 (Nov. 6, 1951).

stainless steels (Fig. 14.2) at the rate of 0.5 mil/hr when the disk was rotating at 50 rpm (lineal velocity approximately 0.9 ft/sec), and the distance between the specimen and disk was 0.005 in. The  $UO_3$  was comminuted during the 12-hr test from an average particle size of 80  $\mu$  to less than 44  $\mu$  (particles no longer flowed freely). The surface hardness of the abraded specimen as measured by a Rockwell superficial hardness tester did not change, indicating no surface work hardening during the course of the test.

The abrasion tester (Fig. 14.1) consists of an Armco iron disk, 4 in. in diameter and 1/8 in. in thickness, mounted on the shaft of a Graham Variable Speed Transmission. The specimen, mounted on a rigid slide, is held a known distance from the rotating disk by counter weights operating against springs. The distance between the specimen and rotating disk can be varied by changing the counter weight loading. A clear plastic box (not shown) encases the assembly to prevent spreading of the  $UO_3$  dust.

The specimen was polished to a minor finish and examined microscopically for any residual scratches. Depth of scratches, if perceptible, were measured for comparison with those produced during the test.

Further experiments are now under way to determine the abrasion rate, using different particle sizes of  $UO_3$ . When the dry runs have been completed, the abrasive action of  $UO_3$  slurries of varying particle size will be studied by pumping slurry between the rotating disk and the specimen.

████████████████████

FOR PERIOD ENDING AUGUST 15, 1951

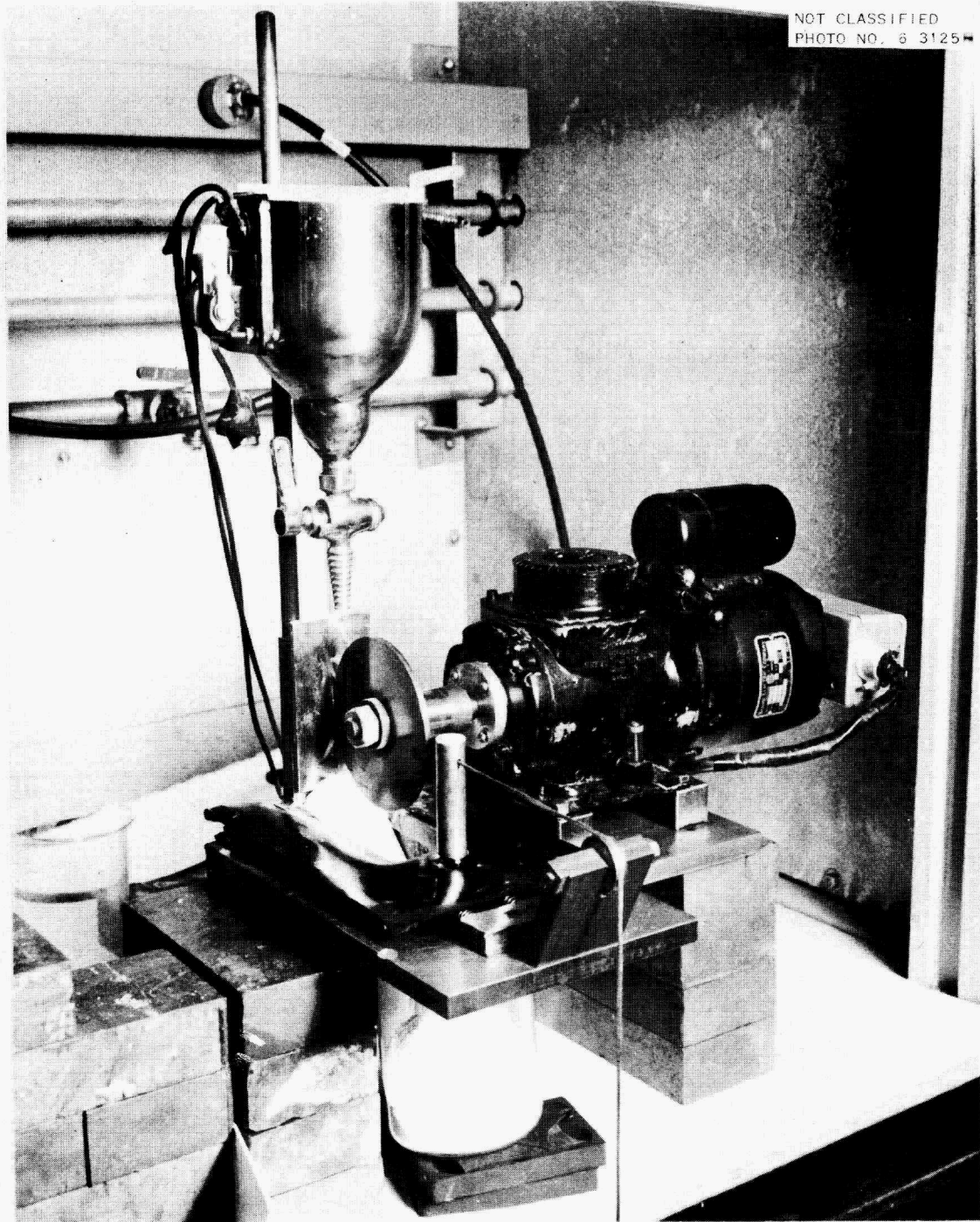


Fig. 14.1 - Abrasion Testing Apparatus.

**UNCLASSIFIED**

# UNCLASSIFIED

## HRP QUARTERLY PROGRESS REPORT

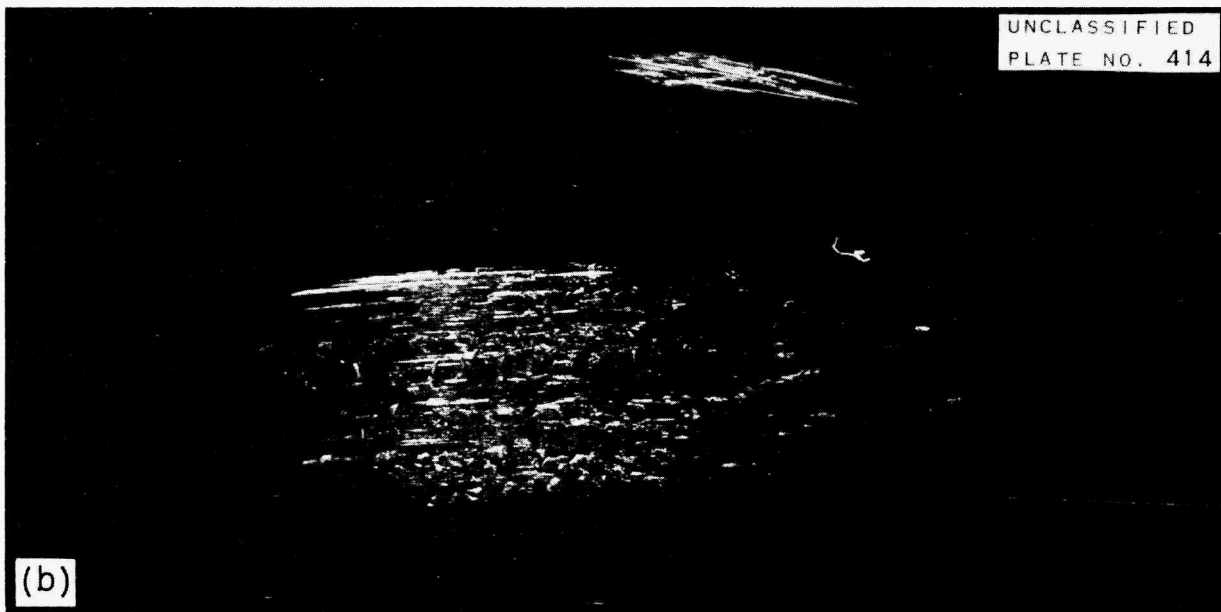


Fig. 14.2 - Abrasion of Stainless Steel Surfaces. (a) Type 321 stainless steel, 9.5X; (b) type 347 stainless steel, 9.5X.

By making a number of assumptions, based on particle abrasion results reported in the literature, an equation has been developed which qualitatively relates the variables affecting conduit wall abrasion at a bend. The equation is advanced tentatively because of the assumptions made in its derivation, and it should not at this time be used as more than an indication of the relationship between the variables. The equation is

$$E = C_6 \left[ \frac{U_{avg}^{3.8} r (\rho_s - \rho_e)}{\mu R \rho_s^{.6}} + \frac{U_{avg}^2 (\rho_s - \rho_e)^{2.8} r^{5.6}}{68 \mu^{2.8} R^{2.8}} \right]$$

where

$E$  = weight loss of wall at a bend per unit weight of particles passing,

$C_6$  = a constant for the system including the elastic and hardness properties of the particles and surface, as well as the shape of the particles,

$U_{avg}$  = mean flow rate of the slurry,

$r$  = radius of particle,

$R$  = radius of the bend (this is postulated to be large compared with the radius of the conduit),

$\mu$  = viscosity of the slurry,

$\rho_s$  = density of solid, and

$\rho_e$  = density of slurry.

The derivation of this equation is presented in ORNL-1071.<sup>(1)</sup>

**Particle-Size Reduction of Circulated Slurry.** It has been reported<sup>(2)</sup> that the  $UO_3$  (10 g of uranium per liter) became discolored when it was pumped through a system consisting of stainless steel and pyrex glass at room temperature. Later it was shown by chemical analysis that the discoloration was due to metallic iron contamination. Apparently the fittings such as elbows and tees were being eroded by the  $UO_3$  slurry. The slurry velocity was approximately 5 ft/sec, and no reduction of the  $UO_3$  to  $U_3O_8$  was evident.

**Particle-Size Change in a Circulated Slurry.** To determine to what extent the  $UO_3$  crystals are comminuted during circulation in a closed system,  $UO_3$  (10 g of uranium per liter) was pumped through a small sphere and through a liquid cyclone separator. The finer fraction from the separator was passed through the pump while the coarser fraction was returned to the finer stream at the throat of a venturi on the high-pressure side of the pump.

The rate of  $UO_3 \cdot H_2O$  crystal breakdown is shown in Fig. 14.3. Samples were taken from regions at five different radial positions in a glass sphere, 8 in. in diameter and operated

<sup>(2)</sup>A. S. Kitzes et al., "Engineering Research on Alternate Reactor Systems," *Homogeneous Reactor Project Quarterly Progress Report for Period Ending May 15, 1951*, ORNL-1057, p. 131 (Oct. 10, 1951).

# HRP QUARTERLY PROGRESS REPORT

with a horizontal vortex. The data indicate that with continued circulation the particle-size distribution of the particles became increasingly uniform, as shown in Fig. 14.4.

Concentration gradients across the glass sphere were also determined. Although the data of one test indicate that the concentration across the sphere becomes essentially uniform because of the comminution of the particles, the experiments are being repeated before the results are reported.

Studies of the crystal growth of  $UO_3$  in stagnant water at temperatures between 50 and 250°C have been planned, and fabrication of the test bombs has been started.

**Temperature Cycle Loop.** During the past quarter a temperature cycle loop (Fig. 14.5) was placed in operation to investigate the heat-transfer and pumping characteristics of a  $UO_3-H_2O$  slurry. In passing around the system, the slurry temperature varies from 110 to 150°C. Erosion,

corrosion, and crystal changes upon thermal cycling are also being studied.

A slurry, containing 100 g of uranium as the oxide per liter of water, is recycled through a stainless steel loop, consisting of a heater, a cooler, and a pump, at a velocity of 10.5 ft/sec. Heat-transfer measurements are made periodically, and samples are drawn off for chemical analyses and particle-size determinations (particle size is determined microscopically). Chemical analyses included pH and iron, nickel, and chromium ion concentrations of

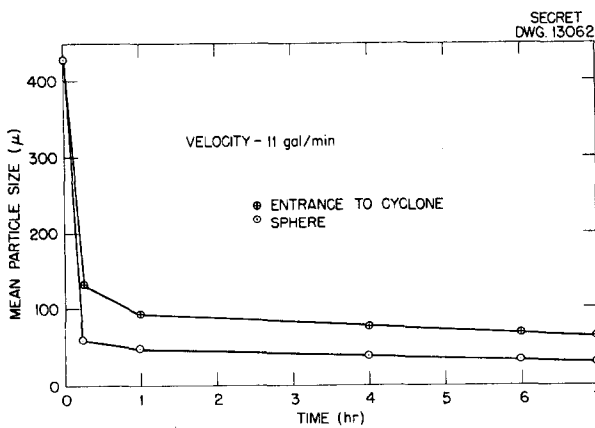


Fig. 14.3 -  $UO_3$  Particle Breakdown.

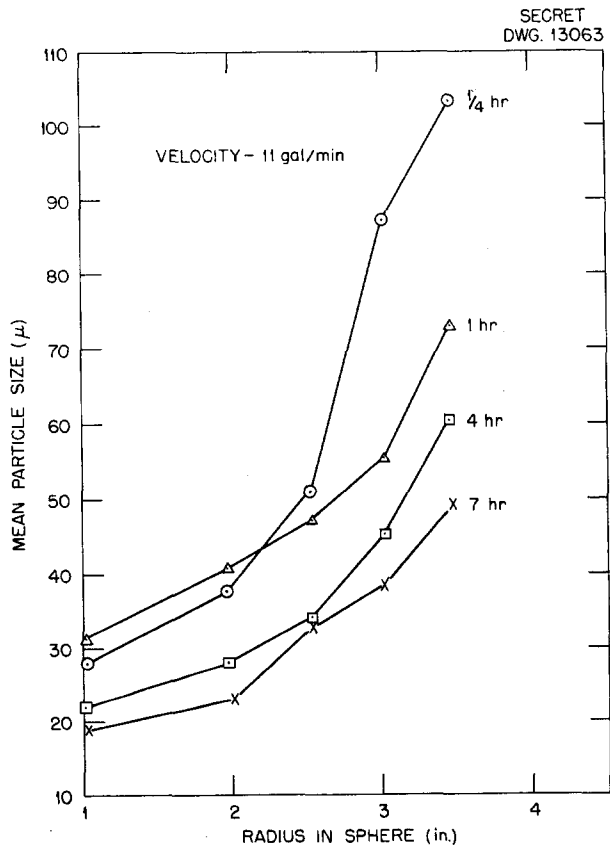


Fig. 14.4 - Particle Distribution in Sphere.

both the solids and filtrates. The system was calibrated by circulating

distilled water. The over-all heat-transfer coefficient,  $710 \text{ Btu/hr-ft}^2\text{-}^\circ\text{F}$ , checked the predicted value within  $\pm 2\%$ . Flow measurements were made with a venturi meter.  $\text{UO}_3$  (particle size - 100% through 325 mesh screen) was washed three to four times with distilled water to reduce the nitrate content and hydrated to  $\text{UO}_3 \cdot \text{H}_2\text{O}$  prior to loading into the loop. Sufficient data are not available at this time to evaluate what is taking place in the loop when operating a slurry.

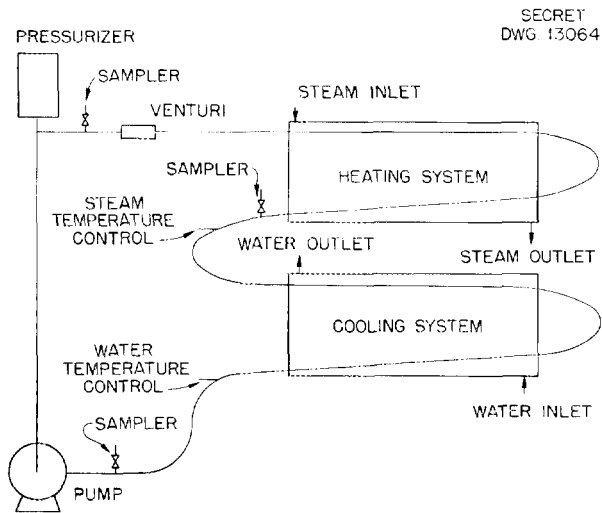


Fig. 14.5 - Slurry Thermal Loop.

Equipment has been designed and fabrication has been started to study the characteristics of a 3-in. Dorr Clone, a liquid cyclone. Materials of varying density and particle size will be used. Work is approximately 20% completed.

100

100

[REDACTED]

**Part III**

**LONG RANGE STUDIES**

[REDACTED]

100

100

## 15. PLUTONIUM CHEMISTRY AND FISSION PRODUCT SOLUBILITIES

W. L. Marshall, Leader  
H. W. Wright      E. V. Jones  
B. Zemel

### PLUTONIUM CHEMISTRY IN AQUEOUS URANYL SULFATE AT 100 to 250°C

H. W. Wright and W. L. Marshall

Intermittent work has been done for the past eight months in preparation for the study of plutonium behavior in aqueous uranyl sulfate solutions from 100 to 250°C; however, interim investigations have delayed the program. Full time effort is now being devoted to this investigation, and the experimental status is as follows:

1. A microsolubility apparatus is under development for synthetic studies above 100°C.
2. The filter disk apparatus of B. Zemel<sup>(1)</sup> of this laboratory will be modified to be used as a direct analytical method. The apparatus probably will be reduced to a smaller scale.
3. The development of a technique will be necessary for the problems inherent in the preparation of pure plutonium compounds.

(1) "Solubilities of Fission Product Sulfates," *Homogeneous Reactor Experiment Quarterly Progress Report for Period Ending August 31, 1950*, ORNL-826, p. 78 (Oct. 24, 1950).

(2) M. H. Lietzke and R. W. Stoughton, *The Measurement of the Solubility of Fission Product Sulfates at High Temperatures and Pressures*, ORNL-970 (Mar. 13, 1951).

### MEASUREMENT OF THE SOLUBILITY OF YTTRIUM SULFATE IN AQUEOUS URANYL SULFATE SOLUTIONS FROM 200 TO 300°C

E. V. Jones

From the standpoint of the homogeneous reactor program, it is very desirable to know the solubilities of fission products in solutions of 5 to 40% uranyl sulfate and in the temperature range of 200 to 300°C. The work covered by this report is an extension of the work of Lietzke and Stoughton<sup>(2)</sup> on the solubility of yttrium sulfate in aqueous uranyl sulfate solutions of higher concentrations. Their study was limited to uranyl sulfate solutions containing 30 g of uranium per liter. At present, solutions containing 258 and 300 g of uranium per liter are under investigation. The method used is the well-known silica-tube synthetic method as described previously.<sup>(2)</sup> A microtechnique devised by W. L. Marshall is also being investigated.

Tentative results of investigations on the solubility of  $Y_2(SO_4)_3$  in uranyl sulfate solutions containing 258 g of uranium per liter are listed as follows:

TEMPERATURE (°C)	$Y_2(SO_4)_3$ SOLUBILITY
208	4.32
215	3.41
230	2.78
245	2.12

## HRP QUARTERLY PROGRESS REPORT

As indicated by the above data, yttrium sulfate shows a negative temperature coefficient of solubility. It also has a strong tendency to supersaturate, and the temperatures recorded are those at which the crystals dissolved completely upon very slow cooling.

Although our results are tentative and are being checked further, several observations may be of some significance:

1. For a given temperature, the solubility of yttrium sulfate is very much greater in more concentrated uranyl sulfate solutions. For example, at 225°C the solubility of yttrium sulfate in uranyl sulfate containing 258 g of uranium per liter is approximately twelve times as great as it is in a solution containing 30 g of uranium per liter. For 300 g of uranium per liter the ratio is about sixteen. The ratios will be somewhat less at 250°C.
2. The temperature of formation of two-liquid phases seems to be considerably lowered by the presence of yttrium sulfate. Secoy<sup>(3)</sup> found this change occurring at the concentration we are using at about 295.5°C. With a sample having 3.41% yttrium sulfate, a  $\text{UO}_2\text{SO}_4$ -rich liquid phase appeared at 260°C. With 2.12% yttrium sulfate the change occurred at 271°C and with 1.43% yttrium sulfate the temperature was 275°C.

<sup>(3)</sup>C. H. Secoy, "The System Uranyl Sulfate-Water. II. Temperature-Concentration Relationships Above 250°," *J. Am. Chem. Soc.* 72, 3343 (1950).

3. We have been unable to extend our measurements into the region of low yttrium sulfate concentrations. For example, with 258 g of uranium per liter and 1.43% of yttrium sulfate in one sample, and 1.08% of yttrium sulfate in another sample, we were unable to obtain any crystals even by heating the solutions to 320°C for 2 hr. The  $\text{UO}_2\text{SO}_4$ -rich layer became very viscous, but no crystals appeared.

### SOLUBILITY OF FISSION PRODUCT SULFATES

B. Zemel

The solubilities of  $\text{Ce}_2(\text{SO}_4)_3$  in  $\text{H}_2\text{O}$ ,  $\text{La}_2(\text{SO}_4)_3$  in  $\text{H}_2\text{O}$ ,  $\text{BaSO}_4$  in  $\text{UO}_2\text{SO}_4$ , and  $\text{Ce}_2(\text{SO}_4)_3$  in  $\text{UO}_2\text{SO}_4$  (concentrations of 30 g of uranium per liter) have been determined up to 350°C.

Several solubility curves for data obtained previously in the presence of  $\text{UO}_2\text{SO}_4$  are now considered invalid since it has been found that the stock  $\text{UO}_2\text{SO}_4$  used contained appreciable amounts of ammonium sulfate. It was further shown that the solubility of the alundum filter disks employed and temperature variations across the bomb were causing spurious results due to precipitation of uranium and distillation of water, respectively.

In order to obviate these factors three measures were taken: (1) The alundum filter disks were replaced by platinum sponge filters; (2) the bomb furnaces were rewound and so arranged that the upper or sampling end of the bomb was kept a few degrees

hotter than the lower or reaction size; and (3) the temperature differential for filtration was kept low enough so as to favor filtration over distillation.

The solubility studies of  $\text{SrSO}_4$  in  $\text{UO}_2\text{SO}_4$  and of  $\text{Y}_2(\text{SO}_4)_3$  in  $\text{UO}_2\text{SO}_4$ , for which impure  $\text{UO}_2\text{SO}_4$  was previously used, have since been almost completely repeated using the pure reagent. The results will be reported later.

The solubility curve of  $\text{Ce}_2(\text{SO}_4)_3$  (Table 15.1 and Fig. 15.1) was determined by adding  $\text{Ce}^{144}$  tracer to natural  $\text{Ce}_2(\text{SO}_4)_3$  in solution. Since the  $\text{Ce}^{144}$  obtained from the Radioisotope Control Department group appeared to be impure, the  $\text{Ce}^{144}$  was

TABLE 15.1

Solubility of  $\text{Ce}_2(\text{SO}_4)_3$  in Water

SAMPLE NO.	TEMP. (°C)	c/m (a)	SOLUBILITY (mg/100 g solution)
10	105	23,857	300
6	139	8,306	113.5
11	169	3,569	50
7	199	1,350	19.1
9	211	1,273	17.3
4	220	959	13.1
5	244	210	2.87
8	269	163	2.2
3	284	36	0.49
2	325	69	0.94
1	350	61	0.83

(a) 100  $\lambda$  samples counted.

(4) D. N. Hume, N. E. Ballou, and L. E. Glendenin, *A Manual of the Radiochemical Determination of Fission Product Activity*, CN-2815 (June 30, 1945).

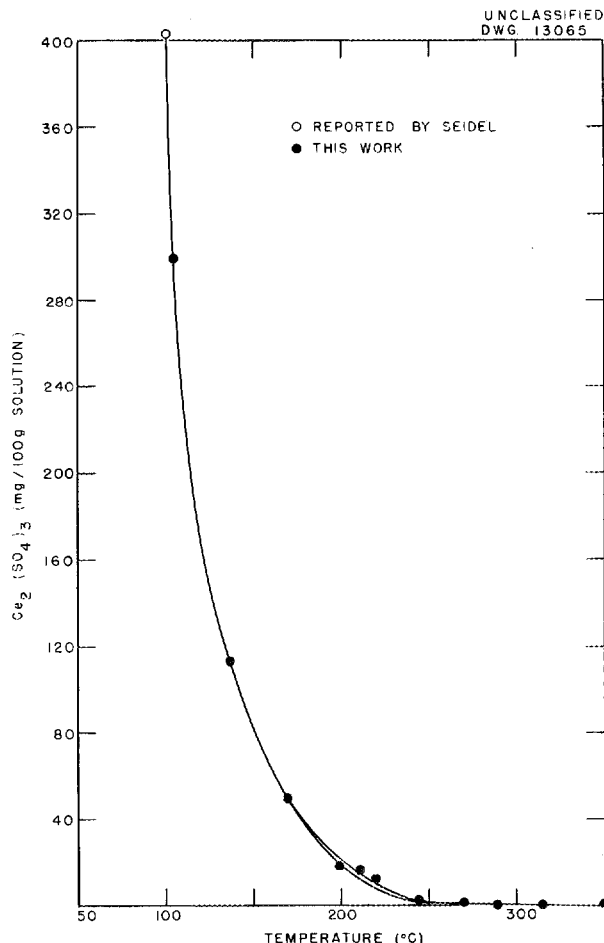


Fig. 15.1 - Solubility of  $\text{Ce}_2(\text{SO}_4)_3$  in  $\text{H}_2\text{O}$  from 100 to 350°C.

first purified by  $\text{CeF}_3$  and  $\text{Ce}(\text{IO}_4)_4$  precipitations(4) and then converted to  $\text{Ce}_2^{144}(\text{SO}_4)_3$  to give a solution containing 1.50 g of  $\text{Ce}_2(\text{SO}_4)_3$  per 100 g of water and giving 100,000 c/m per 100  $\lambda$  of solution on the fourth shelf of a G-M counter.

A solution of  $\text{Ce}_2(\text{SO}_4)_3$  in  $\text{UO}_2\text{SO}_4$  was made by taking 25. ml of  $\text{Ce}_2(\text{SO}_4)_3$  stock solution and then adding 1 ml of  $\text{Ce}_2^{144}(\text{SO}_4)_3$  tracer solution and

**HRP QUARTERLY PROGRESS REPORT**

5.4 g of  $UO_2SO_4$ ; the solution was then diluted to 100 ml. This solution contained 30.75 g of  $UO_2SO_4$  and 1.5 g of  $Ce_2(SO_4)_3$  per liter and was used to obtain the solubility data given in Table 15.2 and Fig. 15.2.

a difficult problem due to its low solubility and to the presence of the  $UO_2SO_4$  which made analysis of the  $Ba^{140}$  after each run more difficult. The procedure employed was as follows:

**TABLE 15.2**

**Solubility of  $Ce_2(SO_4)_3$  in  $UO_2SO_4$  Solution**

SAMPLE NO.	TEMP. (°C)	c/m <sup>(a)</sup>	SOLUBILITY (mg/100 g solution)
5A	137	23,200	290
4A	200	9,097	113.5
8A	220	6,440	80.5
9A	242	3,494	43.7
1A	267	1,865	23.3
6A	338	146	1.82

(a) 100 λ samples counted.

The solubility of  $La_2(SO_4)_3$  has been determined in water using  $La^{140}$  tracer. The lanthanum was obtained in a relatively pure form by purifying  $Ba^{140}$  obtained from the Radioisotope Control Department. The  $Ba^{140}$  was purified by three HCl-ether precipitations followed by a  $Fe(OH)_3$  decontamination step and a TTA-extraction step. The 40-hr  $La^{140}$  was then permitted to grow in and was extracted with TTA. This  $La^{140}$  was then added to a  $La_2(SO_4)_3$  stock solution to make the final  $La_2(SO_4)_3$  solution. The data obtained are given in Table 15.3 and Fig. 15.3.

The determination of the solubility of  $BaSO_4$  in  $UO_2SO_4$  presented

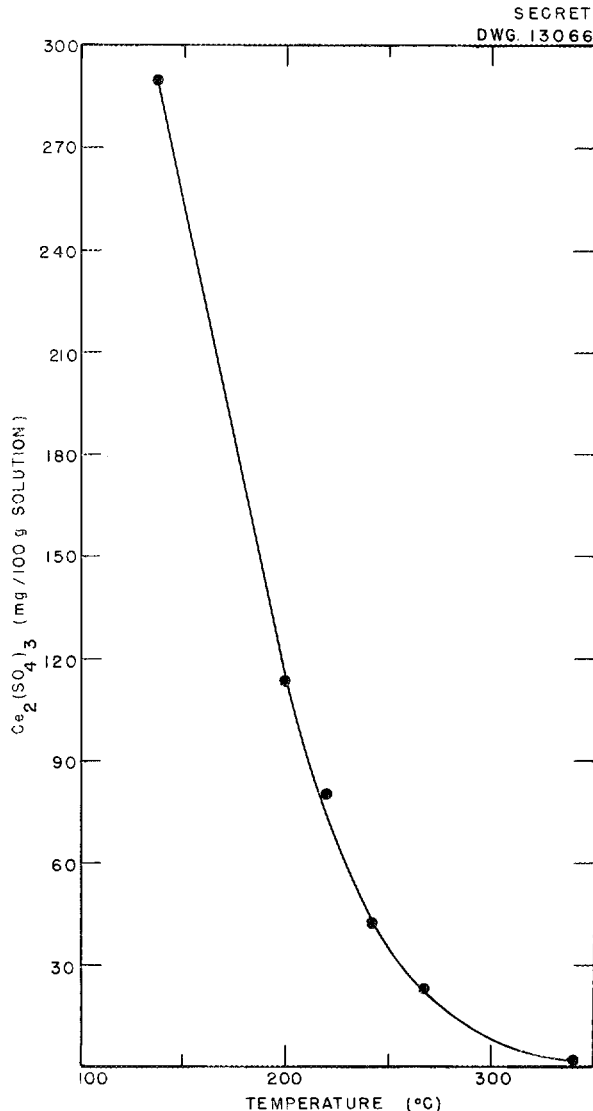


**Fig. 15.2 - Solubility of  $Ce_2(SO_4)_3$  in 0.126 M  $UO_2SO_4$  Solution from 150 to 340°C.**

A known amount of natural barium was added to a solution of  $Ba^{140}$  tracer whereby the specific activity of the stock barium was fixed at  $10^9$  c/m per gram of barium. This barium was precipitated as the sulfate, washed, and dissolved (to the extent of its solubility) in a uranyl sulfate solution containing 30 g of uranium per liter. The centrifuged supernatant solution was analyzed for barium by the addition of carrier barium and sulfuric acid; the barium precipitating as  $BaSO_4$  was centrifuged, washed, metathesized to the carbonate, dissolved in acid, precipitated three times as the chloride from an ether solution, and prepared for counting. A  $Fe(OH)_3$  scavenger precipitate was removed from the  $BaCl_2$  solution before finally preparing the sample for counting. The sample was allowed to stand until the  $La^{140}$  activity grew in to approximately its equilibrium count.

After approximate equilibrium was attained, it was found that the

TABLE 15.3

Solubility of  $La_2(SO_4)_3$  in Water<sup>(a)</sup>

SAMPLE NO.	TEMP. (°C)	SOLUBILITY (mg/100 g solution)
2	350	6.1
1	278	6.2
5	216	12
3	200	24
8	180	41
4	155	142
6	106	598

(a) 500  $\lambda$  samples counted in crystal counter for  $\gamma$  content; a standard sample was counted with each solubility sample due to the short half-life of  $La^{140}$ .

UNCLASSIFIED  
DWG. 13067

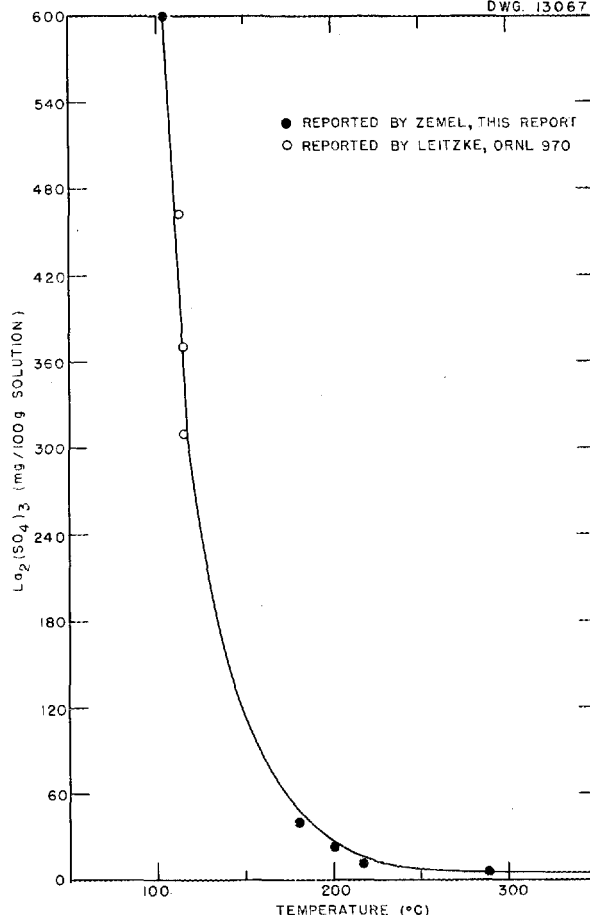


Fig. 15.3 - Solubility of  $La_2(SO_4)_3$  in  $H_2O$  from 100 to 350°C.

$Ba^{140}$ - $La^{140}$  was contaminated with other activities. So through the courtesy of A. R. Brosi the samples were examined on the  $\gamma$ -ray spectrometer, the 1.6-Mev  $La^{140}$  peak being identified and counted. Using the same chemical procedure given above, the original  $Ba^{140}$  solution containing a known weight of natural barium was analyzed. The results were corrected for sample size, chemical yield, and decay, and the

**HRP QUARTERLY PROGRESS REPORT**

stock  $UO_2SO_4$  solution was thus shown to have a concentration of 23 mg of  $BaSO_4$  per 100 g of solution. The barium activity was found to be about a factor of ten less than that due to the disintegration products of uranium.

Additional  $Ba^{140}$  tracer (containing an assumed negligible weight of barium) was then added to the  $BaSO_4$ - $UO_2SO_4$  stock solution. Using

this stock solution and the above chemical procedure, the values in Table 15.4 and Fig. 15.4 were obtained for the solubility of  $BaSO_4$ .

Considering the very high order of dilution and the large number of steps involved in each determination, the above results may be good only to an order of magnitude.

**TABLE 15.4**

**Solubility of  $BaSO_4$  in  $UO_2SO_4$  Solution**

TEMP. (°C)	SOLUBILITY ( $\mu g/100$ g solution)
185	15
200	11
250	9
270	10
296	6

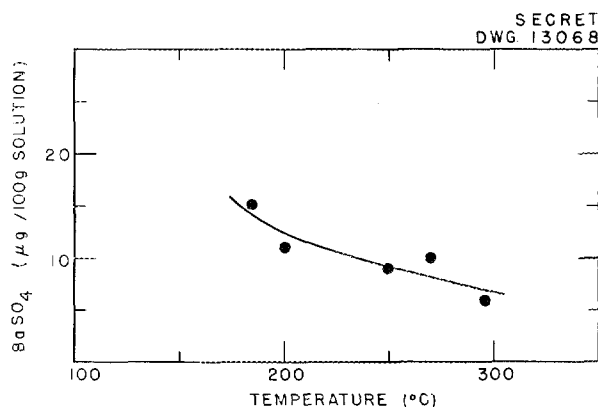


**Fig. 15.4 - Solubility of  $BaSO_4$  in 0.126 M  $UO_2SO_4$  Solution.**

16. CHEMICAL PROCESSING

F. R. Bruce, Leader  
D. E. Ferguson      I. R. Higgins  
D. D. Rauch        W. E. Tomlin

Chemical processing, attendant to the operation of nuclear reactors, has three primary objectives: (1) isolation of the product, (2) removal of fission product poisons, and (3) reclamation of the fuel or source material. The frequency of chemical processing in the case of a plutonium producer is determined by three factors, the first being the rate of formation of  $\text{Pu}^{240}$ , which, if present to the extent of greater than 2%, renders the product less desirable for military use. The second factor determining the processing cycle is the rate of depletion of the reactor fuel, since, on reaching a limiting composition with respect to the fissionable isotope, the fuel must be replenished either by re-enrichment or by adding highly enriched material. The third factor is the rate of build-up of fission product poisons which lower the neutron economy. The purpose of the chemical processing program which is now under way is to develop the best separation method for achieving the three previously mentioned objectives. In this work it is assumed that the most likely homogeneous reactor fuel will be a 1 M solution of uranyl sulfate, and the reactor for which chemical processing has been considered is that described in ORNL CF-51-7-134. (1)

(1) J. A. Lane, *A Comparative Survey of the Feasibility and Economics of Aqueous Homogeneous Reactors for the Large Scale Production of Plutonium*, ORNL CF-51-7-134 (July 27, 1951).

At the present time it is felt that the most attractive chemical process for the separation of uranium and plutonium from a homogeneous reactor will consist of heavy-water recovery by evaporation, and plutonium and uranium decontamination by TBP solvent extraction. A schematic process flow sheet is given in Fig. 16.1.

**Frequency of Chemical Processing for an Aqueous Homogeneous Plutonium Producer.** In the case of a solution homogeneous plutonium producer, three schemes of operation are possible. The reactor may be charged and discharged in one batch, the reactor may be charged and discharged continuously, or plutonium and high cross-section fission products may be removed continuously from the reactor with only a small amount of uranium being removed each day for the enrichment.

Frequency of chemical processing of the reactor fuel for the first two schemes is determined by the amount of  $\text{Pu}^{240}$  which is allowable in the product. If plutonium and fission products are removed continuously, only this part of the processing depends on  $\text{Pu}^{240}$  build-up, and the uranium need not be decontaminated until re-enrichment is necessary.

Calculation of the chemical processing periods, that is, the time in which one reactor charge must be

**HRP QUARTERLY PROGRESS REPORT**

SECRET  
DWG 12057 R1

BASIS: 15-ft REACTOR;  $UO_2SO_4$ - $D_2O$  SYSTEM; OPERATING AT 250°C, 1000 psi, AND 2000 Mw; PRODUCING 1 g OF PLUTONIUM PER MEGAWATT-DAY; AND CONTAINING 30 TONS OF URANIUM.

REACTOR DISCHARGED EVERY 19 DAYS.

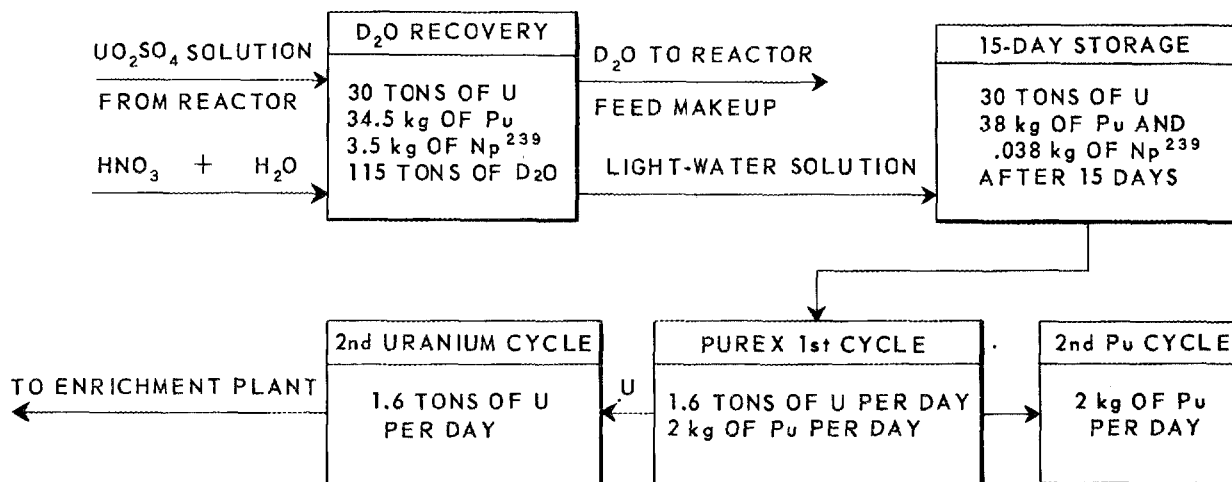


**Fig. 16.1 - Chemical Processing by Purex for Batch Operation of Reactor.**

processed, can be made from solutions of the differential equations which relate the rates of production of  $Np^{239}$ ,  $Pu^{239}$ , and  $Pu^{240}$  to flux and time. If we choose a limiting value for the ratio of  $Pu^{240}$  to total plutonium, the chemical processing period then is a function of flux only. This is shown in Fig. 16.2 for the three different schemes of operation, assuming a  $Pu^{240}$  content of 2%. To illustrate this analysis, consider a homogeneous plutonium producer operating with a 1 M uranyl sulfate in  $D_2O$  solution as fuel, a core diameter of 15 ft, a power level of 2000 mw, and a temperature of

250°C and producing 2000 g of plutonium per day. The thermal flux of this reactor at 2000 mw would be  $1.4 \times 10^{14}$  n/cm<sup>2</sup>/sec. From Fig. 16.2 we see that the chemical processing periods are 19 days for the batch operation of the reactor, 9.5 days for continuous operation, and 6.9 days for continuous removal of plutonium. From this we see that the batch operation of the reactor requires the smallest chemical processing rate, but since removal of plutonium by ion exchange is a simple and inexpensive chemical process, and since the uranium need not be decontaminated until the fuel requires

re-enrichment after 50 days of operation, this scheme competes economically with the batch operation of the reactor followed by a tributyl phosphate extraction process.

**Heavy-Water Recovery.** The first step in chemical processing of the fuel by solvent extraction would consist of heavy-water recovery in order that the subsequent separations might be carried out in a light-water system. The alternate procedure of

carrying out solvent extraction from a heavy-water solution is less desirable since deuterated nitric acid would be required and significant amounts of deuterium would be lost by solvent extraction of deuterated nitric acid and heavy water. The problem of dehydrating uranyl sulfate has not been investigated extensively on the project, and the open literature on the subject is ambiguous. The British have reported preparing uranyl sulfate containing less than 0.2% water by heating to 175°C for 5 to 6 hr. It was also found in this work that extensive decomposition of the uranyl sulfate appeared at about 250°C on heating in a vacuum. For the particular application considered here, decomposition of uranyl sulfate does not present a problem since solvent extraction is carried out in a nitric acid system and nitric acid may be used to dissolve any insoluble oxide formed.

The dehydration of uranyl sulfate on heating has been investigated using the Karl-Fischer reagent. On heating for 72 hr at 400°C no water appeared to be associated with the uranyl sulfate. At the end of this time, it was found that less than 15% of the sulfate ion associated with the uranium had been destroyed. It appears that the Karl-Fischer reagent is not capable of determining all of the water of hydration associated with uranyl sulfate, and an alternate method of studying the dehydration problem is being developed.

**Extraction of Plutonium and Nitric Acid from Solutions Containing Uranyl Sulfate.** It has been found that adequate recovery of uranium and plutonium may be obtained using the standard Purex process, provided the

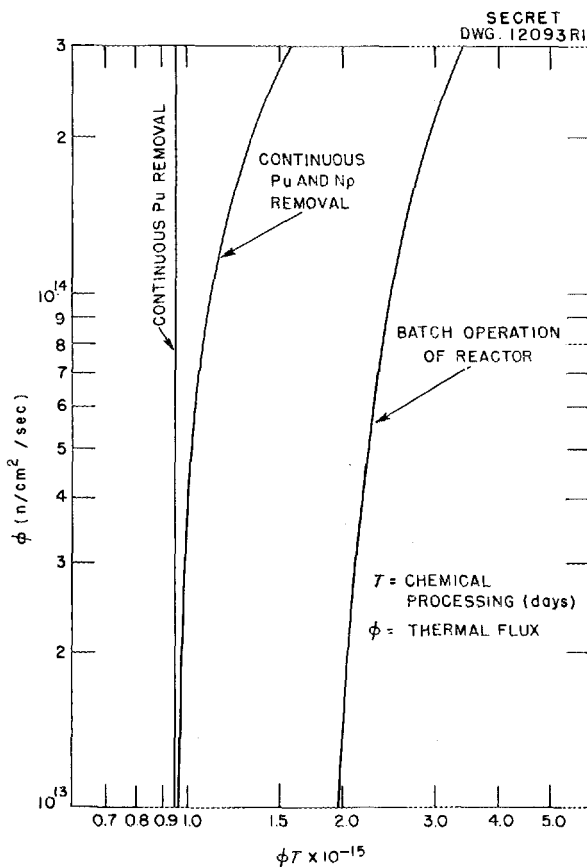


**Fig. 16.2 - Chemical Processing Period for a Homogeneous Plutonium Producer as a Function of Flux To Give 2% Pu<sup>240</sup>.**

**[REDACTED]**

## HRP QUARTERLY PROGRESS REPORT

feed contains a mole ratio of sulfate ion to uranium of 0.5 or greater. This was demonstrated by laboratory countercurrent batch extraction runs in which such a feed was processed through eight stages of extraction with a uranium loss of less than .01% and a plutonium loss of 0.1%. Since the mole ratio of sulfate ion to uranium will probably exceed 0.5 in the contemplated system, unless a special effort is made to destroy the sulfate, an investigation was made of the extraction of plutonium(IV) from nitric acid-sulfuric acid solution by tributyl phosphate diluted with a hydrocarbon diluent. The data which were obtained are summarized in Tables 16.1 through 16.7.

A preliminary correlation of these data yields an equation for

the plutonium(IV) distribution coefficient as a function of nitric acid concentration, tributyl phosphate concentration, and sulfuric acid concentration at 25°C:

$E_A^0$  (Pu(IV) at 25°C)

$$E_A^0 = \frac{2.95 [\text{HNO}_3]_{\text{aq}}^{3.8} [\text{TBP}]_{\text{org}}^{1.4}}{[\text{HNO}_3]_{\text{aq}}^{2.4} + 340 [\text{H}_2\text{SO}_4]_{\text{aq}}}$$

In this equation  $[\text{HNO}_3]$  is the aqueous phase nitric acid molarity,  $[\text{TBP}]$  is the total tributyl phosphate molarity in the organic phase, and  $[\text{H}_2\text{SO}_4]$  is the aqueous phase sulfuric acid molarity. This empirical equation does not present a good fundamental picture of the nature of plutonium(IV) extraction by tributyl

**TABLE 16.1**

Effect of  $\text{HNO}_3$  Concentration on Extraction of Pu(IV) and  $\text{HNO}_3$  by 30% TBP

Equal volumes of 30% TBP in AMSCO and aqueous phase as indicated were equilibrated for 3 min at 25°C.

Trace amount of Pu(IV) present.  
 $\text{SO}_4^{=}$  concentration, 1.0 N.

$\text{HNO}_3$ CONC. (N)	Pu D.C. (O/A)	$\text{HNO}_3$ D.C. (O/A)
0.53	0.004	0.19
0.88	0.01	0.24
1.68	0.1	0.25
2.20	0.4	0.25
2.60	0.7	0.25
3.85	2.7	0.23
4.30	4.1	0.21
5.00	5.6	0.20
6.10	8.4	0.18

**TABLE 16.2**

Effect of  $\text{HNO}_3$  Concentration on Extraction of Pu(IV) and  $\text{HNO}_3$  by 30% TBP from 0.5 N  $\text{H}_2\text{SO}_4$

Equal volumes of 30% TBP in AMSCO and aqueous phase as indicated were equilibrated for 3 min at 25°C.

Trace amount of Pu(IV) present.

$\text{HNO}_3$ CONC. (N)	Pu D.C. (O/A)	$\text{HNO}_3$ D.C. (O/A)
0.52	0.001	0.25
0.98	0.03	0.27
1.68	0.28	0.28
2.10	0.77	0.27
2.60	1.60	0.26
3.40	2.90	0.24
3.80	5.8	0.23
4.10	6.9	0.23
5.20	10.2	0.20
6.15	15.3	0.18

TABLE 16.3

Effect of HNO<sub>3</sub> Concentration on  
Extraction of Pu(IV) and HNO<sub>3</sub>  
by 30% TBP

Equal volumes of 30% TBP in AMSCO and aqueous phase as indicated were equilibrated for 3 min at 25°C.

Trace amount of Pu(IV) present.

HNO <sub>3</sub> CONC. (N)	Pu D.C. (O/A)	HNO <sub>3</sub> D.C. (O/A)
0.52	0.96	0.34
0.93	3.0	0.34
1.78	8.1	0.31
2.13	10.4	0.29
2.40	11.3	0.28
3.50	20.	0.26
3.90	23.0	0.24
4.50	25.	0.23
5.25	34.	0.21
6.25	41.	0.19

TABLE 16.4

Effect of TBP Concentration on  
Extraction of Pu(IV) and HNO<sub>3</sub>  
from HNO<sub>3</sub> Solutions

Equal volumes of TBP in AMSCO and aqueous phase as indicated were equilibrated for 3 min at 25°C.

Trace amount of Pu(IV) present.

TBP CONC. (%)	HNO <sub>3</sub> CONC. (N)	Pu D.C. (O/A)	HNO <sub>3</sub> D.C. (O/A)
5	2.0	0.60	0.04
10	1.95	1.9	0.07
15	1.85	3.6	0.12
20	1.80	4.7	0.15
30	1.66	8.6	0.25

phosphate. However, it was found to express accurately the distribution

TABLE 16.5

Effect of TBP Concentration on  
Extraction of Pu(IV) and HNO<sub>3</sub>  
from HNO<sub>3</sub> Solutions

Equal volumes of TBP in AMSCO and aqueous phase as indicated were equilibrated for 3 min at 25°C.

Trace amount of Pu(IV) present.

TBP CONC. (%)	HNO <sub>3</sub> CONC. (N)	Pu D.C. (O/A)
5	4.4	2.9
10	4.3	8.
15	4.1	13.
20	4.1	20.
30	3.8	36.

TABLE 16.6

Effect of Sodium Nitrate Concentra-  
tion on Extraction of Pu(IV)  
and HNO<sub>3</sub> by 30% TBP from  
HNO<sub>3</sub> Solutions

Equal volumes of 30% TBP in AMSCO and aqueous phase as indicated were equilibrated at 25°C.

Trace amount of Pu(IV) present.

NaNO <sub>3</sub> CONC. (moles/liter)	HNO <sub>3</sub> CONC. (N)	Pu D.C. (O/A)	HNO <sub>3</sub> D.C. (O/A)
0.0	0.96	3.1	0.23
0.5	0.90	5.0	0.31
1.0	0.86	10.	0.35
2.0	0.78	24.	0.49
2.5	0.77	35.	0.54
3.5	0.70	55.	0.67
4.0	0.67	80.	0.76

ratio of plutonium(IV) in the above system over the range of 1 to 5 M nitric acid, 5 to 30% TBP in AMSCO diluent, and 0 to 1 M sulfuric acid.

HRP QUARTERLY PROGRESS REPORT

TABLE 16.7

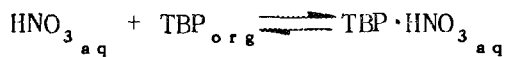
Effect of TBP Concentration on Extraction of Pu(IV) and HNO<sub>3</sub> from 2 M NaNO<sub>3</sub> Solutions of HNO<sub>3</sub>

Equal volumes of TBP in AMSCO and aqueous phase as indicated were equilibrated at 25°C.

Trace amount of Pu(IV) present.

TBP CONC. (%)	HNO <sub>3</sub> CONC. (N)	NaNO <sub>3</sub> CONC. (moles/liter)	Pu D.C. (O/A)	HNO <sub>3</sub> D.C. (O/A)
5	1.10	2.0	1.4	0.07
10	1.02	2.0	4.2	0.12
15	0.98	2.0	8.	0.18
20	0.90	2.0	12.	0.28
25	0.87	2.0	19.	0.33
30	0.80	2.0	23.	0.42

Table 16.8 shows the experimental values obtained for distribution coefficients in the above range of concentrations along with the values calculated from the empirical equation. The agreement is as good as the reproducibility of the distribution coefficients in this type of experiment. It has been reported by workers at Hanford that the extraction of nitric acid may be described by the following equilibrium expression:



In this equation, TBP is interpreted as uncomplexed tributyl phosphate in the organic phase. This equation does not adequately describe the extraction of nitric acid by tributyl phosphate. This may be easily seen from Table 16.1 since

TABLE 16.8

Comparison of Observed and Calculated Pu(IV) Distribution Coefficient

Pu D.C. calculated from

$$E_A^0 (\text{Pu IV}) = \frac{2.95 [\text{NO}_3^-]^{3.8} [\text{TBP}]^{1.4}}{[\text{NO}_3^-]^{2.4} + 340 [\text{SO}_4^-]}$$

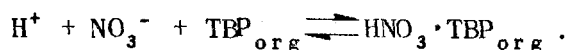
TBP CONC. (M)	HNO <sub>3</sub> CONC. (M)	SO <sub>4</sub> CONC. (M)	Pu D.C. OBSERVED	Pu D.C. CALCULATED
0.185	1.1	0.1	0.009	0.0115
1.11	0.9	0.1	0.06	0.066
0.185	3.0	0.1	0.56	0.39
1.11	2.6	0.1	4.15	2.95
0.185	2.0	0.375	0.04	0.03
0.74	1.8	0.375	0.16	0.14
0.185	5.0	0.375	0.62	0.72
0.74	4.6	0.375	3.90	3.90
0.555	2.8	1.0	0.22	0.18
1.11	2.5	1.0	0.33	0.32
0.555	4.7	1.0	0.94	1.26
1.11	4.3	1.0	1.85	2.44

the nitric acid distribution coefficient changes only from 0.19 at 1 M free TBP in the organic phase to 0.20 at 0.1 M free TBP in the organic phase. However, if the symbol, TBP organic, is interpreted as meaning the total tributyl phosphate, then we have a direct contradiction with the data presented in Table 16.9 where the nitric acid distribution is shown to decrease with increasing nitric acid concentration at constant nitrate ion concentration in the organic phase. From these data it appears that the extraction of nitric acid by 30% TBP in the AMSCO diluent from nitric acid solutions between

[REDACTED]

FOR PERIOD ENDING AUGUST 15, 1951

1 and 4.5 M is better described by the following expression:



The equilibrium constant for this reaction is given by

$$K = \frac{[HNO_3 \cdot TBP]_{org}}{[H^+]_{aq} [NO_3^-]_{aq} [TBP]_{org}}$$

which, if we disregard activity coefficients, becomes

$$K = \frac{E_A^o}{[NO_3^-] [TBP]_{org}}$$

where  $[TBP]_{org}$  is the uncomplexed TBP contained in the organic phase.

TABLE 16.9

Effect of HNO<sub>3</sub> Concentration on  
Extraction of Pu(IV) and HNO<sub>3</sub>  
by 30% TBP at Constant  
Ionic Strength

Equal volumes of 30% TBP in AMSCO and aqueous phase as indicated were equilibrated for 3 min.

Trace amount of Pu(IV) present.

HNO <sub>3</sub> CONC. (N)	NaNO <sub>3</sub> CONC. (moles/liter)	Pu D.C. (O/A)	HNO <sub>3</sub> D.C. (O/A)
0.63	4.0	72	0.70
1.05	3.5	57	0.52
1.48	3.0	42	0.40
2.10	2.5	40	0.34
2.45	1.5	29	0.24
3.25	1.0	29	0.24
4.20	0.0	22	0.20

It is shown in Table 16.10 that  $K$  lies between 0.20 and 0.25 for most of the data which have been obtained to date, with an average of about 0.22. It is also apparent from the data that the above reaction does not adequately describe the phenomenon at lower or higher nitric acid concentrations. This study of nitric acid extraction with TBP will be continued

TABLE 16.10

Values of the Thermodynamic  
Equilibrium Constant at  
25°C for the Reaction



NO <sub>3</sub> CONC. (M)	UNCOMPLEXED TBP (M)	HNO <sub>3</sub> E <sub>A</sub> <sup>o</sup>	K (at 25°C)
0.81	0.95	0.19	0.25
0.93	0.89	0.24	0.29
0.96	0.88	0.23	0.28
1.40	0.83	0.31	0.26
1.66	0.69	0.25	0.22
1.78	0.67	0.25	0.21
1.80	0.47	0.15	0.18
1.85	0.33	0.13	0.22
1.86	0.81	0.35	0.23
1.95	0.23	0.07	0.16
2.00	0.11	0.04	0.19
2.13	0.57	0.25	0.21
2.40	0.51	0.25	0.21
2.78	0.73	0.49	0.24
2.87	0.64	0.33	0.18
3.00	0.38	0.18	0.16
3.10	0.12	0.07	0.19
3.27	0.69	0.55	0.24
3.50	0.31	0.23	0.21
3.90	0.23	0.23	0.24
3.95	0.42	0.28	0.17
4.20	0.64	0.67	0.25
4.48	0.51	0.40	0.18
4.50	0.15	0.21	0.29
4.67	0.60	0.76	0.27

## HRP QUARTERLY PROGRESS REPORT

since it is felt that the behavior of plutonium(IV) in the system cannot be understood until an adequate explanation is found for the nature of nitric acid extraction.

**Plutonium Chemistry in Uranyl Sulfate Solutions.** It was previously shown that the continuous removal of plutonium from a homogeneous reactor considerably improves the economics of plutonium production. Utilization of anion exchange column for achieving this depends upon the plutonium being soluble and in an exchangeable ionic condition. A program was initiated to determine the stable plutonium valence state in uranyl sulfate solution which had been heated at 250°C.

Up to the present time the chemistry of plutonium(III) and plutonium(IV) in uranyl sulfate solutions has been investigated. For this work, plutonium(III) sulfate was prepared by reducing a stock solution of plutonium nitrate with hydrazine nitrate at 65°C. The reduced solution was then passed through a Dowex-50 ion exchange column which adsorbed plutonium(III). The column was then rinsed with water, with 0.25 M sulfuric acid, and finally the plutonium(III) was eluted with 6 N sulfuric acid. The excess sulfuric acid was then neutralized with  $UO_3$  to the pH of neutral uranyl sulfate. To obtain solutions of varying uranium content, neutral uranyl sulfate was added to the stock solution to obtain the desired concentration.

It has been found that the stable plutonium valence state in sulfuric acid and in uranyl sulfate in contact in air at room temperature is the tetravalent state. Likewise, the

heating of a plutonium(III) sulfate solution at 250°C yields plutonium(IV) sulfate. The solubility of plutonium in uranyl sulfate has been investigated as a function of uranium concentration, temperature, and sulfuric acid concentration. In this work, a solution containing plutonium sulfate and uranyl sulfate was heated at 250°C, cooled to room temperature, and the observations were made. This study showed that the solubility of plutonium sulfate in uranyl sulfate is extremely low and increases with increasing uranium concentration and sulfuric acid concentration. The solubility of plutonium in 0.2 M uranyl sulfate after heating at 250°C for 72 hr was found to be 0.9 mg/liter. Increasing the uranium concentration to 1 M increased the plutonium solubility to 6 mg/liter. A 1 M uranyl sulfate solution containing 0.49 N sulfuric acid exhibited a plutonium solubility of 28 mg/liter. Decreasing the heating temperature of 1 M uranyl sulfate, 0.04 N  $H_2SO_4$  solution, containing plutonium, from 250 to 150°C increased the solubility to 4 mg/liter. The solubility of plutonium in uranyl sulfate solutions is summarized in Tables 16.11 through 16.13 and Fig. 16.3.

TABLE 16.11

Plutonium Solubility vs. Uranium Concentration at 250°C

U CONC. (mg/ml)	ORIGINAL Pu CONC. (mg/ml)	FINAL Pu CONC. (mg/ml)
46	0.28	0.0009
91	0.23	0.0016
240	0.24	0.0058
360	0.22	0.0042

TABLE 16.12

Plutonium Solubility vs.  $H_2SO_4$   
Concentration at 250°C

ACID CONC. (N)	Pu SOLUBILITY (mg/ml)	OBSERVATION
0.09 basic	0.00177	Precipitate formed
0.21	0.0179	Precipitate formed
0.49	0.0279	Precipitate formed
0.81	0.123	Precipitate formed
1.32	0.452	No precipitate formed
1.92	0.464	No precipitate formed

By X-ray-diffraction techniques the solid phase precipitating from uranyl sulfate has been identified as  $PuO_2$ . The significance of these solubility determinations to the operation of a homogeneous plutonium producer may be interpreted as follows. A plutonium producer to which a continuous plutonium removal process is attached operates at an equilibrium plutonium concentration of 20 mg of plutonium per liter of uranyl sulfate. In order to achieve this solubility of plutonium the reactor must be operated with uranyl sulfate solution containing 0.33 N sulfuric acid. A plutonium producer

TABLE 16.13

Plutonium Solubility vs.  $H_2SO_4$   
Concentration at 150°C

$H_2SO_4$ (N)	Pu SOLUBILITY (mg/ml)	OBSERVATION
0.04	0.0036	Precipitate formed
0.34	0.392	Slight precipitate formed
0.66	>0.40	No precipitate formed
1.00	>0.40	No precipitate formed

which is processed in the batchwise fashion operates at a maximum plutonium concentration of 60 mg/liter. In order to maintain this plutonium in solution, the solution must be made 0.6 N in sulfuric acid.

In connection with the operation of the circulating loops employing uranyl sulfate solution, the interesting observation was made that uranium decay products appeared to associate themselves with the passive film on the stainless steel. Similarity in the chemistry of tetravalent plutonium and thorium suggested the possibility that plutonium might behave in a similar manner and become associated with the passive film in the reactor system. This was investigated by immersing a piece of passivated stainless steel in uranyl sulfate containing plutonium(IV) at a concentration of 50 mg/liter and heating the mixture to 250°C. At the end of this time, the stainless steel was removed from the solution,

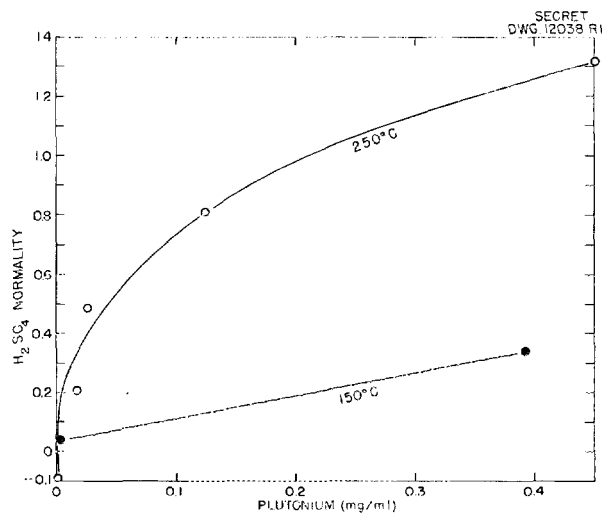


Fig. 16.3 - Solubility of Plutonium Sulfate in  $H_2SO_4$  - 1 M  $UO_2SO_4$ .

HRP QUARTERLY PROGRESS REPORT

TABLE 16.14

Total Radiation Intensities Under Varying Operating Conditions

Power density of reactor = 15 kw/liter.  
 $t_1$  = irradiation time (days).  
 $t_2$  = cooling time (days).  
 Ratio of average to maximum beta energies assumed to be 0.4.

$t_2$	TOTAL FISSION PRODUCT (beta energy watts/liter)	
	$t_1 = 5$	$t_1 = 30$
1	13.	20.
5	3.2	9.2
10	1.8	6.6

washed in water, and the passive film was removed with hydrochloric acid. It was found in this experiment that the plutonium adsorbed on the passive film to the extent of 0.0044 mg/sq in. of surface area. Studies of the adsorption of plutonium on passivated stainless steel will be continued.

**Fission Product Calculations.** The fission product beta activities of fuel solution from a homogeneous reactor have been calculated for several irradiation and cooling periods from data taken from HW-17415. <sup>(2)</sup> The results are presented in Tables 16.14 and 16.15.

Beta activity from fission products is compared (Table 16.16) with the beta activity from neptunium for a homogeneous plutonium producer. The data have been extended to include a

<sup>(2)</sup>P. R. Gillette, *Activity of Fission Products*, HW-17415 (April 14, 1950).

TABLE 16.15

Radiation Intensities from Non-gaseous Fission Products

Power density of reactor = 15 kw/liter.  
 $t_1$  = irradiation time (days).  
 $t_2$  = cooling time (days).

$t_2$	NONGASEOUS FISSION PRODUCT (beta energy watts/liter)	
	$t_1 = 5$	$t_1 = 30$
1	10.	17.
5	2.2	7.5
10	1.5	5.9

breakdown into several individual fission product energies in Tables 16.17 and 16.18.

Estimated fission product concentrations at time of discharge are given in Table 16.19 for a plutonium producer operating to give 600 g of plutonium per ton of uranium.

The total beta energy in watts associated with 1 liter of fuel solution is given in Table 16.14 as a function of irradiation and cooling time for a reactor operating at a power density of 15 kw/liter. The data of Table 16.14 are based on the assumption that *all* fission products remain in solution. Table 16.15 gives results obtained by the assumption that *all* gases and iodine are removed, immediately upon formation, from the reactor system.

The expression

$$P(t_1, t_2) = 41t_2^{-0.2} - [(t_1 + t_2)^{-0.2}]$$

gives satisfactory engineering estimates, at least over the range of

[REDACTED]

FOR PERIOD ENDING AUGUST 15, 1951

TABLE 16.16

**Radiation Intensities of Neptunium Under Varying Conditions**

Reactor power density = 15 kw/liter.  
 Neptunium production = .0154 g/liter per day.  
 $t_1$  = irradiation time (days).  
 $t_2$  = cooling time (days).

$t_2$	TOTAL FISSION PRODUCT (beta energy watts/liter)		Np (beta energy watts/liter)			
			Maximum		Minimum	
	$t_1 = 5$	$t_1 = 30$	$t_1 = 5$	$t_1 = 30$	$t_1 = 5$	$t_1 = 30$
1	13.	21.	20.	25.	13.	17.
5	3.2	9.3	6.0	7.7	4.0	5.1
10	1.9	6.8	1.4	1.7	.90	1.2
15	1.4	4.8	.31	.40	.21	.26

TABLE 16.17

**Radiation Intensities of Uranium Under Varying Conditions**

Reactor power density = 15 kw/liter.  
 $t_1$  = irradiation time (days).  
 $t_2$  = cooling time (days).  
 Uranium concentration = 230 g/liter.

$t_2$	BETA ACTIVITY (disintegrations/min/mg U)									
	Mo <sup>99</sup>		Zr <sup>97</sup>		Zr <sup>95</sup>		Ru <sup>103</sup>		Rh <sup>105</sup>	
	$t_1 = 5$	$t_1 = 30$	$t_1 = 5$	$t_1 = 30$	$t_1 = 5$	$t_1 = 30$	$t_1 = 5$	$t_1 = 30$	$t_1 = 5$	$t_1 = 30$
1	$3.9 \times 10^9$	$5.5 \times 10^9$	$29 \times 10^8$	$30 \times 10^8$	$40 \times 10^7$	$21 \times 10^8$	$28 \times 10^7$	$14 \times 10^8$	$8.1 \times 10^8$	$9.1 \times 10^8$
5	$1.4 \times 10^9$	$2.0 \times 10^9$	$57 \times 10^6$	$58 \times 10^6$	$38 \times 10^7$	$20 \times 10^7$	$26 \times 10^7$	$13 \times 10^8$	$1.3 \times 10^8$	$1.5 \times 10^8$
10	$4.2 \times 10^8$	$5.9 \times 10^8$	$43 \times 10^4$	$36 \times 10^7$	$36 \times 10^7$	$19 \times 10^8$	$24 \times 10^7$	$12 \times 10^8$	$1.4 \times 10^7$	$1.6 \times 10^7$
15	$1.2 \times 10^8$	$1.7 \times 10^8$	$31 \times 10^2$	$32 \times 10^2$	$34 \times 10^7$	$18 \times 10^8$	$22 \times 10^7$	$11 \times 10^8$	$1.5 \times 10^6$	$1.7 \times 10^6$

variables indicated by Tables 16.14 and 16.15, of fission product beta energy in watts per liter corresponding to irradiation and cooling times of  $t_1$  and  $t_2$  days, respectively, for reactor operation at 15 kw/liter.

A comparison between the beta activity due to fission products and the beta activity from neptunium for a plutonium producer operating at 15 kw/liter with a neptunium production rate of .015 g/liter per day

HRP QUARTERLY PROGRESS REPORT

TABLE 16.18

Decontamination Factors Required to Reduce Beta Activity of Uranium to 150 disintegrations/min/mg U Under Conditions Given in Table 16.17

DECONTAMINATION FACTOR										
$t_2$	$Mo^{99}$		$Zr^{97}$		$Zr^{95}$		$Ru^{103}$		$Rh^{105}$	
	$t_1 = 5$	$t_1 = 30$								
1	$2.6 \times 10^7$	$3.7 \times 10^7$	$1.9 \times 10^7$	$1.9 \times 10^7$	$2.6 \times 10^6$	$1.4 \times 10^7$	$1.8 \times 10^6$	$9.1 \times 10^6$	$5.4 \times 10^6$	$6.0 \times 10^6$
5	$9.6 \times 10^6$	$1.4 \times 10^7$	$3.8 \times 10^5$	$3.9 \times 10^5$	$2.5 \times 10^6$	$1.4 \times 10^7$	$1.7 \times 10^6$	$8.6 \times 10^6$	$8.9 \times 10^5$	$1.0 \times 10^6$
10	$2.8 \times 10^6$	$4.0 \times 10^6$	$2.8 \times 10^3$	$2.9 \times 10^3$	$2.4 \times 10^6$	$1.3 \times 10^7$	$1.6 \times 10^6$	$8.0 \times 10^6$	$9.4 \times 10^4$	$1.1 \times 10^5$
15	$8.2 \times 10^5$	$1.2 \times 10^6$	$2.1 \times 10^1$	$2.1 \times 10^1$	$2.3 \times 10^6$	$1.2 \times 10^7$	$1.5 \times 10^6$	$7.3 \times 10^6$	$9.9 \times 10^3$	$1.1 \times 10^4$

is shown in Table 16.16. Maxima and minima are given for neptunium in Table 16.16 since the fractional yields for the various modes of its decay are not available.

Beta disintegrations per minute per milligram of uranium are given in Table 16.17 for  $Mo^{99}$ ,  $Zr^{97}$ ,  $Zr^{95}$ ,  $Ru^{103}$ , and  $Rh^{105}$  for a reactor operating at 15 kw/liter and containing 230 g of uranium per liter. Table 16.18 gives the decontamination factors required to reduce these activities to 150 disintegrations per minute per milligram of uranium.

An estimate of fission product concentrations at the time of discharge is given in Table 16.19 for a plutonium producer operating at 15 kw/liter to produce a total of 600 g of plutonium per ton of uranium, assuming the uranium concentration to be 1 M.

**Alternate Processing Schemes.**

Before it was found that plutonium was insoluble in uranyl sulfate at elevated temperatures, ion exchange

TABLE 16.19

**Fission Product Build-up**

Power density = 15 kw/liter.  
 Uranium concentration = 1 M.  
 Plutonium production = 600 g per ton of uranium.

FISSION PRODUCT	CONCENTRATION (g/liter $\times 10^3$ )
Rare earths	43.
Barium	5.0
Zirconium	15.
Strontium	5.7
Yttrium	3.3
Columbium	3.6
Technetium	2.5
Ruthenium	9.2
Rhodium	.13
Palladium	.60
Tellurium	4.0
Molybdenum	12.

appeared as an attractive method for continuously removing plutonium from a homogeneous reactor.

Recent ion exchange studies indicate that much higher flow rates than those necessary to obtain equilibrium conditions in the ion exchange bed result in good removal of plutonium from uranyl sulfate. It appears at the present time that flow rates as high as 25 ml/min per square centimeter of ion exchange bed cross-sectional area result in reasonably efficient removal of plutonium from uranyl sulfate. The use of such elevated flow rates results in decreased radiation damage to the ion exchange resin. Studies of the radiation stability of ion exchange resins have been continued, and the additional data confirm the fact that the absorption of 1 kw-hr of radiation per kilogram of resin results in a capacity loss of between 10 and 15%.

In the most recent work, phenolic Dowex-30 resin was found to be a factor of 3 more stable than Dowex-50 with respect to radiation. However, Dowex-30 shows only half the capacity for plutonium as Dowex-50. The results which have been obtained on the radiation stability of ion exchange resins are summarized in Fig. 16.4.

An indirect method of preventing the precipitation of plutonium in a homogeneous reactor consists of the removal of neptunium, thus maintaining

the plutonium concentration at a level which does not exceed the solubility. By using a diaphragm electrolysis cell and a porous carbon cathode, about 40% of the neptunium was removed from the uranyl sulfate solution at the cathode, or precipitated with uranium in the catholyte after 18 amp-hr of electrolysis per liter of solution. In a cell with no diaphragm and a porous carbon cathode, no neptunium was deposited in 47 hr at 0.1 amp/liter. Work on electrolysis as a method for removing neptunium and plutonium will be continued.

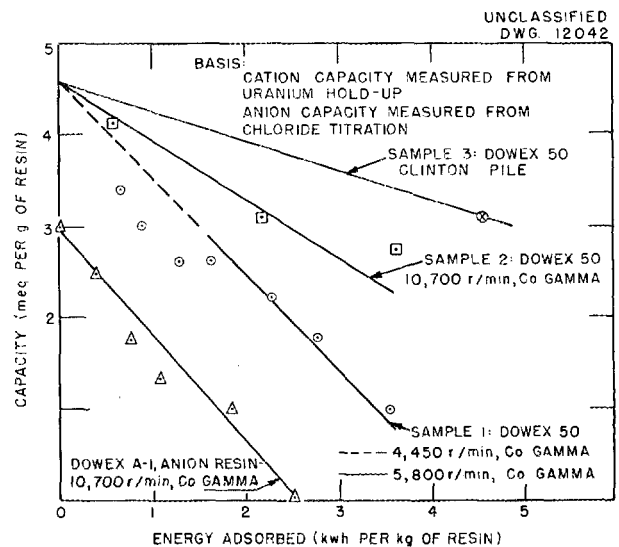


Fig. 16.4 - Dowex-50 Cation and Dowex-A-1 Anion Resin Capacity Loss from Irradiation.

1998

1998

**UNCLASSIFIED**

**APPENDIX**

**UNCLASSIFIED**



# UNCLASSIFIED

## NATURE OF LIQUID FLOW WITHIN A SPHERICAL CONTAINER

Department of Chemical Engineering  
University of Tennessee

**Introduction.** An investigation concerning the nature of liquid flow in spherical containers was begun in May, 1951 at the University of Tennessee in the Department of Chemical Engineering as a subcontract research project of Oak Ridge National Laboratory. This report describes the activities and progress on this investigation during the first quarter since the execution of the subcontract.

The objectives of the research project include studies on the following problems:

1. Liquid pressure drop as a function of liquid flow rate through the spherical container, liquid properties, and dimensions of the equipment.
2. Liquid velocity distribution within a spherical container as a function of the variables stated in (1).
3. Conditions necessary to describe the nature of liquid flow in a spherical container as being "streamline" or turbulent.
4. Effect on (1), (2), and (3) as to the general liquid flow direction within the spherical container, axial, tangential, or a combination of both.
5. Development of relations based on fundamentals of fluid dynamics to explain the experimental data and to allow extrapolation of the data.

6. Treatment of other such related problems as may be mutually agreed upon.

The activities of this first quarter included planning and designing the experimental program and facilities, construction of equipment and experimental work concerning problem (1), literature surveys, and theoretical considerations on the over-all investigation.

**Experimental Program and Facilities.** As an initial phase of the experimental program some pressure-drop measurements have been made using glass spheres which were furnished by ORNL. The details of these tests will be described in a subsequent section of this report.

Upon completion of the preliminary work with the glass spheres, test facilities involving a closed flow system are to be constructed. These facilities include a circulating pump to provide flows up to 200 gpm at 100 psig, appropriate heat exchangers to maintain isothermal conditions, and suitable instrumentation for the measurement of flow rates, static pressures, and liquid velocity direction and magnitude within the spherical container undergoing test. A number of spherical containers ranging in size from 8 to 18 in. in diameter of both metal and plastic construction are to be used in these test facilities.

The design details for the closed flow system have been completed and

UNCLASSIFIED

# UNCLASSIFIED

## HRP QUARTERLY PROGRESS REPORT

construction work is under way. The circulating pump has been purchased and received. Two shell and tube multipass heat exchangers have been made available for this work and prepared for installation. Metal hemispheres, which are to be fabricated into spheres in the departmental shops, are to be furnished by Lukens Steel Co. and Spincraft, Inc. Delivery on these items range from late September to early November.

The effect on liquid properties on the flow characteristics in the spherical containers will be determined by the use of liquids other than water in the flow system. The choice of liquids will give variations in liquid density and viscosity.

Plans are under way to conduct experiments attempting to find suitable methods of showing the flow patterns visually, using plastic spheres. These plans include the use of dye experiments similar to the work at ORNL in the Reactor Experimental Engineering Division, appropriate chemical reactions in liquid solution which produce color as a function of time, and bentonite clay or vanadium pentoxide colloidal solutions to show flow patterns by the birefringent properties of these solutions.

**Pressure-Drop Measurement in Glass Spheres.** The pressure-drop characteristics of glass spheres with two tangential inlets and two axial outlets as a function of flow rate have been determined. The experimental equipment is shown in Fig. 1. The essential features of this equipment include a source of water from the laboratory service lines, orifice meters to measure the liquid flow in influent and effluent pipes, and

mercury manometers to measure pressure drop across the glass sphere. The important dimensions of the glass spheres used in the tests are shown in Table 1.

TABLE 1

Dimensions of Glass Spheres Used in Pressure-Drop Experiments

INSIDE DIAMETER (in.)	INLET PIPE DIAMETER (in.)	EXIT PIPE DIAMETER (in.)
3.84	1.00	1.00
6.16	1.50	2.00

Tests were conducted using the following variations in flow arrangements:

1. Total influent in one inlet, total effluent at one outlet.
2. Total influent in one inlet, equal effluent at two outlets.
3. Equal influent in two inlets, total effluent at one outlet.
4. Equal influent in two inlets, equal effluent at two outlets.

For each flow arrangement the water flow rate was varied from approximately 10 to 70 gpm, and the corresponding pressure drops were measured.

All of the results from these experiments may be briefly summarized as follows:

1. For a given sphere and flow arrangement, the pressure drop increased directly with the square of the total flow rate.

# UNCLASSIFIED

FOR PERIOD ENDING AUGUST 15, 1951

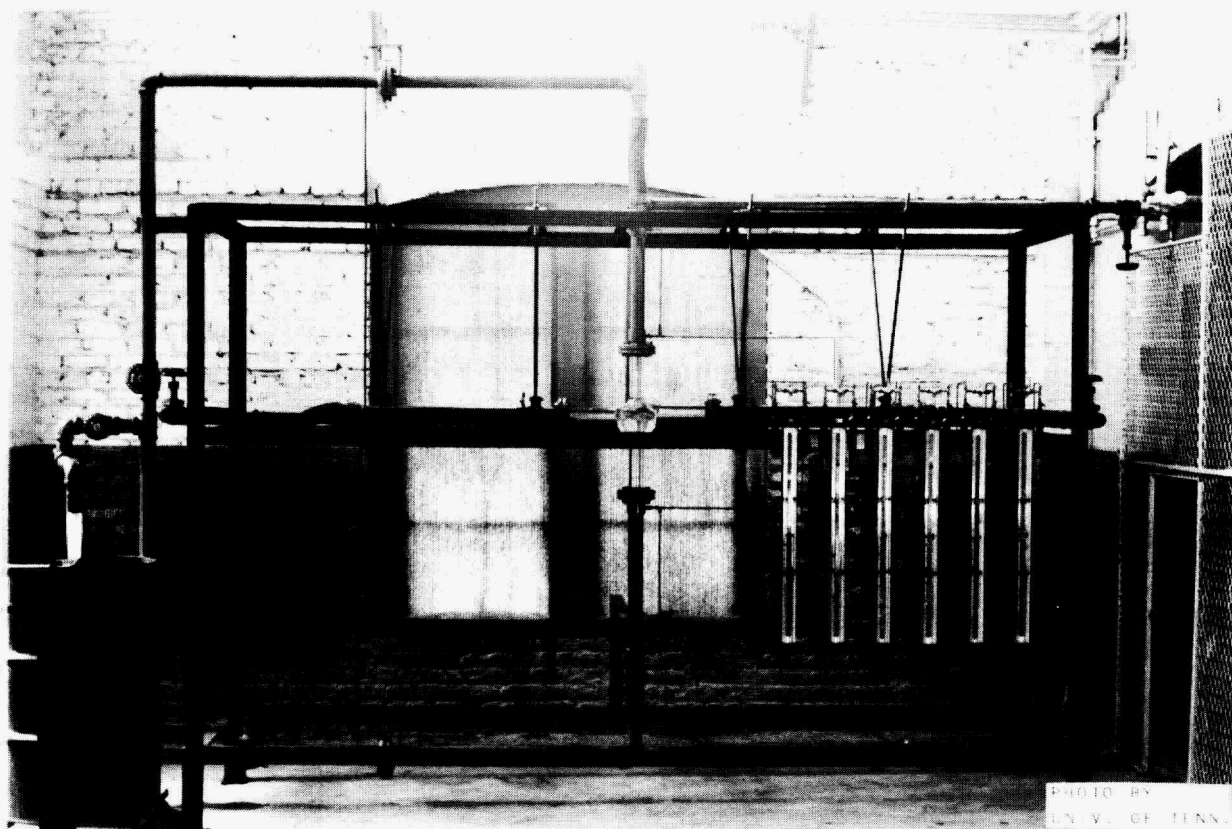


Fig. 1 - Experimental Equipment for Pressure Loss Studies.

2. For a given sphere and a given flow rate, the pressure drop using a single inlet was greater than that using two inlets by a factor of two.
3. For a given sphere and a given flow rate, little variation in the pressure drop was noted as the number of outlets in use was varied.
4. A tentative correlation of all the results based on potential flow considerations of the losses due to the rotary motion within the sphere and exit losses is

$$\Delta P = \frac{\rho V_0^2}{2\pi^2 g_c R_1^4} \left\{ \frac{1}{N_1} \left[ \left( \frac{R_s}{R_2} \right)^2 - 1 \right] + \frac{1}{N_2^2} \left[ \frac{R_1}{R_2} \right]^4 \right\}, \quad (1)$$

where

$\Delta P$  = pressure drop from inlet to outlet of the sphere (pounds force/ft<sup>2</sup>),

UNCLASSIFIED

# UNCLASSIFIED

## HRP QUARTERLY PROGRESS REPORT

- $\rho$  = liquid density (pounds mass/ft<sup>3</sup>),  
 $V_0$  = total liquid flow rate (ft<sup>3</sup>/sec),  
 $R_1$  = radius of inlet pipe (ft),  
 $R_2$  = radius of outlet pipe (ft),  
 $R_s$  = radius of sphere (ft),  
 $N_1$  = number of inlet pipes (dimensionless),  
 $N_2$  = number of outlet pipes (dimensionless), and  
 $g_c$  = gravitational conversion factor [(pounds mass)(ft)/(sec)<sup>2</sup> (pounds force)].

The pressure drop as given by Eq. (1) was found to be greater than the experimental values, but a more satisfactory relation can be given

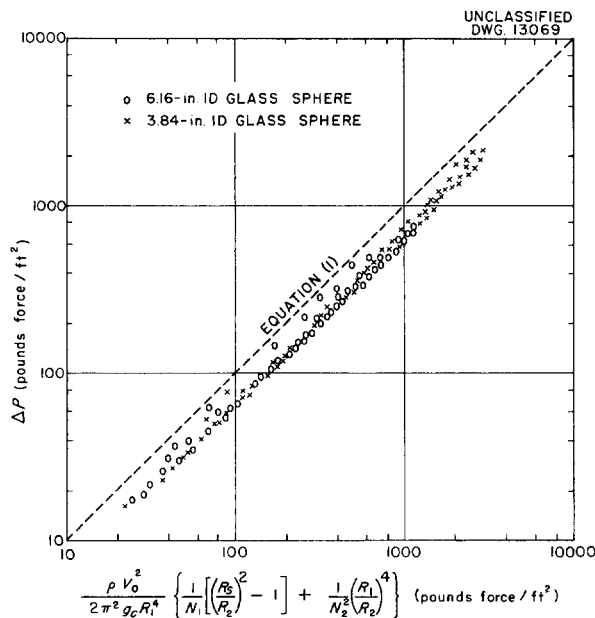


Fig. 2 - Pressure Losses in Spherical Containers.

as more information concerning the liquid velocity distribution within the sphere is known. The comparison of the experimental data with Eq. (1) is shown in Fig. 2.

**Literature Survey and Theoretical Considerations.** A preliminary survey of the literature indicated that the flow of liquid in a spherical container had not been treated either theoretically or experimentally. However, useful information was found regarding theoretical considerations and experimental techniques. Some of the more important references under various headings are given below:

1. *The Instability of Laminar Flow in Curved Channels*

Cornish, J. D., *Proc. Roy. Soc.* A140, 227-40 (1933).

Fage, A., *Proc. Roy. Soc.* A165, 513-17 (1938).

Goldstein, S., *Proc. Cambridge Phil. Soc.* 33, 41-61 (1937).

Lewis, J. W., *Proc. Roy. Soc.* A117, 388-407 (1928).

2. *Turbulent Flow in Curved Channels*

Dean, R. H., *Phil. Mag.* 4, 208-223 (1927); *Phil. Mag.* 5, 673-695 (1928).

Taylor, G. I., *Proc. Roy. Soc.* A124, 243-49 (1929); *Proc. Roy. Soc.* A151, 494-512 (1935); *Proc. Roy. Soc.* A157, 546-579 (1936).

Wattendorf, F. L., *Proc. Roy. Soc.* A148, 565-598 (1935).

White, C. M., *Proc. Roy. Soc.* A123, 645-663 (1929).

3. *Rotary Flow in Cylindrical and Conical Equipment*

Batchelor, G. K., *Quart. J. Mech. App. Math.* IV, 29-41 (1951).

# UNCLASSIFIED

FOR PERIOD ENDING AUGUST 15, 1951

Binnie, A. M., and Davidson, J. F., *Proc. Roy. Soc.* A199, 443-56 (1949).

Binnie, A. M., and Harris, D. P., *Quart. J. Mech. App. Math.* III, 89-106 (1950).

Binnie, A. M., and Hookings, G. A., *Proc. Roy. Soc.* A194, 398-412 (1948).

*Heat Transfer and Fluid Mechanics Institute*, pp. 33-43, Stanford University Press (1951).

Shepherd, C. B., and Lapple, C. E., *Ind. Eng. Chem.* 32, 1246-48 (1950).

Taylor, G. I., *Aero. Research Comm. F. M.*, 788 (1945).

Van Tongeren, H., *Mech. Eng.* 57, 753-59 (1935).

4. *Special Instruments for Measuring Rotary Flow Patterns*

Shubry, A., *Proc. Am. Soc. Civil Engrs.* 75, 713-74 (1949).

Ter Linden, A. J., *Proc. Inst. Mech. Engrs.* 160, 233-55 (1949).

Wattendorf, F. L., *Proc. Roy. Soc.* A148, 565-598 (1935).

Some progress has been made in solving the equations of motion for the type of flow to be encountered in the spherical containers for assumed simple radial and vertical velocity distributions. However, it is realized that the solutions obtained are so limited that this

information will not be discussed in this report.

**Program for September 1 to December 1, 1951.** A tabulation of future work is listed below in the order in which it will be conducted:

1. Extension of the pressure-drop studies in glass spheres using two other sizes of spheres.
2. Continuation of the construction of the closed flow system with the incorporation of metal or plastic spheres as they become available.
3. Initiation of experiments to discover methods of visualizing the flow patterns in the spherical containers.
4. Continuation of the theoretical considerations of the over-all research program.

Submitted 9/20/51/:

H. J. Garber, Professor  
of Chemical Engineering

F. N. Peebles, Asst. Professor  
of Chemical Engineering

Approved:

R. M. Boarts, Head  
Department of Chemical Engineering

UNCLASSIFIED